

**Part I: Kilogram-scale Synthesis of Corannulene**  
**Part II: Deuterium Isotope Effects in the Crystal Structure and Dynamics of**  
**Corannulene**

**Dissertation**  
**zur**  
**Erlangung der naturwissenschaftlichen Doktorwürde**  
**(Dr. sc. nat.)**

**vorgelegt der**  
**Mathematisch-naturwissenschaftlichen Fakultät**  
**der**  
**Universität Zürich**  
**von**  
**Anna Butterfield**  
**aus den Vereinigten Staaten**

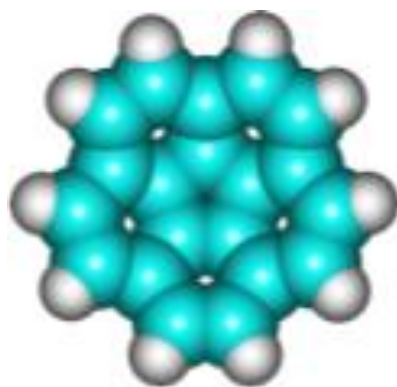
**Promotionskomitee:**

**Prof. Dr. Jay S. Siegel (Vorsitz)**  
**Prof. Dr. Kim K. Baldridge**  
**Prof. Dr. Hans-Beat Bürgi**  
**PD Dr. Thomas Bader**

**Zürich, 2013**

## **Part I: Kilogram-scale Synthesis of Corannulene**

## **Part II: Deuterium Isotope Effects in the Crystal Structure and Dynamics of Corannulene**



## ABSTRACT OF THE DISSERTATION

Part I: Kilogram-scale Synthesis of Corannulene

Part II: Deuterium Isotope Effects in the Crystal Structure and Dynamics of Corannulene

by

Anna Butterfield

University of Zürich, 2012

Professor Dr. Jay S. Siegel, Chair

Corannulene,  $C_{20}H_{10}$ , is a polyaromatic hydrocarbon that has interested chemists for years because it is the smallest subunit of the buckyball motif that still maintains a curved surface. The curvature of corannulene and fullerenes produce unique electronic properties not seen in naphthalene or pyrene. This dissertation is divided into four areas: 1) the kilogram synthesis of corannulene, 2) a study of *sym*-pentasubstituted corannulene derivatives on a water surface, 3) the unit cell volume determination of corannulene and perdeuterocorannulene and 4) an analysis on the temperature dependencies of anisotropic displacement parameters for  $C_{20}H_{10}$  and  $C_{20}D_{10}$ .

The motivation behind the project was outlined in the introduction and possible corannulene derivatives already known in the literature were showcased. An efficient entry process for the synthesis of corannulene has been demonstrated on kilogram scale. Compared to the discovery and gram-scale syntheses, the amounts of solvents and reagents per gram of product were greatly reduced. Priority was given to implement the least toxic agents possible. Improvements in the purification of products obviated the need for column chromatography, alleviating four chromatographic operations. The process now comprises nine steps, each of which runs smoothly at 100-L scale. A total of 1.3 kilograms of corannulene was isolated. This kilogram-scale process reduces material costs by over two orders of magnitude compared to that for the published gram-scale syntheses.

The formation of stable monolayers on the surface of water has proven to be a robust method to apply single layers of material to a solid support in a controlled manner. With the goal to find applications of corannulene derivatives in materials science, one could make use of this technique. A series of *sym*-pentasubstituted corannulene derivatives were synthesized and studied on the surface of water. The derivative containing a hydrophilic tail formed aggregates upon compression and were not good candidates for this technique. The derivatives with hydrophobic tails produced nice isotherms. These derivatives were also studied using Brewster angle microscopy.

Kinetic isotope effect states that a deuterated molecule should have a lower zero-point energy and thus smaller packing radius than its isotopologue. Dunitz showed with benzene and perdeuterobenzene that temperature can also influence the effective size of the molecule and that a deuterated molecule is not always smaller than the protium molecule. The same study was done with corannulene and perdeuterocorannulene by determining their respective unit cell volumes as a function of temperature from 4.5 K to 490 K using x-ray powder diffraction. The  $C_{20}H_{10}$  and  $C_{20}D_{10}$  molecules did not show a crossover point in this range.

An analysis on the temperature dependencies of the anisotropic displacement parameters (ADPs) of  $C_{20}H_{10}$  and  $C_{20}D_{10}$  crystals was presented. The molecules were modeled using the ADPs obtained from neutron diffraction data at 20, 90, 173 K and x-ray diffraction data at 15, 90, 173, 250 K. The neutron and x-ray diffraction data was compared at varying scattering angle cutoff values to determine the most appropriate data set to use. The consistencies between models were determined using the theory of isotope effect. With assistance from *ab initio* calculations of corannulene and perdeuterocorannulene in the gas phase, three additional stretching modes contributing to the out-of-plane components were added to the model.

# ZUSAMMENFASSUNG

Teil I: Synthese von Corannulen im Kilogrammmassstab

Teil II: Untersuchung über Isotopeneffekte von Deuterium in Kristallstrukturen und über die Dynamik von Corannulen

von

Anna Butterfield

Universität Zürich, 2012

Prof. Jay S. Siegel, Vorsitz

Corannulen,  $C_{20}H_{10}$ , ist ein polyaromatischer Kohlenwasserstoff, welcher Chemiker seit Jahren interessiert, weil es die kleinstmögliche Untereinheit des Buckminsterfullerens ( $C_{60}$ ) ist, welche seine gebogene Oberfläche noch beibehalten kann. Die Schalenform von Corannulen und Fulleren erzeugt einzigartige elektronische Eigenschaften, welche zum Beispiel in Naphtalen und Pyren nicht beobachtet werden könne. Diese Dissertation ist in vier Teile unterteilt: 1) Die Corannulen-Synthese im Kilogramm-Massstab, 2) eine Untersuchung von sym-pentasubstituierten Corannulenderivaten auf einer Wasseroberfläche, 3) die Bestimmung des Volumens der Elementarzelle von Corannulen und Perdeutero-Corannulen und 4) eine Analyse der Temperaturabhängigkeit von anisotropischen Verschiebungsparametern von  $C_{20}H_{10}$  und  $C_{20}D_{10}$ .

Ein effizienter Einstiegsprozess für die Synthese von Corannulen im Kilogrammmassstab wurde dargestellt. Verglichen mit den ersten Corannulensynthesen im Gramm-massstab konnten die Mengen an Lösungsmittel und Reagenzien um ein vielfaches reduziert werden. Es wurde darauf geachtet, wenn immer möglich ungiftige Chemikalien oder solche mit geringer Toxizität zu verwenden. Durch Verbesserungen der Reinigungsmethoden wurde es möglich, alle der vier ursprünglichen Reinigungsschritte per Säulenchromatographien zu umgehen. Die gesamte Synthese besteht nun aus neun Stufen, von denen jede problemlos in einem 100 Liter Massstab durchgeführt werden kann. Insgesamt konnten dadurch 1.3 Kilogramm Corannulen hergestellt werden. Durch den Prozess auf Kilogrammskala konnten die Materialkosten

im Vergleich zur Synthese im Grammstabsstab um mehr als zwei Grössenordnungen gesenkt werden.

Die Bildung von stabilen Molekularschichten auf der Wasseroberfläche erwies sich als verlässliche Methode um einzelne Materialschichten kontrolliert auf einen Festphasenträger aufzutragen. Das Ziel, Anwendungsmöglichkeiten für Corannulenderivate in der Materialwissenschaft zu finden, könnte sich diese Technik zu Nutzen machen. Eine Serie von sym-pentasubstituierten Corannulenderivaten wurde hergestellt und auf einer Wasseroberfläche untersucht. Diejenigen Derivate, welche einen hydrophilen Schwanz besaßen, formten unter Druckeinwirkung Aggregate und erwiesen sich dadurch als schlechte Kandidaten für diese Technik. Die Derivate mit hydrophobem Schwanz jedoch formten schöne Isotherme. Diese Derivate wurden ebenfalls mittels Brewster-Winkel Mikroskop untersucht.

Kinetische Isotopeneffekte besagen, dass deuterierte Moleküle eine tiefere Nullpunktsenergie - und dadurch einen kleineren Packungsradius – als ihre Isotopologe haben sollten. Dunitz konnte anhand von Benzen und Perdeuterobenzen zeigen, dass die Temperatur die Grösse der Moleküle beeinflussen kann und dass das deuterierte Molekül nicht immer kleiner ist als das Molekül mit Wasserstoffatomen. Dieselbe Untersuchung wurde mit Corannulen und Perdeuterocorannulen durchgeführt, indem die jeweiligen Elementarzellvolumina in Abhängigkeit der Temperatur zwischen 4.5 K und 490 K mittels Pulverbeugungsverfahren bestimmt wurden. Die  $C_{20}H_{10}$  und  $C_{20}D_{10}$  Moleküle zeigten in diesem Temperaturbereich keinen Überschneidungspunkt.

Eine Temperaturabhängigkeits-Analyse der anisotropischen Verschiebungsparameter (AVP) von  $C_{20}H_{10}$ - und  $C_{20}D_{10}$ -Kristallen wurde vorgestellt. Die Moleküle wurden mit Hilfe der AVP, welche durch Neutronendiffraktion bei 20, 90, 173 K und durch Röntgenstrahlendiffraktion bei 15, 90, 173, 250 K erhalten wurden, modelliert. Die Neutronen- und Röntgenstrahlendiffraktions-Daten wurden bei verschiedenen Streuwinkel-Anhaltewerten verglichen um das am besten geeignete Datenset zu finden. Die Konsistenz zwischen den Modellen wurde mittels Isotopeneffekt-Theorie bestimmt. Mit Hilfe von ab initio Berechnungen von Corannulen und Perdeuterocorannulen in der Gasphase konnten drei zusätzliche Streckungsmodi, die zu

den aus-der-Ebene-Komponenten beitragen, zum Model hinzugefügt und analysiert werden.

## Curriculum Vitae

### ANNA M. BUTTERFIELD

3 Maxwell's Green #402, Somerville, MA 02144 (617) 686 6576  
anna.butterfield@oci.uzh.ch

## EDUCATION

**Ph.D., Organic chemistry, University of Zurich, Switzerland, 2008- 2012**

Thesis research with Prof. Dr. Jay Siegel entitled "Part I: Kilogram-scale Synthesis of Corannulene Part II: Deuterium Isotope Effects in the Crystal Structure and Dynamics of Corannulene"

**M.S., Organic chemistry, University of Zurich, Switzerland, 2006-2008**

**B.S., Chemistry (minor in Spanish), Juniata College, Huntingdon, PA, 2002-2006**

President of *Gamma Sigma Epsilon*, national chemistry honors society.

## Research Experience

**Graduate Researcher, University of Zurich, Switzerland, 2006- September 2012**

- Reduced the cost of target compound, corannulene, from \$1000/ gram to \$10/ gram
- Produced over 1 kilogram of corannulene to drive the development of this class of molecules
- Synthesized a variety of corannulene derivatives and studied their electrochemical and photophysical properties for potential applications in materials science
- Specialized techniques learned: synthetic route design, process chemistry, CV, fluorescence spectroscopy, glovebox, Schlenk, HPLC, LC-MS, GC-MS, NMR, IR, neutron/ powder diffraction, purification using column chromatography
- Presented results at four international conferences

**Undergraduate Researcher (NSF-REU), Juniata College, Huntingdon, PA, 2003-2006**

- Progressed project towards the synthesis of a polyhydroxylated kekulene
- Isolated and characterized intermediates and side products
- Presented results at professional conferences

## LEADERSHIP EXPERIENCE

**Teaching Assistant, University of Zurich, Switzerland, 2009- September 2012**

- Developed individual research program procedures for second and third year students
- Demonstrated advanced lab techniques and how to use ChemDraw/ Scifinder
- Supervised 40-45 students simultaneously



- Monitored and ensured compliance with program requirements
- Created and graded homework assignments in a required undergraduate chemistry course
- Held mandatory weekly problem sessions to further review fundamental concepts

**Laboratory Mentor, University of Zurich, Switzerland, 2008- September 2012**

- Supervised seven students with projects ranging from six weeks to six months in duration
- Responsibilities: planning projects, demonstrating lab techniques and assistance with analyzing data
- Resulted in two publications

**Organic Chemistry Tutor, Juniata College, Huntingdon, PA, 2003-2006**

- Conducted weekly group review sessions for class of 100-150 students
- Held individual tutoring sessions for up to three hours per week

**PROFESSIONAL DEVELOPMENT**

**Participant: Patenting in Life Sciences, Swiss Academy of Sciences, 2012**

- Attended lectures and discussions on the basic knowledge of IP and patenting, technology transfer at universities, patent law, and ethical considerations in life science patenting.
- Participated in a patent infringement workshop and presented results in the final group discussion.

**Skills:**

- Proficient in MS Office Word, Excel, PowerPoint, Keynote, ChemDraw, Scifinder
- Languages: English (native speaking), Spanish (fluent)

**Awards:**

- C&E News highlight of *Org. Process Res. Dev.* **2012** paper (C&EN, March 5, p 49)
- Swiss Chemical Society travel award recipient, **2012**
- Dorothy Crowfoot Hodgkin Symposium poster winner **2011, 2012**
- Juniata College tutor award **2006**
- McKelvey Foundation 4-year full scholarship **2002**

## PUBLICATIONS

1. Duttwyler, S.; Butterfield, A.; Siegel, J. S. Arenium Acid-Catalyzed Deuteration of Aromatic Hydrocarbons, *J. Org. Chem.* **2013**, 78, 2134.
2. Steinauer, A.; Butterfield, A.; Linden, A.; Baldrige, K.; Siegel, J. S. Tunable Redox Properties of *n*-(Phenylthio)corannulenes, *Angew. Chem. Int. Ed.* **2012** *submitted*.
3. Butterfield, A.; Gilomen, B.; Siegel, J. S. Kilogram-Scale Production of Corannulene, *Org. Process Res. Dev.* **2012**, 16, 664.
4. Maag, R.; Northrop, B. H.; Butterfield, A.; Linden, A.; Zerbe, O.; Lee, Y. M. Chi, K-W.; Stang, P. J.; Siegel, J. S. Synthesis and X-ray structural analysis of platinum and ethynyl-platinum corannulenes: supramolecular tectons, *Org. Biomol. Chem.*, **2009**, 7, 4881.
5. Reingold, D. I.; Bowerman, C.; John, M.; Waters, R. S.; Daglen, B. C.; Butterfield, A. M.; Gembicky, M. An Acid-Catalyzed Michael-Aldol Reaction, *Tetrahedron Lett.*, **2006**, 47, 1653.
6. Reingold, D. I.; Butterfield, A. M.; Daglen, B. C.; Walters, R. S.; Allen, K.; Scheuring, S.; Kratz, K.; Gembicky, M.; Baran, P. A New Tricyclic Triketone from Tandem Condensation Reactions, *Tetrahedron Lett.*, **2005**, 46, 3835.

# Table of Contents

<b>Chapter 1 .....</b>	<b>1</b>
<b>Introduction .....</b>	<b>1</b>
1.1 Polycyclic aromatic hydrocarbons .....	1
1.2 First synthesis of corannulene .....	2
1.3 Corannulene derivatives .....	5
1.4 Application of corannulene derivatives.....	11
<b>Chapter 2 .....</b>	<b>22</b>
<b>Kilogram-scale synthesis of corannulene .....</b>	<b>22</b>
2.1 Introduction .....	22
2.2 Historical development.....	22
2.3 Previous work .....	27
2.4 Current work.....	30
2.5 Conclusion.....	39
2.6 Experimental.....	40
<b>Chapter 3 .....</b>	<b>47</b>
<b>Corannulene monolayers.....</b>	<b>47</b>
3.1 History .....	47
3.2 Theory.....	52
3.3 Langmuir films .....	53
3.4 Langmuir-Blodgett films .....	55
3.5 Present work.....	56
3.6 Results and discussion.....	58
3.7 Experimental.....	63
<b>Chapter 4 .....</b>	<b>69</b>
<b>Unit cell volume determination of C<sub>20</sub>H<sub>10</sub> and C<sub>20</sub>D<sub>10</sub>.....</b>	<b>69</b>
4.1 Introduction .....	69
4.2 Isotope Effect .....	69
4.3 Benzene and perdeuterobenzene .....	71
4.4 Corannulene and perdeuterocorannulene .....	72
4.5 Conclusions.....	76
4.6 Experimental.....	76
<b>Chapter 5 .....</b>	<b>78</b>
<b>Temperature dependencies on the anisotropic displacement parameters of C<sub>20</sub>H<sub>10</sub> and C<sub>20</sub>D<sub>10</sub> .....</b>	<b>78</b>
5.1 Introduction .....	78
5.2 Experimental.....	78
5.3 Comparison .....	79
5.4 Results .....	80
5.5 Analysis of models.....	81
5.6 Conclusion.....	89
<b>Appendix A .....</b>	<b>91</b>

## List of Figures

<b>Figure 1.1</b> Smaller PAHs possessing a carbon frame matching that of C <sub>60</sub> .....	2
<b>Figure 1.2</b> Bond lengths and bowl depth of corannulene.....	4
<b>Figure 1.3</b> Proposed mechanism for chlorination.....	7
<b>Figure 1.4</b> C <sub>60</sub> dyads possessing long charge-separation states.....	12
<b>Figure 1.5</b> Three type of nanotubes.....	15
<b>Figure 1.6</b> Corannulene derivative synthesized using a new iron-catalyzed method with potential biological applications.....	16
<b>Figure 2.1</b> Different retrosynthetic approaches to <b>1</b> . Disconnection between the flanking (a) or rim (b) carbons of <b>1</b> results in two different fluoranthene precursors.....	24
<b>Figure 3.1</b> First pressure-area isotherm published by Pockels.....	50
<b>Figure 3.2</b> (Top) Drawing of Langmuir's original film balance. <sup>12</sup> (Bottom) Reconstructed trough at TU Braunschweig.....	52
<b>Figure 3.3</b> Interaction of molecules at the air/water interface.....	53
<b>Figure 3.4</b> Monolayer with a hydrophilic headgroup immersed in the water and hydrophobic tail pointing in the air.....	54
<b>Figure 3.5</b> Schematic surface pressure to mean molecular area isotherm for an amphiphile. <sup>14</sup> .....	55
<b>Figure 3.6</b> Langmuir-Blodgett deposition types Z, Y and X multilayers.....	56
<b>Figure 3.7</b> Surface pressure to area isotherms for single compression of molecules (top) <b>44</b> , (middle) <b>45</b> and (bottom) <b>46</b> .....	60
<b>Figure 3.8</b> Compression/expansion isotherms showing reproducibility in molecule <b>44</b> (top), but not in molecule <b>45</b> (middle) or molecule <b>46</b> (bottom).....	62
<b>Figure 3.9</b> Calculated structure of <b>45</b> showing the PEG ligands expand past the corannulene core of the molecule.....	63
<b>Figure 4.1</b> Diagram of a harmonic oscillator.....	69
<b>Figure 4.2</b> Diagram of an anharmonic oscillator. <sup>3</sup> .....	70
<b>Figure 4.3</b> Molecular volume (V <sub>mol</sub> ) vs. T of benzene (squares) and perdeuterobenzene (circles) obtained from neutron powder diffraction.....	72
<b>Figure 4.4</b> X-ray powder diffractogram corannulene sample fit to the silicon standard.....	74
<b>Figure 4.5</b> Unit cell volume vs. temperature for C <sub>20</sub> H <sub>10</sub> (blue) and C <sub>20</sub> D <sub>10</sub> (red) from 4.5 K to 490 K.....	75
<b>Figure 5.1</b> <i>ab initio</i> calculation of corannulene in the gas phase at 144.75 cm <sup>-1</sup> .....	82

<b>Figure 5.2</b> <i>ab initio</i> calculation of corannulene in the gas phase at 135.33 cm <sup>-1</sup> , showing cosine distribution of the out-of-plane components.....	84
<b>Figure 5.3</b> <i>ab initio</i> calculation of corannulene in the gas phase at 135.33 cm <sup>-1</sup> , showing sine distribution of the out-of-plane components. ....	85

## List of Schemes

<b>Scheme 1.1</b> First synthesis of corannulene ( <b>1</b> ).....	3
<b>Scheme 1.2</b> 2006 synthesis of corannulene .....	4
<b>Scheme 1.3</b> Synthesis of monosubstituted corannulene derivatives .....	6
<b>Scheme 1.4</b> Synthesis of pentachlorocorannulene and decachlorocorannulene .....	6
<b>Scheme 1.5</b> Synthesis of monoborylated corannulene ( <b>26</b> ) from <b>18</b> .....	7
<b>Scheme 1.6</b> Synthesis of pentaalkylcorannulene ( <b>27</b> ) and pentaarylcorannulene ( <b>28</b> ).....	8
<b>Scheme 1.7</b> Synthesis of pentaalkynylcorannulenes from <b>19</b> .....	8
<b>Scheme 1.8</b> Synthesis of pentaborylated corannulene ( <b>30</b> ).....	9
<b>Scheme 1.9</b> Synthesis of corannulenopyrrole ( <b>34</b> ).....	9
<b>Scheme 1.10.</b> Synthesis of azidocorannulene ( <b>36</b> ) .....	10
<b>Scheme 1.11</b> Synthesis of methanofullerenes by addition of diazo compounds to <b>37</b> .....	11
<b>Scheme 2.1</b> First synthesis of corannulene .....	22
<b>Scheme 2.2</b> Flash vacuum pyrolysis method developed by Scott.....	25
<b>Scheme 2.3.</b> First corannulene synthesis by the Siegel group .....	25
<b>Scheme 2.4</b> Solution-phase synthesis of corannulene (2006) .....	27
<b>Scheme 2.6</b> Preparation of isomers <b>13</b> and <b>13b</b> .....	29
<b>Scheme 2.7</b> Separation of <b>13</b> and <b>13b</b> using Girard's Reagent in AcOH.....	31
<b>Scheme 2.8.</b> Optimization of 1,6,7,10-tetramethylfluoranthene ( <b>15</b> ).....	32
<b>Scheme 2.9</b> Benzylic bromination of fluoranthene <b>15</b> .....	34
<b>Scheme 2.11</b> Reduction of <b>17</b> to corannulene using Pd/C.....	38
<b>Scheme 2.12</b> Optimized synthesis of corannulene ( <b>1</b> ) .....	39
<b>Scheme 3.1</b> Synthesis of <b>44</b> .....	57
<b>Scheme 3.2</b> Synthesis of <b>45</b> and <b>46</b> .....	57
<b>Scheme 4.1</b> Synthesis of perdeuterocorannulene ( <b>47</b> ) .....	73

<b>Table 2.4.</b> Comparison of reagents required before (2006) and after (2011) the optimization of 13 and 13b to produce 1 kilogram of corannulene <sup>lxxxvi</sup> .....	31
<b>Table 5.1.</b> Neutron diffraction data minus x-ray diffraction data at various scattering angle cutoffs and temperatures, (H=Corannulene, D=Deuterocorannulene).....	80
<b>Table 5.2.</b> Corannulene minus deuterocorannulene at 0.6 Å and various temperatures, (N=Neutron, X=X-ray) .....	80
<b>Table 5.3.</b> Normal frequencies, $\nu$ (cm <sup>-1</sup> ), and eigenvectors for CorH(A) derived from ADPs pertaining to 3N+4X with additional stretch modes, U <sub>1</sub> , U <sub>2</sub> and U <sub>3</sub> . .....	86
<b>Table 5.4.</b> Normal frequencies, $\nu$ (cm <sup>-1</sup> ), and eigenvectors for CorH(B) derived from ADPs pertaining to 3N+4X with additional stretch modes, U <sub>1</sub> , U <sub>2</sub> and U <sub>3</sub> . .....	86
<b>Table 5.5.</b> Normal frequencies, $\nu$ (cm <sup>-1</sup> ), and eigenvectors for CorD(A) derived from ADPs pertaining to 3N+3X with additional stretch modes, U <sub>1</sub> , U <sub>2</sub> and U <sub>3</sub> . .....	87
<b>Table 5.6.</b> Normal frequencies, $\nu$ (cm <sup>-1</sup> ), and eigenvectors for CorD(B) derived from ADPs pertaining to 3N+3X with additional stretch modes, U <sub>1</sub> , U <sub>2</sub> and U <sub>3</sub> . .....	87
<b>Table 5.7.</b> Libration and translation components determined by the force constant matrix for molecule A in corannulene and perdeuterocorannulene. ....	88
<b>Table 5.8.</b> Libration and translation components determined by the force constant matrix for molecule B in corannulene and perdeuterocorannulene. ....	89

# Chapter 1

## *Introduction*

### **1.1 Polycyclic aromatic hydrocarbons**

Polycyclic aromatic hydrocarbons (PAHs), or polyarenes<sup>1</sup>, consist of a structurally diverse class of organic molecules that have distinct chemical and electronic properties. This unique class of organic molecules is often found in abundance in the environment. Crude oil, karogen shale and coal are the world's primary sources of energy and fuel, therefore providing as a significant source for PAHs in the industrialized world.<sup>2</sup> Byproducts of two important hydrocarbon technologies: the carbonization of hard coal to coke and catalytic reforming to produce gasoline, PAHs can be found in air, water and soil.<sup>3</sup> PAHs have also been detected in meteorites and, through spectroscopic evidence, are believed to be present in interstellar space.<sup>4</sup>

An increase in interest of these polyarenes was brought upon by the discovery of the carcinogenic properties of benzo[*a*]pyrene and other polyarenes in the 1930s.<sup>1</sup> This was an important discovery because until that time, scientist believed that microorganisms and not small, organic molecules caused diseases.<sup>5</sup> Research has now shown that the carcinogenic and mutagenic activities of PAHs may increase with non-planarity.<sup>6</sup>

During the 1980s there was another increase in the interest of PAHs that can be primarily attributed to the discovery of fullerenes in 1985 by Kroto, Curl and Smalley.<sup>7</sup> They were awarded the Nobel Prize in chemistry in 1996 for this research. Until their discovery, natural carbon was only associated with existing as graphite and diamond. Fullerenes opened a new door into the world of carbon allotropes, one that existed as cage-like structures in the shape of spheres, ellipsoids, and tubes.<sup>8</sup>

Within the class of non-planar polyarenes, the one that is most well known is buckminsterfullerene, or C<sub>60</sub>.<sup>9</sup> Fullerenes have a unique structural scaffold that is a model for another class of smaller, curved PAHs whose molecular structure can be “mapped”



onto the fullerene skeleton. Two molecules within this class that have been previously synthesized are the bucky-bowl circumtrindene<sup>10</sup>, C<sub>36</sub>H<sub>12</sub>, and the shallower corannulene<sup>11</sup>, C<sub>20</sub>H<sub>10</sub> (Figure 1.1). The latter will be the primary focus of this thesis.

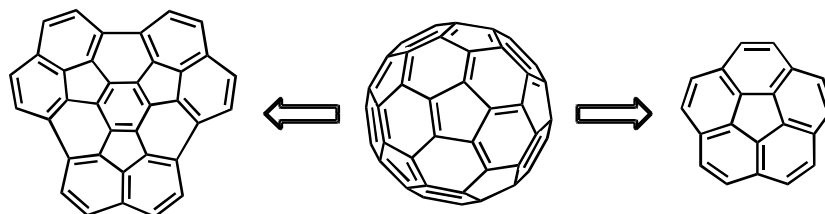


**Figure 1.1** Smaller PAHs possessing a carbon frame matching that of C<sub>60</sub>.

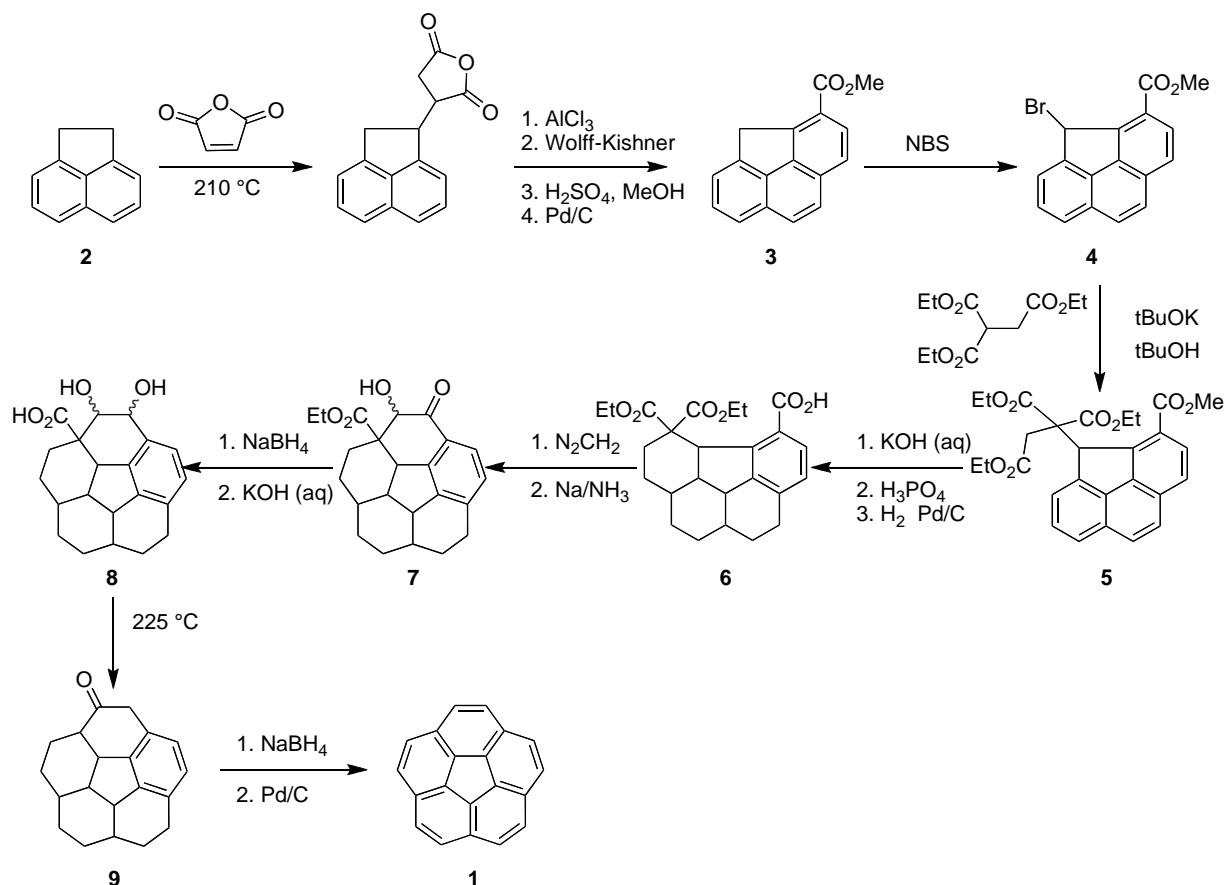
## 1.2 First synthesis of corannulene

Comprising of 20 carbons, corannulene (**1**), or dibenzo[*ghi,mno*]fluoranthene, is one-third the size of C<sub>60</sub> and the smallest subunit of the buckyball motif that still maintains a curved surface.<sup>11</sup> Lawton and Barth first synthesized this PAH in 1966 in a 17-step, 0.4% yield starting from acenaphthene. Despite the poor yield of the synthesis, the work of Lawton and Barth was nonetheless pioneering and considered a remarkable achievement at the time. Their synthetic strategy was to build up the structure ring by ring, introducing strain as late as possible by trading the stabilization from aromatization of the rings for destabilization of the strain due to out-of-plane distortion.

Acenaphthalene (**2**) was converted to 3-carbomethoxy-4*H*-cyclopenta[*def*]phenanthrene (**3**) (Scheme 1) using the method of Sieglitz and Schidlo.<sup>12</sup> The resulting product was then brominated with *N*-bromosuccinimide to **4** followed by alkylation in the presence of potassium *tert*-butoxide and *tert*-butanol to give the tetraester (**5**). Hydrolysis was achieved with aqueous potassium hydroxide that was then subjected to polyphosphoric acid for cyclization of the fourth ring. Hydrogenation was accomplished using Pd/ C to yield a dodecahydro diester acid **6**. Esterification of **6** using diazomethane and subsequent acyloin condensation gave ester **7**, which upon treatment with NaBH<sub>4</sub> then hydrolysis with potassium hydroxide yielded the diol-

ethylester **8**. Thermal decarboxylation at 225 °C converts the diol to the ketone (**9**) and reduction using sodium borohydride followed by palladium on carbon results in corannulene.

**Scheme 1.1** First synthesis of corannulene (**1**)



Despite the poor yield, Lawton and Barth were able to obtain enough material to acquire a crystal structure.<sup>13</sup> Remarkably, elucidation of the crystal structure confirmed the hypothesis of Lawton and Barth that **1** was a non-planar, bowl-shaped polycyclic aromatic hydrocarbon. The bowl depth of corannulene (Figure 1.2) was measured to be 0.89 Å. The four distinct bonds of corannulene, called spoke, rim, hub and flank, were also shown to have distinct bond lengths associated with them. The bond lengths measured were 1.39 Å, 1.40 Å, 1.41 Å, and 1.44 Å respectively.

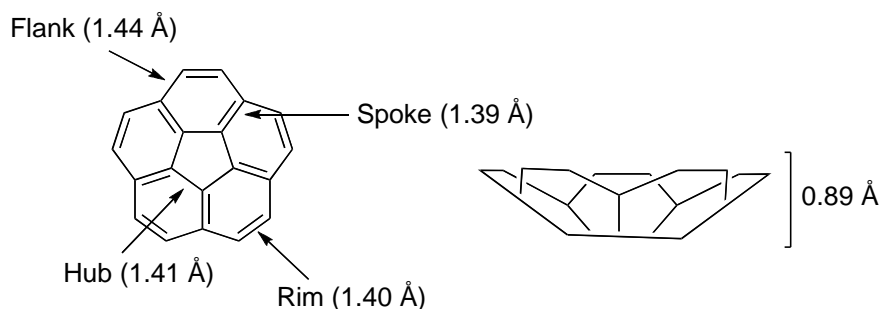
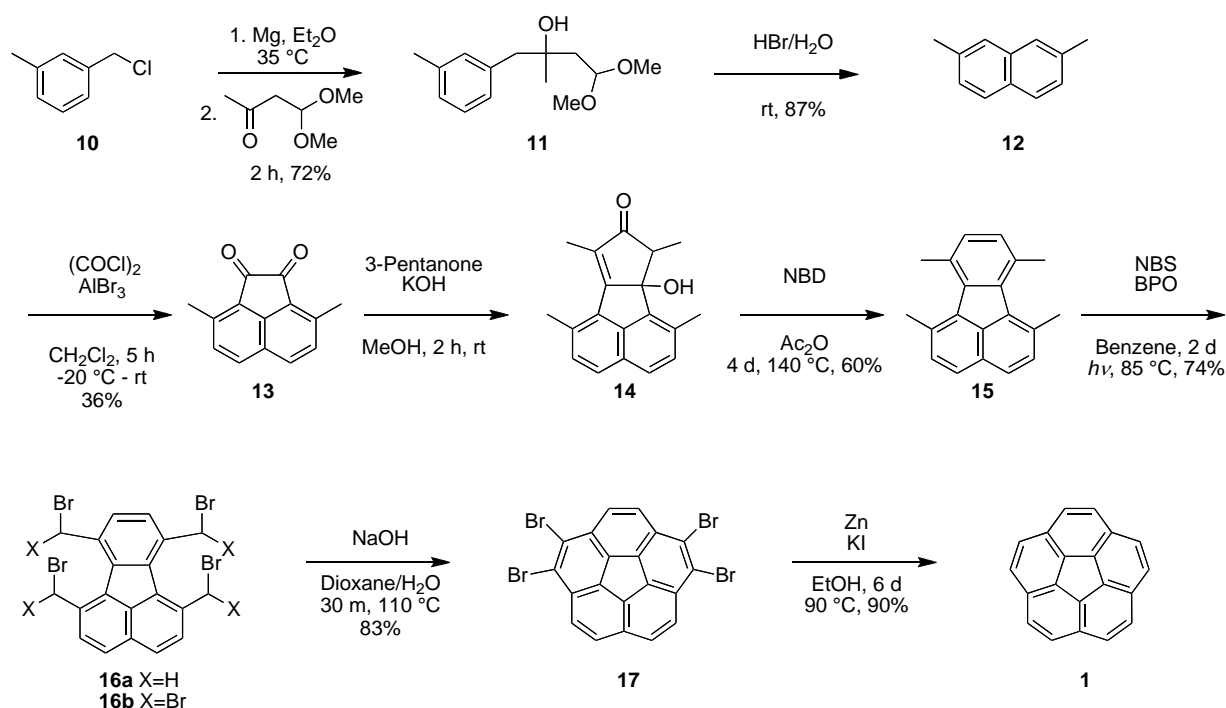


**Figure 1.2** Bond lengths and bowl depth of corannulene

Albeit a pioneering *tour de force*, the synthesis proposed by Lawton and Barth was too lengthy and poor yielding to stimulate a wave of exploration in corannulene chemistry. During the 1970s and 1980s other groups attempted to find a more direct synthesis of **1** but failed.<sup>14</sup> Developing the synthesis of corannulene to the point that grams of **1** were accessible required the contribution of many groups over the span of 30-40 years. This history and individual contributions will be explained in more detail in Chapter 2.

The synthesis of corannulene at the beginning of this thesis was through an 8-step synthesis (Scheme 1.2) starting with  $\alpha$ -chloro-*m*-xylene (**10**). Increased availability of **1** meant that chemists could begin to find ways to derivitize this PAH.

**Scheme 1.2** 2006 synthesis of corannulene

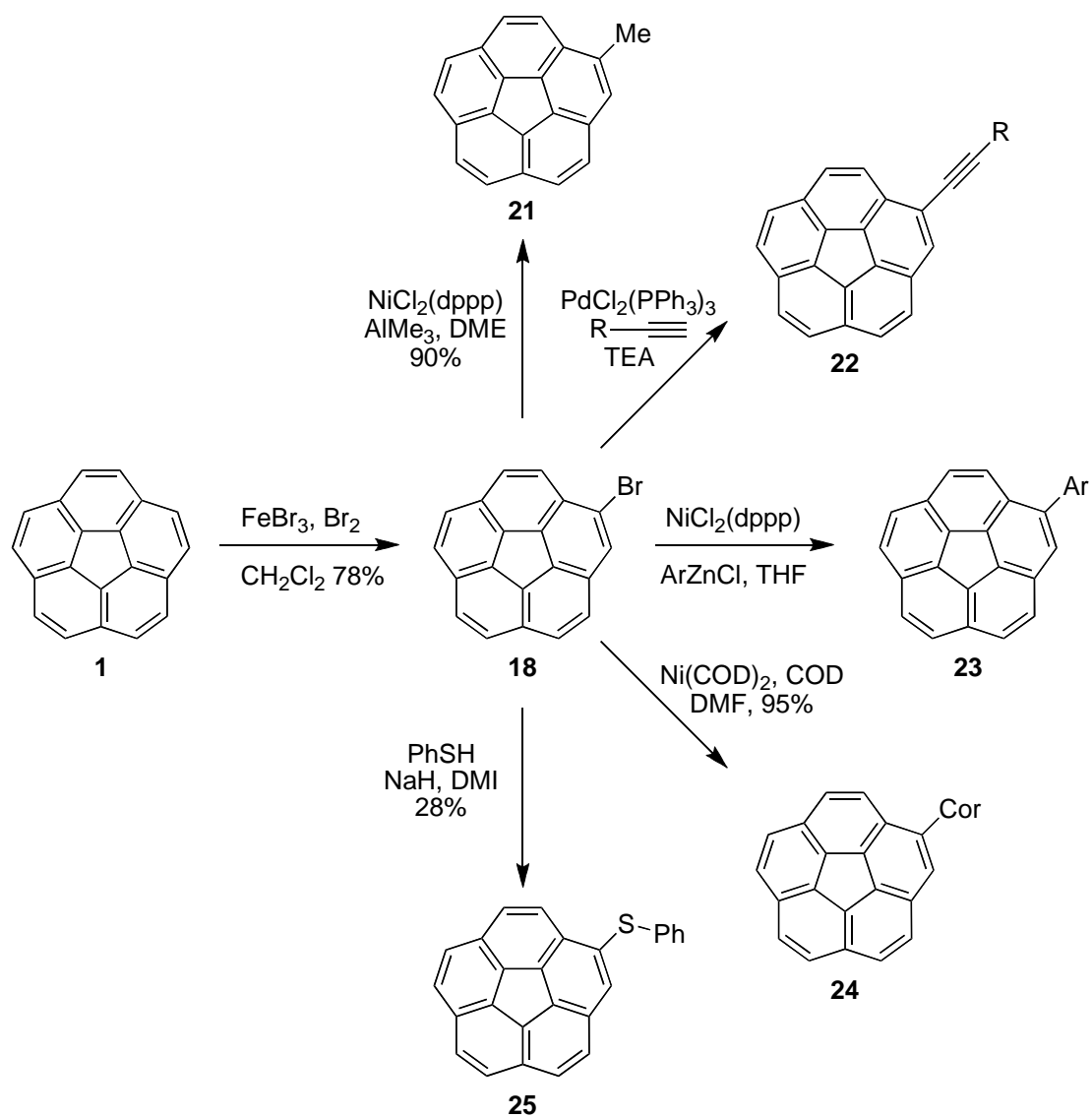


### 1.3 Corannulene derivatives

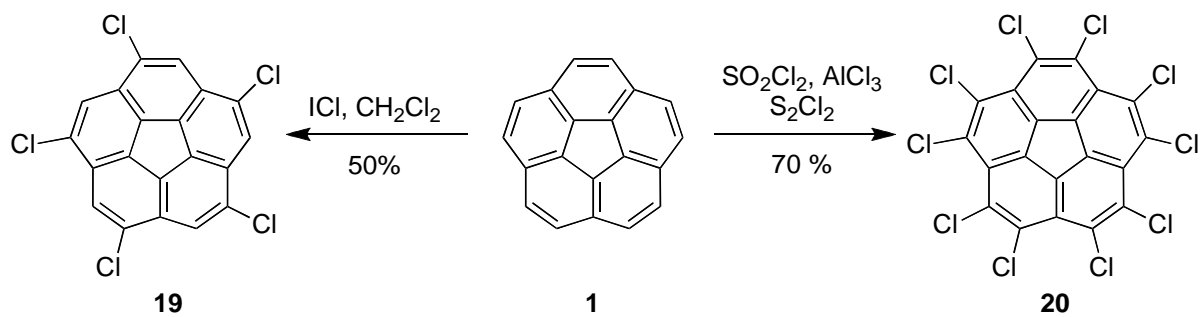
The largest class of corannulene derivatives that have been synthesized and studied to date are the halocorannulenes. This group consists of tetrabromocorannulene (**17**), synthesized *en route* to corannulene, as well as monobromocorannulene, pentachlorocorannulene and decachlorocorannulene. Monobromocorannulene (**18**) was first reported by Larry Scott's group<sup>15</sup> through a direct bromination of **1** using bromine in the presence of a Lewis acid catalyst (Scheme 1.3). *sym*-1,3,5,7,9-Pentachlorocorannulene (**19**) can be obtained in a 50% yield by treating corannulene with a solution of ICl in dichloromethane.<sup>16</sup> Decachlorocorannulene (**20**), although arguably more complicated to synthesize<sup>17</sup> than **18** and **19**, can still be isolated in a 60% yield using the Ballester conditions<sup>18</sup> of sulfonyl chloride, sulfur monochloride and aluminum chloride (Scheme 1.4). The proposed mechanism for this reaction was through a Lewis acid chlorination of the ring (Figure 1.3).

The halocorannulene derivatives **17**, **18**, **19** and **20** are important because with these halocorannulenes in hand, one can alkylate, acylate, alkynylate, arylate or do a nucleophilic aromatic substitution of **1** with select alcohols and thiols, opening the door for new, highly substituted corannulenes. From bromocorannulenes **17** and **18** one can alkylate (**21**) either using trimethylaluminum in the presence of a catalytic amount of NiCl<sub>2</sub>(dppp) (Scheme 1.3) or by treatment with *n*-butyl lithium followed by an alkylchloride.<sup>19</sup> Direct alkylation of **1** is also possible using organolithium reagents followed by reduction with palladium on carbon.<sup>20</sup> Monoalkynylcorannulene (**22**) is accessible through a Sonogashira<sup>21</sup> coupling with **18**; or if an arylcorannulene (**23**) is preferred, one can use Negishi coupling conditions. Biorannulenyne (**24**) was synthesized by Scott's group<sup>22</sup> in 2008 using bromocorannulene and Ni(COD)<sub>2</sub>. Nucleophilic aromatic substitution is also high yielding<sup>23</sup> when using arylthiols (**25**). The conversion of bromocorannulene to a monoborylated corannulene (**26**) was reported<sup>24</sup> by Scott's group using PdCl<sub>2</sub>(dppf) and HBpin (Scheme 1.5). However, recent results show that **26** is accessible directly from **1** under different conditions in one step, making it a more desirable reaction.<sup>25</sup>

**Scheme 1.3** Synthesis of monosubstituted corannulene derivatives



**Scheme 1.4** Synthesis of pentachlorocorannulene and decachlorocorannulene



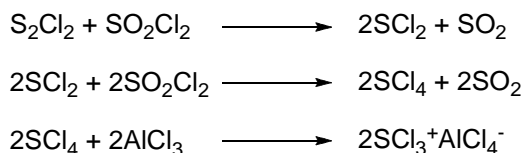
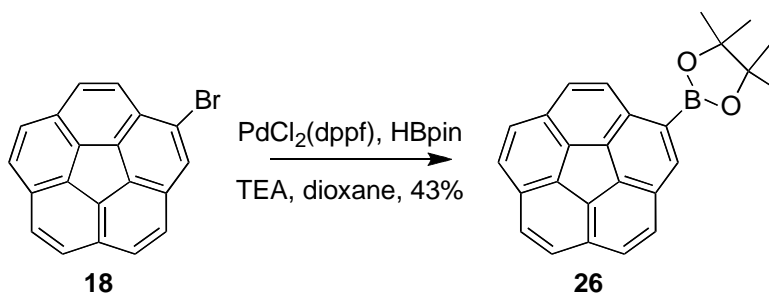


**Figure 1.3** Proposed mechanism for chlorination

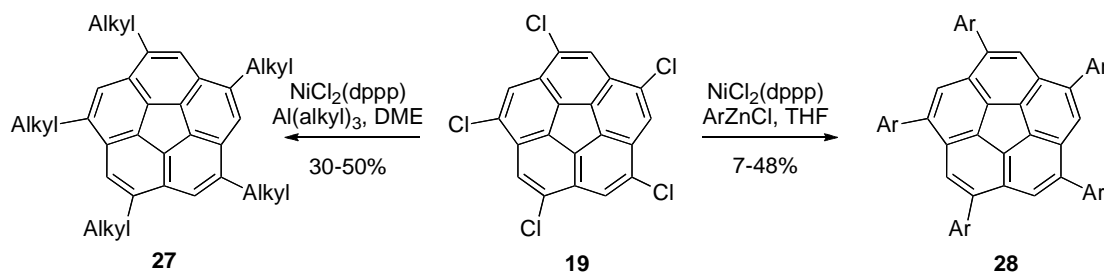
**Scheme 1.5** Synthesis of monoborylated corannulene (**26**) from **18**



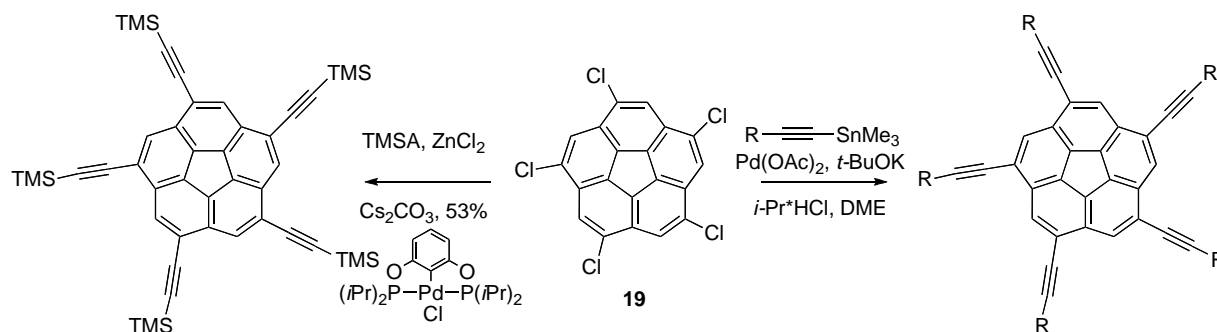
It is now well understood that cross-coupling reactions involving aryl chlorides are more difficult than the same reactions with the corresponding bromides. This trend is also seen with respect to chlorocorannulenes. Not only must **19** and **20** overcome the challenge of the less-active chloride, but also the sparing solubility of these compounds. Adding the fact that **19** and **20** required completing the reaction five or ten times on each respective molecule, developing effective synthetic conditions was no easy task. Nonetheless, both penta- and decachlorocorannulene were shown to make great templates for a variety of penta- and decasubstituted derivatives.

Starting with pentachlorocorannulene, one can obtain pentaalkylcorannulenes (**27**) in a 30-50% overall yield<sup>26</sup> using  $\text{NiCl}_2(\text{dppp})$  and organoaluminum reagents. Pentaarylcorannulenes (**28**) are synthesized in lower yields of 7-48% using  $\text{NiCl}_2(\text{dppp})$  and organozinc reagents (Scheme 1.6). Keinan also showed that **28** can be synthesized from **19** using boronic acids and  $\text{Pd}(0)$  in acceptable yields.<sup>27</sup> Terminal alkynes can be cross coupled using zinc chloride in a 50% yield<sup>28</sup> for trimethylsilyl acetylene, or the alkyne can be converted to the stannane and a Stille coupling using palladium acetate is possible<sup>29</sup> (Scheme 1.7). Similar to the bromocorannulenes, pentachlorocorannulene undergoes nucleophilic aromatic substitution with alkyl and aryl alcohols and thiols.<sup>23</sup> Recently, it has been shown that **19** can also tolerate Grignard reactions.<sup>30</sup>

**Scheme 1.6** Synthesis of pentaalkylcorannulene (**27**) and pentaarylcorynnulene (**28**)



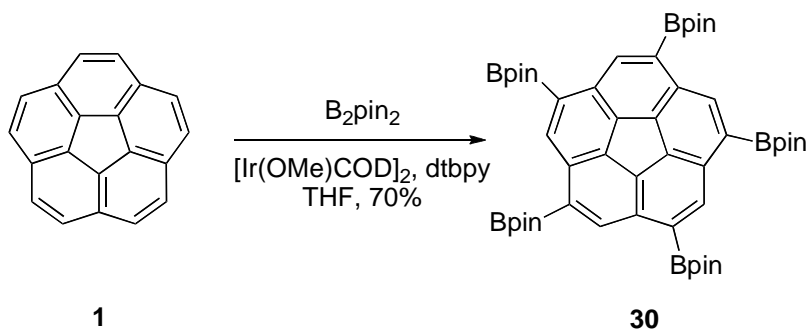
**Scheme 1.7** Synthesis of pentaalkynylcorannulenes from **19**



Methylation of decachlorocorannulene proceeds in a 30% yield<sup>31</sup> through a cross-coupling of **20** with trimethylaluminum and  $\text{NiCl}_2(\text{dppp})$ . One can also replace chlorine with sulfur via nucleophilic aromatic substitution using a series of thiols.<sup>23</sup> Although terminal alkynes do not couple to **20** using zinc chloride, the Stille route for cross-coupling alkynes and **20** does work well.<sup>32</sup>

As mentioned earlier, it was recently shown<sup>25</sup> that monoborylated corannulene (**26**) could be synthesized using iridium-catalyzed conditions with  $\text{B}_2\text{pin}_2$ . Furthermore, increasing the equivalents of catalyst and ligand, one can push the reaction to the pentaborylated corannulene (**30**) (Scheme 1.8). There are a number of advantages to this recent discovery. First, the yield of borylation to chlorination five times on corannulene is 70% to 50% respectively. Second, **30** is better soluble in organic solvents, making purification and subsequent couplings easier. Third, the increased activity of the boronic ester over the chloride paves the way for new coupling reactions. Finally, the remaining 30% of the reaction that is not **30** is often a mixture of borylated material. Conditions to remove these boronic esters and recover corannulene have been developed so corannulene is not lost.

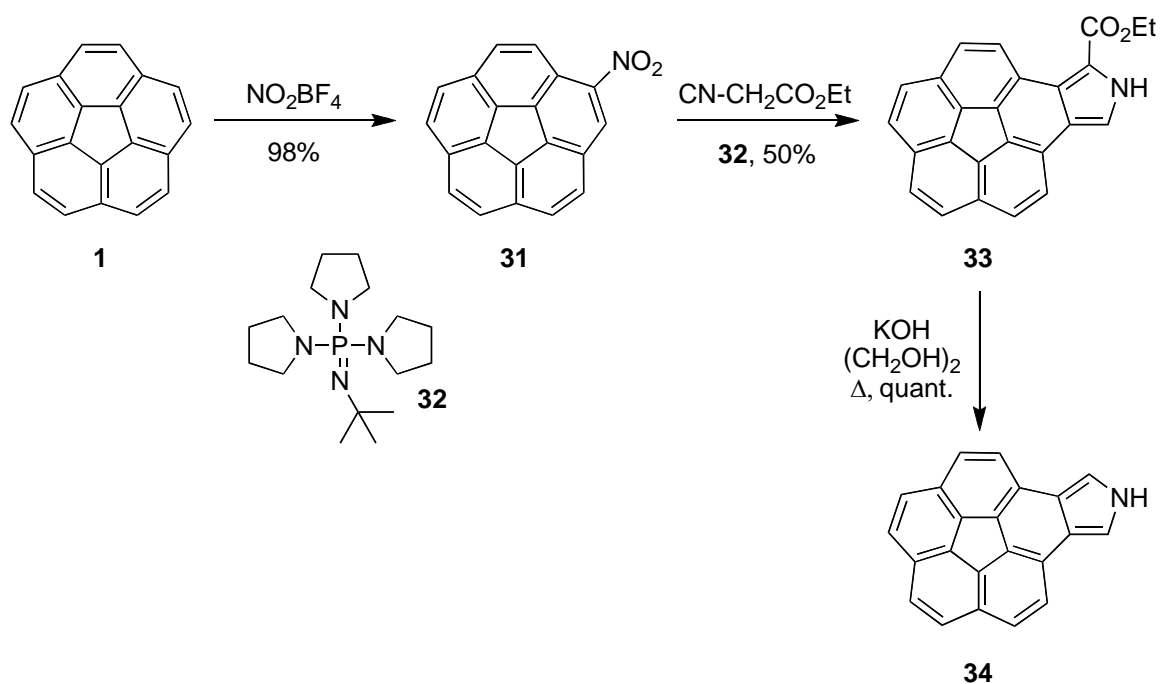
**Scheme 1.8** Synthesis of pentaborylated corannulene (**30**)



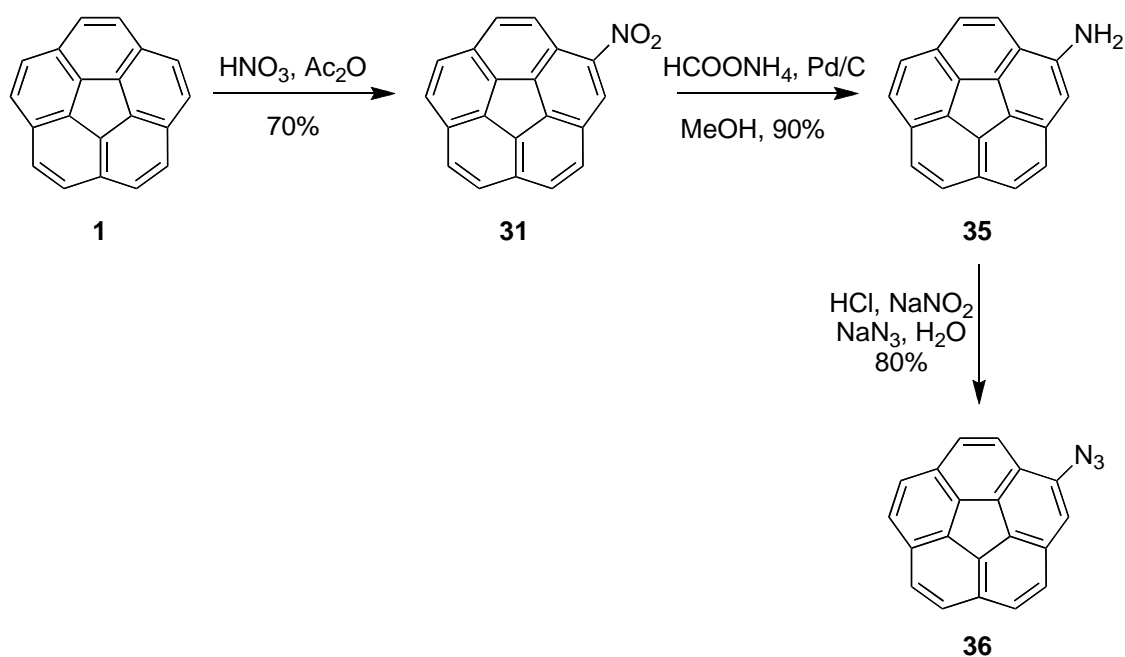
Nitration of corannulene to yield nitrocorannulene (**31**) has been reported under two different conditions. Lash<sup>33</sup> and coworkers first reported the synthesis of nitrocorannulene using nitronium tetrafluoroborate in a 98% crude yield. The nitrocorannulene was then reacted with ethyl isocyanoacetate and a phosphazene base **32** in a Barton-Zard pyrrole condensation to obtain the corannulenopyrrole (**33**), which was saponified and decarboxylated to form **34** (Scheme 1.9). Conditions were also developed in the Siegel group and later reported by Stuparu<sup>34</sup> using nitric acid. Conversion of **31** to aminocorannulene (**35**) was accomplished using ammonium formate and palladium on carbon (Scheme 1.10). The amino group was then treated under acidic conditions to form the diazonium salt, which upon treatment with sodium azide yielded azidocorannulene (**36**).

**Scheme 1.9** Synthesis of corannulenopyrrole (**34**)





**Scheme 1.10.** Synthesis of azidocorannulene (**36**)



As just described, the literature around corannulene abounds with a wide diversity of mono and multi-functionalized derivatives.<sup>35</sup> These derivatives serve as precursors for numerous classes of materials, including graphitic tubes/ caps<sup>36</sup>, liquid crystals<sup>37</sup>, dendrimers<sup>27</sup>, polymers<sup>24,38</sup>, cruciforms<sup>39</sup>, cyclophanes<sup>40</sup> and molecular clefts<sup>41</sup>. Chemists have been looking for ways to utilize corannulene in materials for years. Potential applications and their achievements thus far will be outlined in the following section.

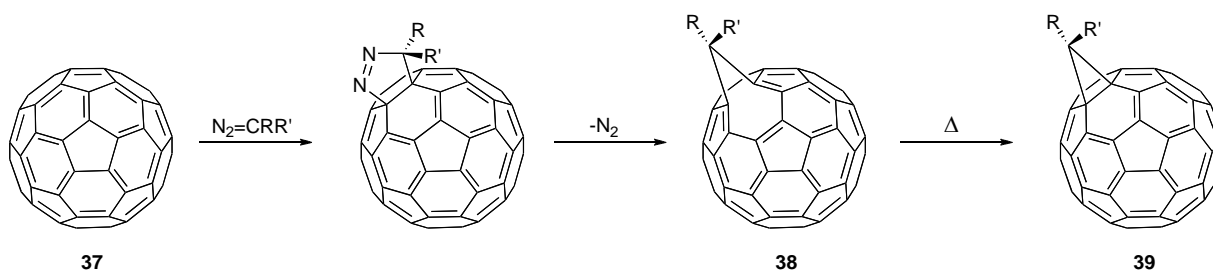
## 1.4 Application of corannulene derivatives

The curvature of **1** and  $C_{60}$  (**37**) give both compounds unique electronic properties that are not observed in planar polyaromatic hydrocarbon (PAH) analogs such as pyrene or naphthalene.<sup>42</sup> The similar properties between these two compounds have been the motivation for corannulene chemists to look to  $C_{60}$  for applications in materials science. Acknowledging the work done by those in the fullerenes field, studying the physicochemical and electronic properties of **37** can stimulate the development of new PAH-based materials with significant potential.

First experimentally observed in 1985, it was believed that buckminsterfullerene,  $C_{60}$ , was a “super aromatic molecule”. This theory was shown<sup>43</sup> to be wrong when X-ray diffraction revealed the molecule to be polyenic in structure and consisting of two types of bonds: those joining two hexagons called 6,6, junctions and those joining a pentagon and a hexagon, coined a 5,6 junction. The unexpected reactivity of  $C_{60}$  is a result of the deviation of its double bonds from planarity<sup>44</sup> with the main driving force of reactivity coming from the relief of strain that the molecule experiences associated with a change in hybridization from  $sp^2$  to  $sp^3$ .

The first to extensively study  $C_{60}$  was the group of Prof. Wudl. They contributed not only to the development of fullerene materials science, but also were the first to show that  $C_{60}$  is an electrophilic reagent that reacts readily with diazo compounds to create a series of functional derivatives called “fulleroids” (**38**) (Scheme 1.11).<sup>45</sup> It was later shown that these fulleroids could be converted to methanofullerenes<sup>46</sup> (**39**), opening the door to derivatives that played an important part in materials science.

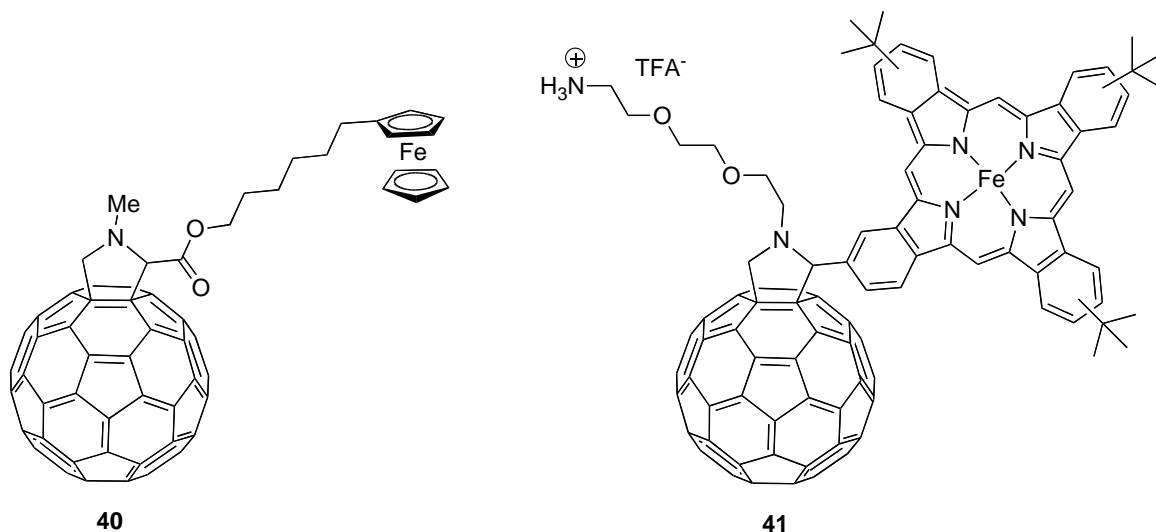
**Scheme 1.11** Synthesis of methanofullerenes by addition of diazo compounds to **37**



An alternative route to **39** is through a [1+2] cycloaddition with carbene<sup>47</sup>. If one instead used nitrenes<sup>48</sup> or silylenes<sup>49</sup>, heteroanalogues of **39** can be obtained. Azafulleroids and azamethanofullerenes can then be converted to the corresponding azafullerenes<sup>50</sup> if desired. Today's literature contains many examples of well-established C<sub>60</sub> functionalization protocols not limited to just carbene addition and [1+2] cycloaddition; other conditions include organometallic addition<sup>51</sup>, cyclopropanation<sup>52</sup>, [2+2]<sup>53</sup>-, [3+2]<sup>54</sup>-, and [4+2]<sup>55</sup> cycloadditions. While developing these reactions have been a crucial component to implementing C<sub>60</sub> derivatives in materials science, they are not the focal point of this thesis and will not be discussed in more detail. Rather, the application of C<sub>60</sub> derivatives and their properties will be outlined.

The use of C<sub>60</sub> derivatives in donor-acceptor systems to transform light into chemical energy has attracted much attention. This phenomenon is efficient in nature because at the photosynthetic reaction center there are many photoactive units coupled together that allows the electron transfer to cascade upon irradiation. With multiple photoactive units, the charge must travel farther and therefore have a longer-lived charge separation state in which the energy is stored. Artificially, chemists have tried to mimic this system by synthesizing dyads consisting of an electron-donor unit and an electron-acceptor unit linked together by a spacer. The high electron-affinity of **37**<sup>56</sup> makes it an excellent candidate as the electron-acceptor component of the dyad. Several dyads using C<sub>60</sub> have been reported to give long charge-separated states (Figure 1.4). Ferrocene-coupled dyad **40** had a measured lifetime of 2.5 μs.<sup>57</sup> The phthalocyanine-linked dyad **41** contains an ethylene glycol chain that aggregates into nanotubules, increasing the charge-separation lifetimes by up to 1 ms.<sup>58</sup> At -150 °C, a 120 s lifetime can be achieved using a zinc chlorin-C<sub>60</sub> dyad.<sup>59</sup>

**Figure 1.4** C<sub>60</sub> dyads possessing long charge-separation states



Fullerenes can also be used in organic solar cells due to their excellent electron-accepting properties. Mixing the fullerene with an electron-donating polymer makes the bulk-heterojunction photovoltaic cells. Due to the sparing solubility of **37**, it cannot be used directly in organic solar cells. Instead, [6,6]-phenyl-C<sub>61</sub>-butyric acid methyl ester (PCBM)<sup>60</sup> is the most widely used derivative in plastic solar cells. The most common polymers used for electron donation to fullerenes are poly(3-hexylthiophene) (P3HT)<sup>61</sup>, or copolymers containing thiophene units. Depending on the blend of the solar cell, different ranges of high power conversion efficiency can be achieved. Currently, efficient cells range from 5-7.5%. PCBM is also one of the most studied fullerene derivatives for organic field-effect transistors (OFETs). OFETs are prepared by growing PCBM on top of organic dielectric divinyltetramethyldisiloxane-bis(benzocyclobutene).<sup>62</sup> Similar to organic solar cells, solubility again plays a role in the success of OFETs.<sup>63</sup>

Attaching an amphiphilic chain to a fullerene can dramatically increase the solubility of the compound to the point that it is partially or totally soluble in water. When deposited on the surface of the water, these compounds may form monolayers at the air-water interface called Langmuir films. Depending on the surface pressure of the system upon compression, the monolayers can then be transferred to a solid support in a controlled manner, forming a Langmuir-Blodgett film. Dendrimers<sup>64</sup>, polyadducts<sup>65</sup>, supramolecular<sup>66</sup> and donor-acceptor systems<sup>67</sup> containing fullerenes have all been studied to determine the stability of their monolayers and multilayers.

Just as fullerenes have been used in donor-acceptor systems, OLEDs, OFETs and LB films, one could imagine replacing C<sub>60</sub> with a corannulene derivative. The high electron-affinity of **37** that made it work well as a component of dyads has been shown to be similar to dibenzo[*g,m*]corannulene,  $1.20 \pm 0.20$  and  $1.00 \pm 0.20$  eV respectively.<sup>68</sup> The first reduction of deca(phenylthio)corannulene is -1.22 volts<sup>62c</sup>, close to the reported<sup>23</sup> value of C<sub>60</sub>, -1.06 volts. The controlled pattern and substitution of corannulene should allow for more variation in the structure of the molecule on the water surface. The overall improved solubility of corannulene versus C<sub>60</sub> in organic solvents would leave one to believe that if the properties of the corannulene derivatives can be tuned, this class of molecules could play an important role in these materials.

Apart from hypothetical applications using corannulene derivatives to replace C<sub>60</sub> in OLEDs or OFETS, chemists have already begun to show the importance of **1** in other applications. One of the most remarkable recent accomplishments was the use of a pentasubstituted corannulene derivative as a template for a nanotube cap.<sup>69</sup> This was the first time that a synthetically designed and controlled end piece to a nanotube was synthesized. The ability to control the chirality, diameter and length of a nanotube is important in tuning its electronic properties. There are three types<sup>70</sup> of nanotubes: armchair, zig-zag and chiral (Figure 1.5). All armchair conformations conduct electricity. The pioneering work of Scott sets a foundation upon which other chemists hope to build. The next goals in this project are to develop conditions for a solution-phase synthesis that would be more tolerant of functional group. Also, one could imagine that with the right precursor and set of conditions, the nanotube could be extended during its ring closure after a cascade of reactions.

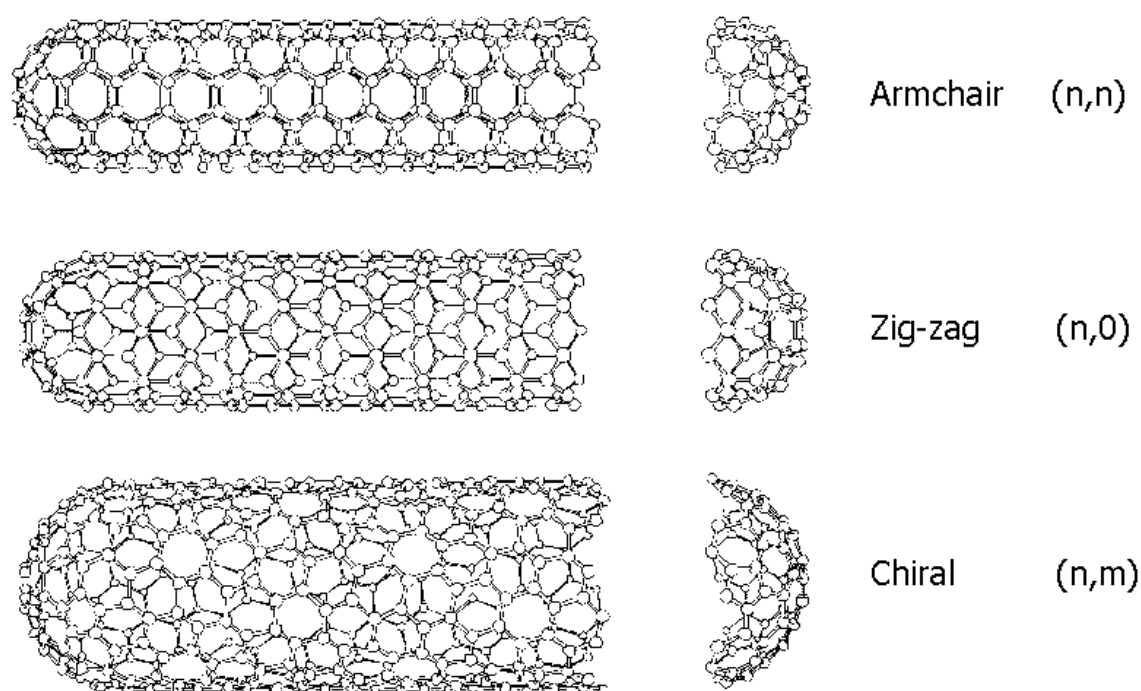


**Figure 1.5** Three type of nanotubes<sup>71</sup>

Another recent discovery was the use of decasubstituted corannulenes as liquid crystalline materials.<sup>72</sup> The bowl shape of **1** results in differences in the electron densities on its convex and concave faces, a property not seen in planar PAH.<sup>73</sup> This difference produces a dipole moment that one might expect to display ferroelectric properties. However, the ease of bowl inversion for the corannulene skeleton,  $2 \times 10^5 \text{ s}^{-1}$  at room temperature<sup>74</sup> makes assembly of a one-dimensional columnar array difficult. The authors successfully obtained hexagonal columnar liquid crystalline assemblies of amide containing corannulene derivatives. This liquid crystal assembly responded to an applied electric field and gave rise to a homeotropic alignment of the hexagonal columns with respect to the electrode surface.

Corannulene derivatives have also found their way into potential biological applications. Recent work in this group<sup>30</sup> has shown that iron-catalyzed aryl-alkyl cross couplings with pentachlorocorannulene can be accomplished with good yields (56-69%). These derivatives were further functionalized to potential building blocks for supramolecular chemistry, dendrimer chemistry, liquid crystals or optoelectronic materials. Additionally, pentapodal  $\omega$ -functional corannulene derivatives believed to be

suitable templates for protein folding mimics or nucleic acid conjugate assemblies were synthesized (Figure 1.6).

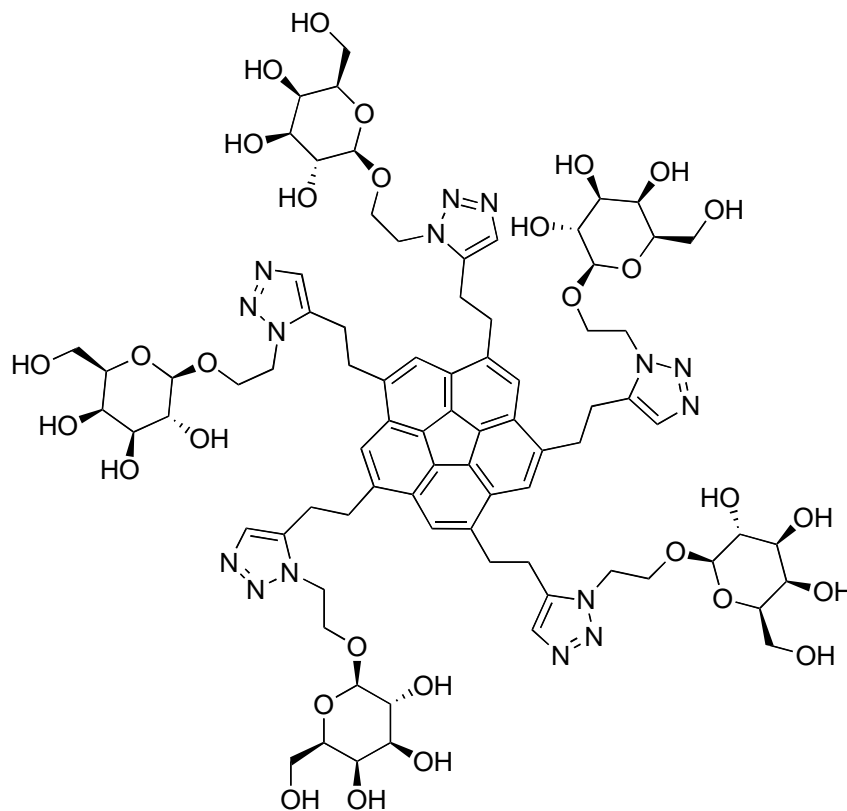


**Figure 1.6** Corannulene derivative synthesized using a new iron-catalyzed method with potential biological applications.

Despite the ever-growing academic interest in **1**, the need for a substantial synthetic commitment to prepare **1** and derivatives is the Achilles heel to broad materials and engineering applications. Thus, a “sustainable” synthesis on scale would go a long way toward allowing corannulene to grow beyond being an esoteric molecule, of academic interest, to an industrially interesting prospect, with direct application in materials chemistry.

---

<sup>1</sup> Harvey, R. G., *Polycyclic Aromatic Hydrocarbons*. Wiley-VCH: New York, 1997.

- 
- <sup>2</sup> Simoneit, B. R. T. *Hand. Environ. Chem.* **1998**, 3, 175.
- <sup>3</sup> (a) Grimmer, G., *Environmental Carcinogens: Polycyclic Aromatic Hydrocarbons*. CRC Press: Boca Raton, FL, 1983. (b) Schoket, B. *Mutat. Res.* **1999**, 424, 143.
- <sup>4</sup> (a) Becker, L. *Astrophysics and Space Science Library*, **1999**, 236, 377. (b) Gutmann, I.; Cyvin, S. J., *Introduction to the Theory of Benzenoid Hydrocarbons*. Springer-Verlag: Berlin, 1989. (c) Heymann, D. *Astrophys. J.* **1997**, 489, L111.
- <sup>5</sup> Harvey, R.G., *Polycyclic Aromatic Hydrocarbons: Chemistry and Carcinogenicity*. 1991.
- <sup>6</sup> (a) Amin, S.; Krzeminski, J.; Rivenson, A.; Kurtzke, C.; Hecht, S. S.; El-Bayoumy, K. *Carcinogenesis* **1995**, 16, 1971. (b) DiGiovanni, J.; Diamond, L.; Harvey, R. G.; Slaga, T. J. *Carcinogenesis* **1983**, 4, 403. (c) Levin, W.; Chang, R. L.; Wood, A. W.; Thakker, D. R.; Yagi, H.; Jerina, D. M.; Conney, A. H. *Cancer Res.* **1986**, 46, 2257. (d) Wu, M.; Yan, S.; Patel, D. J.; Geacintov, N. E.; Broyde, S. *Chem. Res. Toxicol.* **2001**, 14, 1629.
- <sup>7</sup> Kroto, H. W.; Heath, J. R.; O'Brien, S. C.; Curl, R. F.; Smalley, R. E. *Nature* **1985**, 318, 162.
- <sup>8</sup> Lu, X.; Chen, Z. *Chem. Rev.* **2005**, 105, 3643.
- <sup>9</sup> Kroto, H. W. *Pure Appl. Chem.* **1990**, 62, 407.
- <sup>10</sup> Ansems, R. B. M.; Scott, L. T. *J. Am. Chem. Soc.* **2000**, 122, 2719.
- <sup>11</sup> Barth, W. E.; Lawton, R. G. *J. Am. Chem. Soc.* **1966**, 88, 380.
- <sup>12</sup> Sieglitz, A.; Schidlo, W. *Chem. Ber.* **1963**, 96, 1098.
- <sup>13</sup> Hanson, J. C.; Nordman, C. E. *Acta Crystallogr., Sect. B* **1976**, B32, 1147.
- <sup>14</sup> (a) Craig, J. T.; Robins, M. D. W. *Aust. J. Chem.* **1968**, 21, 2237. (b) Davy, J. R.; Iskander, M. N.; Reiss, J. A. *Tetrahedron Lett.* **1978**, 42, 4085.
- <sup>15</sup> Cheng, P.-C. Ph.D. Dissertation, Boston College: Boston, MA, 1996; p212.
- <sup>16</sup> Scott, L. T. *Pure Appl. Chem.* **1996**, 68, 291.
- <sup>17</sup> Baldrige, K. K.; Siegel, J. S. *Theor. Chem. Account*, **2008**, 120, 95.
- <sup>18</sup> Ballester, M.; Castaner, J. *J. Am. Chem. Soc.* **1960**, 82, 4254.
- <sup>19</sup> Seiders, T. J.; Elliott, E. L.; Grube, G. H.; Siegel, J. S. *J. Am. Chem. Soc.* **1999**, 121, 7804.
- <sup>20</sup> Sygula, A.; Sygula, R.; Fronczek, F. R.; Rabideau, P. W. *J. Org. Chem.* **2002**, 67, 6487.
- <sup>21</sup> Jones, C. S.; Elliott, E.; Siegel, J. S. *Synlett* **2004**, 7, 187.



- 
- <sup>22</sup> Eisenberg, D.; Filatov, A. S.; Jackson, E. A.; Rabinovitz, M.; Petrukhina, M. A.; Scott, L. T.; Shenar, R. *J. Org. Chem.* **2008**, *73*, 6073.
- <sup>23</sup> Steinauer, A.; Butterfield, A.; Linden, A.; Baldrige, K.; Siegel, J. S. *Angew. Chem. Int. Ed.* **2012** *submitted*.
- <sup>24</sup> Quimby, J. Ph.D. Dissertation, Boston College: Boston, MA, 2011.
- <sup>25</sup> Eliseeva, M. N.; Scott, L. T. *J. Am. Chem. Soc.* **2012** *submitted*.
- <sup>26</sup> Buncel, E.; Crampton, M. R.; Strauss, T. J.; Terrier, F., *Electron Deficient Aromatic and Heteroaromatic-Base Interactions*; Elsevier: New York, 1984.
- <sup>27</sup> Pappo, D.; Mejuch, T.; Reany, O.; Solel, E.; Gurram, M.; Keinan, E. *Org. Lett.* **2009**, *11*, 1063.
- <sup>28</sup> Sygula, A.; Rabideau, P. W. *J. Am. Chem. Soc.* **2000**, *122*, 6323.
- <sup>29</sup> Hayama, T.; Wu, Y.-T.; Linden, A. L.; Baldrige, K. K.; Siegel, J. S. *J. Am. Chem. Soc.* **2007**, *129*, 12612.
- <sup>30</sup> Mattarella, M.; Siegel, J. S. *Org. Biomol. Chem.* **2012**, *10*, 5799.
- <sup>31</sup> Seiders, T. J.; Baldrige, K. K.; Elliott, E. L.; Grube, G. H.; Siegel, J. S. *J. Am. Chem. Soc.*, **1999**, *121*, 7439.
- <sup>32</sup> Bancu, M.; Rai, A. K.; Cheng, P.-C.; Gilardi, R. D.; Scott, L. T. *Synlett*, **2004**, 173.
- <sup>33</sup> Boedigheimer, H.; Ferrence, G. M.; Lash, T. D. *J. Org. Chem.* **2010**, *75*, 2518.
- <sup>34</sup> Stuparu, M. C. *Tetrahedron* **2012**, *68*, 3527.
- <sup>35</sup> (a) Wu, Y.-T.; Maag, R.; Linden, A.; Baldrige, K. K.; Siegel, J. S. *J. Am. Chem. Soc.* **2008**, *130*, 10729. (b) Seiders, T. J.; Baldrige, K. K.; Grube, G. H.; Siegel, J. S. *J. Am. Chem. Soc.* **2001**, *123*, 517. (c) Reisch, H. A.; Bratcher, M. S.; Scott, L. T. *Org. Lett.* **2000**, *2*, 1427.
- <sup>36</sup> Scanlon, L. G.; Balbuena, P. B.; Zhang, Y.; Sandi, G.; Back, C. K.; Feld, W. A.; Mack, J.; Rottmayer, M. A.; Riepenhoff, J. L. *J. Phys. Chem. B* **2006**, *110*, 7688.
- <sup>37</sup> Miyajima, D.; Tashiro, K.; Araoka, F.; Takezoe, H.; Kim., J.; Kato, K.; Takata, M.; Aida, T. *J. Am. Chem. Soc.* **2009**, *131*, 44.
- <sup>38</sup> Stuparu, M. C. *Chimia*, **2011**, *65*, 799.
- <sup>39</sup> Sygula, A.; Karlen, S. D.; Sygula, R.; Rabideau, P. W. *Org. Lett.* **2002**, *4*, 3135.

- 
- <sup>40</sup> (a) Seiders, T. J.; Baldrige, K. K.; Siegel, J. S. *J. Am. Chem. Soc.* **1996**, *118*, 2754. (b) Seiders, T. J.; Baldrige, K. K.; Siegel, J. S. *Tetrahedron* **2001**, *57*, 3737.
- <sup>41</sup> (a) Sygula, A.; Fronczek, F. R.; Sygula, R.; Rabideau, P. W. *J. Am. Chem. Soc.* **2007**, *129*, 3842. (b) Kobryn, L.; Henry, W. P.; Fronczek, F. R.; Sygula, R.; Sygula, A. *Tetrahedron Lett.* **2009**, *50*, 7124.
- <sup>42</sup> (a) Hirsch, A.; Brettreich, M., *Fullerenes: Chemistry and Reactions*; Wiley-VCH: Weinheim, 2005. (b) Wu, Y.-T.; Siegel, J. S. *Chem. Rev.* **2006**, *106*, 4843. (c) Baldrige, K. K.; Hardcastle, K. I.; Seiders, T. J.; Siegel, J. S. *Org. Biomol. Chem.* **2010**, *8*, 53.
- <sup>43</sup> Hawkings, J. M.; Meyer, A.; Lewis, T. A.; Loren, S.; Hollander, F. J. *Science* **1991**, *252*, 312.
- <sup>44</sup> (a) Haddon, R. C. *Science* **1993**, *261*, 1545. (b) Haddon, R. C. *Acc. Chem. Res.* **1992**, *25*, 127.
- <sup>45</sup> (a) Wudl, F. *Acc. Chem. Res.* **1992**, *25*, 157. (b) Diederich, F.; Isaacs L.; Philp D. *Chem. Soc. Rev.* **1994**, *23*, 243. (c) Suzuki, T.; Li, Q.; Khemani, K.C.; Wudl, F.; Almarsson, Ö. *Science* **1991**, *254*, 1186.
- <sup>46</sup> Suzuki, T.; Li, Q.; Khemani, K.C.; Wudl, F.; Almarsson, Ö. *Science* **1991**, *254*, 1186.
- <sup>47</sup> (a) Vasella, A.; Uhlmann, P.; Waldruff, C. A.; Diederich, F.; Yhilgen, C. *Angew. Chem. Int. Ed.* **1992**, *92*, 1388. (b) Tsuda, M.; Ishida, T.; Nogami, A.; Kurono, S.; Ohashi, M. *Tetrahedron Lett.* **1993**, *34*, 2335. (c) Isaacs L.; Diederich, F. *Helv. Chim. Acta*, **1993**, *76*, 2454. (d) Win, W.; Kao, M.; Eiermann, M.; McNamara, J. J.; Wudl, F.; Pole, D. L.; Kassam, K.; Warkentin, J. *J. Org. Chem.* **1994**, *59*, 5871.
- <sup>48</sup> (a) Ishida, A.; Tanaka, K.; Nogami, A. *Chem. Lett.* **1994**, 56. (b) Schick, G.; Hirsch, A.; Mauser H.; Clark, T. *Chem. Eur. J.* **1996**, *2*, 935. (c) Prato, M.; Lucchini, V.; Maggini, M.; Stimpfl, E.; Scorrano, G.; Eiermann, M.; Suzuki, T.; Wudl, F. *J. Am. Chem. Soc.* **1993**, *115*, 8479. (d) Eiermann, M.; Wudl, F.; Prato, M.; Maggini, M. *J. Am. Chem. Soc.* **1994**, *116*, 8364. (e) Janssen, R. A. J.; Hummelen, J. C.; Wudl, F. *J. Am. Chem. Soc.* **1995**, *117*, 544.
- <sup>49</sup> Akasaka, T.; Komatsu, K.; Murata, Y.; Shiro, M. *J. Am. Chem. Soc.* **1997**, *115*, 1605.
- <sup>50</sup> (a) Prato, M.; Li, Q. C.; Wudl, F.; Lucchini, V. *J. Am. Chem. Soc.* **1993**, *115*, 1148. (b) Grosser, T.; Prato, M.; Lucchini, V.; Hirsch, A.; Wudl, F. *Angew. Chem. Int. Ed.* **1995**, *34*, 1343.
- <sup>51</sup> (a) Zhou, S.; Burger, C.; Chu, B.; Sawamura, M.; Nagahama, N.; Toganoh, M.; Hackler, U. E.; Isobe, H.; Nakamura, E. *Science* **2001**, *291*, 1944. (b) Sawamura, M.; Kawai, K.; Matsuo, Y.; Kanie, K.; Kato, T.; Nakamura, E. *Nature* **2002**, *419*, 702. (c) Matsuo, Y.;

---

Tahara, K.; Sawamura, M.; Nakamura, E. *J. Am. Chem. Soc.* **2004**, *126*, 8725. (d) Zhong, Y.-T.; Matsuo, Y.; Nakamura, E. *J. Am. Chem. Soc.* **2007**, *129*, 3052.

<sup>52</sup> (a) Nierengarten, J.-F.; Gramlich, V.; Cardullo, F.; Diederich, F. *Angew. Chem. Int. Ed.* **1996**, *35*, 2101. (b) Camps, X.; Hirsch, A. *J. Chem. Soc., Perkin Trans. 1* **1997**, *11*, 1595.

<sup>53</sup> (a) Liou, K.-F.; Cheng, C.-H. *J. Chem. Soc., Chem. Commun.* **1995**, 2473. (b) Zhang, X.; Fan, A.; Foote, C. S. *J. Org. Chem.* **1996**, *61*, 5456. (c) Zhang, X.; Foote, C. S. *J. Am. Chem. Soc.* **1995**, *117*, 4271. (d) Zhang, X.; Romero, A.; Foote, C. S. *J. Am. Chem. Soc.* **1993**, *115*, 11024.

<sup>54</sup> (a) Maggini, M.; Scorrano, G.; Prato, M. *J. Am. Chem. Soc.*, **1993**, *115*, 9798. (b) Prato, M.; Maggini, M. *Acc. Chem. Res.* **1998**, *31*, 519. (c) Tagmatarchis, N.; Prato, M. *Synlett.* **2003**, 768.

<sup>55</sup> (a) Ohno, M.; Azuma, T.; Kojima, S.; Shirakawa Y.; Eguchi, S. *Tetrahedron* **1996**, *52*, 4983. (b) Mori, A.; Takamori, Y.; Takeshita, H. *Chem. Lett.* **1997**, 395. (c) Ohno, M.; Shirakawa, Y.; Eguchi, S. *Synthesis*, **1998**, 1812. (d) Mori, S.; Karita, T.; Komatsu, K.; Sugita, N.; Wan, T. *Synth. Commun.* **1997**, *27*, 1475. (e) Krautler, B.; Maynollo, J. *Tetrahedron* **1996**, *52*, 5033. (f) Krautler, B.; Maynollo, J. *Angew. Chem. Int. Ed.* **1995**, *34*, 87.

<sup>56</sup> (a) Echegoyen, L.; Echegoyen, L. E. *Acc. Chem. Res.* **1998**, *31*, 593. (b) Arias, F.; Echegoyen, L.; Wilson, S. R.; Lu, Q. *J. Am. Chem. Soc.* **1995**, *117*, 1422. (c) Echegoyen, L.; Diederich, F.; Echegoyen, L. E., *Electrochemistry of Fullerenes, in Fullerenes: Chemistry, Physics, and Technology*, Wiley: New York, 2000. (d) Guldi, D. M.; Prato, M. *Acc. Chem. Res.* **2000**, *33*, 695.

<sup>57</sup> Guldi, D. M.; Maggini, M.; Scorrano, G.; Prato, M. *J. Am. Chem. Soc.* **1997**, *119*, 974.

<sup>58</sup> Guldi, D. M.; Gouloumis, A.; Vazquez, P.; Torres, T.; Georgakilas, V.; Prato, M. *J. Am. Chem. Soc.* **2005**, *127*, 5811.

<sup>59</sup> Ohkubo, K.; Kotani, H.; Shao, J.; Ou, Z.; Kadish, K. M.; LiPandey, R. K. G.; Fujitsuka, M.; Ito, O.; Imahori, H.; Fukuzumi, S. *Angew. Chem. Int. Ed.* **2004**, *43*, 853.

<sup>60</sup> (a) Yang, C.; Cho, S.; Heeger, A. J.; Wudl, F. *Angew. Chem. Int. Ed.* **2009**, *48*, 1592.

<sup>61</sup> (a) Guenes, S.; Neugebauer, H.; Sariciftci, N. S. *Chem. Rev.* **2007**, *107*, 1324. (b) Shaheen, S.; Brabec, C. J.; Sariciftci, N. S.; Padinger, F.; Fromherz, T.; Hummelen, J. C. *Appl. Phys. Lett.* **2001**, *78*, 841. (c) Mozer, A.; Sariciftci, N. S. *Chem. Phys. Lett.* **2004**, *389*, 438.

<sup>62</sup> (a) Matt, G. J.; Singh, B.; Sariciftci, N. S.; Ramil, A. M.; Sitter, H. *Appl. Phys. Lett.* **2006**, *88*, 263516. (b) Kwiatkowski, J. J.; Frost, J. M.; Nelson, J. *Nano Lett.* **2009**, *9*, 1085.

- 
- <sup>63</sup> (a) Anthopoulos, T. D.; de Leeuw, D. M.; Cantatore, E.; Setayesh, S.; Meijer, C. J.; Tanase, C.; Hummelen, J. C.; Blom, P. M. W. *Appl. Phys. Lett.* **2004**, 85, 4205. (b) Anthopoulos, T. D.; de Leeuw, D. M.; Cantatore, E.; van't Hof, P.; Alma, J.; Hummelen, J. C. *J. Appl. Phys.* **2005**, 98, 54. (c) Anthopoulos, T. D.; Kooistra, F. B.; Wondergem, H. J.; Kronholm, D.; Hummelen, J. C.; de Leeuw, D. M. *Adv. Mater.* **2006**, 18, 1679.
- <sup>64</sup> (a) M. Cochet, M.; Maser, W. K.; Benito, A. M.; Callejas, M. A.; Martinez, M. T.; Benoit, J. M.; Schreiber, J.; Chauvet, O. *Chem. Commun.* **2001**, 1450. (b) Zengin, H.; Zhou, W.; Jin, J.; Czerw, R.; Smith, D. W.; Echegoyen, L.; Carroll, D. L.; Foulger, S. H.; Ballato, J. *Adv. Mater.* **2002**, 14, 1480. (c) Hughes, M.; Chen, G. Z.; Shaffer, M. S. P.; Fray, D. J.; Windle, A. H. *Compos. Sci. Technol.* **2004**, 64, 2325.
- <sup>65</sup> (a) O'Connel, R. J.; Boul, P. J.; Ericson, L. M.; Huffman, C.; Wang, Y.; Haroz, E.; Kuper, C.; Tour, J.; Ausman, K. D.; Smalley, R. E.; *Chem. Phys. Lett.* **2001**, 342, 265. (b) Ago, H.; Petritsch, K.; Shaffer, M. S. P.; Windle, A. H.; Friend, R. H. *Adv. Mater.* **1999**, 11, 1281. (c) Ago, H.; Shaffer, M. S. P.; Ginger, D. S.; Windle, A. H.; Friend, R. H. *Phys. Rev. B: Condens. Matter Mater. Phys.* **2000**, 61, 2286. (d) Gong, X.; Liu, J.; Baskaran, S.; Voise, R. D.; Young, J. S. *Chem. Mater.* **2000**, 12, 1049.
- <sup>66</sup> Jin, Z.; Pramoda, K. P.; Goh, S. H.; Xu, G. *Mater. Res. Bull.* **2002**, 37, 271.
- <sup>67</sup> (a) Petrov, P.; Stassin, F.; Pagnouille, C.; Jernome, R.; *Chem. Commun.* **2003**, 2904. (b) Lou, X.; Daussin, R.; Cuenot, S.; Duwez, A.-S.; Pagnouille, C.; Detrembleur, C.; Bailly, C.; Jernome, R. *Chem. Mater.* **2004**, 16, 4005. (c) Wu, X.; Shi, G. *J. Mater. Chem.* **2005**, 15, 1833.
- <sup>68</sup> Chen, G.; Shuguang, M.; Cooks, R. G.; Bronstein, H. E.; Best, M. D.; Scott, L. T. *J. Mass Spectrom.* **1997**, 32, 1305.
- <sup>69</sup> Scott, L. T.; Jackson, E. A.; Zhang, Q.; Steinberg, B. D.; Bancu, M.; Li B. *J. Am. Chem. Soc.* **2012**, 134, 107.
- <sup>70</sup> Ajayan, P. M. *Chem. Rev.* **1999**, 99, 1787.
- <sup>71</sup> Saito, R. *Appl. Phys. Lett.* **1992**, 60, 2204.
- <sup>72</sup> Miyajima, D.; Tashiro, K.; Araoka, F.; Takezoe, H.; Kim, J.; Kato, K.; Takata, M.; Aida, T. *J. Am. Chem. Soc.* **2009**, 131, 44.
- <sup>73</sup> Scott, L. T.; Hashemi, M. M.; Bratcher, M. S. *J. Am. Chem. Soc.* **1992**, 114, 1920.
- <sup>74</sup> Lovas, F. J.; McMahon, R. J.; Grabow, J.-U.; Schnell, M.; Mack, J.; Scott, L. T.; Kuczkowski, R. L. *J. Am. Chem. Soc.* **2005**, 127, 4345.

## Chapter 2

### *Kilogram-scale synthesis of corannulene<sup>1</sup>*

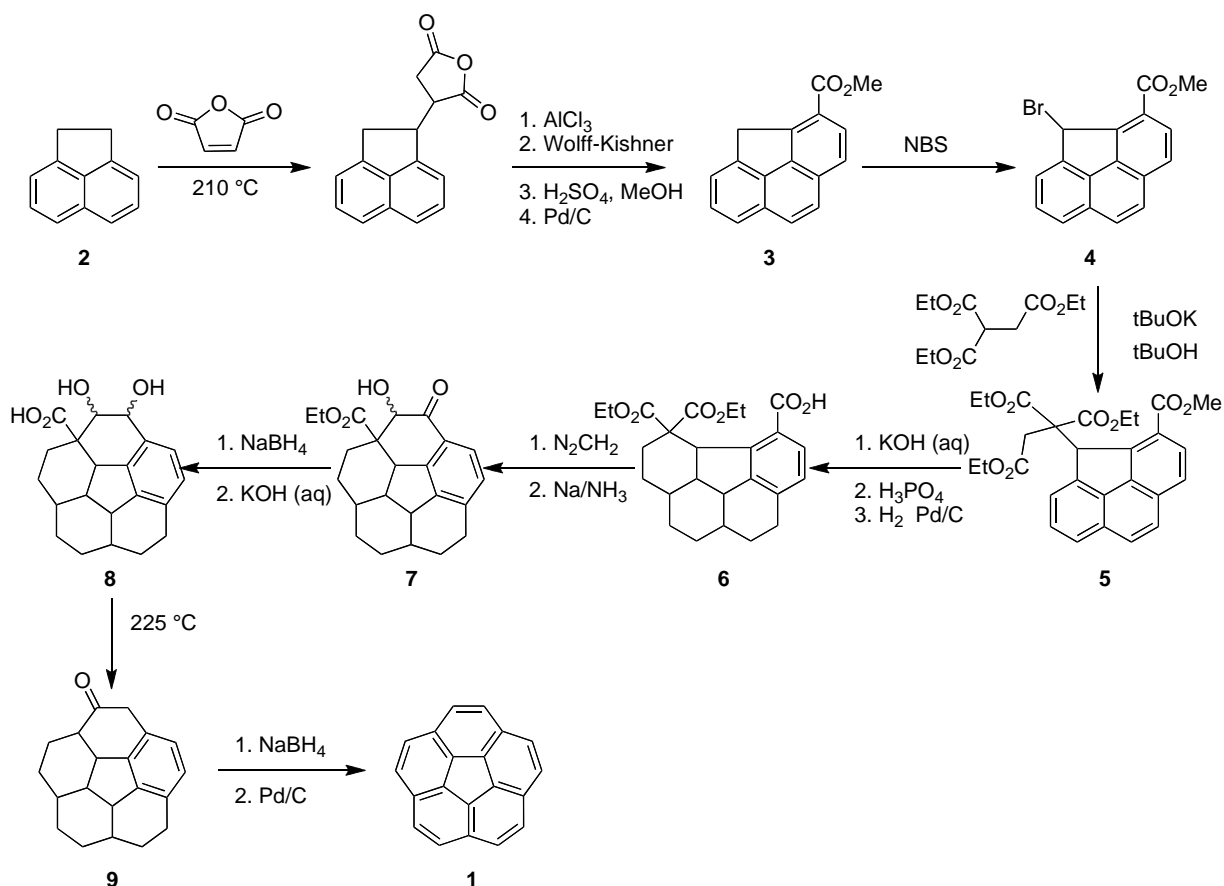
#### 2.1 Introduction

As outlined in Section 1.2, Lawton and Barth's synthesis of corannulene, although pioneering, was also daunting. The low yields and multiple steps required a new synthetic route. This chapter will discuss in detail the development of the corannulene synthesis from the initial synthesis up until the beginning of the optimization for kilogram-scale production. Next, the expected problems of taking the gram-scale synthesis to kilogram-scale will be outlined. Finally, the results of the production will be presented, with a reagent comparison before and after optimization.

#### 2.2 Historical development

The first synthesis of Lawton and Barth (Scheme 2.1) consisted of 17 steps and resulted in a less than 1% yield overall. If one wanted to obtain a kilogram of material, they would need to reproduce this reaction  $10^5$ - $10^6$  times. Clearly, that was not feasible nor was it the intention of chemists at that time. Their goal was to find a shorter synthesis with higher yields to obtain more material and explore the reactivity.

**Scheme 2.1** First synthesis of corannulene



From 1970 to 1990, several groups attempted to find these alternative routes to corannulene but ultimately failed. A basic Friedel-Crafts strategy<sup>2</sup> looked attractive but went fallow. Creation of naphthyl-phenyl cyclophanes as precursors to corannulene also never bore fruit.<sup>3</sup> In the glory of hindsight and physical organic chemical analysis, both these unsuccessful approaches underestimated the strain needed to reach the transition state en route to the final closure, and overestimated the aromatic stabilization benefit one might obtain from creating the corannulene unit. Indeed, higher energy reaction conditions or higher energy synthetic precursors would be needed to bring a new synthesis to fruition.

In the early 1990s two new synthetic strategies to **1** appeared. Both chose a bilaterally symmetric retrosynthetic strategy over the ring-by-ring methods; however, these retrosynthetic approaches differed in their choice of which bond type of **1** to disconnect: (a) flanking or (b) rim (Figure 2.1). The former leads to a relatively low energy and unstrained 7,10-disubstituted fluoranthene, in contrast to the latter, which foresees a sterically crowded 1,6,7,10-tetrasubstituted fluoranthene. Disconnection (a) had been an

unsuccessful strategy when coupled to Friedel-Crafts chemistry in the forward direction. Disconnection (b) resembles the ultimate stage of the classic Lawton-and-Barth strategy, wherein acyloin chemistry enabled a successful synthesis.

The failure of the disconnection (a) when coupled to Friedel-Crafts chemistry can be seen in the additional strain needed to obtain the transition state to attack on the pi face. The molecule must fold to a deeper-bowled and higher-strained conformation before bond formation can occur. Also the reaction conditions are prone to rearrangements that would allow for back reaction to ring-opened products. Disconnection (b) requires a higher energy synthetic precursor; but, in combination with a reductive, radical, or insertion reaction, wherein the transition state to carbon-carbon bond formation can be reached by more or less linear least-motion path of the proximal units, this approach could be much more tractable. The experience of Lawton and Barth with the acyloin reaction empirically supports this analysis.

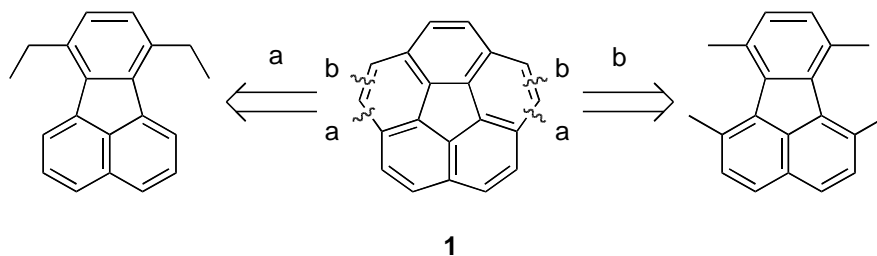


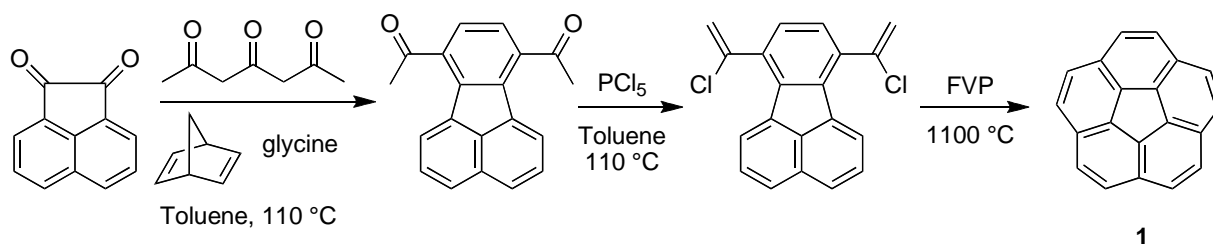
**Figure 2.1** Different retrosynthetic approaches to **1**. Disconnection between the flanking (a) or rim (b) carbons of **1** results in two different fluoranthene precursors.

Larry Scott's and our laboratories independently developed the two pathways simultaneously. The first strategy, from Scott and coworkers,<sup>4</sup> applied high-temperature, gas-phase flash vacuum pyrolysis (FVP) to achieve high reaction energies for short residence times. The idea that this could result in effective ring closure came from the pioneering work of R. F. C. Brown, in which he showed that under FVP conditions acetylenes could isomerize and react as vinylenes.<sup>5</sup> The high energy of the reaction conditions opened a reaction path not available in conventional chemical methods.

The optimized version of the procedure sets out from the chlorovinyl compound (Scheme 2.2), instead of the acetylene originally foreseen from the Brown chemistry. Corannulene was produced on gram-scale in a 20-25% yield starting with commercially

available acenaphthenequinone. Although this route succeeded in a small number of steps, it suffered for the following reasons: only modest yields were obtained, there was essentially no functional group tolerance, there were limitations to scale-up, and extremely high temperatures offered the possibility of undesired thermal rearrangements, increasing the quantity of side products.

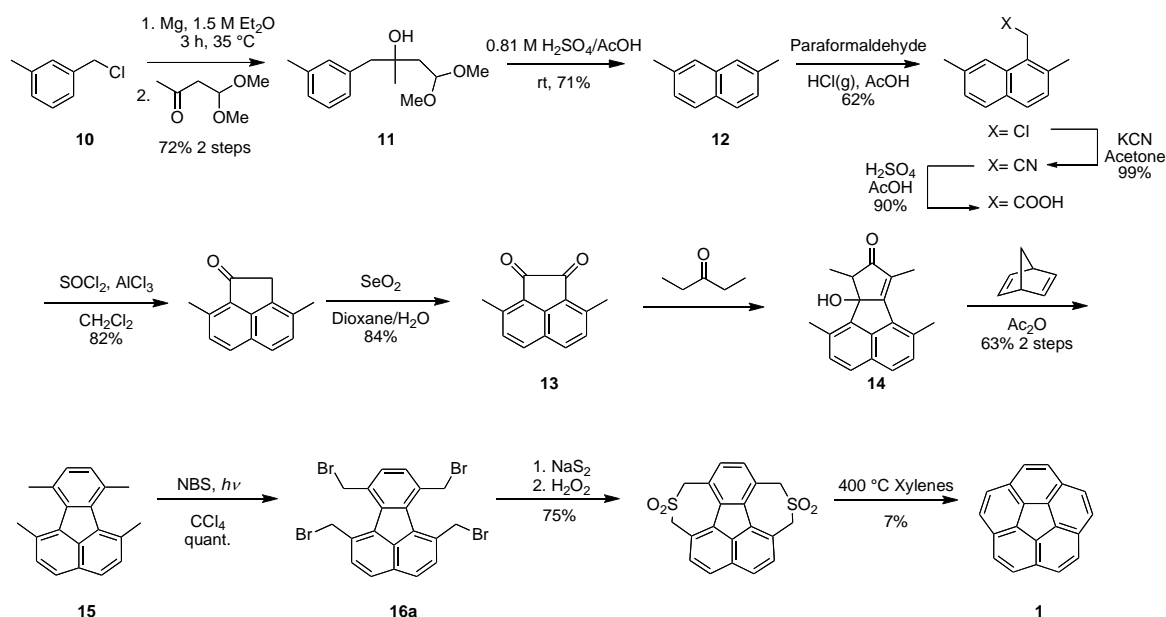
**Scheme 2.2.** Flash vacuum pyrolysis method developed by Scott



The second strategy, pioneered in our group, used milder and more selective solution phase chemistry to achieve the synthesis of corannulene. The initial solution phase synthesis (Scheme 2.3) follows the precedent of Buu-Hoi set back in 1942.<sup>6</sup> It starts by preparing 2,7-dimethylnaphthalene (**12**) by the addition of the Grignard of (**10**) to 4,4-dimethoxy-2-butanone followed by acidic workup leading to deprotection and ring closure.<sup>7</sup> Chloromethylation of **12** occurs regioselectively at the 1 position and homologation with KCN and hydrolysis in sulfuric acid/ water leads to the acetic acid derivative. Formation of the acid chloride and Friedel-Crafts ring closure produces 2,7-dimethylacenaphthone, which is converted to the analogous acenaphthaquinone (**13**) by selenium dioxide oxidation.<sup>8</sup> The crossed-aldol condensation of **5** with 3-pentanone and subsequent Diels-Alder addition yielded 1,6,7,10-tetramethylfluoranthene (**15**), which by Wohl-Ziegler radical bromination was converted to 1,6,7,10-tetrakis(bromomethyl)fluoranthene (**16a**). The bridging thioether was prepared by nucleophilic displacement with sodium sulfide, from which sulfur extrusion and aromatization lead to **1**. This expensive and lengthy synthesis proved the principle of the bilaterally symmetric approach,<sup>8a</sup> but lacked the practicality of anything close to a scalable synthesis. Toxic reagents like selenium dioxide further weakened the practical aspects of this synthesis.

**Scheme 2.3.** First corannulene synthesis by the Siegel group





Further investigations lead to the implementation of a direct formation of **13** from **12** by Friedel-Crafts acylation with oxalyl chloride (Scheme 4). The method yielded two closely related isomers of dimethylacenaphthaquinone, which required stringent chromatographic separation; but, it obviated many steps and the use of selenium dioxide. Benzylic bromination of **15** could be pushed to give the octabromide **16b**, which afforded a ring closure of the flanking bonds by using low valent titanium or vanadium, eliminating the need for pyrolysis.<sup>40,9</sup> Here the first gram scale solution phase synthesis of corannulene was established and shown to produce not only the basic core but also specific derivatives.

Investigations toward the formation of the tetracarboxaldehyde cognate of **15** or **16b** led Sygula and Rabideau to attempt hydrolysis of **16b**.<sup>10</sup> Serendipitously, hydrolysis did not lead to the expected precursor but instead deprotonated the remaining benzylic hydrogen and initiated carbon-carbon bond formation, leading to tetrabromocorannulene (**17**). This reaction was strategically important and offered certain advantages for gram-scale syntheses; however the use of dioxane and the low volume yield of the reaction made this operation very costly and not very "green" if contemplated for synthesis on multi-kilogram scale.

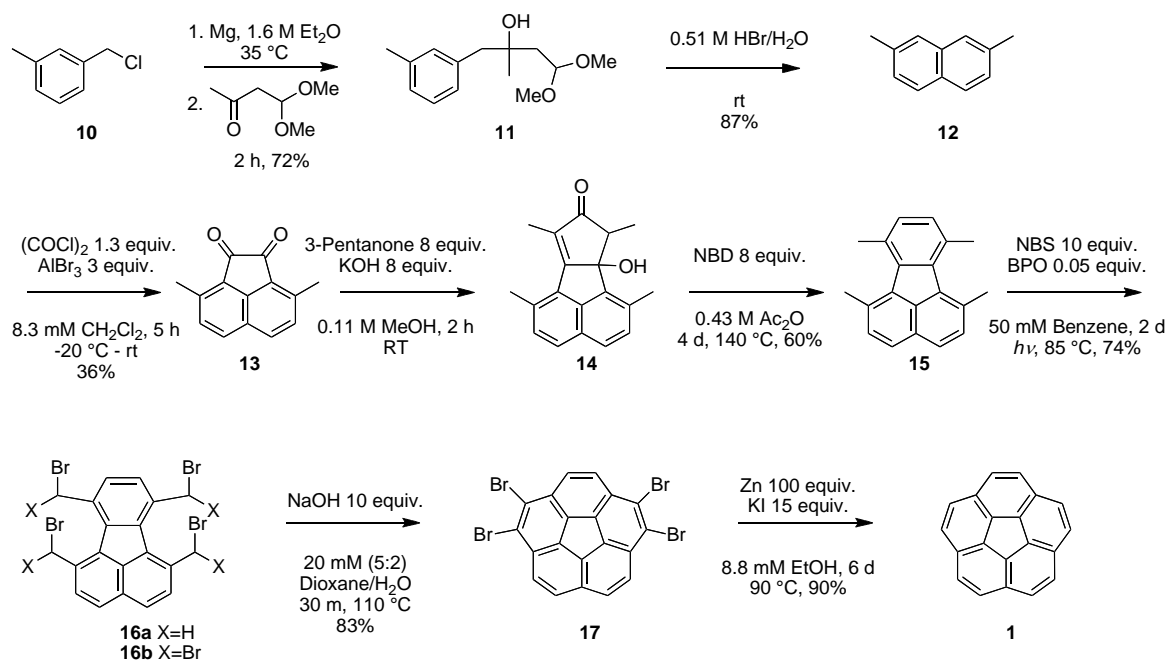
Reduction of **17** was possible using ca. 100 equiv. of zinc and potassium iodide in ethanol. Alternatives using lithium aluminum hydride had also been reported. The

excessive waste of the former and harsh reagents of the latter also required attention for a successful scale-up.

Such was the state of the art in corannulene synthesis when the present investigation in scale-up began; eight steps (overall yield 7.4%), four chromatographic separations (compounds **13**, **15**, **16b**, and **1**), several undesirable solvents, harsh or excessive reagent and no step-volume yield above 3%. To produce 120 grams of corannulene required almost a metric ton of solvent.

Four general challenges were the focus of this initial optimization: 1) Reduce or replace as many costly or toxic reagents as possible; 2) Increase the volume yields toward a target of 10% from values in some cases below 1%; 3) Enhance the robustness throughout the synthesis by mechanistic insight and testing of critical parameters; 4) Remove all chromatographic separations, including that needed to separate the physically similar isomers of dimethylacenaphthenequinone.

**Scheme 2.4** Solution-phase synthesis of corannulene (2006)



## 2.3 Previous work

The work presented in this section was not the work of this thesis. However, for a complete overview of the kilogram-scale production the final conditions will be briefly presented here.

**Synthesis of 2,7-dimethylnaphthalene (12).** Conversion of *a*-chloro-*m*-xylene (**10**) to 2,7-dimethylnaphthalene (**12**) was accomplished through a Grignard addition of dimethoxybutanone followed by acidic ring closure. The production of **11** closely followed the reported procedure<sup>7</sup> and required minimal optimization (Table 2.1).

**Table 2.1.** Comparison of reagents required before (2006) and after (2011) the synthesis of **11** to produce 1 kilogram of corannulene<sup>12</sup>

2006			2011	
	Reagent	Kilograms	Reagent	Kilograms
<b>Reaction:</b>	<b>10</b>	8.0	<b>10</b>	7.7
	Diethyl ether	41	Diethyl ether	40
	Magnesium	1.7	Magnesium	1.6
	Dimethoxybutanone	7.0	Dimethoxybutanone	6.3
<b>Workup:</b>	Water	59	Water	77
	NH <sub>4</sub> Cl solution	55	NH <sub>4</sub> Cl solution	27
	MgSO <sub>4</sub>	5.7	Na <sub>2</sub> SO <sub>4</sub>	3.8
			MTBE	110
<b>Purification:</b>	N/ A		N/ A	
<b>Yield<sup>13</sup>:</b>	72% ( <b>11</b> )	9.2	85% ( <b>11</b> )	9.2
<b>Vol. Yield:</b>	Reaction: 16%	Total: 5.1%	Reaction: 16%	Total: 3.0%
<b>E-factor<sup>14</sup>:</b>		17		28

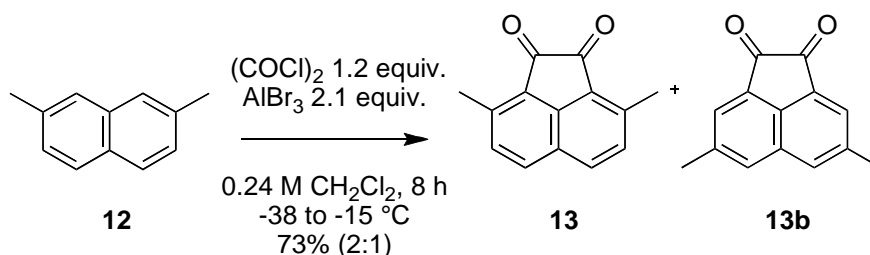
For the ring closure of **11** to yield 2,7-dimethylnaphthalene the original paper reported using a 0.51 M mixture of glacial acetic acid and 48% hydrobromic acid. During production, 95% sulfuric acid replaced the hydrobromic acid (Table 2.2) and a higher concentration of 0.81 M H<sub>2</sub>SO<sub>4</sub> in acetic acid was achieved.

**Table 2.2.** Comparison of reagents required before (2006) and after (2011) the synthesis of **12** to produce 1 kilogram of corannulene<sup>12</sup>

2006			2011	
	Reagent	Kilograms	Reagent	Kilograms
<b>Reaction:</b>	<b>11</b>	9.2	<b>11</b>	9.3
	AcOH	39	AcOH	45
	HBr (48%)	44	H <sub>2</sub> SO <sub>4</sub> (97%)	5.6
<b>Workup:</b>	Water	94	Water	78
			MgSO <sub>4</sub>	3.1
			Toluene	70
			Na <sub>2</sub> CO <sub>3</sub>	2.3
			Sat. NaCl solution	0.43
<b>Purification:</b>	N/ A		Ethanol	19
<b>Yield:</b>	87% ( <b>12</b> )	5.2	71% ( <b>12</b> )	4.3
<b>Vol. Yield:</b>	Reaction: 7.8%	Total: 3.2%	Reaction: 9.4%	Total: 1.9%
<b>E-factor</b>		34		52

**Acylation of dimethylnaphthalene (12) to acenaphthenequinone (13).** The Friedel-Crafts acylation of **12** with oxalyl chloride presented several problems. These problems were addressed in great detail as part of the master's thesis.<sup>15</sup> Although this step was not as improved as one would hope, it was decided to use only AlBr<sub>3</sub>. The concentration and stoichiometry of reagents were varied to determine that the optimal molarity of 0.23 M of **12** in dichloromethane (Table 2.4) resulted in a reproducible combined yield of 73% (2:1) of **13** and **13b** when a temperature gradient of –38 to –15 °C over 6 hours was applied, as shown in Scheme 2.6.

**Scheme 2.6.** Preparation of isomers **13** and **13b**



## 2.4 Current work

After accepting a 2:1 mixture of **13** and **13b** as the best synthetic outcome, the first step of this thesis was to develop an efficient method for isolating and purifying the product. Chromatography was not seen as an option. Both isomers have very similar physical properties; their solubilities were not substantially different in a broad spectrum of solvents.<sup>16</sup> The key chemical difference is the steric environment in the plane of the quinone function. Normal kinetic attack on carbonyls occurs *via* Burgi-Dunitz<sup>17</sup> approaches out of the carbonyl plane, therefore such strategies seemed unlikely to help, and screening revealed no exception to this expectation. Imine formation would occur under thermodynamic control and would place a new substituent in the plane, where the largest steric difference between the isomers could be exploited. Such a process showed greater mechanistic promise and indeed imine formation proceeds for **13b** better than **13**. More importantly, amino acid hydrazides had precedence in the steroid literature as reagents to make water-soluble derivatives that could be separated by simple aqueous extractions. These reagents are sold under the commercial name of Girard's reagents.<sup>18</sup> In particular, limiting amounts of Girard's reagent T (GRT) formed a hydrazone selectively with **13b** in AcOH over two hours at 40 °C. The hydrazone of **13b** was washed away from **13** with water, in a highly selective manner that eliminated the need for column chromatography (Scheme 2.7). The isolation yield for this step was 90% based on the initial amount of **13** in the mixture. The aqueous extract could be hydrolyzed under acidic condition to recover **13b** containing a small amount of **13**. Total recovery of the isomers from the reaction and hydrolysis was 96%. It was also discovered that when this separation procedure was performed at reflux in acetonitrile, with only a small amount of acetic acid for 4 h, one could obtain **13** in 98% yield

following the same workup conditions; however, due to the price of acetonitrile at the time of production, it was not advantageous to use these conditions.

**Scheme 2.7.** Separation of **13** and **13b** using Girard's Reagent in AcOH

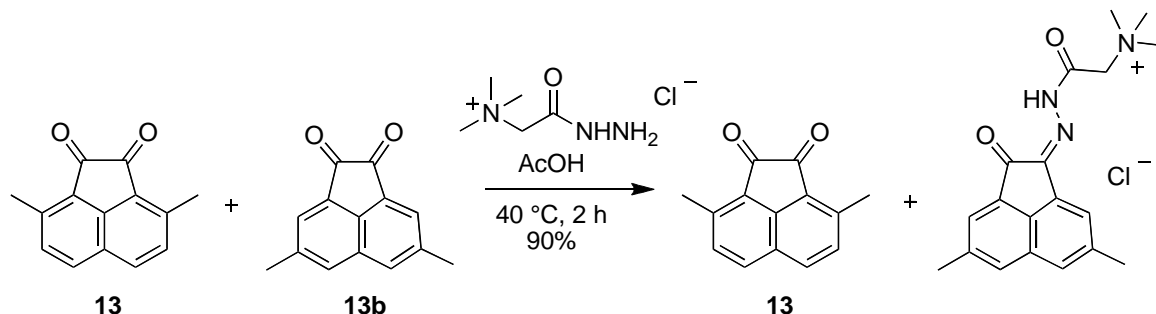


**Table 2.4.** Comparison of reagents required before (2006) and after (2011) the optimization of **13** and **13b** to produce 1 kilogram of corannulene<sup>12</sup>

2006			2011	
	Reagent	Kilograms	Reagent	Kilograms
<b>Reaction:</b>	<b>12</b>	5.2	<b>12</b>	4.3
	Oxalyl chloride	6.6	Oxalyl chloride	4.2
	Aluminum bromide	20	Aluminum bromide	16
	Dichloromethane	540	Dichloromethane	150
<b>Workup:</b>	Water	910	Water	92
	MgSO <sub>4</sub>	40	Na <sub>2</sub> SO <sub>4</sub>	15
	Saturated NaCl sol.	240	Celite	7.8
			Na <sub>2</sub> CO <sub>3</sub>	2.9
			Toluene	67
<b>Yield:</b>	N/ A		73% ( <b>13</b> + <b>13b</b> 2:1)	4.2
<b>Purification:</b>	Silica gel	780	AcOH	29
	Hexane	1300	GRT	1.2
	Dichloromethane	750	Water	47
<b>Yield:</b>	36% ( <b>13</b> )	2.5	42% ( <b>13</b> )	2.5
<b>Vol. Yield:</b>	Reaction: 0.62%	Total: 0.07%	Reaction: 2.2%	Total: 0.70%
<b>E-factor:</b>		1800		170

**Synthesis of 1,6,7,10-tetramethylfluoranthene (15).** The next step of the synthesis was conversion of **13** to 1,6,7,10-tetramethylfluoranthene (**15**) through a crossed-aldol condensation followed by a Diels-Alder, retro Diels-Alder reaction cascade using norbornadiene (Scheme 2.8). Improvements to this step significantly improved volumetric productivity, which reduced the amount of solvents required. The amount of methanol required for the Knoevenagel condensation could be reduced by 50% to that reported<sup>19</sup> and still obtain the same yield (Table 2.5). However, decreasing the equivalents of 3-pentanone<sup>20</sup> and KOH from the reported value led to a decrease in yield. Another important factor in this step was the isolation of the hydroxy intermediate **14** shown below. Careful neutralization of the reaction must be done to avoid protonation and elimination, leading to dimerization of the newly formed cyclopentadienone. Previous attempts to crack the dimer in the subsequent step were unsuccessful. Formation of the dimer dramatically decreases the yield.

Important to the optimization of the workup for the Diels-Alder/ retro-Diels-Alder step was the realization that, with slow quenching of the final reaction mixture, one could precipitate and filter **15** at the end of the reaction. This eliminated the need for the extraction and column chromatography reported in the literature procedure. The final product was obtained in 99.8% purity after recrystallization from an *i*-PrOH/ acetone mixture.

**Scheme 2.8.** Optimization of 1,6,7,10-tetramethylfluoranthene (**15**)

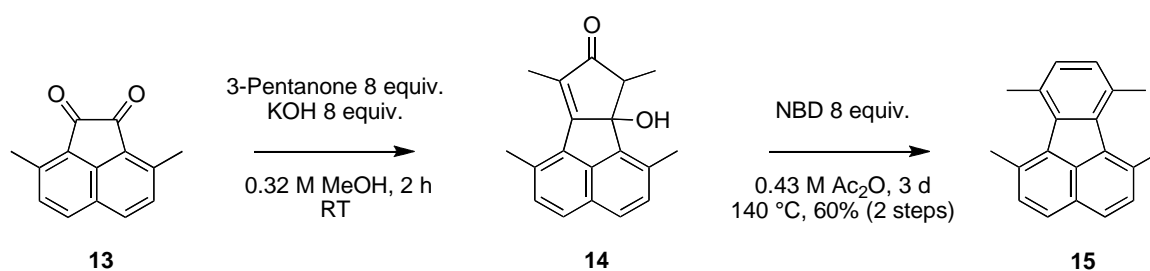


**Table 2.5.** Comparison of reagents required before (2006) and after (2011) the optimization of 15 to produce 1 kilogram of corannulene<sup>12</sup>

2006	2011
------	------

	Reagent	Kilograms	Reagent	Kilograms
<b>Reaction:</b>	<b>13</b>	2.5	<b>13</b>	2.5
	MeOH	88	MeOH	30
	KOH	16	KOH	16
	3-Pentanone	8.3	3-Pentanone	8.0
<b>Workup:</b>	Water	110	Water	87
	Sat. NaCl solution	34	HCl (32%)	30
	HCl (10%)	11		
	Dichloromethane	120		
	MgSO <sub>4</sub>	9.3		
<b>Reaction:</b>	Acetic anhydride	30	Acetic anhydride	32
	NBD	8.4	NBD	8.6
<b>Workup:</b>	Water	74	Water	7.4
	NaOH (10%)	52	NaOH (30%)	6.2
	DCM	50	MeOH	56
	Sat. NaCl solution	54		
<b>Yield:</b>	N/ A		66% ( <b>15</b> ) <sup>a</sup>	2.1
			<sup>a</sup> Assay: 94% Uncorrected Yield: 70%	
<b>Purification:</b>	Silica gel	250	Silica gel	2.1
	Hexane	2000	Cyclohexane	28
			Isopropanol	17
			Acetone	0.52
<b>Yield:</b>	60% ( <b>15</b> )	1.9	65% ( <b>15</b> ) <sup>b</sup>	2.0
			<sup>b</sup> Assay: 99.8% Purification yield: 99%	
<b>Vol. Yield:</b>	Reaction: 1.4%	Total: 0.05%	Reaction: 3.0%	Total: 0.64%
<b>E-factor:</b>		1500		160

**Radical bromination of 15 to yield 1,6,7,10-tetrakis(dibromomethyl)fluoranthene (16b).** The literature bromination of **15** proceeded through a radical bromination using NBS and radical initiation by benzoyl peroxide (BPO) in benzene (or carbon tetrachloride) with a 375 W tungsten lamp as the light source.<sup>21</sup> This step was



challenging to produce on scale due to the safety issues associated with the solvents and with performing a photochemical radical reaction.<sup>22</sup> Specifically, the radical initiator used, BPO, is less effective at stable radical production than other initiators and is not preferred on scale.<sup>23</sup> To overcome these safety issues a series of reactions were screened to try and avoid the need for radical initiators. The solvent of choice turned out to be chlorobenzene at 90-95 °C, but, unfortunately, the higher temperature did not obviate the use of a radical initiator, albeit clear that substantial thermal activation seemed to occur. The better-stabilized radical initiator AIBN, available from the Vazo line of initiators at Dupont, showed good results at these higher temperatures on scale, and was selected (Table 2.6).

There were also hesitations that the light source would not be sufficient on such scale due to the heating mantle and depth of the 100-L reactor. Accordingly, many attempts to find brominating conditions without an extra light source were attempted but unsuccessful, even in the presence of AIBN. Fortunately, radical generation at the outer layer of the reactor sufficed to give a steady and robust process. On the 100 L reactor scale, three lamps were adequate to perform the bromination when shone directly into the solution.

An unforeseen problem arose when scaling the bromination from 10 grams to 50 grams. The dark-red solution unexpectedly turned black and the optimized work-up conditions failed to yield **16b** directly. Column chromatography of the mixture resulted in a 25-30% isolated yield of **16b** while the remainder of the crude mixture stayed on the baseline. This was most likely due to the presence of HBr in the headspace that was responsible for the formation of side products in significant proportions. A slight vacuum of 400 mbar was applied and the reaction proceeded as expected (Scheme 2.9). The product was recrystallized using ethyl acetate, eliminating the column chromatography that was previously required. Given the sensitivity of the octabromo compound, a large-scale chromatography would not only have added cost and material waste from the silica, but likely would have lead to some product decomposition.

#### **Scheme 2.9** Benzylic bromination of fluoranthene **15**

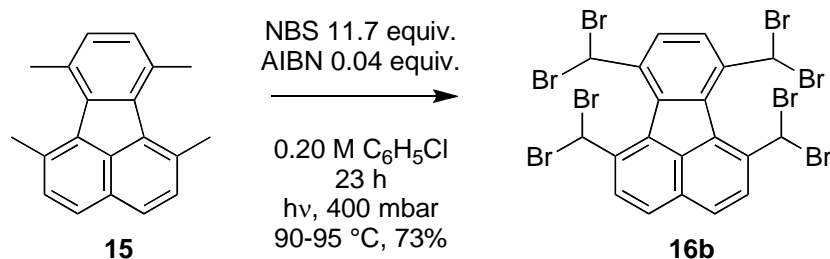


**Table 2.6** Comparison of reagents required before (2006) and after (2011) the optimization of **16b** to produce 1 kilogram of corannulene<sup>12</sup>

2006			2011	
	Reagent	Kilograms	Reagent	Kilograms
Reaction:	15	1.9	15	2.0
	NBS	14	NBS	16
	BPO	0.11	AIBN	0.06
	Benzene	130	Chlorobenzene	46
Workup:	Water	38	Ethyl acetate	15
	Dichloromethane	63		
	MgSO <sub>4</sub>	19		
	Sat. NaCl solution	46		
	Na <sub>2</sub> S <sub>2</sub> O <sub>3</sub>	87		
Purification:	Silica gel	200	N/ A	
	Hexane	1400		
Yield:	74% (16b)	4.8	73% (16b)	5.1
Vol. Yield.	Reaction: 3.3%	Total: 0.19%	Reaction: 12%	Total: 8.8%
E-factor:		410		12

**Synthesis of 1,2,7,8-tetrabromocorannulene (17).** A strategic improvement for the ring closure of **16b** to form the first derivative containing the corannulene core, tetrabromocorannulene **17**, was reported by Sygula *et al.* using a dioxane/ water mixture in the presence of base.<sup>10</sup> Nonetheless, there were still two main areas of optimization for this step: the low volume yield due to reaction concentrations of 20 mM and the cost and toxicity of dioxane as solvent.

In an attempt to overcome the issue of low concentration, the reaction was performed in a ratio of 1 gram **16b** in 10 mL of a solvent mixture (H<sub>2</sub>O:MeOH, H<sub>2</sub>O:Toluene, H<sub>2</sub>O:Dioxane, Toluene:MeOH) with varying bases (NaOH, NaOMe, KOH). These reactions resulted in polymerization of the starting material. The next consideration was portion wise addition of **16b** to the solvent mixture. Upon formation, the product **17** precipitates and allows the starting material to dissolve in the solvent. This would decrease the amount of solvent needed while having minimal effect on the yield. Unfortunately, the strategy proved wrong and instead polymerization of the starting material was the main product isolated upon filtration. A wider screening of solvents showed that isopropanol was a suitable replacement of the dioxane/ water mixture, increasing the allowable reaction concentration from 20 mM to 112 mM (Scheme 2.10). Addition of **16b** to an isopropanol solution with sodium hydroxide at reflux led to the clean formation of **17** in a 79% yield (Table 2.7). The product was filtered and carried through to the next step without further purification.

**Scheme 2.10** Ring closure of **16b** to yield 1,2,7,8-tetrabromocorannulene **17**

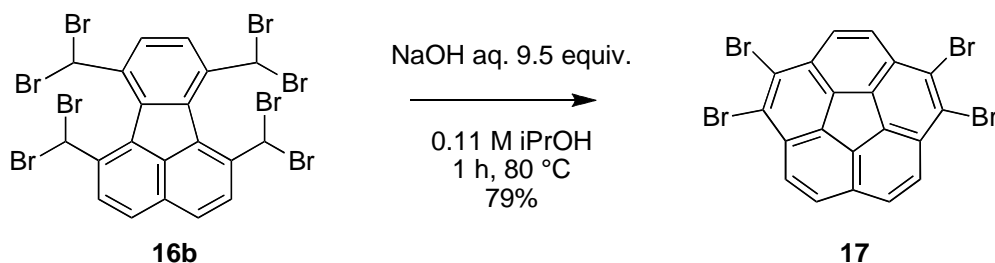


**Table 2.7** Comparison of reagents required before (2006) and after (2011) the optimization of **17** to produce 1 kilogram of corannulene<sup>12</sup>

2006			2011	
	Reagent	Kilograms	Reagent	Kilograms
<b>Reaction:</b>	<b>16b</b>	4.8	<b>16b</b>	5.1
	NaOH	2.2	NaOH (30%)	6.8
	Dioxane	190	Isopropanol	40
	Water	73		

<b>Workup:</b>	Water	380	Water	19
	HCl (10%)	16	Isopropanol	11
	Dichloromethane	250		
	Acetone	150		
<b>Yield:</b>	83% ( <b>17</b> )	2.5	79% ( <b>17</b> )	2.5
<b>Vol. Yield:</b>	Reaction: 0.95%	Total: 0.24%	Reaction: 4.9%	Total: 3.0%
<b>E-factor:</b>		420		30

**Reduction of tetrabromocorannulene (17) to corannulene (1).** The final step of the synthesis, reduction of **17** to **1** had a number of hurdles to overcome.<sup>24</sup> One principal problem for the reaction was the excessive amounts of reagents, solvent, and reaction time required. Although zinc is relatively inexpensive compared to other metals, the large zinc dust excess (100 equiv) and amount of ethanol (8.8 mM) required for agitation proved to be a challenging environmental waste problem. Another difficulty with this reaction was the reported long reaction time of six days. Finally, even after the use of excessive reagents and long reaction times, one would still isolate a mixture of side products that required column chromatography to purify.

A recent paper by Thiemann<sup>25</sup> used zinc dust in the presence of ammonium formate and base to dehalogenated tetrabromobisphenol A (TBBPA), a hazardous pollutant *via* transfer hydrogenation. These results led us to believe that a stoichiometric quantity of ammonium formate and zinc could have the same effect on corannulene, greatly reducing the amount of reagents and solvents required and shortening reaction time to just a few hours. Initial results appeared encouraging with **1** detected after only two hours. Unfortunately the reaction did not proceed to completion and even after 2 days and up to 20 equivalents of zinc powder, GC-MS and TLC identified that there was dibromocorannulene and monobromocorannulene still present in the reaction. Analysis of the reactor headspace indicated the presence of acid. It was hypothesized that HBr formation during the reaction was preventing further reduction of **17** and addition of zinc oxide might solve this problem and push the reaction to completion. We expected the ZnO and HBr to react and form zinc bromide and water. Unfortunately, the addition

of ZnO did not have an effect on the reaction and an alternative reduction method was sought.

A paper by Spatola<sup>26</sup> showed that ammonium formate and Pd/ C were successful at reducing haloaromatics through catalytic transfer hydrogenation. Successful reduction of **17** to **1** was achieved by replacing zinc with 5% palladium on carbon. A setback occurred upon scaleup from 1 gram to 10 grams since formation of ammonium bromide was detected in the condenser. Due to the reactor configuration, salt accumulation would not be easy to remove safely during production although chemically an efficient reaction. We replaced ammonium formate with a triethylamine/ formic acid mixture and further solvent screening showed pyridine was the best to solubilize the formed salts. A less costly alternative to pyridine is 3-picoline, which produced similar results and was used (Table 2.8) in the reduction of **17** (Scheme 2.11).<sup>27</sup>

**Scheme 2.11** Reduction of **17** to corannulene using Pd/ C

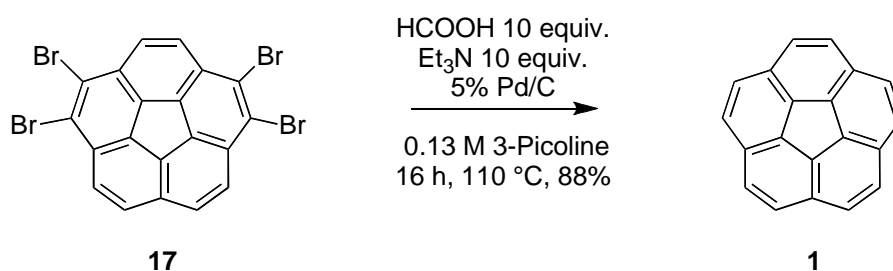


**Table 2.8** Comparison of reagents required before (2006) and after (2011) the optimization to produce 1 kilogram of corannulene<sup>12</sup>

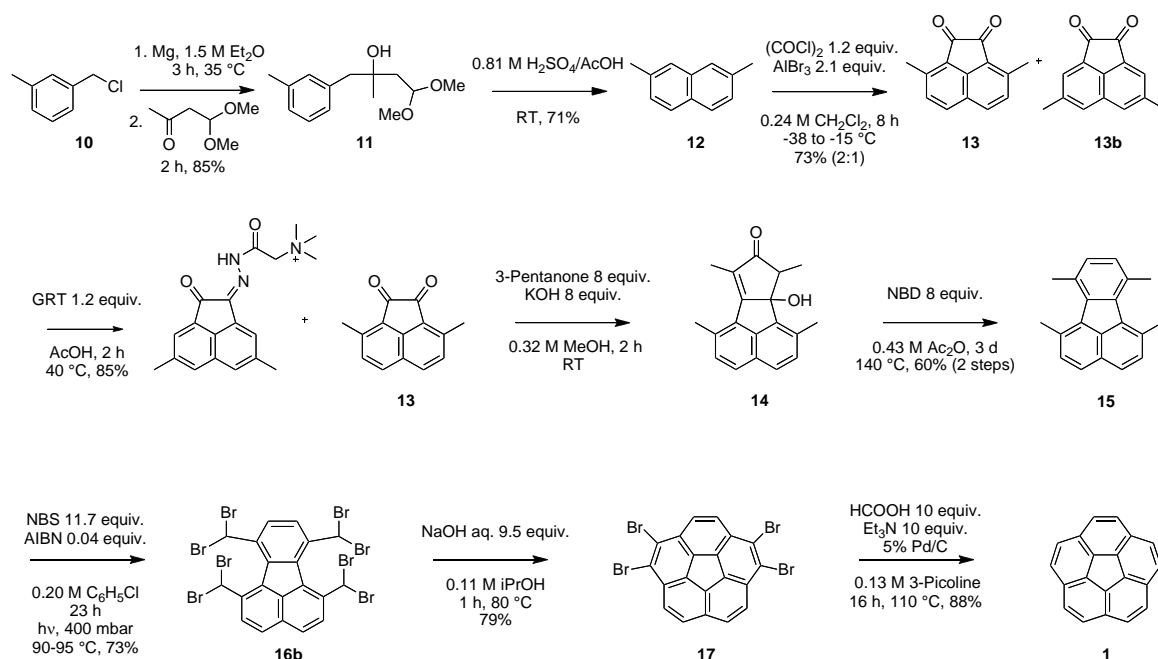
2006			2011	
	Reagent	Kilograms	Reagent	Kilograms
<b>Reaction:</b>	<b>17</b>	2.5	<b>17</b>	2.5
	4% HCl	26	Formic acid	1.7
	Zn	30	Triethylamine	3.6
	KI	11	5% Pd/ C	0.13
	EtOH	390	3-picoline	27
<b>Workup:</b>	Water	250	Water	14

	Dichloromethane	200	HCl (32%)	1.7
	MgSO <sub>4</sub>	15		
<b>Purification:</b>	Silica gel	250	Toluene	27
	Hexane	1900	Activated carbon	0.04
			Celite	0.16
<b>Yield:</b>	90% ( <b>1</b> )	1.0	88% ( <b>1</b> )	1.0
<b>Vol. Yield:</b>	Reaction: 0.19%	Total: 0.03%	Reaction: 3.5%	Total: 1.3%
<b>E-factor:</b>		3100		75

## 2.5 Conclusion

The optimization and production of **1** has been demonstrated on scale. The key successes of the synthesis were to eliminate the column chromatographies previously required for 4 of the 8 steps as well as to find safer and less costly solvents and reagents. Careful evaluation of required solvent volume in the synthesis of **1** starting from dimethylnaphthalene **12** improved the average concentration of each step from 0.04 M to 0.24 M. A total of 1.3 kg of **1** were isolated in an 8.7% yield over 8 steps with the average yield per step being 75% (Scheme 2.12). The campaign also retained an additional 400 g of **17**, 2 kg of **15**, 2 kg of **13**, 2.5 kg of **13b**, and 650 g of **12**. This conversion of the production of corannulene from milligram scale in 1966 to kilogram scale in 2011 also marks the transition of corannulene as esoteric molecular object of academic interest into a chemical entity with a potential engineering/ commercial future.

**Scheme 2.12** Optimized synthesis of corannulene (**1**)



## 2.6 Experimental

**General.** Starting materials were obtained from commercial suppliers and were used without further purification. HPLC analyses were performed on an Agilent Series 1100 liquid chromatograph equipped with a UV detector. NMR data obtained were identical to those reported in the literature. Yield calculation based on HPLC purity, or assay if indicated. Mole amount reported has been corrected based on purity.

**Separation of 3,8-dimethylacenaphthenequinone (13) and 4,7-dimethylacenaphthenequinone (13b).** Acetic acid (31.5 kg) and a mixture of isomers **13** and **13b** (6.00 kg, purity 69% (**5**) [4.1 kg (**5**), 19.7 mol (**5**)] was charged to a 100-L reaction vessel and heated to 40 °C for at least 30 min. During this time, a solution of Girard's Reagent T (1.73 kg, 10.3 mol, 1.2 equiv. of **13b**) in 9.55 kg acetic acid was prepared. This solution was added dropwise to the isomer mixture solution over 2 h. The reaction continued to stir for an additional 2 h then water (60.0 kg) was slowly added to quench the solution over a period of 30 min. The suspension was filtered, washed with 8 kg water, then dried at < 2 mbar overnight to result in 3.72 kg **13** (HPLC assay 97% 3,8-dimethylacenaphthenequinone (**13**) [3.67 kg, 90% HPLC corrected yield]). mp 204-205 °C, <sup>1</sup>H NMR (500 MHz, CDCl<sub>3</sub>): <sup>TM</sup> 2.87 (s, 6H), 7.49 (d, 2H, J = 8.28 Hz), 8.03 (d, 2H, J = 8.28

Hz);  $^{13}\text{C}$  NMR (100 MHz,  $\text{CDCl}_3$ ):  $\delta$  18.12, 76.58, 77.00, 77.42, 124.29, 127.47, 130.63, 131.73, 137.57, 147.10, 188.80.

To the mother liquor, hydrochloric acid (55.7 kg) in water (24.0 kg) was added and stirred at room temperature for 3 h. The precipitate was filtered then dried at < 2 mbar overnight to yield a mixture of isomers **13:13b** (1.88 kg) of 1:4. Total recovery for this step for **5** was 99% (**13+13b** 93%).

**1,6,7,10-tetramethylfluoranthene (15).** Methanol (20 kg) was charged to a 100 L reactor vessel then KOH (11.0 kg, 177 mol) was added in portions. The solution was heated to 60-80 °C until the KOH dissolved. The solution was then cooled to 20 °C and 3-pentanone (5.45 kg, 61.9 mol) was added. 3,8-dimethylacenaphthenequinone (1.70 kg, assay 98% [1.67 kg, 7.86 mol]) was slowly added and a brown solution was obtained. The mixture was stirred at 18-25 °C for at least 2 h. The reaction mixture was cooled to 0 °C and a previously cooled (-3 °C) solution of water (44 kg) and HCl (32%, 20 kg) was added dropwise (so that the internal temperature was less than 20 °C) until the color of the solution changed to a yellow-green and pH was between 5 and 7. The suspension was stirred for 30-60 min at 18-22 °C then filtered and the filter cake was washed with water (15 kg). The product was dried at 40 °C and <10 mbar for 24 h. The vessel was charged with the dried intermediate (2.17 kg), acetic anhydride (21.0 kg), and 2,5-norbornadiene (5.8 kg). The reaction mixture was heated to reflux (135-140 °C) for 2-3 days then cooled to 20-25 °C. A solution of 30% NaOH (4.2 kg) and water (2.5 kg) was added slowly dropwise. The reaction mixture was allowed to stir overnight at 15-30 °C then distilled at 200 mbar and an internal temperature of 70 °C (distillate 16 kg). Water (2.5 kg) was added and the internal temperature was raised to 88 °C then vacuum (300 mbar) was slowly applied. The mixture was cooled to an internal temperature of 20-25 °C and distillate (6.7 kg) was collected. Methanol (2.5 kg) was added to precipitate **14** and the dark brown suspension was filtered and washed with additional MeOH (2.5 kg). The reactor vessel was charged with the filter cake and methanol (25.5 kg) then heated to reflux for 1 h. The suspension was cooled to 20-25 °C and stirred at this temperature overnight then filtered and the filter cake was washed with additional MeOH (2.1 kg).



The product is dried at 40 °C and <10 mbar for 4 h to yield 1.35 kg (HPLC assay 94.5% 1,6,7,10-tetramethylfluoranthene (**15**) [1.28 kg, 63 % HPLC corrected yield]).

For further purification a 50-L reaction vessel was charged with **15** (1.99 kg, assay 94% [1.87 kg, 7.22 mol]) and cyclohexane (26.5 kg). A dark brown suspension was obtained then filtered through a silica gel plug (2.0 kg) with 800 mbar. The filtrate was evaporated and the distilled cyclohexane was used to wash the silica gel until no **15** can be detected on TLC. The residue was then heated in isopropanol (13.9 kg) at 79 °C. Acetone (0.50 kg) was added dropwise until a solution was obtained then the solution is cooled to 20-25 °C and stirred at this temperature overnight. The suspension was filtered and the filtrate was washed with cooled isopropanol (2.3 kg). The product was dried at 50 °C and <10 mbar overnight to yield 1.84 kg (HPLC assay 99.8% 1,6,7,10-tetramethylfluoranthene (**15**) [1.84 kg, 99% HPLC corrected yield]). mp 140.5-143.5 °C, <sup>1</sup>H NMR (500 MHz, CDCl<sub>3</sub>): <sup>1</sup>H 2.74 (s, 6H), 2.84 (s, 6H), 7.13 (s, 2H), 7.35 (d, 2H, J = 8.28), 7.67 (d, 2H, J = 8.28); <sup>13</sup>C NMR (100 MHz, CDCl<sub>3</sub>): <sup>13</sup>C 24.30, 25.13, 126.15, 126.60, 129.63, 130.67, 131.83, 132.00, 133.67, 134.88, 139.91

**1,6,7,10-Tetrakis(dibromomethyl)fluoranthene (16b).** A 100 L vessel was charged with chlorobenzene (55.5 kg) and 1,6,7,10-tetramethylfluoranthene (2.47 kg, assay 99.8% [2.47 kg, 9.56 mol]). The solution was heated to 70-75 °C while illuminating with three 350 W spot bulbs in a distance of 30 cm for the duration of the reaction sequence. AIBN (25.0 g, 0.152 mol) and NBS (20.0 kg, 112 mol) were added and a vacuum (400 mbar) was applied. The mixture was heated to an internal temperature of 90 °C and after 15-30 min an exothermic reaction was detected. The jacket temperature was set to < 98 °C until the internal temperature decreased since decomposition of the product occurs at temperatures above 100 °C. The mixture was stirred vigorously at 90-95 °C, and the reaction was monitored by thin layer chromatography. Additional AIBN (25.0 g, 0.152 mol) was added after 3 h and 10 h. After 23 h the suspension is cooled to 40-45 °C and the suspension was filtered. The filtrate was evaporated at 70 °C (120 mbar to 8 mbar) and the distillate (20 kg) was used to wash the filter cake. Ethyl acetate (8 kg) was added then the solvent was evaporated at 70 °C (120 mbar to 8 mbar). Additional ethyl acetate (2 kg) was added then the suspension was stirred for 1 hr at 70 °C before cooling to 18-25

°C. The suspension was left to stir at this temperature overnight then filtered and washed with ethyl acetate (3.8 kg). The wet product was dried at 40 °C and <10 mbar for 12 h to yield 6.40 kg (HPLC purity 92% 1,6,7,10-tetrakis(dibromomethyl)fluoranthene (**16b**) [5.93 kg, 70% HPLC corrected yield]). mp >300 °C, <sup>1</sup>H NMR (500 MHz, CDCl<sub>3</sub>): <sup>TM</sup> 7.10 (s, 2H), 7.22 (s, 2H), 7.99 (d, <sup>3</sup>J = 8.5 Hz, 2H), 8.22 (s, 2H), 8.28 (d, <sup>3</sup>J = 8.5 Hz, 2H). <sup>13</sup>C NMR (100 MHz, CDCl<sub>3</sub>): <sup>TM</sup> (ppm) 38.5, 39.0, 127.6, 130.1, 130.2, 131.5, 131.8, 132.3, 136.5, 137.9.

**1,2,7,8-tetrabromocorannulene (17).** A 50-L reaction vessel was charged with isopropanol (24.9 kg) and 1,6,7,10-tetrakis(dibromomethyl)fluoranthene (3.19 kg, purity 93% [2.97 kg, 3.35 mol]). The suspension was heated to an internal temperature of 77-82 °C. A NaOH solution (30% aq., 4.25 kg, 31.9 mol) was added dropwise over 40 min. then the reaction mixture was allowed to stir at 77-82 °C for 55-65 min. The suspension was slowly cooled to 20-25 °C over 90-120 min. then filtered through a glass filter and the filter cake was washed with water (12.0 kg) then isopropanol (6.9 kg). The product was dried at 50 °C and <10 mbar for 24 h to yield 1.90 kg (HPLC purity 79% 1,2,7,8-tetrabromocorannulene (**17**) [1.49 kg, 79% HPLC corrected yield]). mp 338-340 °C (dec.), <sup>1</sup>H NMR (400 MHz, CDCl<sub>3</sub>): <sup>TM</sup> 7.98 (s, 2H), 7.95 (d, <sup>3</sup>J = 8.9 Hz), 7.85 (d, <sup>3</sup>J = 8.9 Hz, 2H). <sup>13</sup>C NMR was not obtained due to poor solubility.

**Corannulene (1).** A 50-L reaction vessel was charged with 1,2,7,8-tetrabromocorannulene (4.0 kg, purity 77%, [3.32 kg, 5.87 mol<sup>28</sup>]), 3-picoline (42.0 kg), formic acid (2.62 kg, 55.8 mol), triethylamine (5.76 kg, 56.6 mol), and 5% Pd/ C (50% water, 200 g, 0.41 mol). The suspension was heated to reflux and stirred for 16 h, until the reaction was complete. The mixture was cooled to an internal temperature of 20-25 °C and the solid was filtered through a glass filter then washed with 5.7 kg 3-picoline. The filtrate was returned to the reactor and heated to an internal temperature of 73 °C while applying a vacuum of (p<sub>start</sub>=100 mbar) to remove 45 kg of 3-picoline so that crystallization occurred. Upon crystallization of the product, toluene (23 kg) and a mixture of HCl (32%, 2.7 kg) in water (14 kg) was added until the pH of the water phase was 3. The mixture was heated to an internal temperature of 83-87 °C and activated carbon (57 g) was added. This suspension was stirred for 10 min. then Celite (250 g) was

added and stirred for an additional 10 min. The mixture was filtered through a Celite plug under pressure (700 mbar) and the filtrand was washed with toluene (10 kg). The filtrate was transferred back into the reactor and heated to an internal temperature of 83-87 °C. The organic phase was washed twice with water (5.7 kg total) then filtered (IT = 86-90 °C) through a glass funnel to remove the precipitate. The filtrate was transferred back to the reactor and the organic phase was washed one last time with 15 kg water (IT = 86-90 °C) then the organic layer was distilled (24 kg) at an internal temperature of 87-93 °C under reduced pressure ( $p_{\text{start}} = 800$  mbar,  $p_{\text{end}} = 530$  mbar) until the product started to crystallize. The mixture was heated to reflux and additional toluene (3.5 kg) was added. A clear orange-brown solution was obtained. The solution was cooled using a ramp (jacket temperature = 100 °C to jacket temperature = 70 °C) during 3 h then cooled to jacket temperature = 15 °C and stirred for 15 h. The precipitate was filtered and the filtrand was washed with toluene (0.16 kg) then dried at 40 °C under vacuum for 21 h to yield 1.33 kg pale yellow solid (HPLC purity 98% corannulene (**1**) [1.30 kg, 88% HPLC corrected yield]). mp 268-269 °C,  $^1\text{H}$  NMR (500 MHz,  $\text{CDCl}_3$ ):  $\delta$  7.82 (s, 10H).  $^{13}\text{C}$  NMR (100 MHz,  $\text{CDCl}_3$ ):  $\delta$  127.2, 130.8, 135.8.

- 
- <sup>1</sup> Butterfield, A. M.; Gilomen, B.; Siegel, J. S. *Org. Process. Res. Dev.* **2012**, *16*, 664.
- <sup>2</sup> Craig, J. T.; Robins, M. D. W. *Aust. J. Chem.*, **1968**, *21*, 2237.
- <sup>3</sup> Davy, J. R.; Iskander, M. N.; Reiss, J. A. *Aust. J. Chem.* **1979**, *32*, 1067.
- <sup>4</sup> (a) Scott, L. T.; Hashemi, M. M.; Meyer, D. T.; Warren, H. B. *J. Am. Chem. Soc.* **1991**, *113*, 7082. (b) Scott, L. T.; Cheng, P.-C.; Hashemi, M. M.; Bratcher, M. S. Warren, H. B. *J. Am. Chem. Soc.* **1997**, *119*, 10963. (c) Scott, L. T.; Hashemi, M. M.; Bratcher, M. S. *J. Am. Chem. Soc.* **1992**, *114*, 1920.
- <sup>5</sup> (a) Brown, R. F. C.; Harrington, K. J.; McMullen, G. L. *J. Chem. Soc., Chem. Commun.* **1974**, 123. (b) Brown, R. F. C.; Eastwood, F. W.; Jackman, G. P. *Aust. J. Chem.* **1977**, *30*, 1757. (c) Brown, R. F. C.; Eastwood, F. W.; Jackman, G. P. *Aust. J. Chem.* **1978**, *31*, 579. (d) Brown, R. F. C.; Eastwood, F. W.; Harrington, K. J.; McMullen, G. L. *Aust. J. Chem.* **1974**, *27*, 2393.
- <sup>6</sup> Buu-Hoi; Cagniant, P. *Rev. Sci.* **1942**, *80*, 130.
- <sup>7</sup> Wolinska-Mocydlarz, J.; Canonne, P.; Leitch, L. C. *Synthesis*, **1974**, 556.
- <sup>8</sup> Borchardt, A.; Hardcastle, K.; Gantzel, P.; Siegel, J. S. *Tetrahedron Lett.*, **1993**, *34*, 273.
- <sup>9</sup> (a) Seiders, T. J.; Elliot, E. L.; Grube, G. H.; Siegel, J. S. *J. Am. Chem. Soc.* **1999**, *121*, 7804. (b) Sygula, A.; Rabideau, P.W. *J. Am. Chem. Soc.*, **1998**, *120*, 12666.
- <sup>10</sup> Sygula, A.; Rabideau, P. W. *Tetrahedron* **2001**, *57*, 3637.
- <sup>12</sup> Reaction and workup quantities from 2006 were calculated using reported literature. Purification values, when listed, were determined using the assumption that 50-120 g silica gel were needed to purify 1 gram of product depending on the difficulty of separation. Yield (2006) is uncorrected; yield (2011) is corrected based on assay.
- <sup>13</sup> Based on dimethoxybutanone (assay 95%) as the limiting reagent.
- <sup>14</sup> E-factor determined by kg waste/ kg product. "Waste" included water used and did not assume solvents were recycled.
- <sup>15</sup> Butterfield, A. M. M.Sc. Dissertation, University of Zurich: Zurich, CH, 2008.
- <sup>16</sup> Extremely careful recrystallization from ethyl acetate allowed separation but the conditions were not robust enough for a reliable scale up.
- <sup>17</sup> Bürgi, H. B.; Dunitz, J. D.; Shefter, E. *J. Am. Chem. Soc.* **1973**, *95*, 5065.

- 
- <sup>18</sup> (a) Girard, A.; Sandelescu, G. *Helv. Chim. Acta*, **1936**, *19*, 1095. (b) Henbest, H. B. *Nature*, **1946**, *158*, 950.
- <sup>19</sup> Borchardt, A.; Hardcastle, K.; Gantzel, P.; Siegel, J. S. *Tetrahedron Lett.* **1993**, *34*, 273.
- <sup>20</sup> The self-condensed product of 3-pentanone was never detected but could be one reason that excess reagent was required.
- <sup>21</sup> Sygula, A.; Rabideau, P. W. *J. Am. Chem. Soc.* **1999**, *121*, 7800.
- <sup>22</sup> Bretherick, L. *Hazards in the Chemical Laboratory*; The Royal Society of Chemistry: London, 1986.
- <sup>23</sup> Denisov, E. T.; Denisova, T. G.; Pokidova, T. S. *Handbook of free radical initiators*; Wiley & Sons: New Jersey, 2003.
- <sup>24</sup> Sygula, A.; Rabideau, P. W. *Tetrahedron* **2001**, *57*, 3637.
- <sup>25</sup> Liu, G.-B.; Thiemann, T. *J. Hazard. Mater.* **2009**, *169*, 1150.
- <sup>26</sup> Anwer, M. K.; Sherman, D. B.; Roney, J. G.; Spatola, A. F. *J. Org. Chem.* **1989**, *54*, 1284.
- <sup>27</sup> The importance of fitting the process to the infrastructure at hand is highly emphasized here. We are certain that in an appropriate facility ammonium formate and a cheaper solvent could be implemented with great benefit to the overall process.
- <sup>28</sup> Moles of starting material also include 6% of di- and tribromocorannulene that are present by HPLC analysis of the previous step and should also reduce to **1**.

## Chapter 3

### *Corannulene monolayers*

#### 3.1 History

The earliest written documentation of observing the addition of oil to water was in the 18<sup>th</sup> century BC in Babylon.<sup>1</sup> The Babylonians were very superstitious and believed that the phenomena they observed after oil was poured into a bowl of water was an omen for the future and an answer for things that they could not explain. Their interpretations were written on clay tablets in cuneiform script. The Greeks learned of this practice a thousand years later and called it lecanomancy: *lekani* = bowl and *manteia* = divination.

The transition of using oil in water as a spiritual guide to a practical application happened sometime around the 5<sup>th</sup> century AD. Fulford references<sup>2</sup> two cases in 429 and 651 AD of people pouring oil on stormy waters to calm the wake. At the time, credit was given to the holiness of the oil. It would not be for another 1100 years that the interaction of oil on water would be looked at from a scientific point of view.

The first person to attempt to understand monolayers of organic molecules on a scientific level was Benjamin Franklin.<sup>3</sup> Franklin was the principal representative of the American States for discussions on sovereignty with England and France, which required many trips between the US and Europe. It was during one of these trips that Franklin made an observation<sup>4</sup> that he later reported to the Royal Society:

In 1757, being at sea in a fleet of 96 sail bound against Louisburg, I observed the wakes of two of the ships to be remarkably smooth, while all the others were ruffled by the wind, which blew fresh. Being puzzled with the differing appearance, I at last pointed it out to our captain, and asked him the meaning of it? 'The cooks', says he, 'have, I suppose, been just emptying greasy water through the scuppers, which has greased the sides of those ships a little', and this answer he gave me with an air of some little contempt as to a person ignorant of what everybody else knew. In my own recollecting what I had formerly read in Pliny, I resolved to make some experiment of the effect of oil on water, when I should have the opportunity...

At length being at Clapham where there is, on the common, a large pond, which I observed to be one day very rough with the wind, I fetched out a cruet of oil and the surface ... I then went to the windward side, where [the waves] began to form; and there the oil, though not more than a teaspoonful, produced an instant calm over a space several yards square, which spread amazingly, and extended itself gradually till it reached the lee side, making all that quarter of the pond, perhaps half an acre, as smooth as a looking glass. After this, I contrived to take with me, whenever I went into the country, a little oil in the upper hollow joint of my bamboo cane, with which I might repeat the experiment as opportunity should offer; and I found it constantly to succeed.

In these experiments, one circumstance struck me with particular surprise. This was the sudden, wide and forcible spreading of a drop of oil on the face of the water, which I do not know that anybody has hitherto considered. If a drop of oil is put on a polished marble table, or on a looking-glass that lies horizontally; the drop remains in its place spreading very little. But when put on water it spreads instantly many feet around, becoming so thin as to produce the prismatic colours, for a considerable space, and beyond them so much thinner as to be invisible, except in its effect of smoothing the waves at a much greater distance. It seems as if a mutual repulsion between its particles took place as soon as it touched the water, and a repulsion so strong as to act on other bodies swimming on the surface, as straws, leaves, ships, etc., forcing them to recede every way from the drop, as from a center, leaving a large clear space. The quality of this force and the distance to which it will operate, I have not yet ascertained but I think it a curious enquiry, and I wish to understand whence it arises.

A half-century would pass after Franklin's results were published before lawmakers in England started to see the importance of his findings. It was during the mid-1800s that legislators started to question whether ships should carry supplies of oil to pour into the ocean should they come upon a storm. One particular supporter was Ms. Gordon, who often traveled between the UK, India and the Far East. She suggested that all ships carry tanks of oil or "oil bags" that would slowly discharge into the ocean.

John Shields also understood the potential money one could make having a reliable method to calm the harbor.<sup>5</sup> He conducted two large-scale experiments at two different harbors, Peterhead and Aberdeen, in Scotland. In these experiments, Shields fixed a rubber tube underwater that would dispense oil up to the surface of the harbor. The first round of experiments was successful enough to warrant a patent, issued in 1879.<sup>6</sup> Unfortunately for Shields, the cost of oil to calm the sea for one hour, about 10 GBP, and damage to the piping system were problematic enough that the application did not advance.

The fruits of Shields' labor were not lost because later John Aitken<sup>6</sup> would be the first scientist to carefully study the work of Shields and design important experiments based on his findings. Aitken's experiment consisted of a circular vessel with a jet of air that caused rotary motions when blown overtop. This motion was measured by hanging a submerged horizontal paddle in the middle of the vessel using a thin platinum wire. Aitken first measured the amount of torsion when a jet of air was passed above a sample of clean water, then measured the change in torsion when the water was mixed with oil. When no decrease of deflection was observed, Aitken concluded, "therefore, oil does not reduce the bite, grip or friction of the air on the surface."

Lord Rayleigh, originally interested in sound waves, followed up on the work of Aitken.<sup>7</sup> Rayleigh made observations on the behavior of colliding water jets and water drops. He also studied the effect of static electricity on water drops. Of the five papers<sup>8</sup> published by Rayleigh discussing water surfaces, one publication<sup>9</sup> discusses the effect of superficial layers of olive oil on the surface tension of water. In this paper, Rayleigh is the first scientist to mention that surface films are of a particular molecular thickness, "the great interest which attaches to the determination of molecular magnitudes ...". Specific conclusions made by Rayleigh in this paper that are later supported in other studies include his awareness that surface tension could be lowered by "contamination", that olive oil on water must be ten to twenty angstroms thick because olive oil prevents the movement of camphor, and that molecules on a surface spread until one molecule thick. Rayleigh believed that if an extended layer was used, that one could obtain a direct measure of the size of the organic molecule on a water surface. However, he reports that he was unable to devise such a device.



The call of Rayleigh to build an instrument for such measurements as explained above would be answered by Agnes Pockels, a housewife fascinated by the dirty soap that remained after dishes.<sup>10</sup> The simple device constructed by Pockel consisted of a 70 cm x 5 cm x 2 cm tin trough that was filled to the brim with water. She laid a 1.5 cm tin strip across the top so that it was barely touching the water and could be used to change the area and clean the surface. The variation in surface tension was determined using a balance to measure the force required to lift a small button.

With the recommendation of Rayleigh, Pockels results were published in *Nature*.<sup>11</sup> The comments cited in this first publication set the foundation for many concepts used today. Already, Pockels observed that the surface tension of a contaminated surface varied when the surface was compressed or expanded. Upon compression, the surface tension could decrease by up to a factor of two. When expanded, the surface tension would increase until a maximum value was reached and then remain constant. From these results, Pockels claimed that a water surface could exist in two states: a normal state, where the surface tension was constant regardless of the change in surface size and a anomalous state, where variation in the surface size resulted in a change in surface tension. Her findings also showed that the cleaner the water surface, the more one could compress the system while maintaining the surface pressure at its maximum value.

Pockels furthered her research using the suggestions of Lord Rayleigh to transfer the contaminated substance to the surface using a volatile solvent. She continued to study different oils and acids and created the first isotherm (Figure 3.1) with quantitative units.

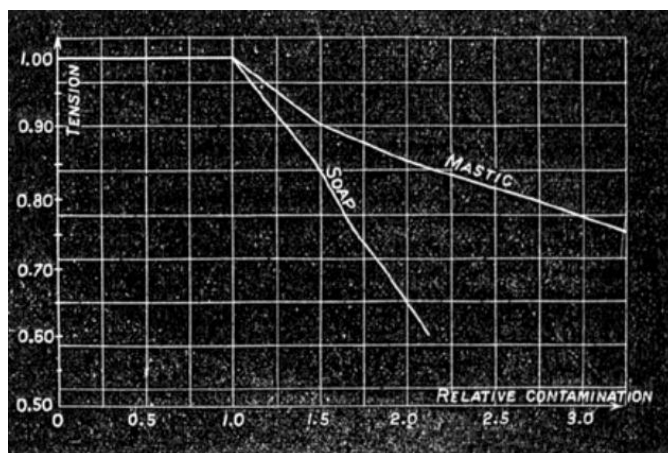


**Figure 3.1** First pressure-area isotherm published by Pockels.

Irwing Langmuir was the first to perform systematic studies of floating monolayers on water and to understand that molecular forces were short ranged and acted only between molecules in contact.<sup>12</sup> Between June and August of 1916, Langmuir studied and tabulated the surface tension of more than 250 substances. As a result of his work he proposed that the main factor in determining the surface tension of liquids comes from the layer of atoms at the surface, and not all components of the molecule contribute equally. Langmuir explained that as molecules arrange themselves in the surface layer, they do so in such a way that their active portions are pulled inwards. This leaves the least active portion of the molecule to form the surface layer. The surface energy, therefore, is not dependent upon the entire molecule but rather depends only on how the least active portions of the molecules can arrange themselves on the surface. He supported this claim by demonstrating that a series of paraffin molecules arrange themselves so that the methyl groups at the end form the surface layer, regardless of chain length. Furthermore, Langmuir was able to show similarities in the surface energies of alcohols (methanol and ethanol) and hydrocarbons. He reasoned that the similarity was due to the fact that both sets of molecules form surface layers with their corresponding CH<sub>3</sub> groups.

Langmuir advanced the technique of studying molecules on a surface to perform the measurements described in his 1917 paper. His original film balance was a modified version of the trough first used in Pockels experiments (Figure 3.2). With Langmuir's improved film balance, he was able to report the first transfer of fatty acid molecules from the water surface to a solid support. The first detailed procedure to transfer a monolayer to a solid support was given by Langmuir's graduate student, Katherine Blodgett in 1935.<sup>13</sup> Langmuir was awarded the Nobel Prize in Chemistry in 1932 for his significant contributions in surface chemistry.

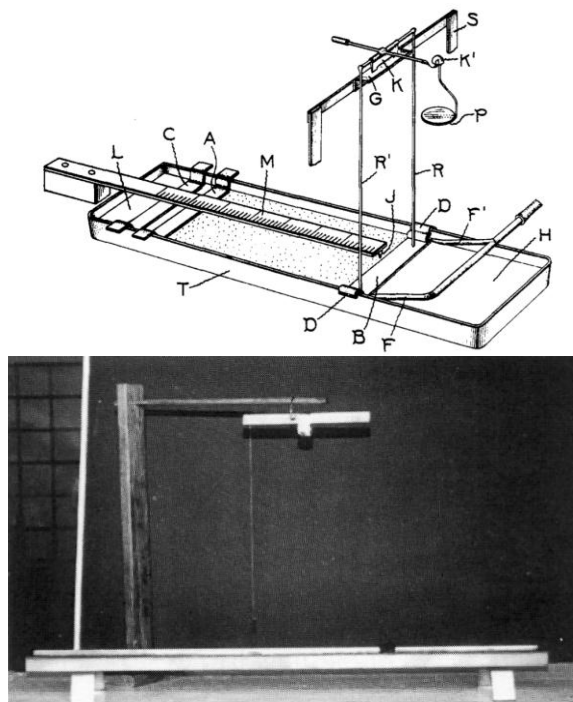


**Figure 3.2** (Top) Drawing of Langmuir's original film balance.<sup>12</sup> (Bottom) Reconstructed trough at TU Braunschweig.<sup>14</sup>

### 3.2 Theory

Molecules in a liquid have a certain amount of attraction towards one another called cohesion. The degree of attraction is dependent on the substance. The molecules deep in the solution have attractive forces pulling equally in all directions, balancing any net attraction. Molecules at the surface, however, have an imbalance of forces and experience a larger attraction towards the liquid (Figure 3.3). This overall imbalance of attraction causes those molecules at the air/ water interface to minimize their areas and contract. The result of this net attraction towards the bulk is the surface free energy and is accessible through measurements of the surface tension,  $\gamma$ , where  $G$  is Gibbs free energy, and  $s$  is the surface area (Eq. 3.1).<sup>15</sup> Temperature,  $T$ , pressure,  $P$ , and number of molecules,  $n_i$  are held constant. For water,  $\gamma$  is around 73 mN/ m at 20 °C.

$$\gamma = \left( \frac{\partial G}{\partial s} \right)_{T, P, n_i} \quad (3.1)$$

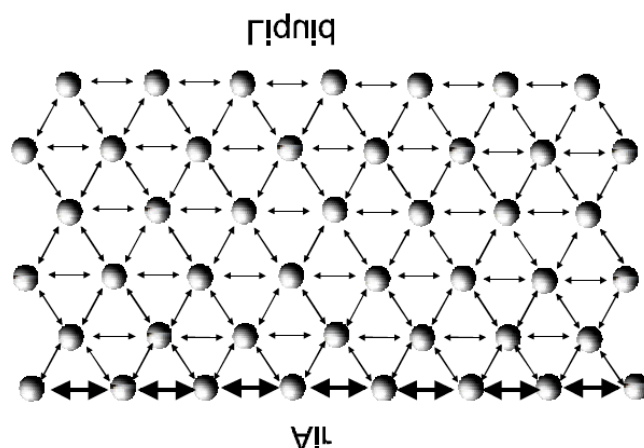


**Figure 3.3** Interaction of molecules at the air/ water interface.<sup>16</sup>

If the molecules interacting in the bulk are polar, such as water, there are strong intermolecular interactions resulting in high surface tensions. To decrease the surface tension, one must decrease the strength of the intermolecular interactions. This can be done by introducing contaminants, such as surfactants, or increasing the temperature of the system.

### 3.3 Langmuir films

A substance is applied to the water surface by first dissolving it in a water insoluble, volatile solvent, such as chloroform. The solution is placed on the water surface using a microsyringe, then the molecules quickly spread to cover the entire available surface. The solvent slowly evaporates and the molecules form a monolayer. When the amphiphile's headgroup is hydrophilic and tail hydrophobic, the tail points towards the air (Figure 3.4<sup>17</sup>). It is also possible to have the reverse situation, where the hydrophilic tail is immersed in the water and the hydrophobic headgroup sits atop the surface in the air.

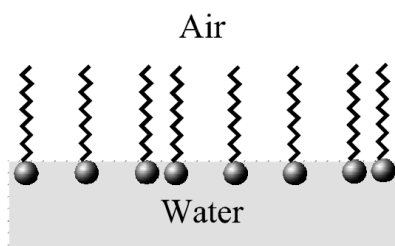


**Figure 3.4** Monolayer with a hydrophilic headgroup immersed in the water and hydrophobic tail pointing in the air.

When the trough is fully open, the available area for the monolayer is large and the intermolecular interactions are weak. The monolayer is considered a two-dimensional gas at this point and has little effect on the surface pressure of water. As the barriers to the system close, the interactions between molecules increases and the molecules repulse one another. The system now experiences an increase in the two-dimensional pressure, called surface pressure<sup>15</sup>,  $\Pi$ , given by the following equation:

$$\Pi = \gamma - \gamma_0$$

where  $\gamma$  is the surface tension without a monolayer and  $\gamma_0$  is the surface tension with a monolayer present.

The most common indicator of the monolayer properties of a material is reported by measuring the surface pressure as a function of mean molecular surface area. Compressing the system at a constant rate and recording the change in surface pressure provides a surface pressure to area isotherm, as shown in Figure 3.5. One can see that at low surface pressure, the molecules are considered to be in a gaseous state and experience minimal repulsion to the surrounding molecules. Upon compression of the barriers, the surface pressure slightly increases as the mean molecular area decreases and the molecules adopt a liquid expanded state. Further compression of the barriers results in a sharp increase in the surface pressure when the molecules begin to transition into the condensed state, also considered the solid state of the monolayer. If one continues to close the barriers past the condensed state the monolayer will collapse into three-dimensional structures and the isotherm will not be reproducible.

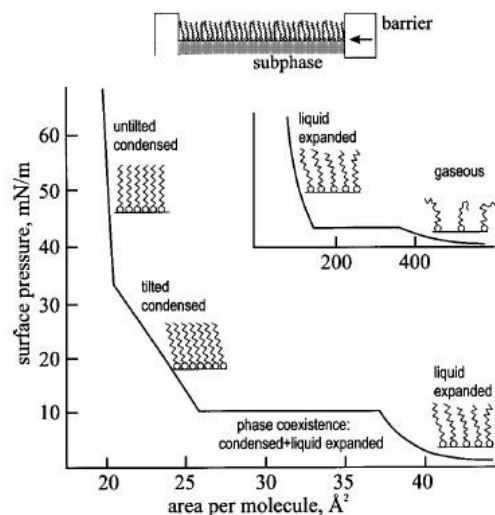


**Figure 3.5** Schematic surface pressure to mean molecular area isotherm for an amphiphile.<sup>14</sup>

### 3.4 Langmuir-Blodgett films

It is possible to transfer the condensed monolayer from the surface of water to a solid substrate. This technique is known as forming a Langmuir-Blodgett film. The initial Langmuir isotherm can provide some insight about the stability of the monolayer and the potential success for a transfer of the monolayer to a solid support. A successful deposition of the material should be done at a surface pressure range between 10 to 40 mN/ mol, often at a rate of 1 mm/ s.<sup>14</sup>

There are many variables that contribute to the final structure of the multilayer film. The composition and position of the substrate depends on the molecule to be deposited. If one wants that the hydrophilic headgroup of the molecule attach to the surface, a hydrophilic subphase should be in the water before the condensed monolayer is formed. Then, as the subphase is slowly lifted from the water, the monolayer will transfer as shown in the top left illustration of Figure 3.6. Furthermore, deposition of the subsequent layers can also be controlled to form three different types of multilayers, X, Y or Z-type.

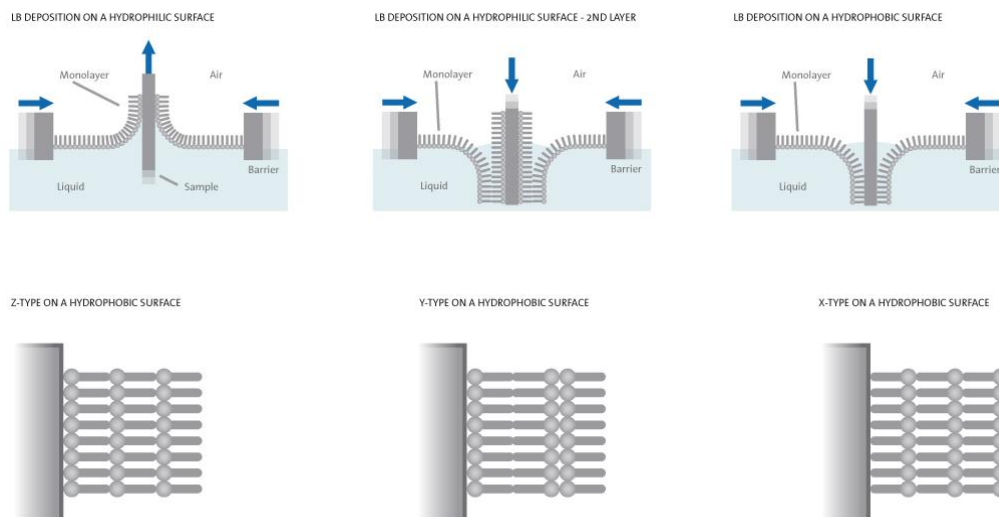


**Figure 3.6** Langmuir-Blodgett deposition types Z, Y and X multilayers.<sup>18</sup>

### 3.5 Present work

The ability to form stable monolayers and deposit them on a solid substrate has opened the door for many new and better controlled applications. These functions range from electronics and optics to biosensors and biochemical probes. The highly organized multilayers allow for controlled intermolecular interactions such as orientation, distance and extent of interaction between molecules.

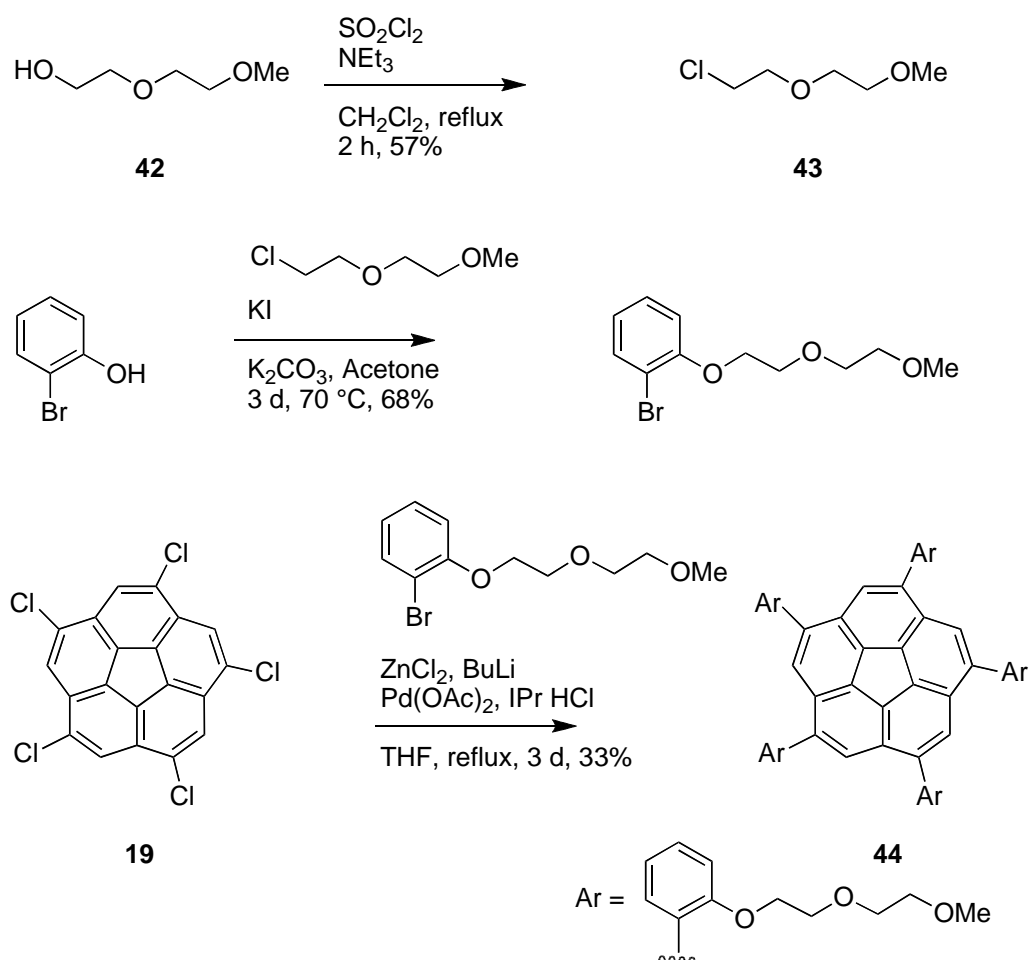
More specifically, there have been many studies of fullerenes, calixarenes, and other aromatic compounds as Langmuir-Blodgett films. One could imagine that studying the stability of corannulene derivatives, as potentially transferable monolayers, would mark the first step towards their potential application in materials. The goal of this project was to probe the formation and stability of Langmuir isotherms with different pentasubstituted corannulene derivatives.

The first series of corannulene derivatives consisted of *sym*-penta(polyethylene glycol)corannulenes, previously reported in this group.<sup>19</sup> The synthesis was reproduced for this study with slightly increased yields.

The polyethylene glycol (PEG) linkers were synthesized by first converting 2-(2-methoxyethoxy)ethanol (**42**) to its chloride derivative (**43**), for the shortest chained derivative. Using the Williamson ether synthesis, **43** was coupled to 2-bromophenol using potassium iodide and potassium carbonate resulting in the aryl(PEG) linker, which

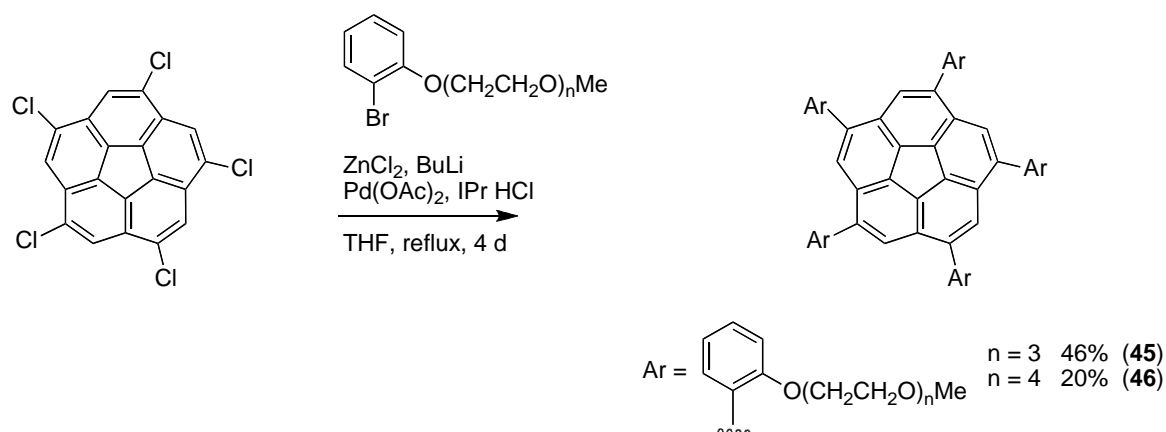
was then coupled to pentachlorocorannulene (**19**) to afford the desired product, *sym*-penta[[2-(2-methoxyethoxy)ethoxy]phenyl]corannulene (**44**), in a 33% yield (Scheme 3.1). Two additional corannulene derivatives were synthesized, **45** and **46**, following the same procedure (Scheme 3.2).

**Scheme 3.1** Synthesis of **44**



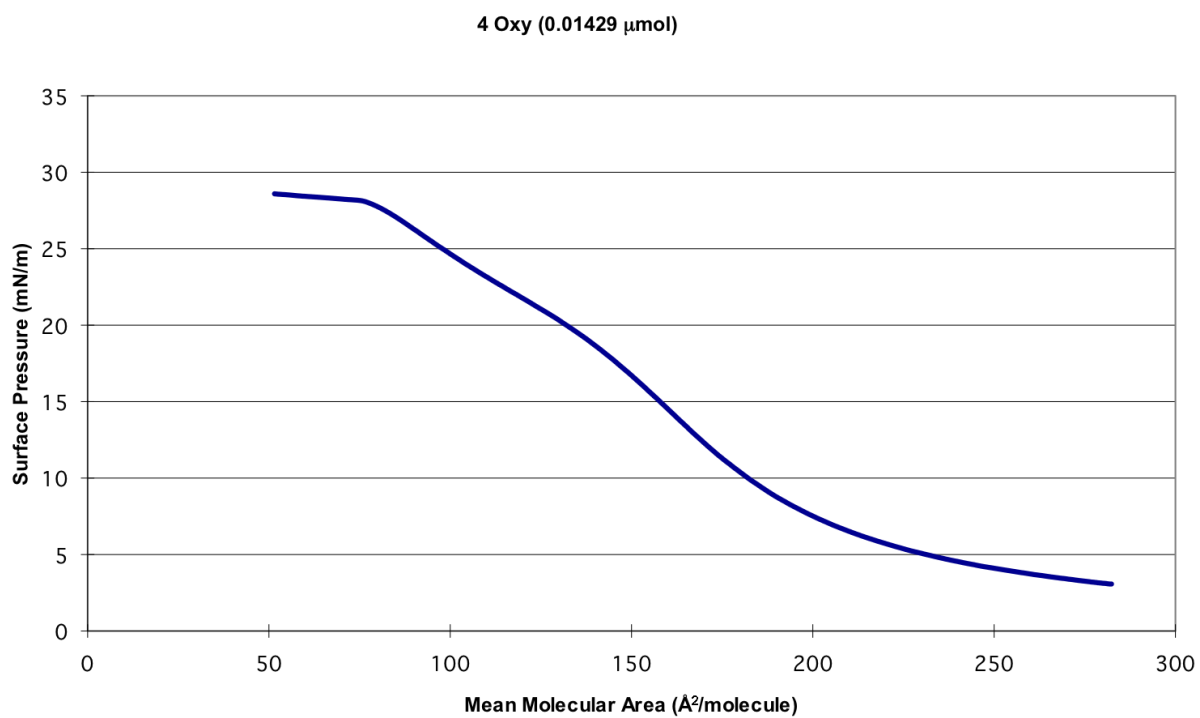
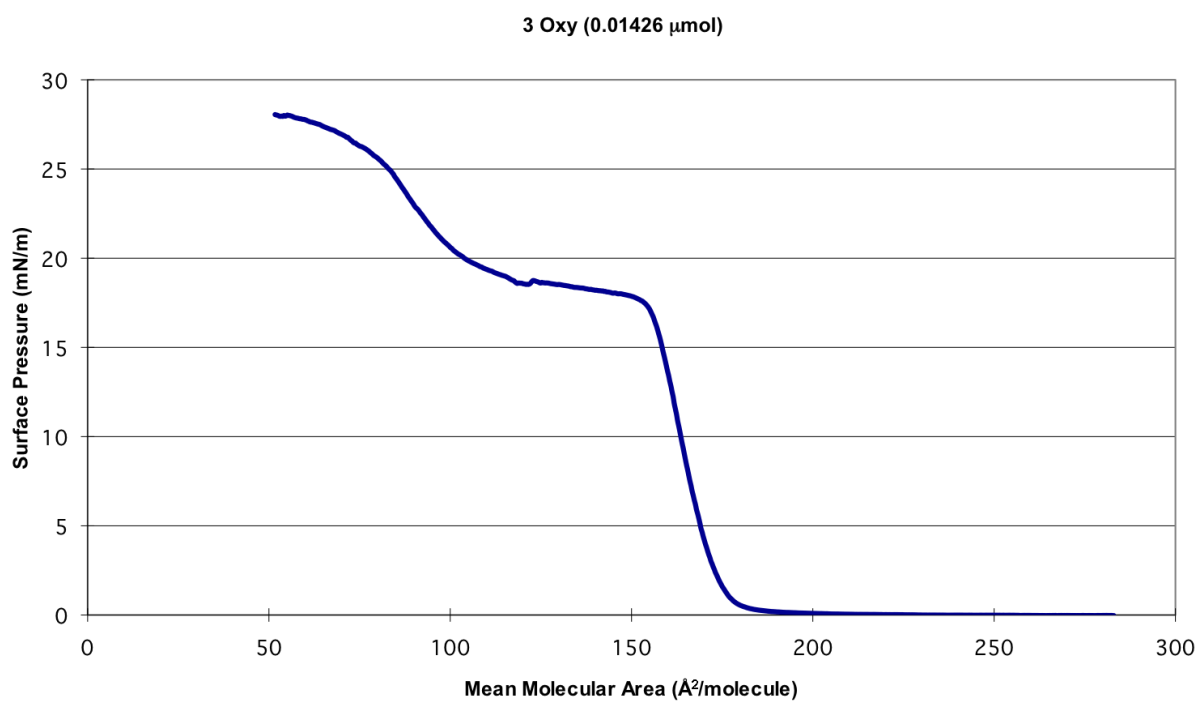
**Scheme 3.2** Synthesis of **45** and **46**





### 3.6 Results and discussion

First, the surface-pressure to area isotherms were measured to determine the various states of the molecule and the collapse point of the monolayers. This provided the pressure to which the isotherm could reproducibly be compressed. The shortest chained PEG derivative, called “3 oxy” for the number of oxygens on one ligand, the collapse point was at approximately 18 mN/ m for a 14 nm concentration. Extending the PEG chain by additional ethylene glycol units to the corresponding “4 oxy” and “5 oxy” derivatives results in unclear collapse points for the isotherms at comparable concentration (Figure 3.7).



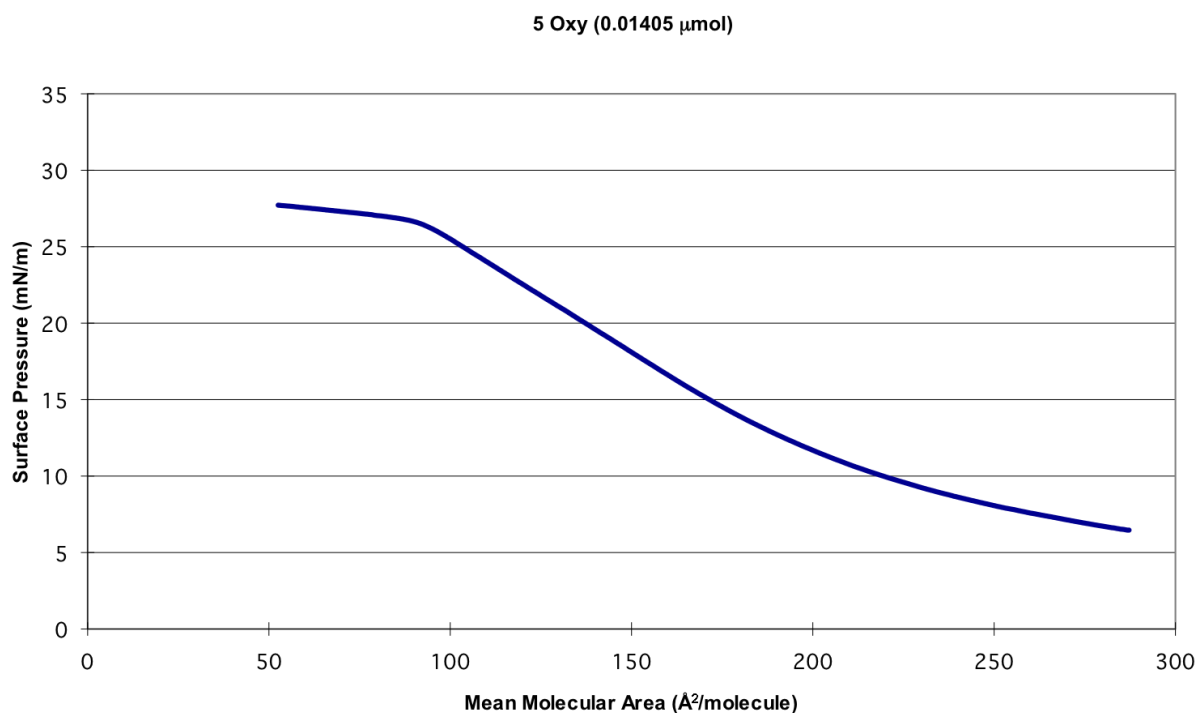
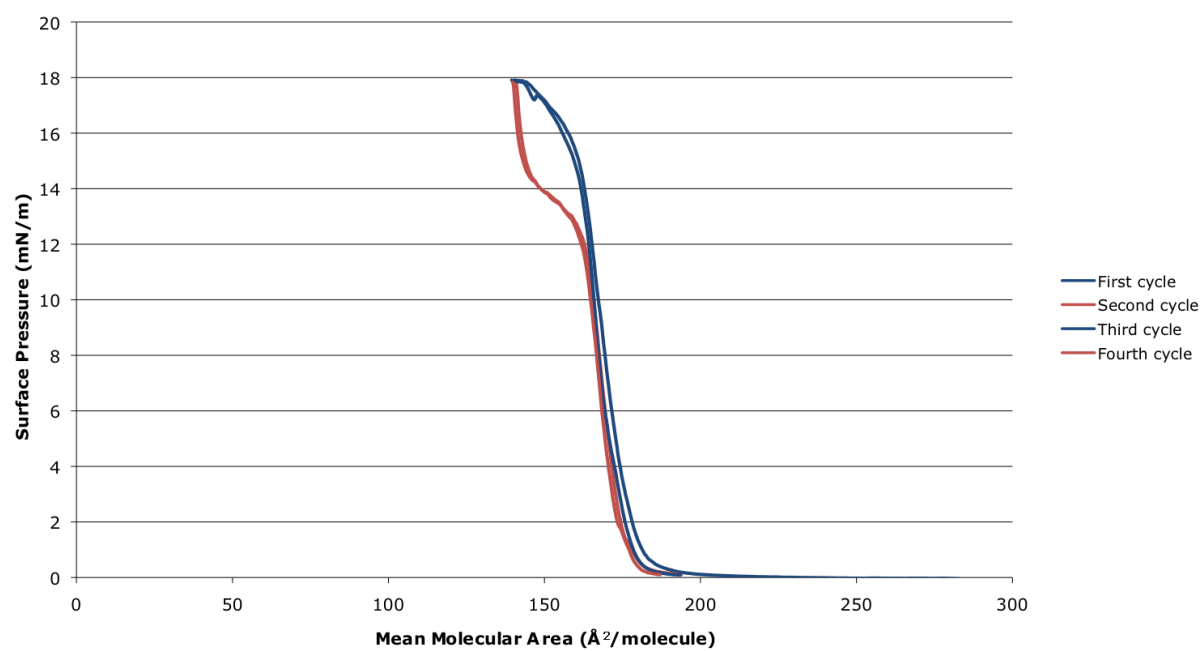


**Figure 3.7** Surface pressure to area isotherms for single compression of molecules (top) **44**, (middle) **45** and (bottom) **46**.

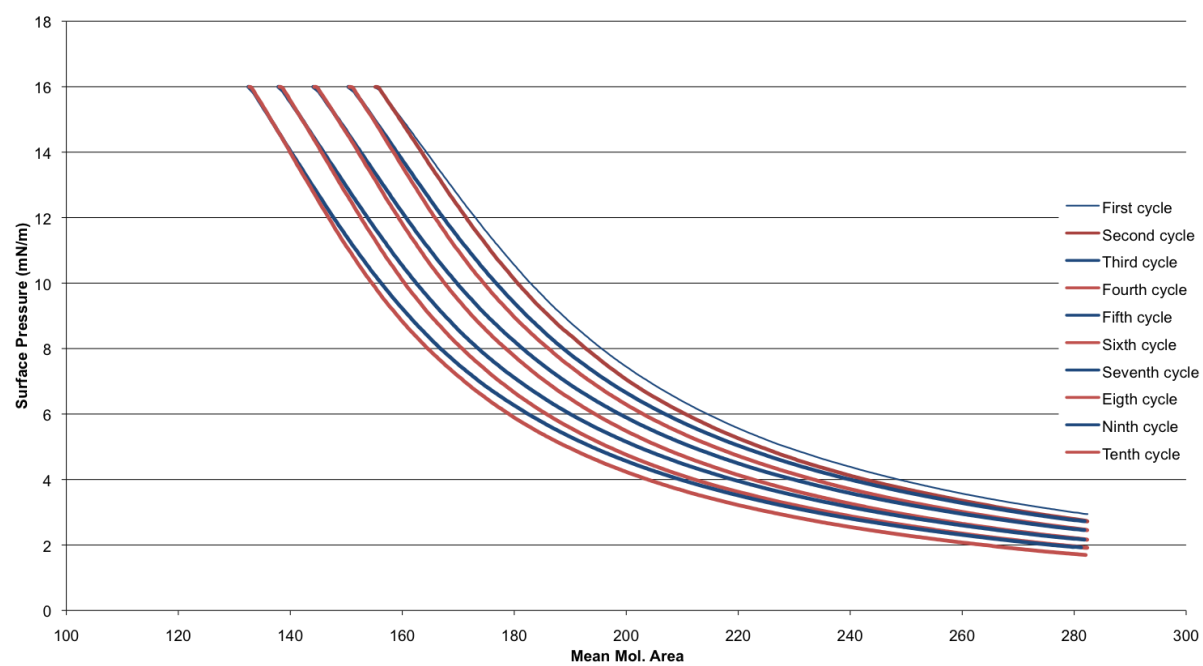
After the initial isotherms were measured, the monolayers were reformed to test reproducibility upon compression. As mentioned earlier, if the isotherm is compressed to a pressure below the collapse point, then upon expanding the troughs then recompressing, the isotherms should be reproducible.

The resulting compression/ expansion isotherms are shown below (Figure 3.8). Odd number cycles are compressions of the system and even number cycles are expansions. The systems were allowed to rest at the end of each cycle. From the first isotherm, one can see that molecule **44** was able to compress/ expand reproducibly. However, in the case of molecules **45** and **46** there was always a systematic shift, regardless of the number of cycles, maximum compression point, or concentration.

### 3 Oxy (0.01426 $\mu\text{mol}$ )



### 4 Oxy (0.01429 mmol)



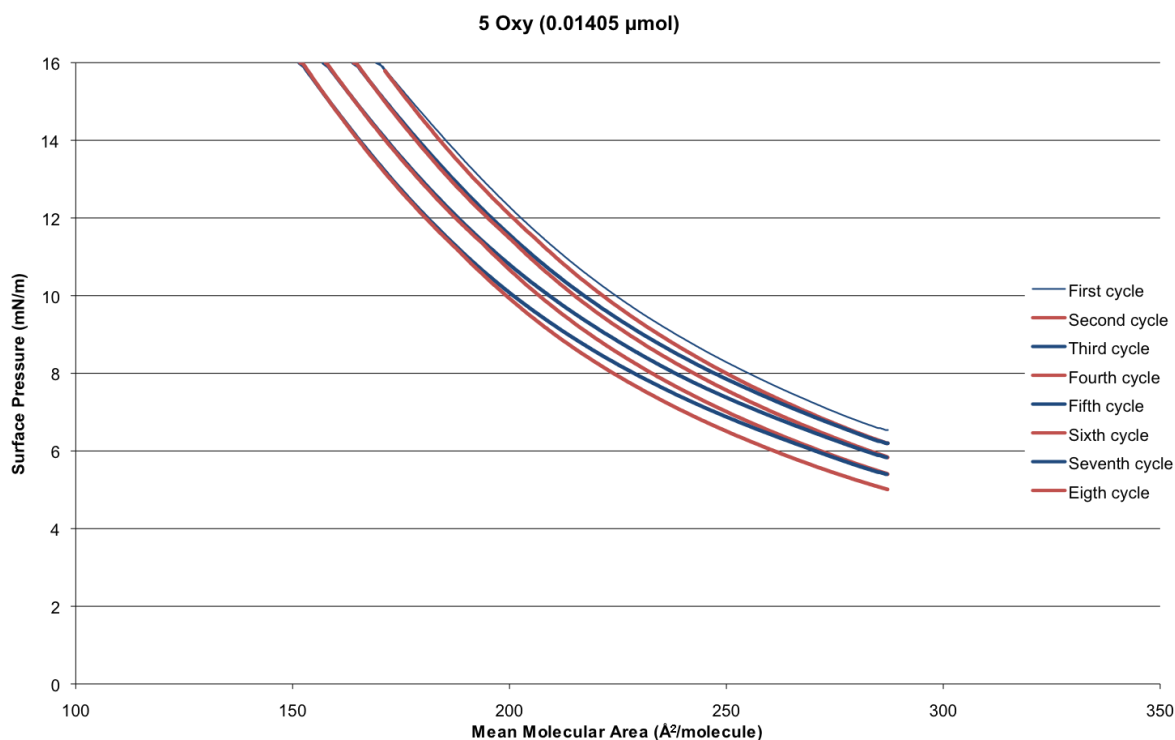


**Figure 3.8** Compression/ expansion isotherms showing reproducibility in molecule **44** (top), but not in molecule **45** (middle) or molecule **46** (bottom).

The fact that the mean molecular area for compounds **45** and **46** always shifted to a smaller area upon compression led us to believe that aggregates were forming. An explanation for this is that upon compression, the molecules find a better fit with one another. As the system is expanded the interactions between molecules are strong enough that the molecules do not disperse to their original expanded state. If one remembers that the polyethylene glycol ligands are water soluble so penetrate the water and do not stick up into the air, it is conceivable that the extra stability in the aggregates are due to hydrogen bonding between the oxygens in the chain. Furthermore, the reason that molecule **44** does not form these aggregates is because the PEG ligands are too short to allow for much intermolecular interaction. Low-level calculations support this explanation. Figure 3.9 shows molecule **45** in its preferred state. One can see that the length of the ligands is just far enough to surpass the diameter of the corannulene core.

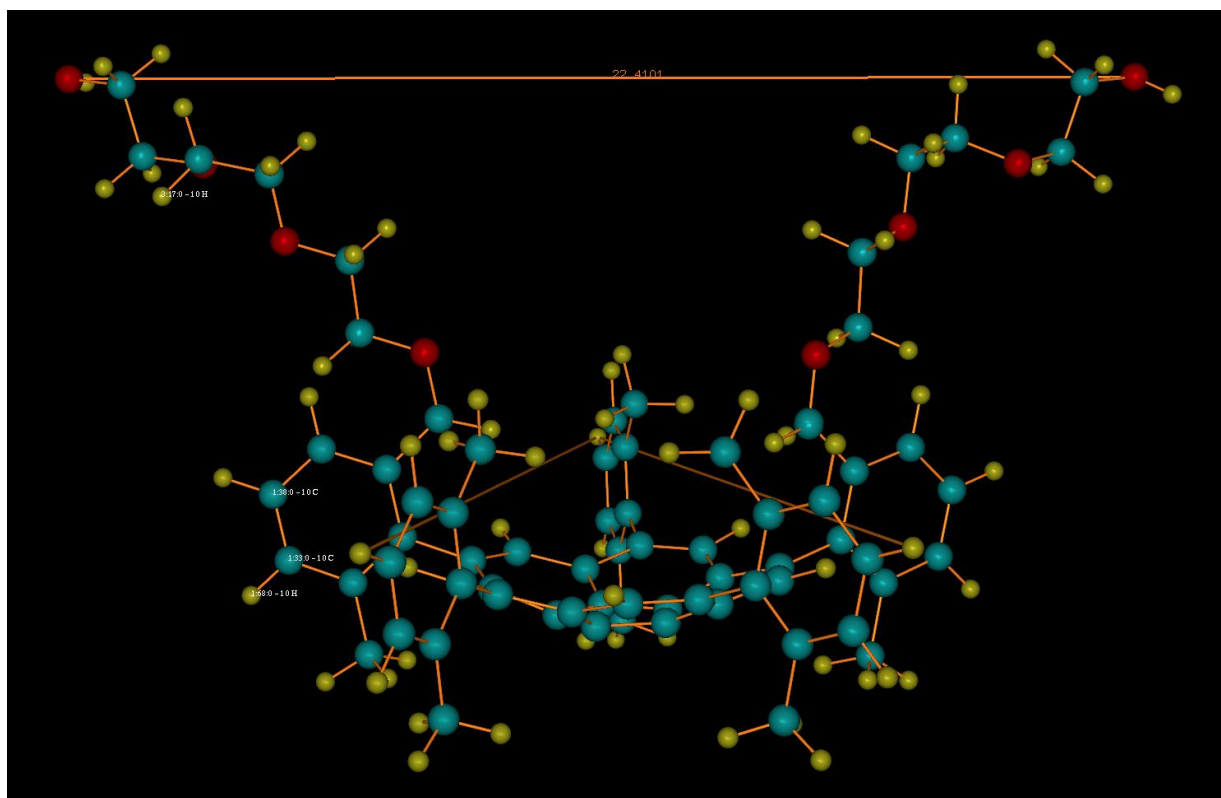


**Figure 3.9** Calculated structure of **45** showing the PEG ligands expand past the corannulene core of the molecule.

### 3.7 Experimental

All reactions were carried out under a nitrogen atmosphere using freshly distilled solvents unless otherwise noted. Pentachlorocorannulene was prepared according to the literature procedure. All commercially available compounds were purchased through Sigma Aldrich. Compounds **44-46** were prepared according to previous work in the group. Spectra matched that of reported.<sup>19</sup>

#### 2-(2-methoxyethoxy)ethoxy chloride (**43**)

To a mixture of 2-(2-methoxyethoxy)ethanol (**42**) (20.0 g, 166 mmol) and triethylamine (25.2 g, 250 mmol) in dichloromethane (600 mL), thionyl chloride (26 g, 218 mmol) was slowly added. The mixture was refluxed for 2.5 h then cooled to 23 °C and quenched with a saturated sodium hydrogen carbonate solution (700 mL). The organic layer was collected and the remaining aqueous phase was washed three times with diethylether.

The organic layers were dried with magnesium sulfate and the solvent was removed under reduced pressure. The product was distilled by fractional distillation to yield 13.13 g (57 % yield) of a colorless oil.

#### **1-bromo-[2-(2-methoxyethoxy)ethoxy]benzene**

2-Bromophenol (3.46 g, 20 mmol), 2-(2-methoxyethoxy)ethoxy chloride (**43**) (3.61 g, 26 mmol), potassium iodide (5.0 g, 30 mmol), and potassium carbonate (4.0 g, 30 mmol) in acetone (20 mL) were refluxed for 3 d. The mixture was cooled to 23 °C, filtered over Celite and washed with diethylether. The organic layer was washed with a 2 M aq. NaOH solution then dried with magnesium sulfate and reduced under pressure. The product was purified by column chromatography (SiO<sub>2</sub>), eluent: hexane/ dichloromethane 3:1 to yield 3.72 g (68%) of a yellow oil.

#### ***sym*-Penta[[2-(2-methoxyethoxy)ethoxy]phenyl]corannulene (**44**)**

A solution of 1-bromo-[2-(2-methoxyethoxy)ethoxy]benzene (1.5 g, 5.45 mmol) in THF (80 mL) was cooled to -78 °C in a dry ice/ acetone bath. *n*-Butyllithium (1.5 M in hexane, 3.93 mL, 5.9 mmol) was slowly added. Zinc chloride (1.12 g, 8.1 mmol) in THF (20 mL) was added and the solution was warmed to room temperature and allowed to stir for 30 min. The solution was then added to a round bottom flask containing pentachlorocorannulene (**19**) (250 mg, 0.570 mmol), Pd(II)OAc (123 mg, 0.545 mmol), and IPrHCl (230 mg, 0.545 mmol) in 40 mL THF. The solution was refluxed for 4 d then cooled to room temperature and filtered over Celite and washed with dichloromethane. The solvent was removed under pressure and the compound was purified by column chromatography (aluminum oxide, 5% deactivated with water), eluent dichloromethane/ ethyl acetate 5:1 to yield 235 mg (33%) of a yellow solid (**44**).

#### **2-[2-(2-methoxyethoxy)ethoxy]ethoxy chloride**

To a mixture of 2-[2-(2-methoxyethoxy)ethoxy]ethanol (40.0 g, 240 mmol) and triethylamine (37 g, 363 mmol) in dichloromethane (1 L), thionyl chloride (40 g, 321 mmol) was slowly added. The mixture was refluxed for 4.5 h then cooled to 23 °C and quenched with a saturated sodium hydrogen carbonate solution (1100 mL). The organic

layer was collected and the remaining aqueous phase was washed three times with diethylether. The organic layers were dried with magnesium sulfate and the solvent was removed under reduced pressure. The product was distilled by fractional distillation to yield 34.5 g (80 % yield) of a pale yellow oil.

#### **1-bromo-[2-[2-(2-methoxyethoxy)ethoxy]ethoxy]benzene**

2-Bromophenol (3.46 g, 20 mmol), 2-[2-(2-methoxyethoxy)ethoxy]ethoxy chloride (4.56 g, 25 mmol), potassium iodide (5.0 g, 30 mmol), and potassium carbonate (4.0 g, 30 mmol) in acetone (20 mL) were refluxed for 3 d. The mixture was cooled to 23 °C, filtered over Celite and washed with diethylether. The organic layer was washed with a 2 M aq. NaOH solution then dried with magnesium sulfate and reduced under pressure. The product was purified by column chromatography (SiO<sub>2</sub>), eluent: hexane/ dichloromethane 1:1 to yield 5.78 g (90%) of a yellow oil.

#### ***sym*-Penta[[2-(2-methoxyethoxy)ethoxy]phenyl]corannulene (**45**)**

A solution of 1-bromo[2-[2-(2-methoxyethoxy)ethoxy]ethoxy]benzene (1.0 g, 3.13 mmol) in THF (40 mL) was cooled to -78 °C in a dry ice/ acetone bath. *n*-Butyllithium (1.5 M in hexane, 2.3 mL, 3.43 mmol) was slowly added. Zinc chloride (640 mg, 4.67 mmol) in THF (20 mL) was added and the solution was warmed to room temperature and allowed to stir for 30 min. The solution was then added to a round bottom flask containing pentachlorocorannulene (**19**) (120 mg, 0.285 mmol), Pd(II)OAc (70 mg, 0.312 mmol), and IPrHCl (135 mg, 0.320 mmol) in 25 mL THF. The solution was refluxed for 4 d then cooled to room temperature and filtered over Celite and washed with dichloromethane. The solvent was removed under pressure and the compound was purified by column chromatography (aluminum oxide, 5% deactivated with water), eluent dichloromethane/ ethyl acetate 4:1 to yield 117 mg (57%) of an orange solid (**45**).

#### **2-[2-[2-(2-methoxyethoxy)ethoxy]ethoxy]ethoxy chloride**

To a mixture of 2-[2[2-(2-methoxyethoxy)ethoxy]ethoxy]ethanol (2.50 g, 12 mmol) and triethylamine (1.82 g, 18 mmol) in dichloromethane (80 mL), thionyl chloride (1.88 g, 15.8 mmol) was slowly added. The mixture was refluxed for 4.5 h then cooled to 23 °C and



quenched with a saturated sodium hydrogen carbonate solution (100 mL). The organic layer was collected and the remaining aqueous phase was washed three times with diethylether. The organic layers were dried with magnesium sulfate and the solvent was removed under reduced pressure. The product was distilled by fractional distillation to yield 1.82 g (67 % yield) of a yellow oil.

**1-bromo-[2-[2-[2-(2-methoxyethoxy)ethoxy]ethoxy]ethoxy]benzene**

2-Bromophenol (0.953 g, 5.5 mmol), 2-[2-[2-(2-methoxyethoxy)ethoxy]ethoxy]ethoxy chloride (1.50 g, 6.6 mmol), potassium iodide (1.35 g, 8.26 mmol), and potassium carbonate (1.14 g, 8.27 mmol) in acetone (12 mL) were refluxed for 3 d. The mixture was cooled to 23 °C, filtered over Celite and washed with diethylether. The organic layer was washed with a 2 M aq. NaOH solution then dried with magnesium sulfate and reduced under pressure. The product was purified by column chromatography (SiO<sub>2</sub>), eluent: 100% ether to yield 2.04 g (quant.) of a yellow oil.

***sym*-Penta[[2-(2-methoxyethoxy)ethoxy]phenyl]corannulene (46)**

A solution of 1-bromo-[2-[2[2-(2-methoxyethoxy)ethoxy]ethoxy]ethoxy]benzene (500 mg, 1.40 mmol) in THF (20 mL) was cooled to -78 °C in a dry ice/ acetone bath. *n*-Butyllithium (1.5 M in hexane, 1.04 mL, 1.56 mmol) was slowly added. Zinc chloride (290 mg, 2.1 mmol) in THF (10 mL) was added and the solution was warmed to room temperature and allowed to stir for 30 min. The solution was then added to a round bottom flask containing pentachlorocorannulene (**19**) (60 mg, 0.140 mmol), Pd(II)OAc (32 mg, 0.142 mmol), and IPrHCl (60 mg, 0.142 mmol) in 10 mL THF. The solution was refluxed for 5 d then cooled to room temperature and filtered over Celite and washed with dichloromethane. The solvent was removed under pressure and the compound was purified by column chromatography (aluminum oxide, 5% deactivated with water), eluent: dichloromethane/ ethyl acetate 20:1 to yield 82 mg (34%) of a yellow solid (**46**).

- 
- <sup>1</sup> Tabor, D. *J. Colloid Interface Sci.* **1980**, 75, 240.
- <sup>2</sup> Fulford, G. D. *Isis* **1968**, 59, 198.
- <sup>3</sup> Franklin, B. *Philos. Trans. R. Soc. London* **1774**, 64, 445.
- <sup>4</sup> Giles, C. H. *Chem. Ind* **1969**, 1616.
- <sup>5</sup> Shields, J. British Patent 3490, **1879**.
- <sup>6</sup> Aitken, J. *Proc. R. Soc. Edinburgh* **1882**, 12, 56.
- <sup>7</sup> (a) Forrester, S. D.; Giles, C. H. *Chem. Ind.* **1979**, 469. (b) Rayleigh, L. *Proc. Lond. Math. Soc.* **1879**, 10, 4.
- <sup>8</sup> (a) Rayleigh, L. *Proc. R. Soc. London* **1890**, 47, 281. (b) Rayleigh, L. *Proc. R. Soc. London* **1890**, 13, 85. (c) Rayleigh, L. *Proc. R. Soc. London* **1890**, 48, 127. (d) Rayleigh, L. *Philos. Mag.* **1890**, 30, 386.
- <sup>9</sup> Rayleigh, L. *Proc. R. Soc. London*, **1890**, 47, 364.
- <sup>10</sup> (a) Giles, C. H.; Forrester, S. D. *Chem. Ind.* **1970**, 90. (b) Giles, C. H.; Forrester, S. D. *Chem. Ind.* **1971**, 43.
- <sup>11</sup> (a) Pockels, A. *Nature* **1891**, 43, 437. (b) Pockels, A. *Nature* **1892**, 46, 418. (c) Pockels, A. *Nature* **1893**, 48, 152.
- <sup>12</sup> Langmuir, I. *J. Am. Chem. Soc.* **1917**, 39, 1848.
- <sup>13</sup> (a) Langmuir, I. *Trans. Faraday Soc.* **1920**, 15, 62. (b) Blodgett, K. B. *J. Am. Chem. Soc.* **1935**, 57, 1007.
- <sup>14</sup> Roberts, G., *Langmuir-Blodgett Films*, Plenum Press: New York, 1990.
- <sup>15</sup> Gaines, G. L., *Insoluble Monolayers at the Liquid-Gas Interface*, Wiley-Interscience: New York, 1966.
- <sup>16</sup> (a) Adamson, A. W., *Physical Chemistry of Surfaces*, Wiley & Sons: New York, 1976. (b) Shaw, D.J., *Introduction to Colloid and Surface Chemistry*, Butterworth & Co: London, 1980.
- <sup>17</sup> Chatteraj, D. K.; Birdi, K. S. *Adsorption and the Gibbs Surface Excess*, Plenum Press: New York, 1984 .
- <sup>18</sup> Binks, B. P. *Adv. Colloid Interface Sci.*, **1991**, 34, 343.

---

<sup>19</sup> Hayama, T. Ph.D. Dissertation, University of Zurich: Zurich, Switzerland, 2008.

## Chapter 4

### *Unit cell volume determination of $C_{20}H_{10}$ and $C_{20}D_{10}$*

#### 4.1 Introduction

A 2008 paper by Dunitz and Ibberson<sup>1</sup> questioned whether deuterium is always smaller than protonium. Although the authors acknowledged that the question, without context, is meaningless, one can nonetheless learn something about the influencing factors contributing to the effective size of protonium and deuterium in a crystal. This chapter will review the theory of isotope effect and answer the question that Dunitz and Ibberson proposed using benzene and perdeuterobenzene. A similar analysis will then be shown with corannulene and perdeuterocorannulene.

#### 4.2 Isotope Effect

Bigeleisen and Mayer first introduced the theory of isotope effect<sup>2</sup>, which is commonly used to describe the difference in reaction rates as a result of isotopic substitution. This change in reaction rate can be understood using the harmonic oscillator approximation to explain the vibrations of diatomic molecules.

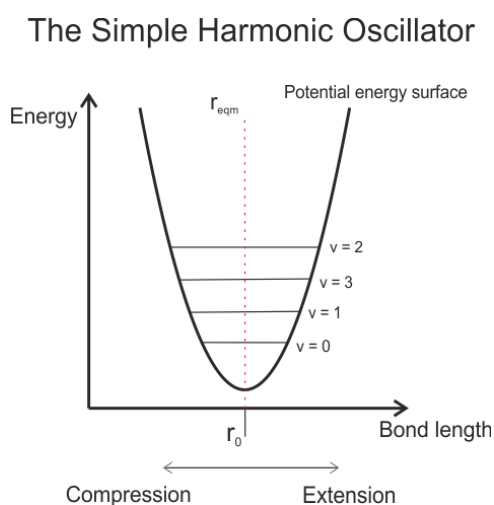


**Figure 4.1** Diagram of a harmonic oscillator<sup>3</sup>

If one considers that the energy of the vibrational levels ( $n$ ) of a bond is given by Eq. 4.1, where  $h$  is Plank's constant and  $\nu$  is the vibrational frequency, then at the zero point energy ( $n=0$ ),  $E=\frac{1}{2} h \nu$ . The vibrational frequency is given by Eq. 4.2, where  $k'$  is the force constant and  $\mu$  is the reduced mass, expressed by Eq. 4.3. It is from Eq. 4.3 that the effects of the heavier, deuterated molecule can be seen. As the fundamental vibrational frequency is inversely proportional to the reduced mass, the heavier mass will result in a lower zero point energy.

$$E_n = (n + \frac{1}{2})h\nu \quad (4.1)$$

$$\nu = \frac{1}{2\pi} \sqrt{\frac{k'}{\mu}} \quad (4.2)$$

$$\mu = \frac{m_1 m_2}{m_1 + m_2} \quad (4.3)$$

Superimposing the harmonic oscillator on a Morse's potential (Figure 4.2) shows that the deuterium atom, with the lower zero-point energy, also has a smaller vibrational amplitude and therefore smaller van der Waals radius than the protonium atom. Subsequently, the smaller effective radius leads to less repulsions and a smaller packing radius for deuterium than hydrogen. At low temperatures then, one should expect the deuterated molecule to have a smaller cell volume.

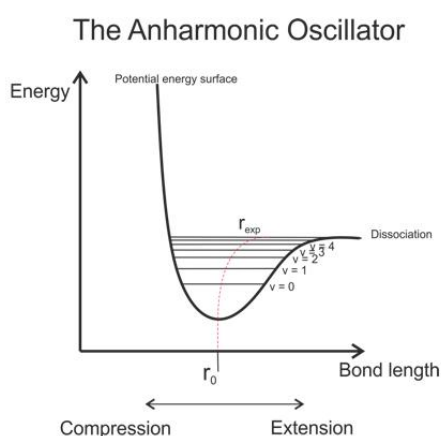


**Figure 4.2** Diagram of an anharmonic oscillator.<sup>3</sup>

The effects of the cell volume as temperature increases is expressed by the mean-square displacement amplitude (Eq. 4.4), which is the Boltzmann distribution over the energy levels of a quantized harmonic oscillator. Again,  $\nu$  is the frequency and  $\mu$  is the reduced mass. The first factor on the right-hand side of Eq. 4.4 is a result of the zero-point motion and similar to Eq. 4.2, is inversely proportional to the mass and hence smaller for the deuterated molecule.

$$\langle u^2 \rangle = (h/8\pi^2\mu\nu) \coth(h\nu/2kT) \quad (4.4)$$

The influence of temperature can be seen in the second factor of Eq. 4.4,  $\coth x$ , where  $x = h\nu/2kT = 0.7914\omega/T$ . At low temperatures,  $\coth x = 1$  and this second factor has no influence on the mean-square displacement amplitude. At higher values of  $T$ ,  $\coth x$  becomes proportional to  $T$  with a slope of  $1.390/\omega$ . The result is that for low-frequency oscillations, as temperature increases, the higher vibrational levels become more populated for deuterated molecules than for their proton isotopologues. One can therefore expect that these larger vibrational amplitudes will result in an enhancement of the frequency effect over the mass effect and that the effective size of deuterium will expand faster than that of hydrogen.

### 4.3 Benzene and perdeuterobenzene

To test this hypothesis, Dunitz and Ibberson looked at the molecular volume ( $V_{\text{mol}}$ ) of benzene ( $\text{C}_6\text{H}_6$ ) and perdeuterobenzene ( $\text{C}_6\text{D}_6$ ). The molecular volume was determined by high-resolution neutron powder diffractometry as a function of temperature (Figure 4.3).

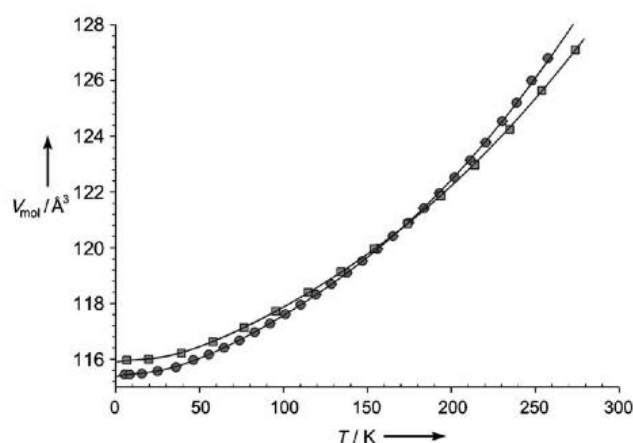


**Figure 4.3** Molecular volume ( $V_{\text{mol}}$ ) vs.  $T$  of benzene (squares) and perdeuterobenzene (circles) obtained from neutron powder diffraction.

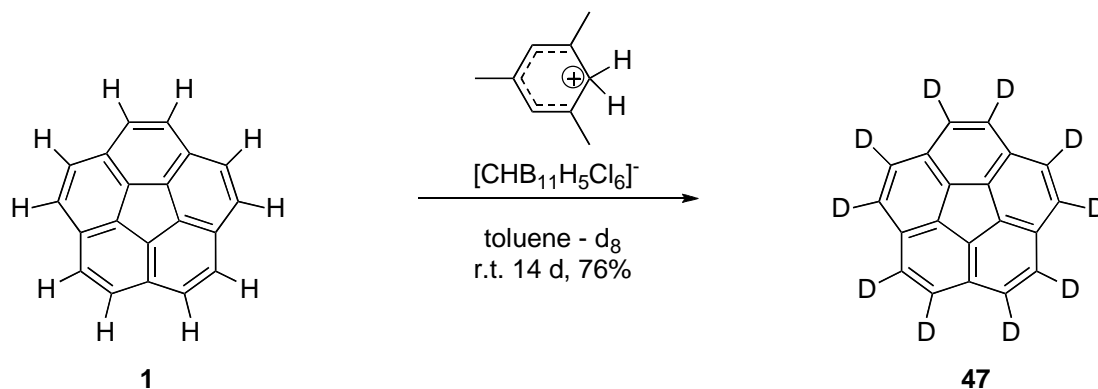
The results of these measurements showed that at low temperatures, 5 K, perdeuterobenzene had a molecular volume of  $115.452(1) \text{ \AA}^3$ , whereas benzene's molecular volume was slightly larger at  $115.967(2) \text{ \AA}^3$ . At higher  $T$ , 250 K, the opposite is seen and the molecular volume of perdeuterobenzene is now larger than that of benzene. The crossover temperature, where both isotopologues' molecular volumes are equal is around 170 K.

#### 4.4 Corannulene and perdeutero­corannulene

We wanted to apply the same analysis that Dunitz and Ibberson applied to  $\text{C}_6\text{H}_6$  and  $\text{C}_6\text{D}_6$  to  $\text{C}_{20}\text{H}_{10}$  (**1**) and  $\text{C}_{20}\text{D}_{10}$  (**47**) to see if these larger aromatic hydrocarbons also showed an inverse kinetic isotope effect. The first task was to make the perdeutero­corannulene. The literature contains many examples of H-/ D- exchange conditions so it was a little surprising when the synthesis was not trivial. Initially, it was believed that if corannulene was dissolved in a deuterated organic solvent and a few drops of acid were added, the H-/ D- exchange would be fast. This however was not the case. After a few days under reflux only starting material could be obtained. If stronger acid was used the reaction turned black and the yield of recovered starting material dropped dramatically, leading one to think that the material was polymerizing. No exchange on **1** could be observed by GC-MS. We were able to obtain

perdeuterocorannulene using a mesitylenium hexachlorocarborane species shown in Scheme 4.1. The corannulene and perdeuterocorannulene samples were purified by prep-HPLC to remove any impurities that might distort the measurements.

**Scheme 4.1** Synthesis of perdeuterocorannulene (**47**)



Powder diffraction data were recorded at the Swiss Light Source (SLS) of the Paul Scherrer Institute in Switzerland. The temperature ranged from 4.5 K to 490 K. Due to restrictions of the instrument setup, data was either collected at the low temperature (LT) range of 4.5 K to 290 K or the high temperature (HT) range of 250 K to 490 K. The overlapping 250 K to 290 K for LT and HT assured us that the data sets were comparable even if the same sample was not used for over the entire range from 4.5 K to 490 K. As the stability of the compound has never been tested under such extreme conditions, there was fear that the material would decompose from prolonged radiation and temperature exposures. The reproducibility for each data point was confirmed by performing the following experiment: the first corannulene sample at low temperature (HCOR1\_LT) was first measured at 4.5 K. The temperature was then increased by increments of 10 K and new samples were taken until 290 K. The capillary was then exchanged with a new sample of corannulene (HCOR2\_LT) and this time the first measurement was at 290 K. If there was any decomposition due to radiation exposure, it should be indicated by difference in the peak profile. Again, samples were taken in 10 K increments down to 4.5 K. The same procedure was followed for perdeuterocorannulene at low temperature and both molecules at high temperature.



The data was processed to obtain the unit cell volume using the program Maud. The silicon sample, which was mixed with both corannulene and perdeuterocorannulene, was first refined using the program. Then, each data set was fit to the silicon (Figure 4.4) and the sides of the unit cell volume,  $a$ ,  $b$ , and  $c$ , along with the angle  $\beta$  were used to calculate  $V_c$ . The data points were plotted unit cell volume vs. temperature (Figure 4.5).

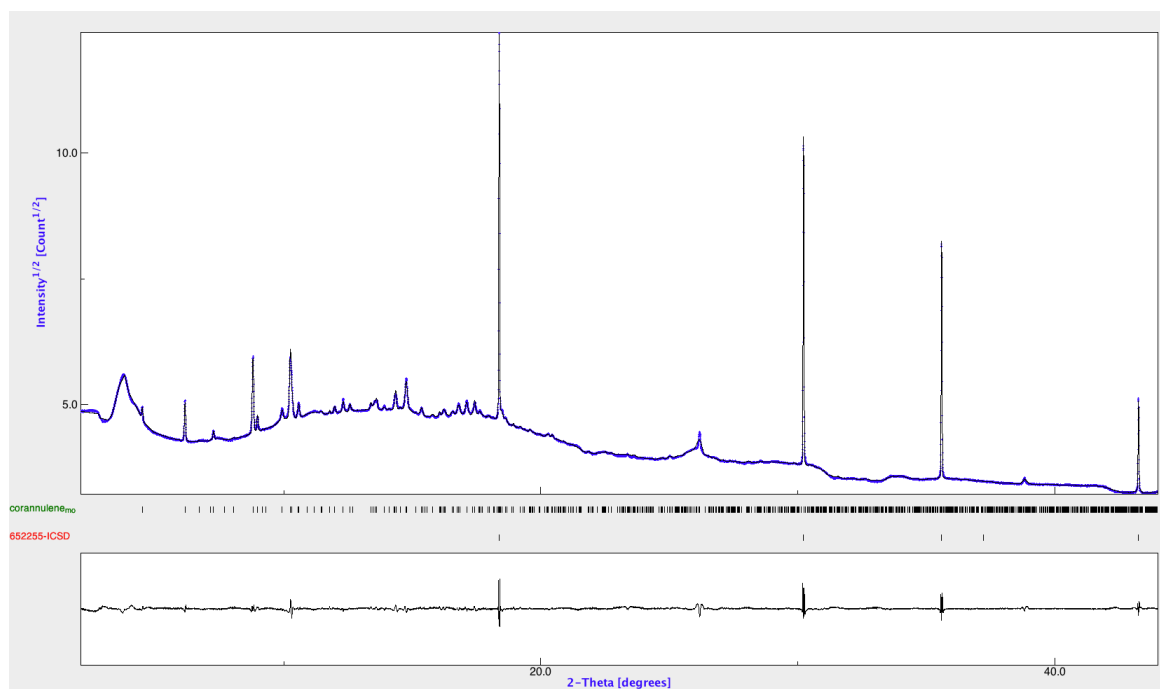


**Figure 4.4** X-ray powder diffractogram corannulene sample fit to the silicon standard.

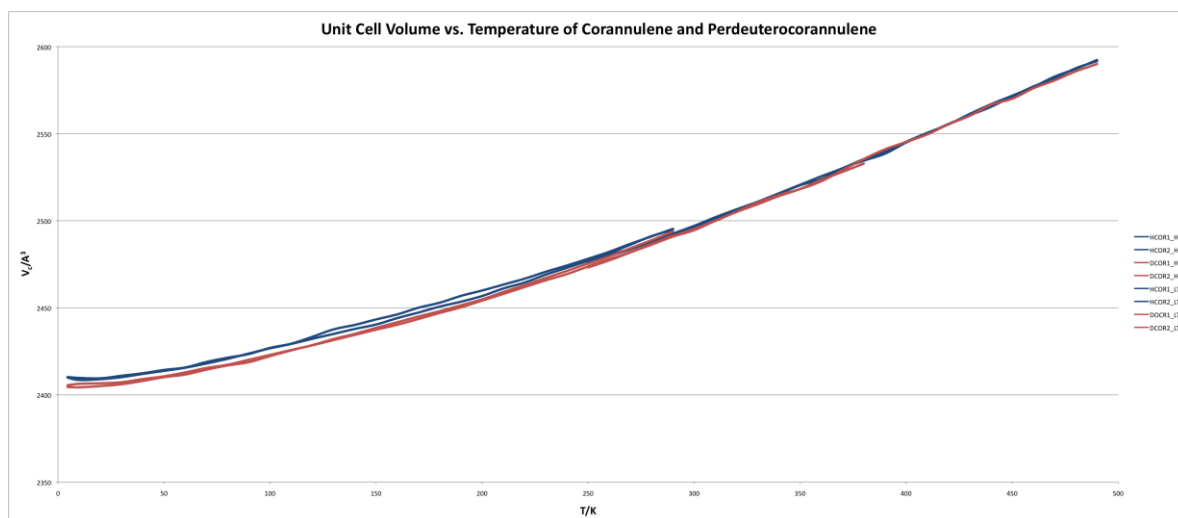


**Figure 4.5** Unit cell volume vs. temperature for  $C_{20}H_{10}$  (blue) and  $C_{20}D_{10}$  (red) from 4.5 K to 490 K.

## 4.5 Conclusions

Perdeuterocorannulene was synthesized in 76% yield using a mesitylenium acid. Variable temperature x-ray powder diffraction measurements were conducted for samples of corannulene and perdeuterocorannulene over a range of 4.5 K to 490 K. Unlike the benzene and perdeuterobenzene samples studied by Dunitz and Ibberson, no crossover point was seen for the  $C_{20}H_{10}/C_{20}D_{10}$  measurements. At 4.5 K, perdeuterobenzene has a unit cell volume of  $2405 \text{ \AA}^3$ , whereas corannulene has a unit cell volume of  $2410 \text{ \AA}^3$ . At 490 K, the unit cell volumes for perdeuterocorannulene and corannulene are closer to one another, at 2590 and  $2591 \text{ \AA}^3$  respectively. It is difficult to say whether or not the system was approaching the crossover point between the two isotopologues. One can imagine that the crystal might decompose at such high temperatures before the unit cell volume for **1** is smaller than perdeuterocorannulene.

## 4.6 Experimental

All reactions were carried out under a nitrogen atmosphere in a Braun Labmaster glovebox. Deuterated solvents were purchased from Armar Chemicals, HPLC solvents were purchased from Merck, and all other solvents for purification were technical grade and freshly distilled prior to use. Melting points (m.p.) were measured with a Büchi Melting Point P-540 apparatus and are uncorrected. IR were recorded on a Jasco FT/IR-410 spectrophotometer. Absorption bands are given in wavenumbers ( $\text{cm}^{-1}$ ), and intensities are characterized as follows: s= strong (0-33% transmission), m= medium (34-66% transmission), w= weak (67-100% transmission). High resolution mass data (HR-MS) were obtained by the Laboratory for Mass Spectroscopy of the Organic Chemistry Institute of the University of Zurich on a Finnigan MAT95 instrument. NMR spectra were recorded on a Bruker AV-500 instrument.  $^{13}\text{C}$  spectrum is proton decoupled. The signals were referenced against  $\text{CDCl}_3$  77.23 ppm. Mesitylenium hexachlorocarborane was prepared according to literature procedure.<sup>4</sup>

**Perdeuterocorannulene (47):** A small vial was charged with corannulene (500 mg, 2.00 mmol), mesitylenium hexachlorocarborane (25 mg, 0.053 mmol) and toluene-d<sub>8</sub> (25 mL) then stirred at 23 °C. After 6 d, additional mesitylenium hexachlorocarborane (5 mg, 0.011 mmol) was added. After 2 weeks the reaction was quenched with D<sub>2</sub>O. The aqueous phase was extracted with EtOAc three times. The combined organic layers were dried over MgSO<sub>4</sub>, filtered and concentrated *in vacuo*. Flash column chromatography (pure hexane) removed baseline impurities and the sample was further purified *via* prep-HPLC to afford **47** as white crystals (395 mg, 76%).

R<sub>f</sub> (hexane): 0.37

M.P.: 250.8-251.2 °C

<sup>13</sup>C-NMR (125.8 MHz, CDCl<sub>3</sub>): <sup>TM</sup> = 136.03, 130.89, 127.11, 127.00, 126.80, 126.60.

IR (neat, cm<sup>-1</sup>): 2956w, 2917w, 2849w, 1291w.

HR-MS (EI): Calculated for C<sub>20</sub>D<sub>10</sub>: 260.1410; measured: 260.1407.

---

<sup>1</sup> Dunitz, J. D.; Ibberson, R. M. *Angew. Chem. Int. Ed.* **2008**, *47*, 4208.

<sup>2</sup> Bigeleisen, J.; Mayer, M. G. *J. Chem. Phys.* **1947**, *15*, 261.

<sup>3</sup> Barnes, K.; Vernon, L. *ChemTube3D*, <http://www.chemtube3d.com/spectrovibcd1-CE-final.html> (accessed June 18, 2012).

<sup>4</sup> Reed, C. A. *Chem. Commun.* **2005**, *13*, 1669.

## Chapter 5

### *Temperature dependencies on the anisotropic displacement parameters of $C_{20}H_{10}$ and $C_{20}D_{10}$*

#### 5.1 Introduction

Although a crystal is defined as a solid material whose constituents are arranged in an ordered (periodic) arrangement, it is not accurate that, as Prof. Leopold Ruzicka once said, “a crystal is a chemical cemetery.”<sup>1</sup> As early as 1913 Debye already demonstrated how increasing the temperature of an x-ray diffraction experiment reduced the intensity of the Bragg diffractions but maintained the position and widths of the peaks.<sup>2</sup> Debye explained this effect to be a result of thermal vibrations of the atoms about their average positions.

X-ray diffraction measurements produce a superposition of a large number of snapshots, each characterized by its instantaneous positions of the atoms. These snapshots are averaged during the experiment and the information available from such data consists of atomic distributions characterized by their centers of electron density (average atomic positions) and by their mean square deviations from these centers (atomic displacement parameters, ADPs), represented by a Gaussian probability density function of the atomic position for each individual atom in the crystal.<sup>3</sup> Occasionally, a given atom permanently takes slightly different positions in different unit cells causing static disorder.<sup>4</sup> If these positions differ by less than the resolution of the experiment, they also contribute to the Gaussian distribution function, or ADPs. Thus, ADPs are the time and space average over the entire crystal and duration of the experiment. They have temperature dependent contributions arising from atomic vibrational motion and temperature independent contributions arising from static disorder. In the following we focus on extracting the vibrational information from the ADPs, assuming that static disorder is negligible.

#### 5.2 Experimental

Corannulene,  $C_{20}H_{10}$ , and deuterocorannulene,  $C_{20}D_{10}$ , were synthesized according to published procedures. Preparative-HPLC was used to remove any impurities in the sample then crystals

were grown from hexane/ *iso*-propanol at 4 °C. Neutron diffraction data was measured at the ILL at 20, 90, 173 K for both corannulene and deuterocorannulene. Scattering angle cutoffs were done at 0.5, 0.6, and 0.7 angstroms. X-ray measurements were also performed at 92, 173 and 250 K using crystals from the same sample. An additional 12 K x-ray measurement for corannulene was recently reported and also used during the development of the dynamic models.

### 5.3 Comparison

The first question that one should address is: how consistent is the data? With crystals grown from the same sample, diffraction data was obtained using two different methods at similar temperatures. One should therefore expect comparable results between the carbon atoms measured using neutron diffraction and x-ray diffraction at corresponding temperatures. That is to say, the average difference between neutron and x-ray data,  $\langle \Delta U_{ii} \rangle$ , is expected to be approximately zero. (Eq. 1) Furthermore, how does the root mean square of the diagonal components of U,  $RMS_{ii}$  (Eq. 2), and the off-diagonal components of U,  $RMS_{ij}$  (Eq. 3), compare to the standard deviation of the neutron data?

$$\langle \Delta U_{ii} \rangle = \frac{[\Sigma(U_{11}^N(T_N) - U_{11}^X(T_X)) + \Sigma(U_{22}^N(T_N) - U_{22}^X(T_X)) + \Sigma(U_{33}^N(T_N) - U_{33}^X(T_X))]}{60} \quad (5.1)$$

$$RMS_{ii} = \sqrt{\frac{\sum [U_{ii}^N(T_N) - U_{ii}^X(T_X)]^2}{60}} \quad (5.2)$$

$$RMS_{ij} = \sqrt{\frac{\sum [U_{ij}^N(T_N) - U_{ij}^X(T_X)]^2}{120}} \quad (5.3)$$

A second method to analyze the consistency of the data comes from the theory of isotope effect on ADPs.<sup>5</sup> This qualitative analysis is possible because at high temperatures,  $\langle U^2 \rangle$  behaves classically and varies linearly with the temperature and with the inverse square of the mass and  $\omega$ . (Eq. 4-5).<sup>6</sup> One should therefore expect the ADPs of deuterium to be lower than hydrogen by 2-4%.

$$\frac{U_H}{U_D} = f\left(\sqrt{\frac{MW_D}{MW_H}}\right) \approx 1.02 \quad (5.4)$$

$$\frac{U_H}{U_D} = f\left(\frac{\omega_D}{\omega_H}\right) \approx 1.04 \quad (5.5)$$

## 5.4 Results

**Table 5.1. Neutron diffraction data minus x-ray diffraction data at various scattering angle cutoffs and temperatures, (H=Corannulene, D=Deuterocorannulene).**

	<U <sub>ii</sub> >	RMS <sub>ii</sub>	Stand. Dev. <sub>ii</sub>	RMS <sub>ij</sub>	Stand. Dev. <sub>ij</sub>		<U <sub>ii</sub> >	RMS <sub>ii</sub>	Stand. Dev. <sub>ii</sub>	RMS <sub>ij</sub>	Stand. Dev. <sub>ij</sub>
<b>0.5</b> <b>H(A)<sub>90.</sub></b> 92K	0.00053	0.00080	0.00018	0.00064	0.00010	<b>0.5</b> <b>D(A)<sub>90.</sub></b> 92K	-0.00010	0.00101	0.00023	0.00087	0.00015
<b>0.6</b> <b>H(A)<sub>90.</sub></b> 92K	-0.00007	0.00064	0.00014	0.00053	0.00009	<b>0.6</b> <b>D(A)<sub>90.</sub></b> 92K	-0.00063	0.00116	0.00026	0.00095	0.00016
<b>0.7</b> <b>H(A)<sub>90.</sub></b> 92K	-0.00009	0.00070	0.00016	0.00058	0.00010	<b>0.7</b> <b>D(A)<sub>90.</sub></b> 92K	-0.00094	0.00138	0.00031	0.00113	0.00018
<b>0.5</b> <b>H(A)<sub>173.</sub></b> 173K	0.00103	0.00117	0.00026	0.00089	0.00010	<b>0.5</b> <b>D(A)<sub>173.</sub></b> 173K	0.00086	0.00115	0.00026	0.00092	0.00014
<b>0.6</b> <b>H(A)<sub>173.</sub></b> 173K	0.00060	0.00085	0.00019	0.00068	0.00010	<b>0.6</b> <b>D(A)<sub>173.</sub></b> 173K	0.00061	0.00096	0.00022	0.00081	0.00014
<b>0.7</b> <b>H(A)<sub>173.</sub></b> 173K	0.00070	0.00092	0.00021	0.00073	0.00010	<b>0.7</b> <b>D(A)<sub>173.</sub></b> 173K	0.00062	0.00100	0.00022	0.00085	0.00015
<b>0.5</b> <b>H(B)<sub>90.</sub></b> 92K	0.00035	0.00059	0.00013	0.00050	0.00009	<b>0.5</b> <b>D(B)<sub>90.</sub></b> 92K	-0.00049	0.00114	0.00026	0.00095	0.00016
<b>0.6</b> <b>H(B)<sub>90.</sub></b> 92K	-0.00024	0.00052	0.00012	0.00045	0.00008	<b>0.6</b> <b>D(B)<sub>90.</sub></b> 92K	-0.00095	0.00144	0.00032	0.00115	0.00017
<b>0.7</b> <b>H(B)<sub>90.</sub></b> 92K	-0.00028	0.00061	0.00014	0.00052	0.00009	<b>0.7</b> <b>D(B)<sub>90.</sub></b> 92K	-0.00122	0.00173	0.00039	0.00135	0.00018
<b>0.5</b> <b>H(B)<sub>173.</sub></b> 173K	0.00096	0.00111	0.00025	0.00085	0.00010	<b>0.5</b> <b>D(B)<sub>173.</sub></b> 173K	0.00073	0.00098	0.00022	0.00084	0.00015
<b>0.6</b> <b>H(B)<sub>173.</sub></b> 173K	0.00057	0.00079	0.00018	0.00063	0.00009	<b>0.6</b> <b>D(B)<sub>173.</sub></b> 173K	0.00047	0.00086	0.00019	0.00077	0.00015
<b>0.7</b> <b>H(B)<sub>173.</sub></b> 173K	0.00065	0.00083	0.00019	0.00065	0.00009	<b>0.7</b> <b>D(B)<sub>173.</sub></b> 173K	0.00047	0.00089	0.00020	0.00078	0.00014

**Table 5.2. Corannulene minus deuterocorannulene at 0.6 Å and various temperatures, (N=Neutron, X=X-ray)**

	$\langle U_{ii} \rangle$	RMS <sub>ii</sub>	Stand. Dev. <sub>ii</sub>	RMS <sub>ij</sub>	Stand. Dev. <sub>ij</sub>		$\langle U_{ii} \rangle$	RMS <sub>ii</sub>	Stand. Dev. <sub>ii</sub>	RMS <sub>ij</sub>	Stand. Dev. <sub>ij</sub>
<b>0.6</b> N(A) <sub>90-92K</sub>	-0.00060	0.00084	0.00019	0.00066	0.00009	<b>0.6</b> X(A) <sub>90-92K</sub>	-0.00115	0.00120	0.00027	0.00087	0.00007
<b>0.6</b> N(A) <sub>173-173K</sub>	-0.00048	0.00091	0.00020	0.00076	0.00013	<b>0.6</b> X(A) <sub>173-173K</sub>	-0.00047	0.00060	0.00013	0.00045	0.00005
<b>0.6</b> N(B) <sub>90-92K</sub>	-0.00064	0.00090	0.00020	0.00069	0.00009	<b>0.6</b> X(B) <sub>90-92K</sub>	-0.00135	0.00146	0.00033	0.00106	0.00008
<b>0.6</b> N(B) <sub>173-173K</sub>	-0.00049	0.00079	0.00018	0.00068	0.00012	<b>0.6</b> X(B) <sub>173-173K</sub>	-0.00058	0.00068	0.00015	0.00050	0.00005

From Table 5.1, one can see that the compatibility between neutron and x-ray diffraction data does not agree for corannulene. When comparing the average difference between data sets, neutron is consistently larger than x-ray. For deuterocorannulene, the noticeable trend is that at 90 K, x-ray is larger whereas at 173 K, neutron is larger. With both molecules one can obtain indirect information about the ellipsoid directions expected based on the root mean square of the off-diagonal elements, RMS<sub>ij</sub>. Consistently, RMS<sub>ij</sub> is smallest for 0.6 Å. Further work is needed to understand why this trend is observed for the data, but is outside the scope of this thesis.

For the analysis of H minus D in Table 5.2, one can see that reliably deuterocorannulene is larger than corannulene for both neutron and x-ray over the temperature range measured. To the first approximation, the ADPs are resulting from either in plane or out of plane, libration and translational, displacement. With a better understanding about the limitations in the quality and consistency of the data, we will next focus on developing dynamic models including the x-ray and neutron diffraction data over all temperature ranges provided.

## 5.5 Analysis of models

The epsilon matrix of the hydrogens in corannulene using *ab initio* calculations is 0.0237. In the corresponding 3N+4X model of CorH(A), the epsilon value was 0.0303. We looked at these *ab initio* calculations done on corannulene and perdeuterocorannulene in the gas phase for an understanding of the out-of-plane components of the ADPs that might add flexibility to the model. The calculations showed three modes of corannulene, one at 144.75 cm<sup>-1</sup> and two



degenerate modes at  $135.33\text{ cm}^{-1}$ , with low enough frequencies that might impact the models. For perdeuterocorannulene the modes are at  $134.66\text{ cm}^{-1}$  and two at  $125.61\text{ cm}^{-1}$ .

The first mode (Figure 5.1) shows significant movement of the hydrogen atoms (H), the peripheral (P) carbons and the central (C) carbons of corannulene. In order to know how much flexibility to add to the rigid-body model, Eq. 5.6-5.8 were used. The coefficients ( $C_H$ ,  $C_P$  and  $C_C$ ) are proportional to the square root of the sum of the squared coordinates from the *ab initio* calculation. The coefficients were averaged for each of the three groups then added to the model.

$$C_H \propto (x_H^2 + y_H^2 + z_H^2)^{1/2} \quad (5.6)$$

$$C_P \propto (x_P^2 + y_P^2 + z_P^2)^{1/2} \quad (5.7)$$

$$C_C \propto (x_C^2 + y_C^2 + z_C^2)^{1/2} \quad (5.8)$$

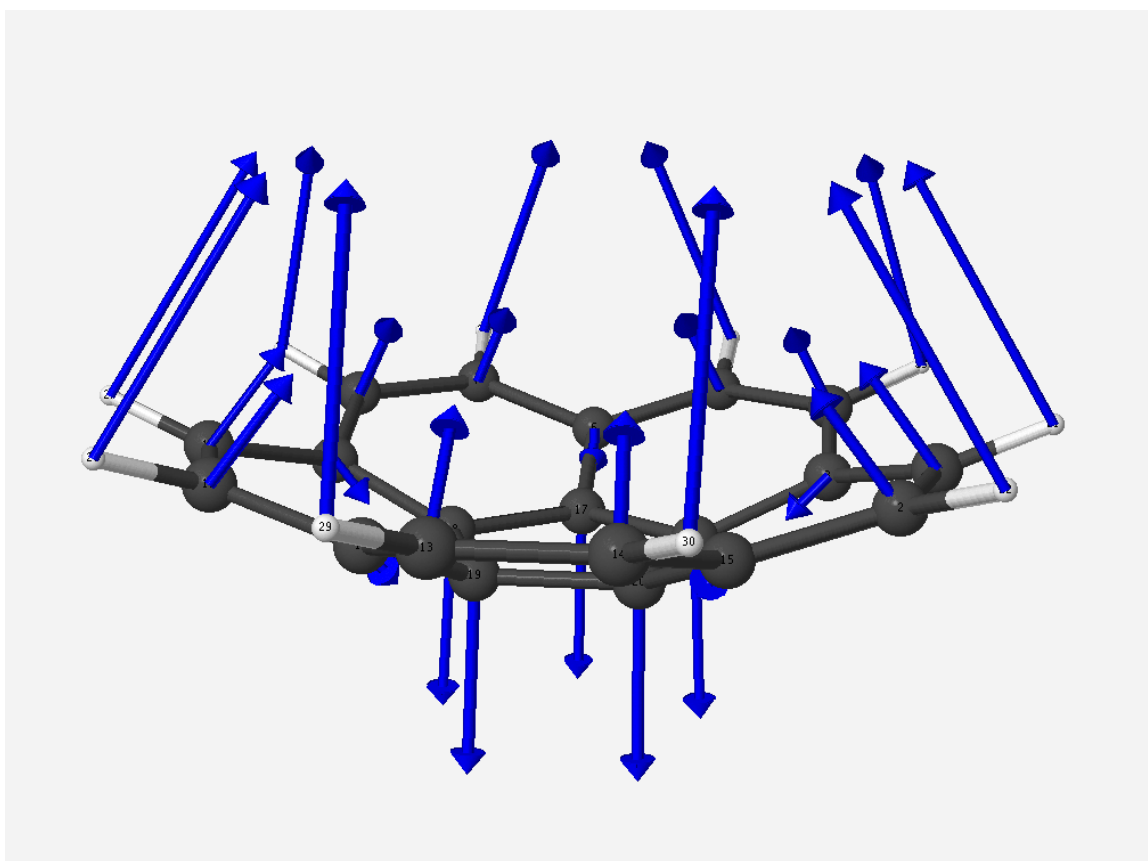


**Figure 5.1** *ab initio* calculation of corannulene in the gas phase at  $144.75\text{ cm}^{-1}$ .

The same idea was used for the two degenerate modes at  $135.33\text{ cm}^{-1}$ , only a little more complicated. From Figures 5.2, one can see that there is a cosine wave associated with the positioning of the out-of-plane components. Therefore, the equation to determine C was modified

to Eq. 5.9, where  $\theta$  is the angle of the atom from the mirror plane. The second degenerate mode shows a corresponding sine function (Figure 5.3), so Eq. 5.10 was used to calculate C. For these two degenerate modes, C was determined for each individual atom and entered accordingly without averaging.

$$C \propto \frac{\sqrt{x^2 + y^2 + z^2}}{\cos 2\theta} \quad (5.9)$$

$$C \propto \frac{\sqrt{x^2 + y^2 + z^2}}{\sin 2\theta} \quad (5.10)$$

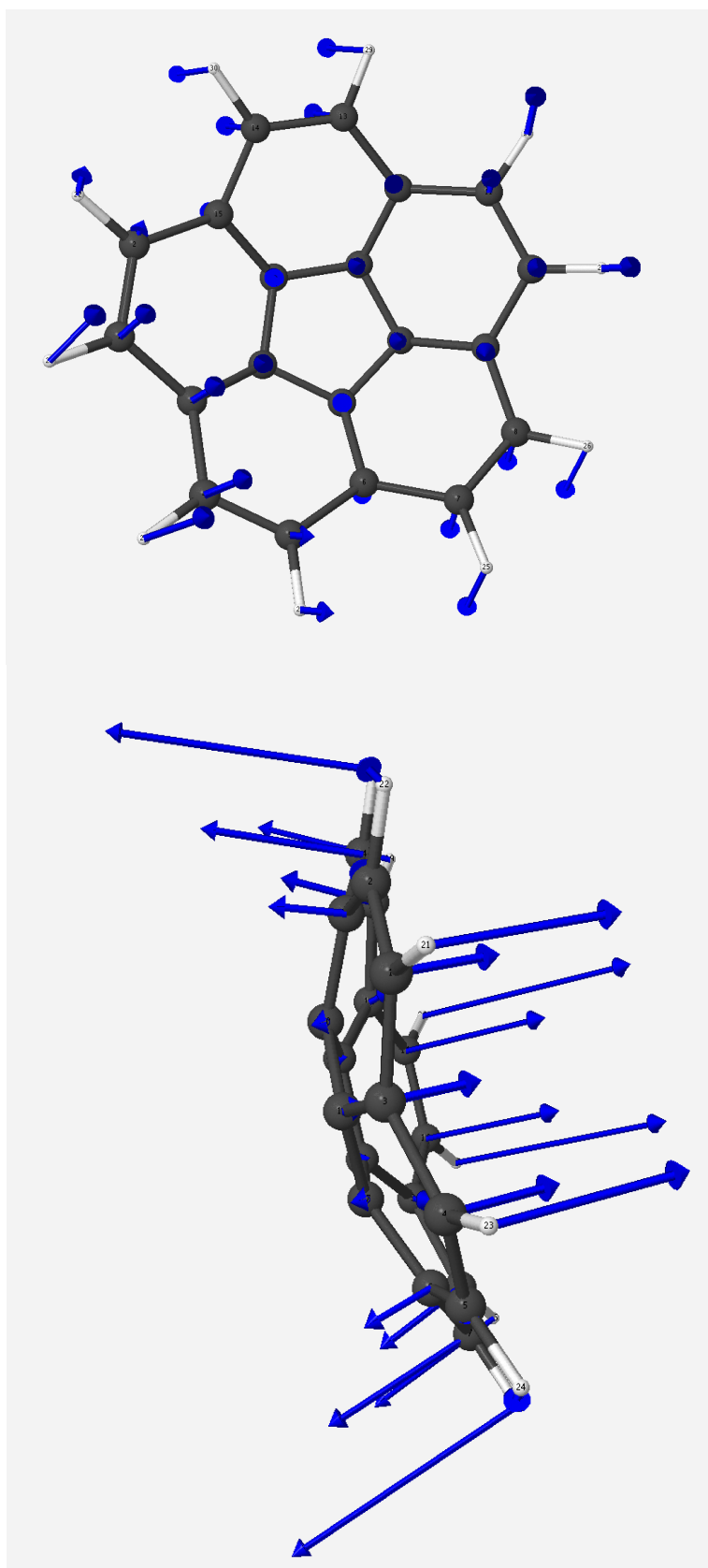


**Figure 5.2** *ab initio* calculation of corannulene in the gas phase at  $135.33\text{ cm}^{-1}$ , showing cosine distribution of the out-of-plane components.

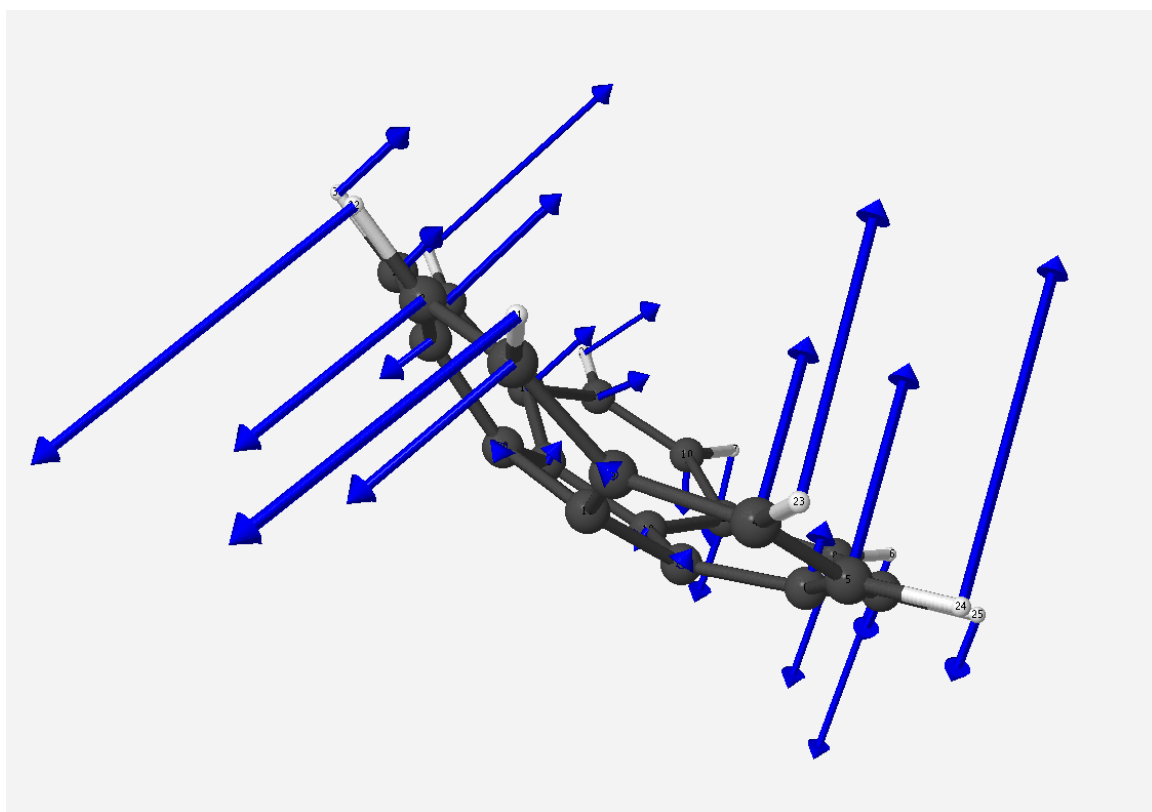
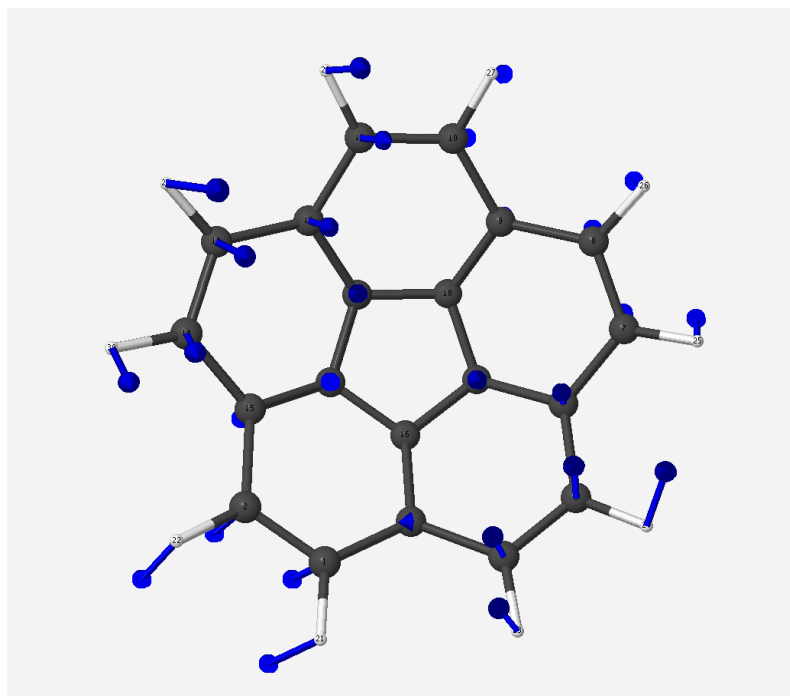


**Figure 5.3** *ab initio* calculation of corannulene in the gas phase at  $135.33\text{ cm}^{-1}$ , showing sine distribution of the out-of-plane components.

The normal frequencies and eigenvectors for CorH(A) derived from ADPs pertaining to (neutron) 20, 90, 173 K and (x-ray) 12, 92, 173, 250 K are given in Table 5.3. The effects of the three

modes are given by  $U_1$ ,  $U_2$  and  $U_3$ . The same information is shown in Table 5.4 for CorH(B), Table 5.5 for CorD(A), and Table 5.6 for CorD(B). There was no 12 K ADP for CorD(A) and CorD(B).

**Table 5.3. Normal frequencies,  $\nu$  ( $\text{cm}^{-1}$ ), and eigenvectors for CorH(A) derived from ADPs pertaining to 3N+4X with additional stretch modes,  $U_1$ ,  $U_2$  and  $U_3$ .**

$\nu(\text{cm}^{-1})$	30.8(2)	27.5(1)	31.5(2)	156(13)	57.4(2.2)
$\mathbf{L}_x$	0.138(36)	-0.048(7)	0.452(15)	-0.159(59)	-0.254(25)
$\mathbf{L}_y$	0.388(10)	0.208(8)	-0.027(29)	0.786(30)	0.228(25)
$\mathbf{L}_z$	0.069(63)	-0.625(11)	-0.207(41)	0.100(17)	-0.545(11)
$\mathbf{T}_x$	0.485(16)	0.395(11)	-0.800(8)	-0.168(26)	-0.219(15)
$\mathbf{T}_y$	-0.741(16)	-0.405(12)	-0.210(55)	0.359(27)	-0.109(16)
$\mathbf{T}_z$	-0.200(21)	0.493(8)	0.262(18)	0.222(25)	-0.725(10)
$\mathbf{U}_1$	-0.025(3)	-0.011(3)	-0.009(4)	0.280(63)	0.004(13)
$\mathbf{U}_2$	-0.002(4)	0.011(3)	-0.004(4)	-0.137(51)	0.032(12)
$\mathbf{U}_3$	0.015(4)	0.008(4)	0.005(4)	-0.210(62)	-0.008(20)

**Table 5.4. Normal frequencies,  $\nu$  ( $\text{cm}^{-1}$ ), and eigenvectors for CorH(B) derived from ADPs pertaining to 3N+4X with additional stretch modes,  $U_1$ ,  $U_2$  and  $U_3$ .**

$\nu(\text{cm}^{-1})$	28.3(1)	31.0(2)	68.6(1.5)	25.9(1)	62.7(2.1)
$\mathbf{L}_x$	-0.148(9)	-0.391(9)	0.788(39)	-0.022(7)	-0.226(128)
$\mathbf{L}_y$	0.362(8)	-0.001(8)	0.437(19)	0.227(9)	-0.057(70)
$\mathbf{L}_z$	0.237(17)	0.109(11)	-0.012(79)	-0.829(6)	-0.483(6)
$\mathbf{T}_x$	-0.291(19)	0.884(6)	0.357(11)	0.005(10)	0.025(60)
$\mathbf{T}_y$	-0.798(7)	-0.229(18)	-0.006(28)	-0.282(16)	0.139(8)
$\mathbf{T}_z$	-0.264(9)	0.032(8)	-0.226(132)	0.425(8)	-0.832(37)
$\mathbf{U}_1$	0.001(4)	-0.010(5)	-0.085(15)	-0.003(3)	-0.021(19)
$\mathbf{U}_2$	0.003(4)	-0.014(5)	0.047(14)	0.002(3)	-0.005(18)
$\mathbf{U}_3$	-0.003(3)	-0.006(4)	0.016(21)	0.003(4)	-0.027(20)

**Table 5.5. Normal frequencies,  $\nu$  (cm<sup>-1</sup>), and eigenvectors for CorD(A) derived from ADPs pertaining to 3N+3X with additional stretch modes, U<sub>1</sub>, U<sub>2</sub> and U<sub>3</sub>.**

$\nu(\text{cm}^{-1})$	57.7(1.9)	28.6(1)	169.7(15)	25.5(1)	29.2(2)
<b>L<sub>x</sub></b>	-0.277(25)	0.109(37)	-0.083(74)	-0.043(6)	-0.476(12)
<b>L<sub>y</sub></b>	0.286(25)	0.418(8)	0.708(53)	0.195(9)	0.016(31)
<b>L<sub>z</sub></b>	-0.516(12)	0.450(14)	0.118(18)	-0.678(10)	0.164(38)
<b>T<sub>x</sub></b>	-0.247(15)	0.108(62)	-0.119(35)	0.340(11)	0.809(9)
<b>T<sub>y</sub></b>	-0.062(16)	-0.755(15)	0.365(40)	-0.368(13)	0.204(55)
<b>T<sub>z</sub></b>	-0.714(14)	-0.172(18)	0.241(30)	0.499(7)	-0.225(16)
<b>U<sub>1</sub></b>	-0.010(13)	-0.019(3)	0.327(88)	-0.004(3)	0.009(4)
<b>U<sub>2</sub></b>	0.022(12)	-0.004(3)	-0.074(76)	0.011(2)	0.009(3)
<b>U<sub>3</sub></b>	-0.015(19)	0.011(4)	-0.400(84)	0.012(4)	-0.011(3)

**Table 5.6. Normal frequencies,  $\nu$  (cm<sup>-1</sup>), and eigenvectors for CorD(B) derived from ADPs pertaining to 3N+3X with additional stretch modes, U<sub>1</sub>, U<sub>2</sub> and U<sub>3</sub>.**

$\nu(\text{cm}^{-1})$	26.7(1)	29.1(2)	64.7(1.2)	23.8(1)	58.9(2.1)
<b>L<sub>x</sub></b>	-0.136(9)	-0.409(8)	0.786(45)	-0.013(5)	-0.266(126)
<b>L<sub>y</sub></b>	0.395(7)	0.006(8)	0.414(15)	0.221(7)	-0.011(62)
<b>L<sub>z</sub></b>	0.216(13)	0.100(10)	-0.031(77)	-0.831(5)	-0.484(8)
<b>T<sub>x</sub></b>	-0.262(18)	0.884(5)	0.377(8)	0.013(7)	-0.001(64)
<b>T<sub>y</sub></b>	-0.806(5)	-0.198(17)	0.014(31)	-0.252(12)	0.160(7)
<b>T<sub>z</sub></b>	-0.247(7)	0.034(7)	-0.246(127)	0.444(6)	-0.816(39)
<b>U<sub>1</sub></b>	0.000(3)	0.000(4)	-0.062(16)	-0.006(2)	0.023(15)
<b>U<sub>2</sub></b>	0.003(3)	-0.012(4)	0.029(14)	-0.000(2)	-0.006(15)
<b>U<sub>3</sub></b>	0.002(3)	-0.001(3)	0.048(22)	0.006(4)	-0.062(18)

From Table 5.3-5.5, one can see that there was not a significant contribution from the incorporation of these additional modes from the low values of U<sub>1</sub>, U<sub>2</sub> and U<sub>3</sub>. Furthermore, the epsilon matrix for CorH(A) with these additional modes was 0.0302, with no improvement from the original 3N+4X model. One explanation for this could be that the *ab initio* calculations are

done in the gas phase. The out-of-plane stretches from the calculations cannot be experienced from the molecules in the crystal due to congestion from nearby molecules.

Finally, using the theory of isotope effect on ADPs<sup>7</sup>, one can determine if the frequencies and eigenvectors obtained for corannulene and perdeuterocorannulene are comparable (Eq. 5.11 and 5.12). In both equations, the force constant matrix can be calculated, and assuming that the temperature is the same, F should also be the same for both models. The relationship between  $\omega_H$  and  $\omega_D$  can further be used to determine the expected error in the eigenvectors. The translation eigenvectors are inversely proportional to the square root of their respective masses (Eq. 5.13). The libration eigenvectors are inversely proportional to the square root of their respective inertial moments.

$$\omega_H^2 = g_H V_H F V_H^T g_H^T \quad (5.11)$$

$$\omega_D^2 = g_D V_D F V_D^T g_D^T \quad (5.12)$$

$$\frac{\omega_H}{\omega_D} = \sqrt{\frac{m_D}{m_H}} \quad (5.13)$$

The force constant matrix was determined for CorH(A), CorD(A), CorH(B) and CorD(B) using the 3N+3X<sup>a</sup> models and summarized in Tables 5.7 and 5.8 with their determined on-diagonal components (librations and translations). The models for molecule B show better comparison than for molecule A. Using Eq. 5.13, the expected error in the eigenvectors was 2-5%. Experimentally, this value was a little higher at 4-7%.

**Table 5.7. Libration and translation components determined by the force constant matrix for molecule A in corannulene and perdeuterocorannulene.**

	<b>CorH(A)</b>	<b>CorD(A)</b>
<b>L<sub>x</sub></b>	37.209	21.972
<b>L<sub>y</sub></b>	692.93	653.05
<b>L<sub>z</sub></b>	161.10	146.98
<b>T<sub>x</sub></b>	13.831	10.164
<b>T<sub>y</sub></b>	49.211	54.778
<b>T<sub>z</sub></b>	35.428	28.955

**Table 5.8. Libration and translation components determined by the force constant matrix for molecule B in corannulene and perdeuterocorannulene.**

	<b>CorH(B)</b>	<b>CorD(B)</b>
<b>L<sub>x</sub></b>	111.68	104.66
<b>L<sub>y</sub></b>	38.834	38.117
<b>L<sub>z</sub></b>	96.748	95.100
<b>T<sub>x</sub></b>	12.147	11.833
<b>T<sub>y</sub></b>	6.0920	5.9256
<b>T<sub>z</sub></b>	26.600	26.928

## 5.6 Conclusion

Models were made for the different (A/ B) molecules in the unit cell for corannulene and perdeuterocorannulene. The neutron and x-ray diffraction data was compared at varying scattering angle cutoff values to determine that 0.6 Å was the most appropriate data set to use. The consistency between models was determined using the theory of isotope effect. With assistance from *ab initio* calculations of corannulene and perdeuterocorannulene in the gas phase, three additional stretching modes contributing to the out-of-plane components were added to the model. Epsilon values from the calculations and the models showed that these out-of-plane components did not contribute very much.



---

<sup>1</sup> Dunitz, J. D. *Trans. Amer. Cryst. Assn.* **1984**, 20, 1.

<sup>2</sup> (a) Debye, P. *Verh. Dtsch. Phys. Ges.* **1913**, 15, 678. (b) Debye, P. *Verh. Dtsch. Phys. Ges.* **1913**, 15, 738. (c) Debye, P. *Verh. Dtsch. Phys. Ges.* **1913**, 15, 857.

<sup>3</sup> Bürgi, H. B.; Capelli, S. C. *Acta Cryst.* **2000**, A 56, 403.

<sup>4</sup> Dunitz, J. D.; Schomaker, V.; Trueblood, K. N.; *J. Phys. Chem.* **1988**, 92, 856.

<sup>5</sup> Bürgi, H. B.; Capelli, S. C.; Goeta, A. E.; Howard, J. A. K.; Spackman, M. A.; Yufit, D. S. *Chem. Eur. J.*, **2002**, 8, 3512.

<sup>6</sup> Bürgi, H. B.; Capelli, S. C.; Birkedal, H. *Acta Cryst.*, **2000**, A 56, 425.

<sup>7</sup> Bürgi, H. B.; Capelli, S. C.; Goeta, A. E.; Howard, J. A. K.; Spackman, M. A.; Yufit, D. S. *Chem. Eur. J.*, **2002**, 8, 3512.

## Appendix A

0.5 Å	N - X										
CorH(A)											
ATOM	X	Y	Z	U11	U22	U33	U12	U13	U23	sum delUii	sum Uii+uij
C1	0.41872	0.30420	0.10953	0.00604	0.00733	0.00657	0.00007	0.00117	0.00023		
C1	0.41947	0.30454	0.10970	0.00660	0.00520	0.00560	0.00040	0.00070	0.00020		
(20k-12k)^2	0.00000	0.00000	0.00000	0.00000	0.00000	0.00000	0.00000	0.00000	0.00000	0.00001	0.00001
C2	0.43766	0.22750	0.17934	0.00616	0.00754	0.00620	0.00016	0.00128	0.00044		
C2	0.43824	0.22785	0.17946	0.00610	0.00570	0.00560	0.00060	0.00090	0.00030		
(20k-12k)^2	0.00000	0.00000	0.00000	0.00000	0.00000	0.00000	0.00000	0.00000	0.00000	0.00000	0.00000
C3	0.34016	0.18265	0.18920	0.00640	0.00761	0.00672	0.00030	0.00143	0.00043		
C3	0.34071	0.18338	0.18934	0.00630	0.00620	0.00580	0.00060	0.00120	0.00060		
(20k-12k)^2	0.00000	0.00000	0.00000	0.00000	0.00000	0.00000	0.00000	0.00000	0.00000	0.00000	0.00000
C4	0.26098	0.23230	0.12590	0.00624	0.00757	0.00706	0.00015	0.00128	0.00055		
C4	0.26169	0.23301	0.12621	0.00620	0.00650	0.00650	0.00080	0.00100	0.00040		
(20k-12k)^2	0.00000	0.00000	0.00000	0.00000	0.00000	0.00000	0.00000	0.00000	0.00000	0.00000	0.00000
C5	0.30971	0.30726	0.07674	0.00636	0.00765	0.00670	0.00011	0.00096	0.00040		
C5	0.31042	0.30783	0.07703	0.00640	0.00590	0.00600	0.00090	0.00080	0.00050		
(20k-12k)^2	0.00000	0.00000	0.00000	0.00000	0.00000	0.00000	0.00000	0.00000	0.00000	0.00000	0.00000
C6	0.49163	0.32550	0.06074	0.00690	0.00759	0.00706	-0.00021	0.00176	0.00024		
C6	0.49215	0.32555	0.06085	0.00700	0.00570	0.00610	0.00000	0.00120	0.00030		
(20k-12k)^2	0.00000	0.00000	0.00000	0.00000	0.00000	0.00000	0.00000	0.00000	0.00000	0.00000	0.00000
C7	0.59475	0.28037	0.09517	0.00671	0.00913	0.00844	-0.00018	0.00225	0.00027		
C7	0.59521	0.28020	0.09516	0.00660	0.00700	0.00770	0.00000	0.00170	0.00030		
(20k-12k)^2	0.00000	0.00000	0.00000	0.00000	0.00000	0.00000	0.00000	0.00000	0.00000	0.00001	0.00001
H7	0.65862	0.29945	0.06361	0.01741	0.03067	0.02681	0.00080	0.01110	0.00610		
H7	0.66055	0.29766	0.06475	0.01910							
(20k-12k)^2	0.00000	0.00000	0.00000	0.00000	0.00094	0.00072	0.00000	0.00012	0.00004		
C8	0.61340	0.20561	0.16388	0.00631	0.00897	0.00859	0.00050	0.00150	0.00047		
C8	0.61378	0.20552	0.16382	0.00620	0.00720	0.00760	0.00070	0.00090	0.00040		
(20k-12k)^2	0.00000	0.00000	0.00000	0.00000	0.00000	0.00000	0.00000	0.00000	0.00000	0.00000	0.00000

<b>H8</b>	0.69125	0.16881	0.18364	0.01419	0.02831	0.02723	0.00676	0.00361	0.00602		
<b>H8</b>	0.69188	0.16925	0.18361	0.01520							
<b>(20k-12k)^2</b>	0.00000	0.00000	0.00000	0.00000	0.00080	0.00074	0.00005	0.00001	0.00004		
<b>C9</b>	0.53050	0.16828	0.20445	0.00618	0.00786	0.00747	0.00040	0.00109	0.00024		
<b>C9</b>	0.53091	0.16838	0.20448	0.00620	0.00610	0.00610	0.00060	0.00070	0.00040		
<b>(20k-12k)^2</b>	0.00000	0.00000	0.00000	0.00000	0.00000	0.00000	0.00000	0.00000	0.00000	0.00000	0.00001
<b>C10</b>	0.52280	0.06476	0.25291	0.00742	0.00874	0.00843	0.00098	0.00053	0.00132		
<b>C10</b>	0.52306	0.06504	0.25289	0.00730	0.00710	0.00720	0.00090	0.00040	0.00150		
<b>(20k-12k)^2</b>	0.00000	0.00000	0.00000	0.00000	0.00000	0.00000	0.00000	0.00000	0.00000	0.00000	0.00000
<b>H10</b>	0.59278	0.01388	0.27766	0.01615	0.02295	0.02922	0.00555	0.00094	0.00680		
<b>H10</b>	0.59348	0.01568	0.27823	0.01800							
<b>(20k-12k)^2</b>	0.00000	0.00000	0.00000	0.00000	0.00053	0.00085	0.00003	0.00000	0.00005		
<b>C11</b>	0.42706	0.02062	0.26213	0.00822	0.00880	0.00776	0.00053	0.00115	0.00182		
<b>C11</b>	0.42736	0.02127	0.26220	0.00790	0.00740	0.00720	0.00080	0.00120	0.00210		
<b>(20k-12k)^2</b>	0.00000	0.00000	0.00000	0.00000	0.00000	0.00000	0.00000	0.00000	0.00000	0.00000	0.00000
<b>H11</b>	0.42569	-0.06193	0.29427	0.02364	0.01874	0.02803	0.00071	0.00476	0.01016		
<b>H11</b>	0.42314	-0.06097	0.29422	0.01880							
<b>(20k-12k)^2</b>	0.00001	0.00000	0.00000	0.00002	0.00035	0.00079	0.00000	0.00002	0.00010		
<b>C12</b>	0.32958	0.07603	0.22459	0.00731	0.00788	0.00737	0.00021	0.00170	0.00094		
<b>C12</b>	0.33004	0.07678	0.22465	0.00700	0.00700	0.00660	0.00040	0.00170	0.00110		
<b>(20k-12k)^2</b>	0.00000	0.00000	0.00000	0.00000	0.00000	0.00000	0.00000	0.00000	0.00000	0.00000	0.00000
<b>C13</b>	0.22547	0.02773	0.20376	0.00766	0.00930	0.00925	-0.00049	0.00245	0.00120		
<b>C13</b>	0.22596	0.02873	0.20394	0.00770	0.00860	0.00930	-0.00050	0.00240	0.00180		
<b>(20k-12k)^2</b>	0.00000	0.00000	0.00000	0.00000	0.00000	0.00000	0.00000	0.00000	0.00000	0.00000	0.00000
<b>H13</b>	0.20934	-0.05399	0.23206	0.02366	0.01992	0.02837	-0.00430	0.00489	0.00854		
<b>H13</b>	0.20897	-0.05373	0.23084	0.02800							
<b>(20k-12k)^2</b>	0.00000	0.00000	0.00000	0.00002	0.00040	0.00080	0.00002	0.00002	0.00007		
<b>C14</b>	0.14798	0.07651	0.14175	0.00700	0.00959	0.01039	-0.00070	0.00205	0.00095		
<b>C14</b>	0.14855	0.07749	0.14207	0.00670	0.00940	0.01050	-0.00040	0.00200	0.00140		
<b>(20k-12k)^2</b>	0.00000	0.00000	0.00000	0.00000	0.00000	0.00000	0.00000	0.00000	0.00000	0.00000	0.00000
<b>H14</b>	0.07347	0.03164	0.12392	0.01490	0.02541	0.03211	-0.00728	0.00146	0.00429		
<b>H14</b>	0.07247	0.03542	0.12443	0.01500							

(20k-12k)^2	0.00000	0.00001	0.00000	0.00000	0.00065	0.00103	0.00005	0.00000	0.00002		
C15	0.16707	0.17766	0.09479	0.00625	0.00879	0.00804	0.00015	0.00135	0.00024		
C15	0.16773	0.17877	0.09515	0.00590	0.00800	0.00840	0.00050	0.00120	0.00080		
(20k-12k)^2	0.00000	0.00000	0.00000	0.00000	0.00000	0.00000	0.00000	0.00000	0.00000	0.00000	0.00000
C16	0.11436	0.21623	0.01184	0.00643	0.01068	0.00936	0.00017	0.00028	0.00052		
C16	0.11497	0.21748	0.01226	0.00620	0.01030	0.00940	0.00050	0.00000	0.00100		
(20k-12k)^2	0.00000	0.00000	0.00000	0.00000	0.00000	0.00000	0.00000	0.00000	0.00000	0.00000	0.00000
H16	0.03773	0.18083	-0.01610	0.01430	0.03236	0.02486	-0.00637	-0.00178	0.00168		
H16	0.03727	0.18417	-0.01488	0.02010							
(20k-12k)^2	0.00000	0.00001	0.00000	0.00003	0.00105	0.00062	0.00004	0.00000	0.00000		
C17	0.16263	0.28880	-0.03680	0.00731	0.01028	0.00801	0.00044	-0.00004	0.00089		
C17	0.16318	0.28992	-0.03633	0.00740	0.00910	0.00800	0.00100	-0.00070	0.00120		
(20k-12k)^2	0.00000	0.00000	0.00000	0.00000	0.00000	0.00000	0.00000	0.00000	0.00000	0.00000	0.00000
H17	0.12324	0.30711	-0.10153	0.02177	0.03184	0.01683	-0.00195	-0.00319	0.00539		
H17	0.12467	0.31000	-0.10116	0.01940							
(20k-12k)^2	0.00000	0.00001	0.00000	0.00001	0.00101	0.00028	0.00000	0.00001	0.00003		
C18	0.26767	0.33087	-0.00701	0.00717	0.00850	0.00672	0.00015	0.00054	0.00075		
C18	0.26832	0.33163	-0.00664	0.00740	0.00660	0.00630	0.00100	0.00020	0.00090		
(20k-12k)^2	0.00000	0.00000	0.00000	0.00000	0.00000	0.00000	0.00000	0.00000	0.00000	0.00000	0.00000
C19	0.34170	0.37242	-0.05501	0.00899	0.00980	0.00723	0.00007	0.00144	0.00143		
C19	0.34222	0.37276	-0.05476	0.00920	0.00740	0.00660	0.00050	0.00070	0.00170		
(20k-12k)^2	0.00000	0.00000	0.00000	0.00000	0.00001	0.00000	0.00000	0.00000	0.00000	0.00001	0.00001
H19	0.31379	0.39825	-0.12059	0.02335	0.03410	0.01489	0.00042	0.00089	0.00795		
H19	0.31351	0.40015	-0.11994	0.01770							
(20k-12k)^2	0.00000	0.00000	0.00000	0.00003	0.00116	0.00022	0.00000	0.00000	0.00006		
C20	0.44860	0.36960	-0.02287	0.00832	0.00877	0.00752	-0.00047	0.00183	0.00110		
C20	0.44914	0.36968	-0.02273	0.00910	0.00680	0.00660	-0.00040	0.00140	0.00130		
(20k-12k)^2	0.00000	0.00000	0.00000	0.00000	0.00000	0.00000	0.00000	0.00000	0.00000	0.00001	0.00001
H20	0.50071	0.39397	-0.06427	0.02077	0.03140	0.02012	-0.00259	0.00920	0.00521		
H20	0.50215	0.39216	-0.06402	0.01930							
(20k-12k)^2	0.00000	0.00000	0.00000	0.00000	0.00099	0.00040	0.00001	0.00008	0.00003		
	X	Y	Z	U11	U22	U33	U12	U13	U23	0.00006	0.00007

<delta>	-0.00053	-0.00055	-0.00019	0.00000	0.00146	0.00059	-0.00033	0.00032	-0.00019	0.00068	
RMS:	0.00055	0.00069	0.00024	0.00028	0.00158	0.00075	0.00040	0.00039	0.00028	0.00102	0.00077
0.5 Angstroms	N - X										
CorH(B)											
ATOM	X	Y	Z	U11	U22	U33	U12	U13	U23	sum delUii	sum Uii+uij
C21	0.15424	0.69848	0.46823	0.00667	0.00693	0.00683	0.00009	0.00131	-0.00064		
C21	0.15442	0.69786	0.46838	0.00710	0.00520	0.00690	0.00000	0.00100	-0.00100		
(20k-12k)^2	0.00000	0.00000	0.00000	0.00000	0.00000	0.00000	0.00000	0.00000	0.00000	0.00000	0.00000
C22	0.09848	0.69601	0.38330	0.00645	0.00693	0.00730	0.00033	0.00096	-0.00036		
C22	0.09862	0.69546	0.38347	0.00690	0.00560	0.00710	0.00030	0.00060	-0.00100		
(20k-12k)^2	0.00000	0.00000	0.00000	0.00000	0.00000	0.00000	0.00000	0.00000	0.00000	0.00000	0.00000
C23	0.12313	0.59147	0.34646	0.00674	0.00701	0.00710	0.00000	0.00112	-0.00058		
C23	0.12325	0.59102	0.34664	0.00700	0.00610	0.00680	-0.00010	0.00100	-0.00130		
(20k-12k)^2	0.00000	0.00000	0.00000	0.00000	0.00000	0.00000	0.00000	0.00000	0.00000	0.00000	0.00000
C24	0.19467	0.52963	0.40855	0.00701	0.00672	0.00750	0.00021	0.00148	-0.00016		
C24	0.19469	0.52914	0.40869	0.00770	0.00490	0.00760	0.00010	0.00160	-0.00090		
(20k-12k)^2	0.00000	0.00000	0.00000	0.00000	0.00000	0.00000	0.00000	0.00000	0.00000	0.00000	0.00000
C25	0.21460	0.59612	0.48353	0.00710	0.00691	0.00713	0.00029	0.00134	0.00008		
C25	0.21459	0.59572	0.48368	0.00760	0.00510	0.00680	0.00010	0.00120	-0.00060		
(20k-12k)^2	0.00000	0.00000	0.00000	0.00000	0.00000	0.00000	0.00000	0.00000	0.00000	0.00000	0.00000
C26	0.18134	0.79981	0.51239	0.00792	0.00740	0.00765	0.00005	0.00142	-0.00100		
C26	0.18146	0.79906	0.51248	0.00770	0.00540	0.00750	0.00000	0.00070	-0.00140		
(20k-12k)^2	0.00000	0.00000	0.00000	0.00000	0.00000	0.00000	0.00000	0.00000	0.00000	0.00000	0.00000
C27	0.13360	0.90230	0.46989	0.00955	0.00689	0.01036	0.00047	0.00127	-0.00082		
C27	0.13379	0.90150	0.46994	0.00970	0.00550	0.00990	0.00070	0.00070	-0.00150		
(20k-12k)^2	0.00000	0.00000	0.00000	0.00000	0.00000	0.00000	0.00000	0.00000	0.00000	0.00000	0.00000
H27	0.14596	0.98569	0.50165	0.03208	0.01485	0.02515	0.00012	0.00124	-0.00559		
H27	0.14551	0.98402	0.50321	0.01860							
(20k-12k)^2	0.00000	0.00000	0.00000	0.00018	0.00022	0.00063	0.00000	0.00000	0.00003		
C28	0.07969	0.89998	0.38629	0.00937	0.00751	0.01049	0.00158	0.00059	-0.00007		
C28	0.07992	0.89924	0.38631	0.00990	0.00610	0.01030	0.00150	-0.00020	-0.00030		

(20k-12k)^2	0.00000	0.00000	0.00000	0.00000	0.00000	0.00000	0.00000	0.00000	0.00000	0.00000	0.00000
H28	0.05254	0.98133	0.35572	0.03169	0.01566	0.02552	0.00578	-0.00027	0.00414		
H28	0.05159	0.98116	0.35670	0.02090							
(20k-12k)^2	0.00000	0.00000	0.00000	0.00012	0.00025	0.00065	0.00003	0.00000	0.00002		
C29	0.06682	0.79451	0.33710	0.00724	0.00759	0.00852	0.00086	0.00059	0.00036		
C29	0.06703	0.79395	0.33718	0.00770	0.00650	0.00810	0.00080	0.00010	-0.00030		
(20k-12k)^2	0.00000	0.00000	0.00000	0.00000	0.00000	0.00000	0.00000	0.00000	0.00000	0.00000	0.00000
C30	0.04576	0.77800	0.24651	0.00896	0.00948	0.00826	0.00095	0.00039	0.00103		
C30	0.04594	0.77751	0.24666	0.00940	0.00860	0.00840	0.00130	-0.00020	0.00060		
(20k-12k)^2	0.00000	0.00000	0.00000	0.00000	0.00000	0.00000	0.00000	0.00000	0.00000	0.00000	0.00000
H30	0.01534	0.84967	0.20498	0.03150	0.02070	0.02082	0.00643	0.00166	0.00642		
H30	0.01178	0.84990	0.20712	0.01900							
(20k-12k)^2	0.00001	0.00000	0.00000	0.00016	0.00043	0.00043	0.00004	0.00000	0.00004		
C31	0.07064	0.67543	0.21027	0.00882	0.01072	0.00722	0.00046	0.00068	0.00017		
C31	0.07065	0.67514	0.21043	0.00930	0.00960	0.00710	0.00070	-0.00020	-0.00050		
(20k-12k)^2	0.00000	0.00000	0.00000	0.00000	0.00000	0.00000	0.00000	0.00000	0.00000	0.00000	0.00000
H31	0.06052	0.67171	0.14178	0.03094	0.02858	0.01253	0.00338	0.00278	0.00021		
H31	0.06163	0.67100	0.14200	0.01830							
(20k-12k)^2	0.00000	0.00000	0.00000	0.00016	0.00082	0.00016	0.00001	0.00001	0.00000		
C32	0.11816	0.57897	0.26086	0.00742	0.00846	0.00694	-0.00010	0.00106	-0.00096		
C32	0.11808	0.57852	0.26103	0.00790	0.00760	0.00690	0.00010	0.00060	-0.00160		
(20k-12k)^2	0.00000	0.00000	0.00000	0.00000	0.00000	0.00000	0.00000	0.00000	0.00000	0.00000	0.00000
C33	0.17817	0.48282	0.23884	0.00883	0.00972	0.00832	0.00003	0.00158	-0.00215		
C33	0.17819	0.48267	0.23909	0.00910	0.00820	0.00770	0.00040	0.00140	-0.00260		
(20k-12k)^2	0.00000	0.00000	0.00000	0.00000	0.00000	0.00000	0.00000	0.00000	0.00000	0.00000	0.00000
H33	0.17345	0.46022	0.17276	0.02999	0.02942	0.01446	0.00397	0.00335	-0.00481		
H33	0.17372	0.46114	0.17284	0.01770							
(20k-12k)^2	0.00000	0.00000	0.00000	0.00015	0.00087	0.00021	0.00002	0.00001	0.00002		
C34	0.24844	0.42223	0.29999	0.00917	0.00814	0.00970	0.00066	0.00240	-0.00150		
C34	0.24834	0.42205	0.30019	0.00980	0.00680	0.00910	0.00080	0.00230	-0.00210		
(20k-12k)^2	0.00000	0.00000	0.00000	0.00000	0.00000	0.00000	0.00000	0.00000	0.00000	0.00000	0.00000
H34	0.29627	0.35545	0.27926	0.02644	0.02268	0.02443	0.00918	0.00799	-0.00472		

<b>H34</b>	0.29652	0.35578	0.27917	0.02040							
<b>(20k-12k)^2</b>	0.00000	0.00000	0.00000	0.00004	0.00051	0.00060	0.00008	0.00006	0.00002		
<b>C35</b>	0.26565	0.45178	0.38851	0.00773	0.00670	0.00859	0.00044	0.00185	-0.00071		
<b>C35</b>	0.26561	0.45149	0.38877	0.00850	0.00530	0.00840	0.00060	0.00190	-0.00090		
<b>(20k-12k)^2</b>	0.00000	0.00000	0.00000	0.00000	0.00000	0.00000	0.00000	0.00000	0.00000	0.00000	0.00000
<b>C36</b>	0.35516	0.43068	0.45579	0.00847	0.00767	0.01021	0.00142	0.00177	0.00052		
<b>C36</b>	0.35508	0.43027	0.45594	0.00960	0.00590	0.00960	0.00170	0.00140	0.00060		
<b>(20k-12k)^2</b>	0.00000	0.00000	0.00000	0.00000	0.00000	0.00000	0.00000	0.00000	0.00000	0.00000	0.00001
<b>H36</b>	0.41281	0.36610	0.44724	0.02101	0.02140	0.02777	0.00925	0.00354	-0.00237		
<b>H36</b>	0.41492	0.36874	0.44687	0.02060							
<b>(20k-12k)^2</b>	0.00000	0.00001	0.00000	0.00000	0.00046	0.00077	0.00009	0.00001	0.00001		
<b>C37</b>	0.37482	0.49645	0.52922	0.00846	0.00853	0.00860	0.00125	0.00098	0.00118		
<b>C37</b>	0.37483	0.49614	0.52935	0.00960	0.00690	0.00830	0.00180	0.00090	0.00110		
<b>(20k-12k)^2</b>	0.00000	0.00000	0.00000	0.00000	0.00000	0.00000	0.00000	0.00000	0.00000	0.00000	0.00000
<b>H37</b>	0.44732	0.48159	0.57480	0.01796	0.02859	0.02188	0.00576	-0.00361	-0.00024		
<b>H37</b>	0.44757	0.48239	0.57526	0.01980							
<b>(20k-12k)^2</b>	0.00000	0.00000	0.00000	0.00000	0.00082	0.00048	0.00003	0.00001	0.00000		
<b>C38</b>	0.30687	0.58993	0.54259	0.00737	0.00810	0.00731	0.00047	0.00083	0.00018		
<b>C38</b>	0.30692	0.58950	0.54279	0.00840	0.00610	0.00670	0.00060	0.00080	0.00030		
<b>(20k-12k)^2</b>	0.00000	0.00000	0.00000	0.00000	0.00000	0.00000	0.00000	0.00000	0.00000	0.00001	0.00001
<b>C39</b>	0.32831	0.68910	0.59787	0.00890	0.00952	0.00712	0.00001	0.00015	-0.00028		
<b>C39</b>	0.32831	0.68863	0.59798	0.00950	0.00770	0.00670	0.00030	0.00000	-0.00060		
<b>(20k-12k)^2</b>	0.00000	0.00000	0.00000	0.00000	0.00000	0.00000	0.00000	0.00000	0.00000	0.00000	0.00000
<b>H39</b>	0.39727	0.68907	0.64890	0.02150	0.02663	0.02006	0.00117	-0.00553	-0.00261		
<b>H39</b>	0.39915	0.68926	0.64725	0.02080							
<b>(20k-12k)^2</b>	0.00000	0.00000	0.00000	0.00000	0.00071	0.00040	0.00000	0.00003	0.00001		
<b>C40</b>	0.26805	0.78899	0.58378	0.00906	0.00893	0.00798	-0.00023	0.00100	-0.00148		
<b>C40</b>	0.26814	0.78833	0.58389	0.00940	0.00700	0.00740	-0.00010	0.00000	-0.00190		
<b>(20k-12k)^2</b>	0.00000	0.00000	0.00000	0.00000	0.00000	0.00000	0.00000	0.00000	0.00000	0.00000	0.00001
<b>H40</b>	0.29206	0.86371	0.62416	0.02606	0.02056	0.02379	-0.00103	-0.00171	-0.00960		
<b>H40</b>	0.29314	0.86455	0.62248	0.01620							
<b>(20k-12k)^2</b>	0.00000	0.00000	0.00000	0.00010	0.00042	0.00057	0.00000	0.00000	0.00009		

	X	Y	Z	U11	U22	U33	U12	U13	U23	0.00006	0.00007
<delta>	-0.00006	0.00047	-0.00015	-0.00053	0.00149	0.00029	-0.00012	0.00036	0.00044	0.00042	
RMS:	0.00012	0.00051	0.00016	0.00062	0.00153	0.00038	0.00023	0.00048	0.00051	0.00098	0.00075
0.6 Angstroms	N - X										
CorH(A)											
ATOM	X	Y	Z	U11	U22	U33	U12	U13	U23	sum delUii	sum Uii+uij
C1	0.41874	0.30418	0.10952	0.00537	0.00641	0.00572	0.00011	0.00114	0.00016		
C1	0.41947	0.30454	0.10970	0.00660	0.00520	0.00560	0.00040	0.00070	0.00020		
(20k-12k)^2	0.00000	0.00000	0.00000	0.00000	0.00000	0.00000	0.00000	0.00000	0.00000	0.00000	0.00000
C2	0.43763	0.22746	0.17940	0.00518	0.00654	0.00548	0.00020	0.00111	0.00046		
C2	0.43824	0.22785	0.17946	0.00610	0.00570	0.00560	0.00060	0.00090	0.00030		
(20k-12k)^2	0.00000	0.00000	0.00000	0.00000	0.00000	0.00000	0.00000	0.00000	0.00000	0.00000	0.00000
C3	0.34016	0.18267	0.18921	0.00571	0.00660	0.00604	0.00018	0.00154	0.00058		
C3	0.34071	0.18338	0.18934	0.00630	0.00620	0.00580	0.00060	0.00120	0.00060		
(20k-12k)^2	0.00000	0.00000	0.00000	0.00000	0.00000	0.00000	0.00000	0.00000	0.00000	0.00000	0.00000
C4	0.26094	0.23226	0.12591	0.00512	0.00670	0.00649	0.00014	0.00104	0.00037		
C4	0.26169	0.23301	0.12621	0.00620	0.00650	0.00650	0.00080	0.00100	0.00040		
(20k-12k)^2	0.00000	0.00000	0.00000	0.00000	0.00000	0.00000	0.00000	0.00000	0.00000	0.00000	0.00000
C5	0.30967	0.30723	0.07672	0.00553	0.00669	0.00566	0.00046	0.00068	0.00035		
C5	0.31042	0.30783	0.07703	0.00640	0.00590	0.00600	0.00090	0.00080	0.00050		
(20k-12k)^2	0.00000	0.00000	0.00000	0.00000	0.00000	0.00000	0.00000	0.00000	0.00000	0.00000	0.00000
C6	0.49161	0.32548	0.06073	0.00619	0.00675	0.00645	-0.00033	0.00191	0.00007		
C6	0.49215	0.32555	0.06085	0.00700	0.00570	0.00610	0.00000	0.00120	0.00030		
(20k-12k)^2	0.00000	0.00000	0.00000	0.00000	0.00000	0.00000	0.00000	0.00000	0.00000	0.00000	0.00000
C7	0.59477	0.28033	0.09516	0.00571	0.00839	0.00792	-0.00034	0.00194	0.00000		
C7	0.59521	0.28020	0.09516	0.00660	0.00700	0.00770	0.00000	0.00170	0.00030		
(20k-12k)^2	0.00000	0.00000	0.00000	0.00000	0.00000	0.00000	0.00000	0.00000	0.00000	0.00000	0.00000
H7	0.65858	0.29947	0.06366	0.01649	0.02973	0.02575	0.00038	0.01062	0.00569		
H7	0.66055	0.29766	0.06475	0.01910							
(20k-12k)^2	0.00000	0.00000	0.00000	0.00001	0.00088	0.00066	0.00000	0.00011	0.00003		
C8	0.61340	0.20560	0.16387	0.00557	0.00807	0.00802	0.00059	0.00123	0.00023		



C8	0.61378	0.20552	0.16382	0.00620	0.00720	0.00760	0.00070	0.00090	0.00040		
(20k-12k)^2	0.00000	0.00000	0.00000	0.00000	0.00000	0.00000	0.00000	0.00000	0.00000	0.00000	0.00000
H8	0.69121	0.16880	0.18367	0.01337	0.02847	0.02612	0.00631	0.00333	0.00546		
H8	0.69188	0.16925	0.18361	0.01520							
(20k-12k)^2	0.00000	0.00000	0.00000	0.00000	0.00081	0.00068	0.00004	0.00001	0.00003		
C9	0.53044	0.16831	0.20442	0.00539	0.00702	0.00653	0.00061	0.00097	0.00019		
C9	0.53091	0.16838	0.20448	0.00620	0.00610	0.00610	0.00060	0.00070	0.00040		
(20k-12k)^2	0.00000	0.00000	0.00000	0.00000	0.00000	0.00000	0.00000	0.00000	0.00000	0.00000	0.00000
C10	0.52277	0.06473	0.25293	0.00656	0.00818	0.00773	0.00096	0.00062	0.00117		
C10	0.52306	0.06504	0.25289	0.00730	0.00710	0.00720	0.00090	0.00040	0.00150		
(20k-12k)^2	0.00000	0.00000	0.00000	0.00000	0.00000	0.00000	0.00000	0.00000	0.00000	0.00000	0.00000
H10	0.59264	0.01399	0.27756	0.01515	0.02282	0.02801	0.00529	0.00129	0.00656		
H10	0.59348	0.01568	0.27823	0.01800							
(20k-12k)^2	0.00000	0.00000	0.00000	0.00001	0.00052	0.00078	0.00003	0.00000	0.00004		
C11	0.42710	0.02064	0.26217	0.00723	0.00813	0.00725	0.00061	0.00131	0.00173		
C11	0.42736	0.02127	0.26220	0.00790	0.00740	0.00720	0.00080	0.00120	0.00210		
(20k-12k)^2	0.00000	0.00000	0.00000	0.00000	0.00000	0.00000	0.00000	0.00000	0.00000	0.00000	0.00000
H11	0.42582	-0.06187	0.29421	0.02308	0.01786	0.02724	0.00058	0.00513	0.01009		
H11	0.42314	-0.06097	0.29422	0.01880							
(20k-12k)^2	0.00001	0.00000	0.00000	0.00002	0.00032	0.00074	0.00000	0.00003	0.00010		
C12	0.32957	0.07607	0.22459	0.00645	0.00725	0.00645	0.00006	0.00170	0.00082		
C12	0.33004	0.07678	0.22465	0.00700	0.00700	0.00660	0.00040	0.00170	0.00110		
(20k-12k)^2	0.00000	0.00000	0.00000	0.00000	0.00000	0.00000	0.00000	0.00000	0.00000	0.00000	0.00000
C13	0.22544	0.02776	0.20372	0.00717	0.00820	0.00861	-0.00060	0.00240	0.00129		
C13	0.22596	0.02873	0.20394	0.00770	0.00860	0.00930	-0.00050	0.00240	0.00180		
(20k-12k)^2	0.00000	0.00000	0.00000	0.00000	0.00000	0.00000	0.00000	0.00000	0.00000	0.00000	0.00000
H13	0.20945	-0.05376	0.23209	0.02249	0.01955	0.02792	-0.00377	0.00517	0.00884		
H13	0.20897	-0.05373	0.23084	0.02800							
(20k-12k)^2	0.00000	0.00000	0.00000	0.00003	0.00038	0.00078	0.00001	0.00003	0.00008		
C14	0.14804	0.07650	0.14180	0.00595	0.00875	0.01011	-0.00065	0.00217	0.00069		
C14	0.14855	0.07749	0.14207	0.00670	0.00940	0.01050	-0.00040	0.00200	0.00140		
(20k-12k)^2	0.00000	0.00000	0.00000	0.00000	0.00000	0.00000	0.00000	0.00000	0.00000	0.00000	0.00000

H14	0.07354	0.03169	0.12390	0.01513	0.02496	0.03000	-0.00711	0.00167	0.00406		
H14	0.07247	0.03542	0.12443	0.01500							
(20k-12k)^2	0.00000	0.00001	0.00000	0.00000	0.00062	0.00090	0.00005	0.00000	0.00002		
C15	0.16702	0.17774	0.09479	0.00519	0.00790	0.00747	0.00025	0.00128	0.00017		
C15	0.16773	0.17877	0.09515	0.00590	0.00800	0.00840	0.00050	0.00120	0.00080		
(20k-12k)^2	0.00000	0.00000	0.00000	0.00000	0.00000	0.00000	0.00000	0.00000	0.00000	0.00000	0.00000
C16	0.11435	0.21621	0.01182	0.00555	0.00985	0.00872	0.00025	0.00022	0.00044		
C16	0.11497	0.21748	0.01226	0.00620	0.01030	0.00940	0.00050	0.00000	0.00100		
(20k-12k)^2	0.00000	0.00000	0.00000	0.00000	0.00000	0.00000	0.00000	0.00000	0.00000	0.00000	0.00000
H16	0.03787	0.18100	-0.01605	0.01374	0.03160	0.02378	-0.00633	-0.00222	0.00205		
H16	0.03727	0.18417	-0.01488	0.02010							
(20k-12k)^2	0.00000	0.00001	0.00000	0.00004	0.00100	0.00057	0.00004	0.00000	0.00000		
C17	0.16257	0.28883	-0.03681	0.00623	0.00945	0.00732	0.00062	-0.00015	0.00084		
C17	0.16318	0.28992	-0.03633	0.00740	0.00910	0.00800	0.00100	-0.00070	0.00120		
(20k-12k)^2	0.00000	0.00000	0.00000	0.00000	0.00000	0.00000	0.00000	0.00000	0.00000	0.00000	0.00000
H17	0.12321	0.30711	-0.10143	0.02121	0.03098	0.01576	-0.00175	-0.00341	0.00559		
H17	0.12467	0.31000	-0.10116	0.01940							
(20k-12k)^2	0.00000	0.00001	0.00000	0.00000	0.00096	0.00025	0.00000	0.00001	0.00003		
C18	0.26764	0.33087	-0.00703	0.00672	0.00709	0.00616	0.00054	0.00054	0.00072		
C18	0.26832	0.33163	-0.00664	0.00740	0.00660	0.00630	0.00100	0.00020	0.00090		
(20k-12k)^2	0.00000	0.00000	0.00000	0.00000	0.00000	0.00000	0.00000	0.00000	0.00000	0.00000	0.00000
C19	0.34172	0.37238	-0.05504	0.00835	0.00855	0.00662	0.00027	0.00125	0.00139		
C19	0.34222	0.37276	-0.05476	0.00920	0.00740	0.00660	0.00050	0.00070	0.00170		
(20k-12k)^2	0.00000	0.00000	0.00000	0.00000	0.00000	0.00000	0.00000	0.00000	0.00000	0.00000	0.00000
H19	0.31396	0.39834	-0.12045	0.02255	0.03325	0.01430	0.00019	0.00075	0.00773		
H19	0.31351	0.40015	-0.11994	0.01770							
(20k-12k)^2	0.00000	0.00000	0.00000	0.00002	0.00111	0.00020	0.00000	0.00000	0.00006		
C20	0.44865	0.36958	-0.02289	0.00775	0.00771	0.00683	-0.00047	0.00168	0.00094		
C20	0.44914	0.36968	-0.02273	0.00910	0.00680	0.00660	-0.00040	0.00140	0.00130		
(20k-12k)^2	0.00000	0.00000	0.00000	0.00000	0.00000	0.00000	0.00000	0.00000	0.00000	0.00000	0.00000
H20	0.50080	0.39408	-0.06425	0.02026	0.03026	0.01950	-0.00232	0.00897	0.00539		
H20	0.50215	0.39216	-0.06402	0.01930							

(20k-12k)^2	0.00000	0.00000	0.00000	0.00000	0.00092	0.00038	0.00001	0.00008	0.00003		
	X	Y	Z	U11	U22	U33	U12	U13	U23	0.00003	0.00004
<delta>	-0.00054	-0.00055	-0.00019	-0.00082	0.00055	-0.00008	-0.00027	0.00025	-0.00028	-0.00012	
RMS:	0.00056	0.00068	0.00024	0.00085	0.00080	0.00042	0.00032	0.00032	0.00035	0.00072	0.00056
0.6 Angstroms	N - X										
CorH(B)											
ATOM	X	Y	Z	U11	U22	U33	U12	U13	U23	sum delUii	sum Uii+uij
C21	0.15425	0.69847	0.46826	0.00590	0.00607	0.00616	0.00013	0.00128	-0.00065		
C21	0.15442	0.69786	0.46838	0.00710	0.00520	0.00690	0.00000	0.00100	-0.00100		
(20k-12k)^2	0.00000	0.00000	0.00000	0.00000	0.00000	0.00000	0.00000	0.00000	0.00000	0.00000	0.00000
C22	0.09847	0.69606	0.38331	0.00546	0.00576	0.00655	0.00042	0.00060	-0.00034		
C22	0.09862	0.69546	0.38347	0.00690	0.00560	0.00710	0.00030	0.00060	-0.00100		
(20k-12k)^2	0.00000	0.00000	0.00000	0.00000	0.00000	0.00000	0.00000	0.00000	0.00000	0.00000	0.00000
C23	0.12314	0.59147	0.34647	0.00597	0.00616	0.00640	-0.00005	0.00108	-0.00065		
C23	0.12325	0.59102	0.34664	0.00700	0.00610	0.00680	-0.00010	0.00100	-0.00130		
(20k-12k)^2	0.00000	0.00000	0.00000	0.00000	0.00000	0.00000	0.00000	0.00000	0.00000	0.00000	0.00000
C24	0.19470	0.52962	0.40854	0.00598	0.00572	0.00693	0.00012	0.00138	-0.00018		
C24	0.19469	0.52914	0.40869	0.00770	0.00490	0.00760	0.00010	0.00160	-0.00090		
(20k-12k)^2	0.00000	0.00000	0.00000	0.00000	0.00000	0.00000	0.00000	0.00000	0.00000	0.00000	0.00000
C25	0.21454	0.59616	0.48352	0.00625	0.00606	0.00647	0.00033	0.00114	0.00005		
C25	0.21459	0.59572	0.48368	0.00760	0.00510	0.00680	0.00010	0.00120	-0.00060		
(20k-12k)^2	0.00000	0.00000	0.00000	0.00000	0.00000	0.00000	0.00000	0.00000	0.00000	0.00000	0.00000
C26	0.18136	0.79973	0.51238	0.00702	0.00639	0.00723	-0.00004	0.00145	-0.00111		
C26	0.18146	0.79906	0.51248	0.00770	0.00540	0.00750	0.00000	0.00070	-0.00140		
(20k-12k)^2	0.00000	0.00000	0.00000	0.00000	0.00000	0.00000	0.00000	0.00000	0.00000	0.00000	0.00000
C27	0.13359	0.90230	0.46986	0.00866	0.00620	0.00987	0.00022	0.00134	-0.00096		
C27	0.13379	0.90150	0.46994	0.00970	0.00550	0.00990	0.00070	0.00070	-0.00150		
(20k-12k)^2	0.00000	0.00000	0.00000	0.00000	0.00000	0.00000	0.00000	0.00000	0.00000	0.00000	0.00000
H27	0.14613	0.98561	0.50155	0.03093	0.01440	0.02445	0.00024	0.00118	-0.00546		
H27	0.14551	0.98402	0.50321	0.01860							
(20k-12k)^2	0.00000	0.00000	0.00000	0.00015	0.00021	0.00060	0.00000	0.00000	0.00003		

C28	0.07967	0.89999	0.38628	0.00852	0.00659	0.01009	0.00139	0.00070	-0.00017		
C28	0.07992	0.89924	0.38631	0.00990	0.00610	0.01030	0.00150	-0.00020	-0.00030		
(20k-12k)^2	0.00000	0.00000	0.00000	0.00000	0.00000	0.00000	0.00000	0.00000	0.00000	0.00000	0.00000
H28	0.05260	0.98127	0.35568	0.03031	0.01456	0.02507	0.00538	-0.00022	0.00399		
H28	0.05159	0.98116	0.35670	0.02090							
(20k-12k)^2	0.00000	0.00000	0.00000	0.00009	0.00021	0.00063	0.00003	0.00000	0.00002		
C29	0.06686	0.79452	0.33708	0.00632	0.00680	0.00804	0.00068	0.00061	0.00021		
C29	0.06703	0.79395	0.33718	0.00770	0.00650	0.00810	0.00080	0.00010	-0.00030		
(20k-12k)^2	0.00000	0.00000	0.00000	0.00000	0.00000	0.00000	0.00000	0.00000	0.00000	0.00000	0.00000
C30	0.04570	0.77801	0.24645	0.00814	0.00865	0.00765	0.00096	0.00024	0.00090		
C30	0.04594	0.77751	0.24666	0.00940	0.00860	0.00840	0.00130	-0.00020	0.00060		
(20k-12k)^2	0.00000	0.00000	0.00000	0.00000	0.00000	0.00000	0.00000	0.00000	0.00000	0.00000	0.00000
H30	0.01540	0.84967	0.20500	0.03109	0.01962	0.02012	0.00671	0.00181	0.00621		
H30	0.01178	0.84990	0.20712	0.01900							
(20k-12k)^2	0.00001	0.00000	0.00000	0.00015	0.00038	0.00040	0.00005	0.00000	0.00004		
C31	0.07063	0.67546	0.21028	0.00786	0.00996	0.00663	0.00045	0.00037	0.00005		
C31	0.07065	0.67514	0.21043	0.00930	0.00960	0.00710	0.00070	-0.00020	-0.00050		
(20k-12k)^2	0.00000	0.00000	0.00000	0.00000	0.00000	0.00000	0.00000	0.00000	0.00000	0.00000	0.00000
H31	0.06063	0.67161	0.14190	0.02995	0.02776	0.01191	0.00325	0.00271	-0.00028		
H31	0.06163	0.67100	0.14200	0.01830							
(20k-12k)^2	0.00000	0.00000	0.00000	0.00014	0.00077	0.00014	0.00001	0.00001	0.00000		
C32	0.11816	0.57889	0.26082	0.00642	0.00787	0.00616	0.00006	0.00091	-0.00093		
C32	0.11808	0.57852	0.26103	0.00790	0.00760	0.00690	0.00010	0.00060	-0.00160		
(20k-12k)^2	0.00000	0.00000	0.00000	0.00000	0.00000	0.00000	0.00000	0.00000	0.00000	0.00000	0.00000
C33	0.17819	0.48282	0.23888	0.00814	0.00884	0.00747	-0.00008	0.00163	-0.00216		
C33	0.17819	0.48267	0.23909	0.00910	0.00820	0.00770	0.00040	0.00140	-0.00260		
(20k-12k)^2	0.00000	0.00000	0.00000	0.00000	0.00000	0.00000	0.00000	0.00000	0.00000	0.00000	0.00000
H33	0.17338	0.46037	0.17287	0.02911	0.02876	0.01357	0.00418	0.00347	-0.00508		
H33	0.17372	0.46114	0.17284	0.01770							
(20k-12k)^2	0.00000	0.00000	0.00000	0.00013	0.00083	0.00018	0.00002	0.00001	0.00003		
C34	0.24844	0.42222	0.29996	0.00848	0.00731	0.00898	0.00085	0.00232	-0.00152		
C34	0.24834	0.42205	0.30019	0.00980	0.00680	0.00910	0.00080	0.00230	-0.00210		

(20k-12k)^2	0.00000	0.00000	0.00000	0.00000	0.00000	0.00000	0.00000	0.00000	0.00000	0.00000	0.00000
H34	0.29603	0.35568	0.27928	0.02561	0.02246	0.02342	0.00927	0.00702	-0.00464		
H34	0.29652	0.35578	0.27917	0.02040							
(20k-12k)^2	0.00000	0.00000	0.00000	0.00003	0.00050	0.00055	0.00009	0.00005	0.00002		
C35	0.26565	0.45178	0.38856	0.00689	0.00571	0.00796	0.00042	0.00192	-0.00056		
C35	0.26561	0.45149	0.38877	0.00850	0.00530	0.00840	0.00060	0.00190	-0.00090		
(20k-12k)^2	0.00000	0.00000	0.00000	0.00000	0.00000	0.00000	0.00000	0.00000	0.00000	0.00000	0.00000
C36	0.35515	0.43062	0.45575	0.00751	0.00655	0.00968	0.00161	0.00161	0.00050		
C36	0.35508	0.43027	0.45594	0.00960	0.00590	0.00960	0.00170	0.00140	0.00060		
(20k-12k)^2	0.00000	0.00000	0.00000	0.00000	0.00000	0.00000	0.00000	0.00000	0.00000	0.00000	0.00000
H36	0.41261	0.36627	0.44721	0.02076	0.02060	0.02679	0.00884	0.00356	-0.00208		
H36	0.41492	0.36874	0.44687	0.02060							
(20k-12k)^2	0.00001	0.00001	0.00000	0.00000	0.00042	0.00072	0.00008	0.00001	0.00000		
C37	0.37481	0.49640	0.52920	0.00755	0.00782	0.00831	0.00127	0.00103	0.00142		
C37	0.37483	0.49614	0.52935	0.00960	0.00690	0.00830	0.00180	0.00090	0.00110		
(20k-12k)^2	0.00000	0.00000	0.00000	0.00000	0.00000	0.00000	0.00000	0.00000	0.00000	0.00001	0.00001
H37	0.44719	0.48170	0.57485	0.01722	0.02754	0.02104	0.00558	-0.00336	-0.00046		
H37	0.44757	0.48239	0.57526	0.01980							
(20k-12k)^2	0.00000	0.00000	0.00000	0.00001	0.00076	0.00044	0.00003	0.00001	0.00000		
C38	0.30688	0.58990	0.54262	0.00652	0.00721	0.00670	0.00048	0.00091	0.00043		
C38	0.30692	0.58950	0.54279	0.00840	0.00610	0.00670	0.00060	0.00080	0.00030		
(20k-12k)^2	0.00000	0.00000	0.00000	0.00000	0.00000	0.00000	0.00000	0.00000	0.00000	0.00000	0.00000
C39	0.32825	0.68916	0.59787	0.00817	0.00884	0.00635	0.00001	0.00016	-0.00017		
C39	0.32831	0.68863	0.59798	0.00950	0.00770	0.00670	0.00030	0.00000	-0.00060		
(20k-12k)^2	0.00000	0.00000	0.00000	0.00000	0.00000	0.00000	0.00000	0.00000	0.00000	0.00000	0.00000
H39	0.39714	0.68918	0.64888	0.02054	0.02556	0.02042	0.00156	-0.00532	-0.00219		
H39	0.39915	0.68926	0.64725	0.02080							
(20k-12k)^2	0.00000	0.00000	0.00000	0.00000	0.00065	0.00042	0.00000	0.00003	0.00000		
C40	0.26809	0.78899	0.58377	0.00827	0.00793	0.00734	-0.00026	0.00089	-0.00155		
C40	0.26814	0.78833	0.58389	0.00940	0.00700	0.00740	-0.00010	0.00000	-0.00190		
(20k-12k)^2	0.00000	0.00000	0.00000	0.00000	0.00000	0.00000	0.00000	0.00000	0.00000	0.00000	0.00000
H40	0.29196	0.86353	0.62415	0.02581	0.01904	0.02345	-0.00033	-0.00183	-0.00889		

<b>H40</b>	0.29314	0.86455	0.62248	0.01620							
<b>(20k-12k)^2</b>	0.00000	0.00000	0.00000	0.00009	0.00036	0.00055	0.00000	0.00000	0.00008		
	<b>X</b>	<b>Y</b>	<b>Z</b>	<b>U11</b>	<b>U22</b>	<b>U33</b>	<b>U12</b>	<b>U13</b>	<b>U23</b>	<b>0.00005</b>	<b>0.00006</b>
<b>&lt;delta&gt;</b>	<b>-0.00007</b>	<b>0.00047</b>	<b>-0.00015</b>	<b>-0.00139</b>	<b>0.00062</b>	<b>-0.00032</b>	<b>-0.00013</b>	<b>0.00030</b>	<b>0.00043</b>	<b>-0.00036</b>	
<b>RMS:</b>	<b>0.00012</b>	<b>0.00050</b>	<b>0.00016</b>	<b>0.00143</b>	<b>0.00070</b>	<b>0.00041</b>	<b>0.00025</b>	<b>0.00043</b>	<b>0.00047</b>	<b>0.00095</b>	<b>0.00073</b>
<b>0.7 Angstroms</b>	<b>N - X</b>										
<b>CorH(A)</b>											
<b>ATOM</b>	<b>X</b>	<b>Y</b>	<b>Z</b>	<b>U11</b>	<b>U22</b>	<b>U33</b>	<b>U12</b>	<b>U13</b>	<b>U23</b>	<b>sum delUii</b>	<b>sum Uii+uij</b>
<b>C1</b>	0.41872	0.30414	0.10952	0.00505	0.00638	0.00547	0.00019	0.00107	0.00029		
<b>C1</b>	0.41947	0.30454	0.10970	0.00660	0.00520	0.00560	0.00040	0.00070	0.00020		
<b>(20k-12k)^2</b>	0.00000	0.00000	0.00000	0.00000	0.00000	0.00000	0.00000	0.00000	0.00000	0.00000	0.00000
<b>C2</b>	0.43761	0.22743	0.17939	0.00489	0.00663	0.00502	0.00036	0.00106	0.00040		
<b>C2</b>	0.43824	0.22785	0.17946	0.00610	0.00570	0.00560	0.00060	0.00090	0.00030		
<b>(20k-12k)^2</b>	0.00000	0.00000	0.00000	0.00000	0.00000	0.00000	0.00000	0.00000	0.00000	0.00000	0.00000
<b>C3</b>	0.34011	0.18272	0.18919	0.00522	0.00647	0.00565	0.00037	0.00124	0.00063		
<b>C3</b>	0.34071	0.18338	0.18934	0.00630	0.00620	0.00580	0.00060	0.00120	0.00060		
<b>(20k-12k)^2</b>	0.00000	0.00000	0.00000	0.00000	0.00000	0.00000	0.00000	0.00000	0.00000	0.00000	0.00000
<b>C4</b>	0.26095	0.23225	0.12590	0.00467	0.00624	0.00627	0.00020	0.00083	0.00031		
<b>C4</b>	0.26169	0.23301	0.12621	0.00620	0.00650	0.00650	0.00080	0.00100	0.00040		
<b>(20k-12k)^2</b>	0.00000	0.00000	0.00000	0.00000	0.00000	0.00000	0.00000	0.00000	0.00000	0.00000	0.00000
<b>C5</b>	0.30963	0.30719	0.07675	0.00528	0.00644	0.00553	0.00044	0.00067	0.00041		
<b>C5</b>	0.31042	0.30783	0.07703	0.00640	0.00590	0.00600	0.00090	0.00080	0.00050		
<b>(20k-12k)^2</b>	0.00000	0.00000	0.00000	0.00000	0.00000	0.00000	0.00000	0.00000	0.00000	0.00000	0.00000
<b>C6</b>	0.49163	0.32548	0.06074	0.00606	0.00670	0.00591	-0.00060	0.00181	-0.00004		
<b>C6</b>	0.49215	0.32555	0.06085	0.00700	0.00570	0.00610	0.00000	0.00120	0.00030		
<b>(20k-12k)^2</b>	0.00000	0.00000	0.00000	0.00000	0.00000	0.00000	0.00000	0.00000	0.00000	0.00000	0.00000
<b>C7</b>	0.59484	0.28037	0.09517	0.00555	0.00802	0.00780	-0.00046	0.00185	0.00022		
<b>C7</b>	0.59521	0.28020	0.09516	0.00660	0.00700	0.00770	0.00000	0.00170	0.00030		
<b>(20k-12k)^2</b>	0.00000	0.00000	0.00000	0.00000	0.00000	0.00000	0.00000	0.00000	0.00000	0.00000	0.00000
<b>H7</b>	0.65855	0.29952	0.06370	0.01645	0.02999	0.02500	-0.00001	0.01042	0.00607		
<b>H7</b>	0.66055	0.29766	0.06475	0.01910							
<b>(20k-12k)^2</b>	0.00000	0.00000	0.00000	0.00001	0.00090	0.00063	0.00000	0.00011	0.00004		

C8	0.61346	0.20561	0.16392	0.00536	0.00801	0.00754	0.00066	0.00139	0.00040		
C8	0.61378	0.20552	0.16382	0.00620	0.00720	0.00760	0.00070	0.00090	0.00040		
(20k-12k)^2	0.00000	0.00000	0.00000	0.00000	0.00000	0.00000	0.00000	0.00000	0.00000	0.00000	0.00000
H8	0.69122	0.16896	0.18372	0.01326	0.02795	0.02553	0.00632	0.00351	0.00554		
H8	0.69188	0.16925	0.18361	0.01520							
(20k-12k)^2	0.00000	0.00000	0.00000	0.00000	0.00078	0.00065	0.00004	0.00001	0.00003		
C9	0.53047	0.16831	0.20444	0.00486	0.00732	0.00606	0.00075	0.00070	0.00029		
C9	0.53091	0.16838	0.20448	0.00620	0.00610	0.00610	0.00060	0.00070	0.00040		
(20k-12k)^2	0.00000	0.00000	0.00000	0.00000	0.00000	0.00000	0.00000	0.00000	0.00000	0.00000	0.00000
C10	0.52274	0.06465	0.25292	0.00629	0.00807	0.00751	0.00100	0.00076	0.00136		
C10	0.52306	0.06504	0.25289	0.00730	0.00710	0.00720	0.00090	0.00040	0.00150		
(20k-12k)^2	0.00000	0.00000	0.00000	0.00000	0.00000	0.00000	0.00000	0.00000	0.00000	0.00000	0.00000
H10	0.59263	0.01410	0.27755	0.01468	0.02271	0.02681	0.00530	0.00123	0.00670		
H10	0.59348	0.01568	0.27823	0.01800							
(20k-12k)^2	0.00000	0.00000	0.00000	0.00001	0.00052	0.00072	0.00003	0.00000	0.00004		
C11	0.42705	0.02065	0.26217	0.00698	0.00775	0.00734	0.00047	0.00120	0.00169		
C11	0.42736	0.02127	0.26220	0.00790	0.00740	0.00720	0.00080	0.00120	0.00210		
(20k-12k)^2	0.00000	0.00000	0.00000	0.00000	0.00000	0.00000	0.00000	0.00000	0.00000	0.00000	0.00000
H11	0.42584	-0.06196	0.29422	0.02268	0.01793	0.02674	0.00047	0.00502	0.01022		
H11	0.42314	-0.06097	0.29422	0.01880							
(20k-12k)^2	0.00001	0.00000	0.00000	0.00002	0.00032	0.00072	0.00000	0.00003	0.00010		
C12	0.32953	0.07607	0.22459	0.00632	0.00701	0.00625	0.00019	0.00173	0.00086		
C12	0.33004	0.07678	0.22465	0.00700	0.00700	0.00660	0.00040	0.00170	0.00110		
(20k-12k)^2	0.00000	0.00000	0.00000	0.00000	0.00000	0.00000	0.00000	0.00000	0.00000	0.00000	0.00000
C13	0.22541	0.02774	0.20370	0.00669	0.00796	0.00830	-0.00062	0.00250	0.00116		
C13	0.22596	0.02873	0.20394	0.00770	0.00860	0.00930	-0.00050	0.00240	0.00180		
(20k-12k)^2	0.00000	0.00000	0.00000	0.00000	0.00000	0.00000	0.00000	0.00000	0.00000	0.00000	0.00000
H13	0.20945	-0.05370	0.23206	0.02238	0.01927	0.02825	-0.00388	0.00516	0.00899		
H13	0.20897	-0.05373	0.23084	0.02800							
(20k-12k)^2	0.00000	0.00000	0.00000	0.00003	0.00037	0.00080	0.00002	0.00003	0.00008		
C14	0.14795	0.07648	0.14176	0.00575	0.00847	0.01000	-0.00055	0.00245	0.00071		
C14	0.14855	0.07749	0.14207	0.00670	0.00940	0.01050	-0.00040	0.00200	0.00140		

(20k-12k)^2	0.00000	0.00000	0.00000	0.00000	0.00000	0.00000	0.00000	0.00000	0.00000	0.00000	0.00000
H14	0.07347	0.03163	0.12391	0.01459	0.02491	0.03032	-0.00726	0.00128	0.00384		
H14	0.07247	0.03542	0.12443	0.01500							
(20k-12k)^2	0.00000	0.00001	0.00000	0.00000	0.00062	0.00092	0.00005	0.00000	0.00001		
C15	0.16704	0.17773	0.09477	0.00497	0.00745	0.00734	0.00031	0.00126	0.00033		
C15	0.16773	0.17877	0.09515	0.00590	0.00800	0.00840	0.00050	0.00120	0.00080		
(20k-12k)^2	0.00000	0.00000	0.00000	0.00000	0.00000	0.00000	0.00000	0.00000	0.00000	0.00000	0.00000
C16	0.11437	0.21625	0.01184	0.00564	0.00961	0.00829	0.00042	0.00037	0.00060		
C16	0.11497	0.21748	0.01226	0.00620	0.01030	0.00940	0.00050	0.00000	0.00100		
(20k-12k)^2	0.00000	0.00000	0.00000	0.00000	0.00000	0.00000	0.00000	0.00000	0.00000	0.00000	0.00000
H16	0.03788	0.18107	-0.01609	0.01412	0.03150	0.02291	-0.00624	-0.00185	0.00171		
H16	0.03727	0.18417	-0.01488	0.02010							
(20k-12k)^2	0.00000	0.00001	0.00000	0.00004	0.00099	0.00052	0.00004	0.00000	0.00000		
C17	0.16257	0.28885	-0.03677	0.00577	0.00927	0.00719	0.00070	-0.00015	0.00076		
C17	0.16318	0.28992	-0.03633	0.00740	0.00910	0.00800	0.00100	-0.00070	0.00120		
(20k-12k)^2	0.00000	0.00000	0.00000	0.00000	0.00000	0.00000	0.00000	0.00000	0.00000	0.00000	0.00000
H17	0.12317	0.30697	-0.10145	0.02122	0.03113	0.01588	-0.00181	-0.00367	0.00518		
H17	0.12467	0.31000	-0.10116	0.01940							
(20k-12k)^2	0.00000	0.00001	0.00000	0.00000	0.00097	0.00025	0.00000	0.00001	0.00003		
C18	0.26765	0.33083	-0.00701	0.00657	0.00651	0.00617	0.00057	0.00065	0.00076		
C18	0.26832	0.33163	-0.00664	0.00740	0.00660	0.00630	0.00100	0.00020	0.00090		
(20k-12k)^2	0.00000	0.00000	0.00000	0.00000	0.00000	0.00000	0.00000	0.00000	0.00000	0.00000	0.00000
C19	0.34168	0.37232	-0.05502	0.00795	0.00812	0.00689	0.00012	0.00152	0.00115		
C19	0.34222	0.37276	-0.05476	0.00920	0.00740	0.00660	0.00050	0.00070	0.00170		
(20k-12k)^2	0.00000	0.00000	0.00000	0.00000	0.00000	0.00000	0.00000	0.00000	0.00000	0.00000	0.00000
H19	0.31408	0.39828	-0.12041	0.02245	0.03259	0.01450	0.00008	0.00089	0.00729		
H19	0.31351	0.40015	-0.11994	0.01770							
(20k-12k)^2	0.00000	0.00000	0.00000	0.00002	0.00106	0.00021	0.00000	0.00000	0.00005		
C20	0.44862	0.36956	-0.02289	0.00742	0.00737	0.00657	-0.00051	0.00161	0.00090		
C20	0.44914	0.36968	-0.02273	0.00910	0.00680	0.00660	-0.00040	0.00140	0.00130		
(20k-12k)^2	0.00000	0.00000	0.00000	0.00000	0.00000	0.00000	0.00000	0.00000	0.00000	0.00000	0.00000
H20	0.50077	0.39391	-0.06422	0.02007	0.03003	0.01930	-0.00268	0.00884	0.00495		



<b>H20</b>	0.50215	0.39216	-0.06402	0.01930							
<b>(20k-12k)^2</b>	0.00000	0.00000	0.00000	0.00000	0.00090	0.00037	0.00001	0.00008	0.00002		
	<b>X</b>	<b>Y</b>	<b>Z</b>	<b>U11</b>	<b>U22</b>	<b>U33</b>	<b>U12</b>	<b>U13</b>	<b>U23</b>	<b>0.00004</b>	<b>0.00005</b>
<b>&lt;delta&gt;</b>	<b>-0.00055</b>	<b>-0.00056</b>	<b>-0.00018</b>	<b>-0.00111</b>	<b>0.00033</b>	<b>-0.00030</b>	<b>-0.00024</b>	<b>0.00025</b>	<b>-0.00025</b>	<b>-0.00036</b>	
<b>RMS:</b>	<b>0.00057</b>	<b>0.00069</b>	<b>0.00024</b>	<b>0.00115</b>	<b>0.00074</b>	<b>0.00051</b>	<b>0.00032</b>	<b>0.00036</b>	<b>0.00034</b>	<b>0.00084</b>	<b>0.00064</b>
<b>0.7 Angstroms</b>	<b>N - X</b>										
<b>CorH(A)</b>											
<b>ATOM</b>	<b>X</b>	<b>Y</b>	<b>Z</b>	<b>U11</b>	<b>U22</b>	<b>U33</b>	<b>U12</b>	<b>U13</b>	<b>U23</b>	<b>sum delUii</b>	<b>sum Uii+uij</b>
<b>C21</b>	0.15423	0.69841	0.46826	0.00569	0.00558	0.00652	0.00018	0.00140	-0.00091		
<b>C21</b>	0.15442	0.69786	0.46838	0.00710	0.00520	0.00690	0.00000	0.00100	-0.00100		
<b>(20k-12k)^2</b>	0.00000	0.00000	0.00000	0.00000	0.00000	0.00000	0.00000	0.00000	0.00000	0.00000	0.00000
<b>C22</b>	0.09845	0.69604	0.38325	0.00523	0.00559	0.00662	0.00029	0.00062	-0.00032		
<b>C22</b>	0.09862	0.69546	0.38347	0.00690	0.00560	0.00710	0.00030	0.00060	-0.00100		
<b>(20k-12k)^2</b>	0.00000	0.00000	0.00000	0.00000	0.00000	0.00000	0.00000	0.00000	0.00000	0.00000	0.00000
<b>C23</b>	0.12317	0.59146	0.34648	0.00566	0.00599	0.00597	0.00024	0.00101	-0.00054		
<b>C23</b>	0.12325	0.59102	0.34664	0.00700	0.00610	0.00680	-0.00010	0.00100	-0.00130		
<b>(20k-12k)^2</b>	0.00000	0.00000	0.00000	0.00000	0.00000	0.00000	0.00000	0.00000	0.00000	0.00000	0.00000
<b>C24</b>	0.19473	0.52962	0.40853	0.00584	0.00541	0.00680	0.00035	0.00139	-0.00024		
<b>C24</b>	0.19469	0.52914	0.40869	0.00770	0.00490	0.00760	0.00010	0.00160	-0.00090		
<b>(20k-12k)^2</b>	0.00000	0.00000	0.00000	0.00000	0.00000	0.00000	0.00000	0.00000	0.00000	0.00000	0.00000
<b>C25</b>	0.21455	0.59617	0.48352	0.00607	0.00604	0.00614	0.00019	0.00143	-0.00006		
<b>C25</b>	0.21459	0.59572	0.48368	0.00760	0.00510	0.00680	0.00010	0.00120	-0.00060		
<b>(20k-12k)^2</b>	0.00000	0.00000	0.00000	0.00000	0.00000	0.00000	0.00000	0.00000	0.00000	0.00000	0.00000
<b>C26</b>	0.18132	0.79967	0.51239	0.00686	0.00642	0.00693	-0.00007	0.00159	-0.00114		
<b>C26</b>	0.18146	0.79906	0.51248	0.00770	0.00540	0.00750	0.00000	0.00070	-0.00140		
<b>(20k-12k)^2</b>	0.00000	0.00000	0.00000	0.00000	0.00000	0.00000	0.00000	0.00000	0.00000	0.00000	0.00000
<b>C27</b>	0.13356	0.90238	0.46985	0.00845	0.00600	0.00926	0.00018	0.00128	-0.00112		
<b>C27</b>	0.13379	0.90150	0.46994	0.00970	0.00550	0.00990	0.00070	0.00070	-0.00150		
<b>(20k-12k)^2</b>	0.00000	0.00000	0.00000	0.00000	0.00000	0.00000	0.00000	0.00000	0.00000	0.00000	0.00000
<b>H27</b>	0.14612	0.98556	0.50161	0.03081	0.01444	0.02408	0.00024	0.00157	-0.00605		
<b>H27</b>	0.14551	0.98402	0.50321	0.01860							
<b>(20k-12k)^2</b>	0.00000	0.00000	0.00000	0.00015	0.00021	0.00058	0.00000	0.00000	0.00004		

C28	0.07966	0.89999	0.38628	0.00810	0.00675	0.00975	0.00137	0.00068	-0.00034		
C28	0.07992	0.89924	0.38631	0.00990	0.00610	0.01030	0.00150	-0.00020	-0.00030		
(20k-12k)^2	0.00000	0.00000	0.00000	0.00000	0.00000	0.00000	0.00000	0.00000	0.00000	0.00000	0.00000
H28	0.05268	0.98133	0.35560	0.03002	0.01448	0.02382	0.00517	-0.00085	0.00427		
H28	0.05159	0.98116	0.35670	0.02090							
(20k-12k)^2	0.00000	0.00000	0.00000	0.00008	0.00021	0.00057	0.00003	0.00000	0.00002		
C29	0.06688	0.79453	0.33707	0.00596	0.00661	0.00768	0.00089	0.00078	0.00020		
C29	0.06703	0.79395	0.33718	0.00770	0.00650	0.00810	0.00080	0.00010	-0.00030		
(20k-12k)^2	0.00000	0.00000	0.00000	0.00000	0.00000	0.00000	0.00000	0.00000	0.00000	0.00000	0.00000
C30	0.04566	0.77802	0.24648	0.00783	0.00818	0.00764	0.00098	0.00032	0.00085		
C30	0.04594	0.77751	0.24666	0.00940	0.00860	0.00840	0.00130	-0.00020	0.00060		
(20k-12k)^2	0.00000	0.00000	0.00000	0.00000	0.00000	0.00000	0.00000	0.00000	0.00000	0.00000	0.00000
H30	0.01543	0.84971	0.20497	0.02991	0.02016	0.01980	0.00686	0.00138	0.00600		
H30	0.01178	0.84990	0.20712	0.01900							
(20k-12k)^2	0.00001	0.00000	0.00000	0.00012	0.00041	0.00039	0.00005	0.00000	0.00004		
C31	0.07065	0.67546	0.21028	0.00741	0.00954	0.00670	0.00065	0.00053	-0.00002		
C31	0.07065	0.67514	0.21043	0.00930	0.00960	0.00710	0.00070	-0.00020	-0.00050		
(20k-12k)^2	0.00000	0.00000	0.00000	0.00000	0.00000	0.00000	0.00000	0.00000	0.00000	0.00000	0.00000
H31	0.06062	0.67146	0.14184	0.03003	0.02731	0.01245	0.00301	0.00296	-0.00071		
H31	0.06163	0.67100	0.14200	0.01830							
(20k-12k)^2	0.00000	0.00000	0.00000	0.00014	0.00075	0.00016	0.00001	0.00001	0.00000		
C32	0.11815	0.57884	0.26083	0.00609	0.00784	0.00587	0.00006	0.00110	-0.00081		
C32	0.11808	0.57852	0.26103	0.00790	0.00760	0.00690	0.00010	0.00060	-0.00160		
(20k-12k)^2	0.00000	0.00000	0.00000	0.00000	0.00000	0.00000	0.00000	0.00000	0.00000	0.00000	0.00001
C33	0.17816	0.48283	0.23891	0.00763	0.00874	0.00746	-0.00009	0.00190	-0.00202		
C33	0.17819	0.48267	0.23909	0.00910	0.00820	0.00770	0.00040	0.00140	-0.00260		
(20k-12k)^2	0.00000	0.00000	0.00000	0.00000	0.00000	0.00000	0.00000	0.00000	0.00000	0.00000	0.00000
H33	0.17338	0.46025	0.17286	0.02920	0.02801	0.01380	0.00453	0.00398	-0.00499		
H33	0.17372	0.46114	0.17284	0.01770							
(20k-12k)^2	0.00000	0.00000	0.00000	0.00013	0.00078	0.00019	0.00002	0.00002	0.00002		
C34	0.24844	0.42223	0.29998	0.00807	0.00739	0.00871	0.00103	0.00230	-0.00171		
C34	0.24834	0.42205	0.30019	0.00980	0.00680	0.00910	0.00080	0.00230	-0.00210		

(20k-12k)^2	0.00000	0.00000	0.00000	0.00000	0.00000	0.00000	0.00000	0.00000	0.00000	0.00000	0.00000
H34	0.29594	0.35578	0.27938	0.02557	0.02243	0.02232	0.00979	0.00696	-0.00422		
H34	0.29652	0.35578	0.27917	0.02040							
(20k-12k)^2	0.00000	0.00000	0.00000	0.00003	0.00050	0.00050	0.00010	0.00005	0.00002		
C35	0.26565	0.45179	0.38858	0.00663	0.00565	0.00781	0.00057	0.00228	-0.00038		
C35	0.26561	0.45149	0.38877	0.00850	0.00530	0.00840	0.00060	0.00190	-0.00090		
(20k-12k)^2	0.00000	0.00000	0.00000	0.00000	0.00000	0.00000	0.00000	0.00000	0.00000	0.00000	0.00000
C36	0.35513	0.43061	0.45573	0.00723	0.00638	0.00961	0.00180	0.00179	0.00082		
C36	0.35508	0.43027	0.45594	0.00960	0.00590	0.00960	0.00170	0.00140	0.00060		
(20k-12k)^2	0.00000	0.00000	0.00000	0.00001	0.00000	0.00000	0.00000	0.00000	0.00000	0.00001	0.00001
H36	0.41258	0.36637	0.44728	0.01997	0.02034	0.02644	0.00878	0.00341	-0.00189		
H36	0.41492	0.36874	0.44687	0.02060							
(20k-12k)^2	0.00001	0.00001	0.00000	0.00000	0.00041	0.00070	0.00008	0.00001	0.00000		
C37	0.37480	0.49638	0.52919	0.00724	0.00755	0.00817	0.00118	0.00098	0.00140		
C37	0.37483	0.49614	0.52935	0.00960	0.00690	0.00830	0.00180	0.00090	0.00110		
(20k-12k)^2	0.00000	0.00000	0.00000	0.00001	0.00000	0.00000	0.00000	0.00000	0.00000	0.00001	0.00001
H37	0.44716	0.48168	0.57480	0.01683	0.02710	0.02095	0.00542	-0.00323	-0.00017		
H37	0.44757	0.48239	0.57526	0.01980							
(20k-12k)^2	0.00000	0.00000	0.00000	0.00001	0.00073	0.00044	0.00003	0.00001	0.00000		
C38	0.30692	0.58990	0.54261	0.00599	0.00705	0.00657	0.00026	0.00088	0.00019		
C38	0.30692	0.58950	0.54279	0.00840	0.00610	0.00670	0.00060	0.00080	0.00030		
(20k-12k)^2	0.00000	0.00000	0.00000	0.00001	0.00000	0.00000	0.00000	0.00000	0.00000	0.00001	0.00001
C39	0.32828	0.68911	0.59785	0.00804	0.00852	0.00605	0.00013	0.00044	-0.00005		
C39	0.32831	0.68863	0.59798	0.00950	0.00770	0.00670	0.00030	0.00000	-0.00060		
(20k-12k)^2	0.00000	0.00000	0.00000	0.00000	0.00000	0.00000	0.00000	0.00000	0.00000	0.00000	0.00000
H39	0.39712	0.68906	0.64881	0.02018	0.02602	0.02034	0.00150	-0.00519	-0.00219		
H39	0.39915	0.68926	0.64725	0.02080							
(20k-12k)^2	0.00000	0.00000	0.00000	0.00000	0.00068	0.00041	0.00000	0.00003	0.00000		
C40	0.26807	0.78898	0.58376	0.00797	0.00762	0.00692	-0.00032	0.00090	-0.00157		
C40	0.26814	0.78833	0.58389	0.00940	0.00700	0.00740	-0.00010	0.00000	-0.00190		
(20k-12k)^2	0.00000	0.00000	0.00000	0.00000	0.00000	0.00000	0.00000	0.00000	0.00000	0.00000	0.00000
H40	0.29203	0.86346	0.62412	0.02508	0.01856	0.02365	-0.00026	-0.00197	-0.00885		

<b>H40</b>	0.29314	0.86455	0.62248	0.01620							
<b>(20k-12k)^2</b>	0.00000	0.00000	0.00000	0.00008	0.00034	0.00056	0.00000	0.00000	0.00008		
	<b>X</b>	<b>Y</b>	<b>Z</b>	<b>U11</b>	<b>U22</b>	<b>U33</b>	<b>U12</b>	<b>U13</b>	<b>U23</b>	<b>0.00007</b>	<b>0.00008</b>
<b>&lt;delta&gt;</b>	<b>-0.00007</b>	<b>0.00046</b>	<b>-0.00015</b>	<b>-0.00169</b>	<b>0.00044</b>	<b>-0.00051</b>	<b>-0.00009</b>	<b>0.00040</b>	<b>0.00041</b>	<b>-0.00059</b>	
<b>RMS:</b>	<b>0.00013</b>	<b>0.00050</b>	<b>0.00016</b>	<b>0.00173</b>	<b>0.00058</b>	<b>0.00057</b>	<b>0.00027</b>	<b>0.00051</b>	<b>0.00047</b>	<b>0.00110</b>	<b>0.00084</b>
<b>0.5 Angstroms</b>	<b>N - X</b>										
<b>CorH(A)</b>											
<b>ATOM</b>	<b>X</b>	<b>Y</b>	<b>Z</b>	<b>U11</b>	<b>U22</b>	<b>U33</b>	<b>U12</b>	<b>U13</b>	<b>U23</b>	<b>sum delUii</b>	<b>sum Uii+uij</b>
<b>C1</b>	0.41802	0.30400	0.10987	0.01292	0.01235	0.01194	0.00055	0.00245	-0.00108		
<b>C1</b>	0.41799	0.30396	0.10988	0.01292	0.01083	0.01118	0.00030	0.00208	-0.00153		
<b>(90k-92k)^2</b>	0.00000	0.00000	0.00000	0.00000	0.00000	0.00000	0.00000	0.00000	0.00000	0.00000	0.00000
<b>C2</b>	0.43703	0.22757	0.17956	0.01244	0.01345	0.01074	0.00106	0.00220	-0.00097		
<b>C2</b>	0.43696	0.22753	0.17950	0.01242	0.01240	0.00965	0.00092	0.00166	-0.00170		
<b>(90k-92k)^2</b>	0.00000	0.00000	0.00000	0.00000	0.00000	0.00000	0.00000	0.00000	0.00000	0.00000	0.00000
<b>C3</b>	0.33973	0.18281	0.18939	0.01338	0.01481	0.01111	0.00145	0.00352	-0.00028		
<b>C3</b>	0.33972	0.18281	0.18935	0.01321	0.01372	0.01020	0.00156	0.00356	-0.00075		
<b>(90k-92k)^2</b>	0.00000	0.00000	0.00000	0.00000	0.00000	0.00000	0.00000	0.00000	0.00000	0.00000	0.00000
<b>C4</b>	0.26064	0.23205	0.12610	0.01183	0.01457	0.01372	0.00183	0.00330	-0.00090		
<b>C4</b>	0.26065	0.23195	0.12622	0.01187	0.01362	0.01291	0.00242	0.00352	-0.00110		
<b>(90k-92k)^2</b>	0.00000	0.00000	0.00000	0.00000	0.00000	0.00000	0.00000	0.00000	0.00000	0.00000	0.00000
<b>C5</b>	0.30916	0.30679	0.07710	0.01334	0.01271	0.01275	0.00180	0.00209	-0.00038		
<b>C5</b>	0.30910	0.30675	0.07714	0.01310	0.01150	0.01210	0.00220	0.00191	-0.00068		
<b>(90k-92k)^2</b>	0.00000	0.00000	0.00000	0.00000	0.00000	0.00000	0.00000	0.00000	0.00000	0.00000	0.00000
<b>C6</b>	0.49075	0.32522	0.06119	0.01508	0.01263	0.01382	-0.00145	0.00401	-0.00107		
<b>C6</b>	0.49070	0.32524	0.06126	0.01498	0.01160	0.01323	-0.00179	0.00371	-0.00171		
<b>(90k-92k)^2</b>	0.00000	0.00000	0.00000	0.00000	0.00000	0.00000	0.00000	0.00000	0.00000	0.00000	0.00000
<b>C7</b>	0.59388	0.28030	0.09557	0.01358	0.01660	0.01761	-0.00172	0.00490	-0.00273		
<b>C7</b>	0.59376	0.28022	0.09560	0.01350	0.01557	0.01681	-0.00197	0.00468	-0.00358		
<b>(90k-92k)^2</b>	0.00000	0.00000	0.00000	0.00000	0.00000	0.00000	0.00000	0.00000	0.00000	0.00000	0.00000
<b>H7</b>	0.65756	0.29969	0.06403	0.02460	0.04018	0.03746	-0.00263	0.01510	0.00100		
<b>H7</b>	0.65847	0.30553	0.06688	0.01809							

(90k-92k)^2	0.00000	0.00003	0.00001	0.00004	0.00161	0.00140	0.00001	0.00023	0.00000		
C8	0.61257	0.20566	0.16403	0.01189	0.01735	0.01666	0.00029	0.00198	-0.00282		
C8	0.61253	0.20579	0.16402	0.01173	0.01619	0.01638	0.00069	0.00157	-0.00354		
(90k-92k)^2	0.00000	0.00000	0.00000	0.00000	0.00000	0.00000	0.00000	0.00000	0.00000	0.00000	0.00000
H8	0.69020	0.16907	0.18373	0.01899	0.03963	0.03912	0.00796	0.00403	0.00156		
H8	0.69161	0.17453	0.18785	0.01796							
(90k-92k)^2	0.00000	0.00003	0.00002	0.00000	0.00157	0.00153	0.00006	0.00002	0.00000		
C9	0.52983	0.16843	0.20460	0.01261	0.01525	0.01237	0.00157	0.00091	-0.00150		
C9	0.52980	0.16853	0.20460	0.01272	0.01423	0.01105	0.00132	0.00018	-0.00195		
(90k-92k)^2	0.00000	0.00000	0.00000	0.00000	0.00000	0.00000	0.00000	0.00000	0.00000	0.00000	0.00000
C10	0.52235	0.06542	0.25296	0.01639	0.01714	0.01305	0.00270	0.00024	0.00077		
C10	0.52235	0.06540	0.25294	0.01674	0.01657	0.01173	0.00319	-0.00048	0.00050		
(90k-92k)^2	0.00000	0.00000	0.00000	0.00000	0.00000	0.00000	0.00000	0.00000	0.00000	0.00000	0.00000
H10	0.59230	0.01486	0.27747	0.02642	0.03241	0.03606	0.00851	-0.00109	0.00726		
H10	0.59369	0.02087	0.28295	0.01862							
(90k-92k)^2	0.00000	0.00004	0.00003	0.00006	0.00105	0.00130	0.00007	0.00000	0.00005		
C11	0.42696	0.02142	0.26221	0.01884	0.01725	0.01295	0.00193	0.00271	0.00265		
C11	0.42688	0.02144	0.26225	0.02011	0.01666	0.01118	0.00235	0.00294	0.00243		
(90k-92k)^2	0.00000	0.00000	0.00000	0.00000	0.00000	0.00000	0.00000	0.00000	0.00000	0.00001	0.00001
H11	0.42563	-0.06113	0.29408	0.03869	0.02807	0.03417	0.00264	0.00675	0.01262		
H11	0.42548	-0.05691	0.29904	0.01924							
(90k-92k)^2	0.00000	0.00002	0.00002	0.00038	0.00079	0.00117	0.00001	0.00005	0.00016		
C12	0.32948	0.07646	0.22463	0.01629	0.01697	0.01225	0.00110	0.00483	0.00136		
C12	0.32944	0.07640	0.22465	0.01656	0.01581	0.01130	0.00102	0.00538	0.00084		
(90k-92k)^2	0.00000	0.00000	0.00000	0.00000	0.00000	0.00000	0.00000	0.00000	0.00000	0.00000	0.00000
C13	0.22559	0.02809	0.20377	0.01672	0.01967	0.01928	-0.00084	0.00855	0.00211		
C13	0.22555	0.02805	0.20380	0.01750	0.01907	0.01882	-0.00100	0.00927	0.00148		
(90k-92k)^2	0.00000	0.00000	0.00000	0.00000	0.00000	0.00000	0.00000	0.00000	0.00000	0.00000	0.00000
H13	0.20983	-0.05359	0.23206	0.03551	0.03199	0.04354	-0.00521	0.01323	0.01041		
H13	0.20770	-0.04812	0.23746	0.02120							
(90k-92k)^2	0.00000	0.00003	0.00003	0.00020	0.00102	0.00190	0.00003	0.00018	0.00011		
C14	0.14810	0.07642	0.14196	0.01349	0.02076	0.02346	-0.00052	0.00754	0.00045		

C14	0.14812	0.07635	0.14195	0.01303	0.02053	0.02300	-0.00063	0.00801	-0.00016		
(90k-92k)^2	0.00000	0.00000	0.00000	0.00000	0.00000	0.00000	0.00000	0.00000	0.00000	0.00000	0.00000
H14	0.07362	0.03153	0.12396	0.02093	0.04085	0.05009	-0.00820	0.00731	0.00317		
H14	0.07091	0.03705	0.12823	0.02188							
(90k-92k)^2	0.00001	0.00003	0.00002	0.00000	0.00167	0.00251	0.00007	0.00005	0.00001		
C15	0.16692	0.17741	0.09506	0.01123	0.01859	0.01871	0.00177	0.00434	-0.00094		
C15	0.16699	0.17745	0.09516	0.01066	0.01772	0.01819	0.00207	0.00424	-0.00125		
(90k-92k)^2	0.00000	0.00000	0.00000	0.00000	0.00000	0.00000	0.00000	0.00000	0.00000	0.00000	0.00000
C16	0.11427	0.21576	0.01236	0.01122	0.02204	0.02100	0.00287	0.00049	-0.00066		
C16	0.11425	0.21587	0.01235	0.01105	0.02165	0.02078	0.00330	0.00036	-0.00134		
(90k-92k)^2	0.00000	0.00000	0.00000	0.00000	0.00000	0.00000	0.00000	0.00000	0.00000	0.00000	0.00000
H16	0.03765	0.18064	-0.01561	0.02019	0.04719	0.04060	-0.00522	-0.00192	0.00048		
H16	0.03463	0.18717	-0.01274	0.02191							
(90k-92k)^2	0.00001	0.00004	0.00001	0.00000	0.00223	0.00165	0.00003	0.00000	0.00000		
C17	0.16219	0.28838	-0.03624	0.01497	0.01991	0.01784	0.00409	-0.00116	0.00066		
C17	0.16222	0.28828	-0.03606	0.01495	0.01880	0.01730	0.00474	-0.00171	0.00025		
(90k-92k)^2	0.00000	0.00000	0.00000	0.00000	0.00000	0.00000	0.00000	0.00000	0.00000	0.00000	0.00000
H17	0.12301	0.30623	-0.10075	0.03050	0.04508	0.02703	0.00261	-0.00688	0.00554		
H17	0.11944	0.31410	-0.09839	0.02131							
(90k-92k)^2	0.00001	0.00006	0.00001	0.00008	0.00203	0.00073	0.00001	0.00005	0.00003		
C18	0.26711	0.33043	-0.00643	0.01581	0.01402	0.01378	0.00288	0.00062	0.00098		
C18	0.26705	0.33045	-0.00640	0.01581	0.01303	0.01345	0.00335	0.00049	0.00102		
(90k-92k)^2	0.00000	0.00000	0.00000	0.00000	0.00000	0.00000	0.00000	0.00000	0.00000	0.00000	0.00000
C19	0.34092	0.37185	-0.05445	0.02169	0.01562	0.01403	0.00092	0.00274	0.00318		
C19	0.34094	0.37179	-0.05431	0.02237	0.01451	0.01339	0.00135	0.00234	0.00287		
(90k-92k)^2	0.00000	0.00000	0.00000	0.00000	0.00000	0.00000	0.00000	0.00000	0.00000	0.00000	0.00000
H19	0.31299	0.39780	-0.11973	0.04143	0.04360	0.02178	0.00200	0.00161	0.01202		
H19	0.31202	0.40601	-0.11750	0.02035							
(90k-92k)^2	0.00000	0.00007	0.00000	0.00044	0.00190	0.00047	0.00000	0.00000	0.00014		
C20	0.44776	0.36928	-0.02225	0.02045	0.01471	0.01495	-0.00176	0.00517	0.00140		
C20	0.44769	0.36916	-0.02216	0.02135	0.01335	0.01440	-0.00207	0.00522	0.00104		
(90k-92k)^2	0.00000	0.00000	0.00000	0.00000	0.00000	0.00000	0.00000	0.00000	0.00000	0.00000	0.00000

<b>H20</b>	0.49998	0.39372	-0.06354	0.03732	0.04048	0.02967	-0.00641	0.01528	0.00576		
<b>H20</b>	0.50039	0.40102	-0.06081	0.01938							
<b>(90k-92k)^2</b>	0.00000	0.00005	0.00001	0.00032	0.00164	0.00088	0.00004	0.00023	0.00003		
	<b>X</b>	<b>Y</b>	<b>Z</b>	<b>U11</b>	<b>U22</b>	<b>U33</b>	<b>U12</b>	<b>U13</b>	<b>U23</b>	<b>0.00004</b>	<b>0.00005</b>
<b>&lt;delta&gt;</b>	<b>0.00003</b>	<b>0.00002</b>	<b>-0.00004</b>	<b>-0.00012</b>	<b>0.00095</b>	<b>0.00075</b>	<b>-0.00014</b>	<b>0.00013</b>	<b>0.00045</b>	<b>0.00053</b>	
<b>RMS:</b>	<b>0.00005</b>	<b>0.00007</b>	<b>0.00007</b>	<b>0.00047</b>	<b>0.00100</b>	<b>0.00084</b>	<b>0.00036</b>	<b>0.00042</b>	<b>0.00050</b>	<b>0.00080</b>	<b>0.00064</b>
<b>0.5 Angstroms</b>	<b>N - X</b>										
<b>CorH(B)</b>											
<b>ATOM</b>	<b>X</b>	<b>Y</b>	<b>Z</b>	<b>U11</b>	<b>U22</b>	<b>U33</b>	<b>U12</b>	<b>U13</b>	<b>U23</b>	<b>sum delUii</b>	<b>sum Uii+uij</b>
<b>C21</b>	0.15469	0.69810	0.46774	0.01269	0.01306	0.01529	-0.00120	0.00432	-0.00139		
<b>C21</b>	0.15478	0.69807	0.46766	0.01193	0.01262	0.01469	-0.00121	0.00452	-0.00138		
<b>(90k-92k)^2</b>	0.00000	0.00000	0.00000	0.00000	0.00000	0.00000	0.00000	0.00000	0.00000	0.00000	0.00000
<b>C22</b>	0.09901	0.69540	0.38290	0.01097	0.01342	0.01667	-0.00055	0.00300	-0.00109		
<b>C22</b>	0.09910	0.69539	0.38287	0.00991	0.01315	0.01602	-0.00092	0.00294	-0.00112		
<b>(90k-92k)^2</b>	0.00000	0.00000	0.00000	0.00000	0.00000	0.00000	0.00000	0.00000	0.00000	0.00000	0.00000
<b>C23</b>	0.12361	0.59100	0.34642	0.01158	0.01416	0.01526	-0.00202	0.00312	-0.00223		
<b>C23</b>	0.12367	0.59089	0.34647	0.01083	0.01328	0.01527	-0.00243	0.00311	-0.00214		
<b>(90k-92k)^2</b>	0.00000	0.00000	0.00000	0.00000	0.00000	0.00000	0.00000	0.00000	0.00000	0.00000	0.00000
<b>C24</b>	0.19488	0.52953	0.40856	0.01352	0.01160	0.01675	-0.00076	0.00465	-0.00038		
<b>C24</b>	0.19493	0.52951	0.40859	0.01375	0.01057	0.01591	-0.00155	0.00488	-0.00040		
<b>(90k-92k)^2</b>	0.00000	0.00000	0.00000	0.00000	0.00000	0.00000	0.00000	0.00000	0.00000	0.00000	0.00000
<b>C25</b>	0.21478	0.59617	0.48329	0.01449	0.01322	0.01417	-0.00071	0.00464	0.00064		
<b>C25</b>	0.21474	0.59618	0.48316	0.01413	0.01229	0.01376	-0.00115	0.00458	0.00092		
<b>(90k-92k)^2</b>	0.00000	0.00000	0.00000	0.00000	0.00000	0.00000	0.00000	0.00000	0.00000	0.00000	0.00000
<b>C26</b>	0.18188	0.79918	0.51156	0.01503	0.01501	0.01705	-0.00136	0.00483	-0.00376		
<b>C26</b>	0.18198	0.79916	0.51145	0.01482	0.01441	0.01736	-0.00151	0.00547	-0.00384		
<b>(90k-92k)^2</b>	0.00000	0.00000	0.00000	0.00000	0.00000	0.00000	0.00000	0.00000	0.00000	0.00000	0.00000
<b>C27</b>	0.13443	0.90128	0.46880	0.01819	0.01380	0.02606	0.00043	0.00547	-0.00382		
<b>C27</b>	0.13467	0.90119	0.46883	0.01801	0.01305	0.02645	0.00014	0.00555	-0.00414		
<b>(90k-92k)^2</b>	0.00000	0.00000	0.00000	0.00000	0.00000	0.00000	0.00000	0.00000	0.00000	0.00000	0.00000
<b>H27</b>	0.14716	0.98457	0.50023	0.04459	0.02181	0.04647	0.00046	0.00605	-0.01156		

H27	0.14140	0.98252	0.50314	0.02285							
(90k-92k)^2	0.00003	0.00000	0.00001	0.00047	0.00048	0.00216	0.00000	0.00004	0.00013		
C28	0.08071	0.89869	0.38539	0.01687	0.01461	0.02795	0.00243	0.00264	0.00019		
C28	0.08084	0.89864	0.38534	0.01643	0.01369	0.02843	0.00275	0.00296	0.00041		
(90k-92k)^2	0.00000	0.00000	0.00000	0.00000	0.00000	0.00000	0.00000	0.00000	0.00000	0.00000	0.00000
H28	0.05415	0.98003	0.35477	0.04282	0.02341	0.04999	0.00869	0.00089	0.00641		
H28	0.04747	0.97827	0.35575	0.02372							
(90k-92k)^2	0.00004	0.00000	0.00000	0.00036	0.00055	0.00250	0.00008	0.00000	0.00004		
C29	0.06774	0.79355	0.33659	0.01193	0.01583	0.02040	0.00121	0.00113	0.00101		
C29	0.06780	0.79337	0.33656	0.01118	0.01555	0.02043	0.00106	0.00110	0.00111		
(90k-92k)^2	0.00000	0.00000	0.00000	0.00000	0.00000	0.00000	0.00000	0.00000	0.00000	0.00000	0.00000
C30	0.04666	0.77664	0.24626	0.01462	0.02348	0.01963	0.00095	-0.00075	0.00365		
C30	0.04672	0.77636	0.24618	0.01365	0.02325	0.01970	0.00044	-0.00136	0.00401		
(90k-92k)^2	0.00000	0.00000	0.00000	0.00000	0.00000	0.00000	0.00000	0.00000	0.00000	0.00000	0.00000
H30	0.01641	0.84813	0.20463	0.03934	0.03907	0.03562	0.00692	-0.00050	0.01267		
H30	0.01041	0.84574	0.20499	0.02349							
(90k-92k)^2	0.00004	0.00001	0.00000	0.00025	0.00153	0.00127	0.00005	0.00000	0.00016		
C31	0.07139	0.67427	0.21033	0.01429	0.02660	0.01571	-0.00185	-0.00037	0.00012		
C31	0.07143	0.67416	0.21040	0.01356	0.02701	0.01517	-0.00245	-0.00074	-0.00018		
(90k-92k)^2	0.00000	0.00000	0.00000	0.00000	0.00000	0.00000	0.00000	0.00000	0.00000	0.00000	0.00000
H31	0.06152	0.66975	0.14213	0.03836	0.05296	0.02037	-0.00079	0.00167	0.00033		
H31	0.05470	0.66614	0.14189	0.02295							
(90k-92k)^2	0.00005	0.00001	0.00000	0.00024	0.00280	0.00041	0.00000	0.00000	0.00000		
C32	0.11858	0.57808	0.26115	0.01280	0.01952	0.01576	-0.00336	0.00241	-0.00361		
C32	0.11866	0.57796	0.26113	0.01214	0.01941	0.01540	-0.00388	0.00202	-0.00415		
(90k-92k)^2	0.00000	0.00000	0.00000	0.00000	0.00000	0.00000	0.00000	0.00000	0.00000	0.00000	0.00000
C33	0.17857	0.48219	0.23950	0.01755	0.02111	0.01927	-0.00370	0.00508	-0.00755		
C33	0.17870	0.48202	0.23959	0.01736	0.02091	0.01918	-0.00456	0.00536	-0.00814		
(90k-92k)^2	0.00000	0.00000	0.00000	0.00000	0.00000	0.00000	0.00000	0.00000	0.00000	0.00000	0.00000
H33	0.17388	0.45963	0.17351	0.04053	0.04730	0.02747	-0.00064	0.00815	-0.01367		
H33	0.16865	0.45626	0.17372	0.02271							
(90k-92k)^2	0.00003	0.00001	0.00000	0.00032	0.00224	0.00075	0.00000	0.00007	0.00019		



C34	0.24873	0.42201	0.30072	0.01917	0.01546	0.02383	-0.00148	0.00764	-0.00596		
C34	0.24872	0.42201	0.30066	0.01943	0.01450	0.02409	-0.00209	0.00827	-0.00651		
(90k-92k)^2	0.00000	0.00000	0.00000	0.00000	0.00000	0.00000	0.00000	0.00000	0.00000	0.00000	0.00000
H34	0.29646	0.35543	0.28031	0.04090	0.03036	0.04406	0.00629	0.01537	-0.01154		
H34	0.29211	0.35034	0.28138	0.02256							
(90k-92k)^2	0.00002	0.00003	0.00000	0.00034	0.00092	0.00194	0.00004	0.00024	0.00013		
C35	0.26572	0.45185	0.38897	0.01644	0.01159	0.02130	-0.00026	0.00629	-0.00056		
C35	0.26575	0.45179	0.38904	0.01664	0.01041	0.02098	-0.00031	0.00642	-0.00063		
(90k-92k)^2	0.00000	0.00000	0.00000	0.00000	0.00000	0.00000	0.00000	0.00000	0.00000	0.00000	0.00000
C36	0.35499	0.43085	0.45615	0.01860	0.01348	0.02483	0.00303	0.00602	0.00401		
C36	0.35508	0.43086	0.45631	0.01894	0.01255	0.02461	0.00294	0.00614	0.00447		
(90k-92k)^2	0.00000	0.00000	0.00000	0.00000	0.00000	0.00000	0.00000	0.00000	0.00000	0.00000	0.00000
H36	0.41267	0.36670	0.44796	0.03330	0.02906	0.04979	0.01257	0.00991	0.00190		
H36	0.40860	0.36135	0.44951	0.02216							
(90k-92k)^2	0.00002	0.00003	0.00000	0.00012	0.00084	0.00248	0.00016	0.00010	0.00000		
C37	0.37470	0.49653	0.52931	0.01794	0.01804	0.01959	0.00265	0.00317	0.00640		
C37	0.37471	0.49664	0.52930	0.01820	0.01718	0.01909	0.00249	0.00315	0.00705		
(90k-92k)^2	0.00000	0.00000	0.00000	0.00000	0.00000	0.00000	0.00000	0.00000	0.00000	0.00000	0.00000
H37	0.44681	0.48182	0.57502	0.02939	0.04154	0.03392	0.00782	-0.00269	0.00761		
H37	0.44324	0.47741	0.57825	0.02192							
(90k-92k)^2	0.00001	0.00002	0.00001	0.00006	0.00173	0.00115	0.00006	0.00001	0.00006		
C38	0.30681	0.58999	0.54234	0.01660	0.01693	0.01420	0.00015	0.00306	0.00294		
C38	0.30691	0.58995	0.54232	0.01670	0.01648	0.01323	-0.00034	0.00305	0.00361		
(90k-92k)^2	0.00000	0.00000	0.00000	0.00000	0.00000	0.00000	0.00000	0.00000	0.00000	0.00000	0.00000
C39	0.32833	0.68900	0.59730	0.01926	0.02225	0.01319	-0.00165	0.00169	0.00004		
C39	0.32831	0.68903	0.59725	0.01960	0.02269	0.01236	-0.00230	0.00176	0.00031		
(90k-92k)^2	0.00000	0.00000	0.00000	0.00000	0.00000	0.00000	0.00000	0.00000	0.00000	0.00000	0.00000
H39	0.39698	0.68900	0.64837	0.03377	0.04620	0.02650	-0.00063	-0.00718	-0.00186		
H39	0.39330	0.68550	0.65154	0.02214							
(90k-92k)^2	0.00001	0.00001	0.00001	0.00014	0.00213	0.00070	0.00000	0.00005	0.00000		
C40	0.26838	0.78852	0.58291	0.01946	0.02020	0.01590	-0.00300	0.00419	-0.00457		
C40	0.26853	0.78846	0.58286	0.01959	0.02045	0.01497	-0.00357	0.00420	-0.00461		

<b>(90k-92k)^2</b>	0.00000	0.00000	0.00000	0.00000	0.00000	0.00000	0.00000	0.00000	0.00000	0.00000	0.00000
<b>H40</b>	0.29250	0.86296	0.62310	0.03936	0.03562	0.03409	-0.00550	0.00220	-0.01573		
<b>H40</b>	0.28729	0.86048	0.62654	0.02190							
<b>(90k-92k)^2</b>	0.00003	0.00001	0.00001	0.00030	0.00127	0.00116	0.00003	0.00000	0.00025		
	<b>X</b>	<b>Y</b>	<b>Z</b>	<b>U11</b>	<b>U22</b>	<b>U33</b>	<b>U12</b>	<b>U13</b>	<b>U23</b>	<b>0.00002</b>	<b>0.00003</b>
<b>&lt;delta&gt;</b>	<b>-0.00007</b>	<b>0.00006</b>	<b>0.00001</b>	<b>0.00026</b>	<b>0.00050</b>	<b>0.00029</b>	<b>0.00037</b>	<b>-0.00006</b>	<b>-0.00003</b>	<b>0.00035</b>	
<b>RMS:</b>	<b>0.00010</b>	<b>0.00010</b>	<b>0.00007</b>	<b>0.00053</b>	<b>0.00069</b>	<b>0.00053</b>	<b>0.00047</b>	<b>0.00030</b>	<b>0.00036</b>	<b>0.00059</b>	<b>0.00050</b>
<b>0.6 Angstroms</b>	<b>N - X</b>										
<b>CorH(A)</b>											
<b>ATOM</b>	<b>X</b>	<b>Y</b>	<b>Z</b>	<b>U11</b>	<b>U22</b>	<b>U33</b>	<b>U12</b>	<b>U13</b>	<b>U23</b>	<b>sum delUii</b>	<b>sum Uii+uij</b>
<b>C1</b>	0.41805	0.30398	0.10985	0.01235	0.01145	0.01149	0.00045	0.00233	-0.00085		
<b>C1</b>	0.41799	0.30396	0.10988	0.01292	0.01083	0.01118	0.00030	0.00208	-0.00153		
<b>(90k-92k)^2</b>	0.00000	0.00000	0.00000	0.00000	0.00000	0.00000	0.00000	0.00000	0.00000	0.00000	0.00000
<b>C2</b>	0.43702	0.22755	0.17952	0.01157	0.01260	0.01043	0.00100	0.00220	-0.00112		
<b>C2</b>	0.43696	0.22753	0.17950	0.01242	0.01240	0.00965	0.00092	0.00166	-0.00170		
<b>(90k-92k)^2</b>	0.00000	0.00000	0.00000	0.00000	0.00000	0.00000	0.00000	0.00000	0.00000	0.00000	0.00000
<b>C3</b>	0.33977	0.18280	0.18937	0.01276	0.01388	0.01070	0.00130	0.00355	-0.00044		
<b>C3</b>	0.33972	0.18281	0.18935	0.01321	0.01372	0.01020	0.00156	0.00356	-0.00075		
<b>(90k-92k)^2</b>	0.00000	0.00000	0.00000	0.00000	0.00000	0.00000	0.00000	0.00000	0.00000	0.00000	0.00000
<b>C4</b>	0.26063	0.23200	0.12611	0.01115	0.01396	0.01319	0.00192	0.00330	-0.00106		
<b>C4</b>	0.26065	0.23195	0.12622	0.01187	0.01362	0.01291	0.00242	0.00352	-0.00110		
<b>(90k-92k)^2</b>	0.00000	0.00000	0.00000	0.00000	0.00000	0.00000	0.00000	0.00000	0.00000	0.00000	0.00000
<b>C5</b>	0.30913	0.30676	0.07708	0.01268	0.01217	0.01203	0.00207	0.00203	-0.00055		
<b>C5</b>	0.30910	0.30675	0.07714	0.01310	0.01150	0.01210	0.00220	0.00191	-0.00068		
<b>(90k-92k)^2</b>	0.00000	0.00000	0.00000	0.00000	0.00000	0.00000	0.00000	0.00000	0.00000	0.00000	0.00000
<b>C6</b>	0.49076	0.32524	0.06120	0.01418	0.01214	0.01336	-0.00160	0.00378	-0.00111		
<b>C6</b>	0.49070	0.32524	0.06126	0.01498	0.01160	0.01323	-0.00179	0.00371	-0.00171		
<b>(90k-92k)^2</b>	0.00000	0.00000	0.00000	0.00000	0.00000	0.00000	0.00000	0.00000	0.00000	0.00000	0.00000
<b>C7</b>	0.59389	0.28031	0.09558	0.01315	0.01592	0.01709	-0.00170	0.00491	-0.00263		
<b>C7</b>	0.59376	0.28022	0.09560	0.01350	0.01557	0.01681	-0.00197	0.00468	-0.00358		
<b>(90k-92k)^2</b>	0.00000	0.00000	0.00000	0.00000	0.00000	0.00000	0.00000	0.00000	0.00000	0.00000	0.00000

H7	0.65751	0.29965	0.06407	0.02417	0.03974	0.03703	-0.00244	0.01456	0.00117		
H7	0.65847	0.30553	0.06688	0.01809							
(90k-92k)^2	0.00000	0.00003	0.00001	0.00004	0.00158	0.00137	0.00001	0.00021	0.00000		
C8	0.61258	0.20568	0.16402	0.01107	0.01663	0.01607	0.00031	0.00167	-0.00292		
C8	0.61253	0.20579	0.16402	0.01173	0.01619	0.01638	0.00069	0.00157	-0.00354		
(90k-92k)^2	0.00000	0.00000	0.00000	0.00000	0.00000	0.00000	0.00000	0.00000	0.00000	0.00000	0.00000
H8	0.69008	0.16914	0.18365	0.01862	0.03940	0.03815	0.00823	0.00396	0.00169		
H8	0.69161	0.17453	0.18785	0.01796							
(90k-92k)^2	0.00000	0.00003	0.00002	0.00000	0.00155	0.00146	0.00007	0.00002	0.00000		
C9	0.52981	0.16846	0.20459	0.01169	0.01452	0.01202	0.00152	0.00076	-0.00150		
C9	0.52980	0.16853	0.20460	0.01272	0.01423	0.01105	0.00132	0.00018	-0.00195		
(90k-92k)^2	0.00000	0.00000	0.00000	0.00000	0.00000	0.00000	0.00000	0.00000	0.00000	0.00000	0.00000
C10	0.52235	0.06540	0.25295	0.01571	0.01651	0.01251	0.00303	0.00007	0.00081		
C10	0.52235	0.06540	0.25294	0.01674	0.01657	0.01173	0.00319	-0.00048	0.00050		
(90k-92k)^2	0.00000	0.00000	0.00000	0.00000	0.00000	0.00000	0.00000	0.00000	0.00000	0.00000	0.00000
H10	0.59218	0.01505	0.27740	0.02562	0.03247	0.03527	0.00834	-0.00095	0.00668		
H10	0.59369	0.02087	0.28295	0.01862							
(90k-92k)^2	0.00000	0.00003	0.00003	0.00005	0.00105	0.00124	0.00007	0.00000	0.00004		
C11	0.42697	0.02140	0.26221	0.01835	0.01679	0.01241	0.00175	0.00288	0.00267		
C11	0.42688	0.02144	0.26225	0.02011	0.01666	0.01118	0.00235	0.00294	0.00243		
(90k-92k)^2	0.00000	0.00000	0.00000	0.00000	0.00000	0.00000	0.00000	0.00000	0.00000	0.00000	0.00001
H11	0.42569	-0.06096	0.29414	0.03855	0.02797	0.03324	0.00267	0.00667	0.01265		
H11	0.42548	-0.05691	0.29904	0.01924							
(90k-92k)^2	0.00000	0.00002	0.00002	0.00037	0.00078	0.00110	0.00001	0.00004	0.00016		
C12	0.32943	0.07642	0.22463	0.01567	0.01612	0.01201	0.00108	0.00498	0.00135		
C12	0.32944	0.07640	0.22465	0.01656	0.01581	0.01130	0.00102	0.00538	0.00084		
(90k-92k)^2	0.00000	0.00000	0.00000	0.00000	0.00000	0.00000	0.00000	0.00000	0.00000	0.00000	0.00000
C13	0.22562	0.02812	0.20380	0.01619	0.01898	0.01890	-0.00067	0.00857	0.00231		
C13	0.22555	0.02805	0.20380	0.01750	0.01907	0.01882	-0.00100	0.00927	0.00148		
(90k-92k)^2	0.00000	0.00000	0.00000	0.00000	0.00000	0.00000	0.00000	0.00000	0.00000	0.00000	0.00000
H13	0.20980	-0.05343	0.23206	0.03486	0.03200	0.04255	-0.00492	0.01338	0.01038		
H13	0.20770	-0.04812	0.23746	0.02120							

(90k-92k)^2	0.00000	0.00003	0.00003	0.00019	0.00102	0.00181	0.00002	0.00018	0.00011		
C14	0.14809	0.07640	0.14195	0.01274	0.02034	0.02323	-0.00071	0.00766	0.00016		
C14	0.14812	0.07635	0.14195	0.01303	0.02053	0.02300	-0.00063	0.00801	-0.00016		
(90k-92k)^2	0.00000	0.00000	0.00000	0.00000	0.00000	0.00000	0.00000	0.00000	0.00000	0.00000	0.00000
H14	0.07377	0.03167	0.12397	0.02096	0.03999	0.04897	-0.00794	0.00753	0.00324		
H14	0.07091	0.03705	0.12823	0.02188							
(90k-92k)^2	0.00001	0.00003	0.00002	0.00000	0.00160	0.00240	0.00006	0.00006	0.00001		
C15	0.16691	0.17748	0.09508	0.01033	0.01780	0.01851	0.00170	0.00423	-0.00097		
C15	0.16699	0.17745	0.09516	0.01066	0.01772	0.01819	0.00207	0.00424	-0.00125		
(90k-92k)^2	0.00000	0.00000	0.00000	0.00000	0.00000	0.00000	0.00000	0.00000	0.00000	0.00000	0.00000
C16	0.11425	0.21578	0.01233	0.01035	0.02176	0.02051	0.00316	0.00026	-0.00057		
C16	0.11425	0.21587	0.01235	0.01105	0.02165	0.02078	0.00330	0.00036	-0.00134		
(90k-92k)^2	0.00000	0.00000	0.00000	0.00000	0.00000	0.00000	0.00000	0.00000	0.00000	0.00000	0.00000
H16	0.03778	0.18070	-0.01558	0.01970	0.04726	0.03920	-0.00532	-0.00198	0.00049		
H16	0.03463	0.18717	-0.01274	0.02191							
(90k-92k)^2	0.00001	0.00004	0.00001	0.00000	0.00223	0.00154	0.00003	0.00000	0.00000		
C17	0.16217	0.28840	-0.03624	0.01440	0.01924	0.01732	0.00444	-0.00109	0.00078		
C17	0.16222	0.28828	-0.03606	0.01495	0.01880	0.01730	0.00474	-0.00171	0.00025		
(90k-92k)^2	0.00000	0.00000	0.00000	0.00000	0.00000	0.00000	0.00000	0.00000	0.00000	0.00000	0.00000
H17	0.12298	0.30621	-0.10072	0.03000	0.04438	0.02646	0.00248	-0.00734	0.00557		
H17	0.11944	0.31410	-0.09839	0.02131							
(90k-92k)^2	0.00001	0.00006	0.00001	0.00008	0.00197	0.00070	0.00001	0.00005	0.00003		
C18	0.26710	0.33039	-0.00641	0.01510	0.01337	0.01324	0.00288	0.00052	0.00089		
C18	0.26705	0.33045	-0.00640	0.01581	0.01303	0.01345	0.00335	0.00049	0.00102		
(90k-92k)^2	0.00000	0.00000	0.00000	0.00000	0.00000	0.00000	0.00000	0.00000	0.00000	0.00000	0.00000
C19	0.34090	0.37184	-0.05442	0.02114	0.01483	0.01367	0.00101	0.00242	0.00305		
C19	0.34094	0.37179	-0.05431	0.02237	0.01451	0.01339	0.00135	0.00234	0.00287		
(90k-92k)^2	0.00000	0.00000	0.00000	0.00000	0.00000	0.00000	0.00000	0.00000	0.00000	0.00000	0.00000
H19	0.31299	0.39778	-0.11966	0.04041	0.04258	0.02190	0.00217	0.00127	0.01147		
H19	0.31202	0.40601	-0.11750	0.02035							
(90k-92k)^2	0.00000	0.00007	0.00000	0.00040	0.00181	0.00048	0.00000	0.00000	0.00013		
C20	0.44778	0.36928	-0.02223	0.01968	0.01410	0.01457	-0.00179	0.00523	0.00133		

C20	0.44769	0.36916	-0.02216	0.02135	0.01335	0.01440	-0.00207	0.00522	0.00104		
(90k-92k)^2	0.00000	0.00000	0.00000	0.00000	0.00000	0.00000	0.00000	0.00000	0.00000	0.00000	0.00000
H20	0.49987	0.39370	-0.06354	0.03617	0.04011	0.02879	-0.00629	0.01441	0.00507		
H20	0.50039	0.40102	-0.06081	0.01938							
(90k-92k)^2	0.00000	0.00005	0.00001	0.00028	0.00161	0.00083	0.00004	0.00021	0.00003		
	X	Y	Z	U11	U22	U33	U12	U13	U23	0.00002	0.00003
<delta>	0.00003	0.00001	-0.00004	-0.00082	0.00029	0.00031	-0.00011	0.00007	0.00042	-0.00007	
RMS:	0.00006	0.00006	0.00006	0.00091	0.00038	0.00051	0.00030	0.00034	0.00050	0.00064	0.00053
0.6 Angstroms	N - X										
CorH(B)											
ATOM	X	Y	Z	U11	U22	U33	U12	U13	U23	sum delUii	sum Uii+uij
C21	0.15468	0.69813	0.46776	0.01208	0.01236	0.01491	-0.00109	0.00447	-0.00145		
C21	0.15478	0.69807	0.46766	0.01193	0.01262	0.01469	-0.00121	0.00452	-0.00138		
(90k-92k)^2	0.00000	0.00000	0.00000	0.00000	0.00000	0.00000	0.00000	0.00000	0.00000	0.00000	0.00000
C22	0.09905	0.69542	0.38290	0.01025	0.01275	0.01606	-0.00052	0.00296	-0.00100		
C22	0.09910	0.69539	0.38287	0.00991	0.01315	0.01602	-0.00092	0.00294	-0.00112		
(90k-92k)^2	0.00000	0.00000	0.00000	0.00000	0.00000	0.00000	0.00000	0.00000	0.00000	0.00000	0.00000
C23	0.12362	0.59101	0.34641	0.01096	0.01352	0.01480	-0.00210	0.00305	-0.00247		
C23	0.12367	0.59089	0.34647	0.01083	0.01328	0.01527	-0.00243	0.00311	-0.00214		
(90k-92k)^2	0.00000	0.00000	0.00000	0.00000	0.00000	0.00000	0.00000	0.00000	0.00000	0.00000	0.00000
C24	0.19491	0.52954	0.40856	0.01282	0.01058	0.01635	-0.00083	0.00448	-0.00057		
C24	0.19493	0.52951	0.40859	0.01375	0.01057	0.01591	-0.00155	0.00488	-0.00040		
(90k-92k)^2	0.00000	0.00000	0.00000	0.00000	0.00000	0.00000	0.00000	0.00000	0.00000	0.00000	0.00000
C25	0.21476	0.59617	0.48325	0.01373	0.01245	0.01390	-0.00076	0.00435	0.00049		
C25	0.21474	0.59618	0.48316	0.01413	0.01229	0.01376	-0.00115	0.00458	0.00092		
(90k-92k)^2	0.00000	0.00000	0.00000	0.00000	0.00000	0.00000	0.00000	0.00000	0.00000	0.00000	0.00000
C26	0.18193	0.79916	0.51155	0.01451	0.01435	0.01651	-0.00122	0.00484	-0.00382		
C26	0.18198	0.79916	0.51145	0.01482	0.01441	0.01736	-0.00151	0.00547	-0.00384		
(90k-92k)^2	0.00000	0.00000	0.00000	0.00000	0.00000	0.00000	0.00000	0.00000	0.00000	0.00000	0.00000
C27	0.13443	0.90124	0.46880	0.01765	0.01316	0.02572	0.00026	0.00533	-0.00396		
C27	0.13467	0.90119	0.46883	0.01801	0.01305	0.02645	0.00014	0.00555	-0.00414		

(90k-92k)^2	0.00000	0.00000	0.00000	0.00000	0.00000	0.00000	0.00000	0.00000	0.00000	0.00000	0.00000
H27	0.14719	0.98450	0.50023	0.04379	0.02167	0.04550	0.00025	0.00544	-0.01119		
H27	0.14140	0.98252	0.50314	0.02285							
(90k-92k)^2	0.00003	0.00000	0.00001	0.00044	0.00047	0.00207	0.00000	0.00003	0.00013		
C28	0.08068	0.89870	0.38535	0.01631	0.01366	0.02740	0.00243	0.00261	0.00019		
C28	0.08084	0.89864	0.38534	0.01643	0.01369	0.02843	0.00275	0.00296	0.00041		
(90k-92k)^2	0.00000	0.00000	0.00000	0.00000	0.00000	0.00000	0.00000	0.00000	0.00000	0.00000	0.00000
H28	0.05408	0.97995	0.35473	0.04169	0.02370	0.04961	0.00841	0.00042	0.00618		
H28	0.04747	0.97827	0.35575	0.02372							
(90k-92k)^2	0.00004	0.00000	0.00000	0.00032	0.00056	0.00246	0.00007	0.00000	0.00004		
C29	0.06770	0.79352	0.33659	0.01129	0.01561	0.01985	0.00121	0.00108	0.00103		
C29	0.06780	0.79337	0.33656	0.01118	0.01555	0.02043	0.00106	0.00110	0.00111		
(90k-92k)^2	0.00000	0.00000	0.00000	0.00000	0.00000	0.00000	0.00000	0.00000	0.00000	0.00000	0.00000
C30	0.04664	0.77663	0.24623	0.01411	0.02287	0.01903	0.00087	-0.00079	0.00366		
C30	0.04672	0.77636	0.24618	0.01365	0.02325	0.01970	0.00044	-0.00136	0.00401		
(90k-92k)^2	0.00000	0.00000	0.00000	0.00000	0.00000	0.00000	0.00000	0.00000	0.00000	0.00000	0.00000
H30	0.01652	0.84811	0.20469	0.03900	0.03853	0.03474	0.00722	-0.00037	0.01257		
H30	0.01041	0.84574	0.20499	0.02349							
(90k-92k)^2	0.00004	0.00001	0.00000	0.00024	0.00148	0.00121	0.00005	0.00000	0.00016		
C31	0.07139	0.67429	0.21033	0.01395	0.02625	0.01494	-0.00206	-0.00025	-0.00019		
C31	0.07143	0.67416	0.21040	0.01356	0.02701	0.01517	-0.00245	-0.00074	-0.00018		
(90k-92k)^2	0.00000	0.00000	0.00000	0.00000	0.00000	0.00000	0.00000	0.00000	0.00000	0.00000	0.00000
H31	0.06146	0.66973	0.14222	0.03790	0.05170	0.01970	-0.00034	0.00138	0.00057		
H31	0.05470	0.66614	0.14189	0.02295							
(90k-92k)^2	0.00005	0.00001	0.00000	0.00022	0.00267	0.00039	0.00000	0.00000	0.00000		
C32	0.11860	0.57809	0.26112	0.01202	0.01905	0.01513	-0.00358	0.00218	-0.00360		
C32	0.11866	0.57796	0.26113	0.01214	0.01941	0.01540	-0.00388	0.00202	-0.00415		
(90k-92k)^2	0.00000	0.00000	0.00000	0.00000	0.00000	0.00000	0.00000	0.00000	0.00000	0.00000	0.00000
C33	0.17858	0.48220	0.23950	0.01683	0.02073	0.01855	-0.00375	0.00513	-0.00757		
C33	0.17870	0.48202	0.23959	0.01736	0.02091	0.01918	-0.00456	0.00536	-0.00814		
(90k-92k)^2	0.00000	0.00000	0.00000	0.00000	0.00000	0.00000	0.00000	0.00000	0.00000	0.00000	0.00000
H33	0.17384	0.45969	0.17358	0.03991	0.04673	0.02679	-0.00065	0.00825	-0.01383		

H33	0.16865	0.45626	0.17372	0.02271							
(90k-92k)^2	0.00003	0.00001	0.00000	0.00030	0.00218	0.00072	0.00000	0.00007	0.00019		
C34	0.24875	0.42198	0.30069	0.01844	0.01484	0.02343	-0.00143	0.00748	-0.00597		
C34	0.24872	0.42201	0.30066	0.01943	0.01450	0.02409	-0.00209	0.00827	-0.00651		
(90k-92k)^2	0.00000	0.00000	0.00000	0.00000	0.00000	0.00000	0.00000	0.00000	0.00000	0.00000	0.00000
H34	0.29635	0.35564	0.28032	0.04082	0.02998	0.04315	0.00645	0.01516	-0.01159		
H34	0.29211	0.35034	0.28138	0.02256							
(90k-92k)^2	0.00002	0.00003	0.00000	0.00033	0.00090	0.00186	0.00004	0.00023	0.00013		
C35	0.26572	0.45188	0.38900	0.01572	0.01099	0.02071	-0.00006	0.00617	-0.00043		
C35	0.26575	0.45179	0.38904	0.01664	0.01041	0.02098	-0.00031	0.00642	-0.00063		
(90k-92k)^2	0.00000	0.00000	0.00000	0.00000	0.00000	0.00000	0.00000	0.00000	0.00000	0.00000	0.00000
C36	0.35498	0.43086	0.45610	0.01792	0.01286	0.02453	0.00310	0.00597	0.00392		
C36	0.35508	0.43086	0.45631	0.01894	0.01255	0.02461	0.00294	0.00614	0.00447		
(90k-92k)^2	0.00000	0.00000	0.00000	0.00000	0.00000	0.00000	0.00000	0.00000	0.00000	0.00000	0.00000
H36	0.41250	0.36671	0.44788	0.03253	0.02878	0.04910	0.01252	0.00984	0.00214		
H36	0.40860	0.36135	0.44951	0.02216							
(90k-92k)^2	0.00002	0.00003	0.00000	0.00011	0.00083	0.00241	0.00016	0.00010	0.00000		
C37	0.37472	0.49654	0.52931	0.01731	0.01754	0.01901	0.00271	0.00289	0.00673		
C37	0.37471	0.49664	0.52930	0.01820	0.01718	0.01909	0.00249	0.00315	0.00705		
(90k-92k)^2	0.00000	0.00000	0.00000	0.00000	0.00000	0.00000	0.00000	0.00000	0.00000	0.00000	0.00000
H37	0.44667	0.48192	0.57492	0.02929	0.04048	0.03342	0.00873	-0.00271	0.00775		
H37	0.44324	0.47741	0.57825	0.02192							
(90k-92k)^2	0.00001	0.00002	0.00001	0.00005	0.00164	0.00112	0.00008	0.00001	0.00006		
C38	0.30679	0.58995	0.54233	0.01599	0.01616	0.01359	0.00007	0.00303	0.00297		
C38	0.30691	0.58995	0.54232	0.01670	0.01648	0.01323	-0.00034	0.00305	0.00361		
(90k-92k)^2	0.00000	0.00000	0.00000	0.00000	0.00000	0.00000	0.00000	0.00000	0.00000	0.00000	0.00000
C39	0.32831	0.68897	0.59725	0.01852	0.02211	0.01251	-0.00164	0.00147	0.00018		
C39	0.32831	0.68903	0.59725	0.01960	0.02269	0.01236	-0.00230	0.00176	0.00031		
(90k-92k)^2	0.00000	0.00000	0.00000	0.00000	0.00000	0.00000	0.00000	0.00000	0.00000	0.00000	0.00000
H39	0.39694	0.68900	0.64834	0.03366	0.04545	0.02581	-0.00065	-0.00637	-0.00188		
H39	0.39330	0.68550	0.65154	0.02214							
(90k-92k)^2	0.00001	0.00001	0.00001	0.00013	0.00207	0.00067	0.00000	0.00004	0.00000		

C40	0.26838	0.78854	0.58289	0.01888	0.01954	0.01542	-0.00301	0.00394	-0.00455		
C40	0.26853	0.78846	0.58286	0.01959	0.02045	0.01497	-0.00357	0.00420	-0.00461		
(90k-92k)^2	0.00000	0.00000	0.00000	0.00000	0.00000	0.00000	0.00000	0.00000	0.00000	0.00000	0.00000
H40	0.29245	0.86285	0.62313	0.03869	0.03525	0.03353	-0.00543	0.00202	-0.01530		
H40	0.28729	0.86048	0.62654	0.02190							
(90k-92k)^2	0.00003	0.00001	0.00001	0.00028	0.00124	0.00112	0.00003	0.00000	0.00023		
	X	Y	Z	U11	U22	U33	U12	U13	U23	0.00002	0.00002
<delta>	-0.00007	0.00006	0.00000	-0.00038	-0.00010	-0.00024	0.00035	-0.00015	-0.00005	-0.00024	
RMS:	0.00010	0.00010	0.00007	0.00063	0.00040	0.00050	0.00043	0.00034	0.00034	0.00052	0.00045
0.7 Angstroms	N - X										
CorH(A)											
ATOM	X	Y	Z	U11	U22	U33	U12	U13	U23	sum delUii	sum Uii+uij
C1	0.41800	0.30400	0.10988	0.01204	0.01178	0.01146	0.00043	0.00234	-0.00067		
C1	0.41799	0.30396	0.10988	0.01292	0.01083	0.01118	0.00030	0.00208	-0.00153		
(90k-92k)^2	0.00000	0.00000	0.00000	0.00000	0.00000	0.00000	0.00000	0.00000	0.00000	0.00000	0.00000
C2	0.43698	0.22755	0.17950	0.01160	0.01237	0.01050	0.00128	0.00217	-0.00125		
C2	0.43696	0.22753	0.17950	0.01242	0.01240	0.00965	0.00092	0.00166	-0.00170		
(90k-92k)^2	0.00000	0.00000	0.00000	0.00000	0.00000	0.00000	0.00000	0.00000	0.00000	0.00000	0.00000
C3	0.33975	0.18275	0.18935	0.01257	0.01366	0.01125	0.00119	0.00353	-0.00034		
C3	0.33972	0.18281	0.18935	0.01321	0.01372	0.01020	0.00156	0.00356	-0.00075		
(90k-92k)^2	0.00000	0.00000	0.00000	0.00000	0.00000	0.00000	0.00000	0.00000	0.00000	0.00000	0.00000
C4	0.26066	0.23203	0.12614	0.01115	0.01387	0.01343	0.00172	0.00350	-0.00072		
C4	0.26065	0.23195	0.12622	0.01187	0.01362	0.01291	0.00242	0.00352	-0.00110		
(90k-92k)^2	0.00000	0.00000	0.00000	0.00000	0.00000	0.00000	0.00000	0.00000	0.00000	0.00000	0.00000
C5	0.30913	0.30681	0.07710	0.01248	0.01205	0.01206	0.00210	0.00210	-0.00028		
C5	0.30910	0.30675	0.07714	0.01310	0.01150	0.01210	0.00220	0.00191	-0.00068		
(90k-92k)^2	0.00000	0.00000	0.00000	0.00000	0.00000	0.00000	0.00000	0.00000	0.00000	0.00000	0.00000
C6	0.49074	0.32530	0.06118	0.01404	0.01220	0.01328	-0.00186	0.00385	-0.00120		
C6	0.49070	0.32524	0.06126	0.01498	0.01160	0.01323	-0.00179	0.00371	-0.00171		
(90k-92k)^2	0.00000	0.00000	0.00000	0.00000	0.00000	0.00000	0.00000	0.00000	0.00000	0.00000	0.00000
C7	0.59386	0.28031	0.09554	0.01333	0.01574	0.01715	-0.00172	0.00501	-0.00249		



C7	0.59376	0.28022	0.09560	0.01350	0.01557	0.01681	-0.00197	0.00468	-0.00358		
(90k-92k)^2	0.00000	0.00000	0.00000	0.00000	0.00000	0.00000	0.00000	0.00000	0.00000	0.00000	0.00000
H7	0.65745	0.29963	0.06410	0.02484	0.03971	0.03790	-0.00231	0.01510	0.00173		
H7	0.65847	0.30553	0.06688	0.01809							
(90k-92k)^2	0.00000	0.00003	0.00001	0.00005	0.00158	0.00144	0.00001	0.00023	0.00000		
C8	0.61264	0.20570	0.16404	0.01090	0.01650	0.01620	0.00056	0.00173	-0.00281		
C8	0.61253	0.20579	0.16402	0.01173	0.01619	0.01638	0.00069	0.00157	-0.00354		
(90k-92k)^2	0.00000	0.00000	0.00000	0.00000	0.00000	0.00000	0.00000	0.00000	0.00000	0.00000	0.00000
H8	0.69010	0.16916	0.18371	0.01843	0.03938	0.03831	0.00820	0.00383	0.00210		
H8	0.69161	0.17453	0.18785	0.01796							
(90k-92k)^2	0.00000	0.00003	0.00002	0.00000	0.00155	0.00147	0.00007	0.00001	0.00000		
C9	0.52981	0.16855	0.20456	0.01161	0.01416	0.01221	0.00134	0.00089	-0.00160		
C9	0.52980	0.16853	0.20460	0.01272	0.01423	0.01105	0.00132	0.00018	-0.00195		
(90k-92k)^2	0.00000	0.00000	0.00000	0.00000	0.00000	0.00000	0.00000	0.00000	0.00000	0.00000	0.00000
C10	0.52235	0.06542	0.25291	0.01554	0.01676	0.01232	0.00301	0.00013	0.00103		
C10	0.52235	0.06540	0.25294	0.01674	0.01657	0.01173	0.00319	-0.00048	0.00050		
(90k-92k)^2	0.00000	0.00000	0.00000	0.00000	0.00000	0.00000	0.00000	0.00000	0.00000	0.00000	0.00000
H10	0.59217	0.01514	0.27739	0.02568	0.03243	0.03554	0.00854	-0.00044	0.00578		
H10	0.59369	0.02087	0.28295	0.01862							
(90k-92k)^2	0.00000	0.00003	0.00003	0.00005	0.00105	0.00126	0.00007	0.00000	0.00003		
C11	0.42697	0.02138	0.26219	0.01823	0.01710	0.01229	0.00155	0.00283	0.00236		
C11	0.42688	0.02144	0.26225	0.02011	0.01666	0.01118	0.00235	0.00294	0.00243		
(90k-92k)^2	0.00000	0.00000	0.00000	0.00000	0.00000	0.00000	0.00000	0.00000	0.00000	0.00000	0.00001
H11	0.42564	-0.06091	0.29408	0.03775	0.02870	0.03381	0.00276	0.00685	0.01252		
H11	0.42548	-0.05691	0.29904	0.01924							
(90k-92k)^2	0.00000	0.00002	0.00002	0.00034	0.00082	0.00114	0.00001	0.00005	0.00016		
C12	0.32941	0.07643	0.22463	0.01562	0.01624	0.01175	0.00100	0.00500	0.00118		
C12	0.32944	0.07640	0.22465	0.01656	0.01581	0.01130	0.00102	0.00538	0.00084		
(90k-92k)^2	0.00000	0.00000	0.00000	0.00000	0.00000	0.00000	0.00000	0.00000	0.00000	0.00000	0.00000
C13	0.22558	0.02811	0.20376	0.01615	0.01843	0.01876	-0.00105	0.00837	0.00223		
C13	0.22555	0.02805	0.20380	0.01750	0.01907	0.01882	-0.00100	0.00927	0.00148		
(90k-92k)^2	0.00000	0.00000	0.00000	0.00000	0.00000	0.00000	0.00000	0.00000	0.00000	0.00000	0.00000

H13	0.20981	-0.05341	0.23204	0.03489	0.03126	0.04315	-0.00509	0.01414	0.01117		
H13	0.20770	-0.04812	0.23746	0.02120							
(90k-92k)^2	0.00000	0.00003	0.00003	0.00019	0.00098	0.00186	0.00003	0.00020	0.00012		
C14	0.14807	0.07641	0.14189	0.01277	0.02041	0.02360	-0.00056	0.00807	0.00017		
C14	0.14812	0.07635	0.14195	0.01303	0.02053	0.02300	-0.00063	0.00801	-0.00016		
(90k-92k)^2	0.00000	0.00000	0.00000	0.00000	0.00000	0.00000	0.00000	0.00000	0.00000	0.00000	0.00000
H14	0.07380	0.03161	0.12395	0.02158	0.04008	0.04895	-0.00817	0.00807	0.00323		
H14	0.07091	0.03705	0.12823	0.02188							
(90k-92k)^2	0.00001	0.00003	0.00002	0.00000	0.00161	0.00240	0.00007	0.00007	0.00001		
C15	0.16688	0.17746	0.09505	0.01019	0.01752	0.01859	0.00152	0.00408	-0.00103		
C15	0.16699	0.17745	0.09516	0.01066	0.01772	0.01819	0.00207	0.00424	-0.00125		
(90k-92k)^2	0.00000	0.00000	0.00000	0.00000	0.00000	0.00000	0.00000	0.00000	0.00000	0.00000	0.00000
C16	0.11426	0.21573	0.01233	0.01068	0.02206	0.02080	0.00328	0.00064	-0.00045		
C16	0.11425	0.21587	0.01235	0.01105	0.02165	0.02078	0.00330	0.00036	-0.00134		
(90k-92k)^2	0.00000	0.00000	0.00000	0.00000	0.00000	0.00000	0.00000	0.00000	0.00000	0.00000	0.00000
H16	0.03777	0.18064	-0.01558	0.02021	0.04727	0.03987	-0.00480	-0.00124	0.00094		
H16	0.03463	0.18717	-0.01274	0.02191							
(90k-92k)^2	0.00001	0.00004	0.00001	0.00000	0.00223	0.00159	0.00002	0.00000	0.00000		
C17	0.16216	0.28835	-0.03622	0.01394	0.01926	0.01713	0.00461	-0.00124	0.00080		
C17	0.16222	0.28828	-0.03606	0.01495	0.01880	0.01730	0.00474	-0.00171	0.00025		
(90k-92k)^2	0.00000	0.00000	0.00000	0.00000	0.00000	0.00000	0.00000	0.00000	0.00000	0.00000	0.00000
H17	0.12298	0.30619	-0.10068	0.03033	0.04438	0.02615	0.00250	-0.00722	0.00534		
H17	0.11944	0.31410	-0.09839	0.02131							
(90k-92k)^2	0.00001	0.00006	0.00001	0.00008	0.00197	0.00068	0.00001	0.00005	0.00003		
C18	0.26708	0.33035	-0.00640	0.01529	0.01325	0.01297	0.00288	0.00056	0.00101		
C18	0.26705	0.33045	-0.00640	0.01581	0.01303	0.01345	0.00335	0.00049	0.00102		
(90k-92k)^2	0.00000	0.00000	0.00000	0.00000	0.00000	0.00000	0.00000	0.00000	0.00000	0.00000	0.00000
C19	0.34088	0.37182	-0.05439	0.02096	0.01495	0.01408	0.00071	0.00261	0.00298		
C19	0.34094	0.37179	-0.05431	0.02237	0.01451	0.01339	0.00135	0.00234	0.00287		
(90k-92k)^2	0.00000	0.00000	0.00000	0.00000	0.00000	0.00000	0.00000	0.00000	0.00000	0.00000	0.00000
H19	0.31296	0.39778	-0.11969	0.03949	0.04296	0.02215	0.00194	0.00128	0.01068		
H19	0.31202	0.40601	-0.11750	0.02035							

(90k-92k)^2	0.00000	0.00007	0.00000	0.00037	0.00185	0.00049	0.00000	0.00000	0.00011		
C20	0.44774	0.36922	-0.02221	0.01986	0.01384	0.01461	-0.00178	0.00512	0.00125		
C20	0.44769	0.36916	-0.02216	0.02135	0.01335	0.01440	-0.00207	0.00522	0.00104		
(90k-92k)^2	0.00000	0.00000	0.00000	0.00000	0.00000	0.00000	0.00000	0.00000	0.00000	0.00000	0.00000
H20	0.49984	0.39365	-0.06346	0.03712	0.03945	0.02925	-0.00642	0.01446	0.00569		
H20	0.50039	0.40102	-0.06081	0.01938							
(90k-92k)^2	0.00000	0.00005	0.00001	0.00031	0.00156	0.00086	0.00004	0.00021	0.00003		
	X	Y	Z	U11	U22	U33	U12	U13	U23	0.00003	0.00004
<delta>	0.00001	0.00001	-0.00005	-0.00088	0.00024	0.00037	-0.00016	0.00012	0.00045	-0.00009	
RMS:	0.00006	0.00007	0.00006	0.00098	0.00042	0.00058	0.00036	0.00037	0.00054	0.00070	0.00058
0.7 Angstroms	N - X										
CorH(B)											
ATOM	X	Y	Z	U11	U22	U33	U12	U13	U23	sum delUii	sum Uii+uij
C21	0.15466	0.69812	0.46774	0.01213	0.01230	0.01503	-0.00106	0.00460	-0.00148		
C21	0.15478	0.69807	0.46766	0.01193	0.01262	0.01469	-0.00121	0.00452	-0.00138		
(90k-92k)^2	0.00000	0.00000	0.00000	0.00000	0.00000	0.00000	0.00000	0.00000	0.00000	0.00000	0.00000
C22	0.09904	0.69541	0.38291	0.01020	0.01237	0.01587	-0.00044	0.00290	-0.00131		
C22	0.09910	0.69539	0.38287	0.00991	0.01315	0.01602	-0.00092	0.00294	-0.00112		
(90k-92k)^2	0.00000	0.00000	0.00000	0.00000	0.00000	0.00000	0.00000	0.00000	0.00000	0.00000	0.00000
C23	0.12362	0.59102	0.34639	0.01104	0.01323	0.01481	-0.00191	0.00313	-0.00233		
C23	0.12367	0.59089	0.34647	0.01083	0.01328	0.01527	-0.00243	0.00311	-0.00214		
(90k-92k)^2	0.00000	0.00000	0.00000	0.00000	0.00000	0.00000	0.00000	0.00000	0.00000	0.00000	0.00000
C24	0.19496	0.52951	0.40857	0.01259	0.01054	0.01647	-0.00093	0.00469	-0.00073		
C24	0.19493	0.52951	0.40859	0.01375	0.01057	0.01591	-0.00155	0.00488	-0.00040		
(90k-92k)^2	0.00000	0.00000	0.00000	0.00000	0.00000	0.00000	0.00000	0.00000	0.00000	0.00000	0.00000
C25	0.21475	0.59620	0.48325	0.01356	0.01251	0.01396	-0.00072	0.00428	0.00056		
C25	0.21474	0.59618	0.48316	0.01413	0.01229	0.01376	-0.00115	0.00458	0.00092		
(90k-92k)^2	0.00000	0.00000	0.00000	0.00000	0.00000	0.00000	0.00000	0.00000	0.00000	0.00000	0.00000
C26	0.18194	0.79913	0.51152	0.01460	0.01429	0.01640	-0.00129	0.00464	-0.00338		
C26	0.18198	0.79916	0.51145	0.01482	0.01441	0.01736	-0.00151	0.00547	-0.00384		
(90k-92k)^2	0.00000	0.00000	0.00000	0.00000	0.00000	0.00000	0.00000	0.00000	0.00000	0.00000	0.00000

C27	0.13439	0.90128	0.46878	0.01725	0.01305	0.02592	0.00013	0.00519	-0.00356		
C27	0.13467	0.90119	0.46883	0.01801	0.01305	0.02645	0.00014	0.00555	-0.00414		
(90k-92k)^2	0.00000	0.00000	0.00000	0.00000	0.00000	0.00000	0.00000	0.00000	0.00000	0.00000	0.00000
H27	0.14715	0.98449	0.50021	0.04390	0.02129	0.04626	-0.00014	0.00603	-0.01127		
H27	0.14140	0.98252	0.50314	0.02285							
(90k-92k)^2	0.00003	0.00000	0.00001	0.00044	0.00045	0.00214	0.00000	0.00004	0.00013		
C28	0.08071	0.89875	0.38539	0.01603	0.01411	0.02726	0.00255	0.00259	0.00022		
C28	0.08084	0.89864	0.38534	0.01643	0.01369	0.02843	0.00275	0.00296	0.00041		
(90k-92k)^2	0.00000	0.00000	0.00000	0.00000	0.00000	0.00000	0.00000	0.00000	0.00000	0.00000	0.00000
H28	0.05407	0.97979	0.35471	0.04116	0.02397	0.04989	0.00856	0.00110	0.00649		
H28	0.04747	0.97827	0.35575	0.02372							
(90k-92k)^2	0.00004	0.00000	0.00000	0.00030	0.00057	0.00249	0.00007	0.00000	0.00004		
C29	0.06769	0.79351	0.33663	0.01132	0.01564	0.01921	0.00123	0.00106	0.00128		
C29	0.06780	0.79337	0.33656	0.01118	0.01555	0.02043	0.00106	0.00110	0.00111		
(90k-92k)^2	0.00000	0.00000	0.00000	0.00000	0.00000	0.00000	0.00000	0.00000	0.00000	0.00000	0.00000
C30	0.04666	0.77668	0.24623	0.01427	0.02245	0.01890	0.00089	-0.00067	0.00355		
C30	0.04672	0.77636	0.24618	0.01365	0.02325	0.01970	0.00044	-0.00136	0.00401		
(90k-92k)^2	0.00000	0.00000	0.00000	0.00000	0.00000	0.00000	0.00000	0.00000	0.00000	0.00000	0.00000
H30	0.01656	0.84797	0.20466	0.03864	0.03817	0.03599	0.00747	-0.00053	0.01292		
H30	0.01041	0.84574	0.20499	0.02349							
(90k-92k)^2	0.00004	0.00000	0.00000	0.00023	0.00146	0.00130	0.00006	0.00000	0.00017		
C31	0.07134	0.67423	0.21030	0.01378	0.02631	0.01521	-0.00176	-0.00014	-0.00005		
C31	0.07143	0.67416	0.21040	0.01356	0.02701	0.01517	-0.00245	-0.00074	-0.00018		
(90k-92k)^2	0.00000	0.00000	0.00000	0.00000	0.00000	0.00000	0.00000	0.00000	0.00000	0.00000	0.00000
H31	0.06138	0.66962	0.14218	0.03729	0.05186	0.02110	-0.00029	0.00159	0.00053		
H31	0.05470	0.66614	0.14189	0.02295							
(90k-92k)^2	0.00004	0.00001	0.00000	0.00021	0.00269	0.00045	0.00000	0.00000	0.00000		
C32	0.11858	0.57808	0.26114	0.01184	0.01883	0.01505	-0.00331	0.00227	-0.00335		
C32	0.11866	0.57796	0.26113	0.01214	0.01941	0.01540	-0.00388	0.00202	-0.00415		
(90k-92k)^2	0.00000	0.00000	0.00000	0.00000	0.00000	0.00000	0.00000	0.00000	0.00000	0.00000	0.00000
C33	0.17851	0.48222	0.23946	0.01679	0.02048	0.01902	-0.00374	0.00532	-0.00779		
C33	0.17870	0.48202	0.23959	0.01736	0.02091	0.01918	-0.00456	0.00536	-0.00814		

(90k-92k)^2	0.00000	0.00000	0.00000	0.00000	0.00000	0.00000	0.00000	0.00000	0.00000	0.00000	0.00000
H33	0.17387	0.45964	0.17355	0.04064	0.04659	0.02711	-0.00010	0.00887	-0.01357		
H33	0.16865	0.45626	0.17372	0.02271							
(90k-92k)^2	0.00003	0.00001	0.00000	0.00032	0.00217	0.00073	0.00000	0.00008	0.00018		
C34	0.24870	0.42201	0.30067	0.01873	0.01475	0.02340	-0.00124	0.00764	-0.00627		
C34	0.24872	0.42201	0.30066	0.01943	0.01450	0.02409	-0.00209	0.00827	-0.00651		
(90k-92k)^2	0.00000	0.00000	0.00000	0.00000	0.00000	0.00000	0.00000	0.00000	0.00000	0.00000	0.00000
H34	0.29621	0.35570	0.28033	0.04029	0.02966	0.04311	0.00706	0.01569	-0.01113		
H34	0.29211	0.35034	0.28138	0.02256							
(90k-92k)^2	0.00002	0.00003	0.00000	0.00031	0.00088	0.00186	0.00005	0.00025	0.00012		
C35	0.26574	0.45187	0.38900	0.01582	0.01104	0.02100	-0.00004	0.00660	-0.00059		
C35	0.26575	0.45179	0.38904	0.01664	0.01041	0.02098	-0.00031	0.00642	-0.00063		
(90k-92k)^2	0.00000	0.00000	0.00000	0.00000	0.00000	0.00000	0.00000	0.00000	0.00000	0.00000	0.00000
C36	0.35495	0.43086	0.45607	0.01747	0.01314	0.02461	0.00309	0.00600	0.00409		
C36	0.35508	0.43086	0.45631	0.01894	0.01255	0.02461	0.00294	0.00614	0.00447		
(90k-92k)^2	0.00000	0.00000	0.00000	0.00000	0.00000	0.00000	0.00000	0.00000	0.00000	0.00000	0.00000
H36	0.41240	0.36671	0.44779	0.03218	0.02856	0.04972	0.01263	0.01007	0.00297		
H36	0.40860	0.36135	0.44951	0.02216							
(90k-92k)^2	0.00001	0.00003	0.00000	0.00010	0.00082	0.00247	0.00016	0.00010	0.00001		
C37	0.37473	0.49653	0.52930	0.01723	0.01777	0.01897	0.00265	0.00303	0.00688		
C37	0.37471	0.49664	0.52930	0.01820	0.01718	0.01909	0.00249	0.00315	0.00705		
(90k-92k)^2	0.00000	0.00000	0.00000	0.00000	0.00000	0.00000	0.00000	0.00000	0.00000	0.00000	0.00000
H37	0.44663	0.48189	0.57492	0.02924	0.04109	0.03266	0.00824	-0.00294	0.00757		
H37	0.44324	0.47741	0.57825	0.02192							
(90k-92k)^2	0.00001	0.00002	0.00001	0.00005	0.00169	0.00107	0.00007	0.00001	0.00006		
C38	0.30683	0.58996	0.54237	0.01573	0.01608	0.01356	-0.00025	0.00301	0.00281		
C38	0.30691	0.58995	0.54232	0.01670	0.01648	0.01323	-0.00034	0.00305	0.00361		
(90k-92k)^2	0.00000	0.00000	0.00000	0.00000	0.00000	0.00000	0.00000	0.00000	0.00000	0.00000	0.00000
C39	0.32830	0.68902	0.59722	0.01850	0.02204	0.01256	-0.00188	0.00148	-0.00009		
C39	0.32831	0.68903	0.59725	0.01960	0.02269	0.01236	-0.00230	0.00176	0.00031		
(90k-92k)^2	0.00000	0.00000	0.00000	0.00000	0.00000	0.00000	0.00000	0.00000	0.00000	0.00000	0.00000
H39	0.39699	0.68899	0.64832	0.03423	0.04559	0.02576	-0.00156	-0.00681	-0.00188		

<b>H39</b>	0.39330	0.68550	0.65154	0.02214							
<b>(90k-92k)^2</b>	0.00001	0.00001	0.00001	0.00015	0.00208	0.00066	0.00000	0.00005	0.00000		
<b>C40</b>	0.26838	0.78851	0.58287	0.01877	0.01943	0.01544	-0.00267	0.00399	-0.00449		
<b>C40</b>	0.26853	0.78846	0.58286	0.01959	0.02045	0.01497	-0.00357	0.00420	-0.00461		
<b>(90k-92k)^2</b>	0.00000	0.00000	0.00000	0.00000	0.00000	0.00000	0.00000	0.00000	0.00000	0.00000	0.00000
<b>H40</b>	0.29243	0.86279	0.62312	0.03900	0.03564	0.03291	-0.00499	0.00203	-0.01505		
<b>H40</b>	0.28729	0.86048	0.62654	0.02190							
<b>(90k-92k)^2</b>	0.00003	0.00001	0.00001	0.00029	0.00127	0.00108	0.00002	0.00000	0.00023		
	<b>X</b>	<b>Y</b>	<b>Z</b>	<b>U11</b>	<b>U22</b>	<b>U33</b>	<b>U12</b>	<b>U13</b>	<b>U23</b>	<b>0.00002</b>	<b>0.00003</b>
<b>&lt;delta&gt;</b>	<b>-0.00008</b>	<b>0.00006</b>	<b>-0.00001</b>	<b>-0.00046</b>	<b>-0.00015</b>	<b>-0.00022</b>	<b>0.00039</b>	<b>-0.00009</b>	<b>-0.00003</b>	<b>-0.00028</b>	
<b>RMS:</b>	<b>0.00011</b>	<b>0.00011</b>	<b>0.00008</b>	<b>0.00073</b>	<b>0.00052</b>	<b>0.00057</b>	<b>0.00049</b>	<b>0.00036</b>	<b>0.00039</b>	<b>0.00061</b>	<b>0.00052</b>
<b>0.5 Angstroms</b>	<b>N - X</b>										
<b>CorH(A)</b>											
<b>ATOM</b>	<b>X</b>	<b>Y</b>	<b>Z</b>	<b>U11</b>	<b>U22</b>	<b>U33</b>	<b>U12</b>	<b>U13</b>	<b>U23</b>	<b>sum delUii</b>	<b>sum Uii+uij</b>
<b>C1</b>	0.41698	0.30378	0.11032	0.02252	0.01963	0.01960	0.00039	0.00398	-0.00287		
<b>C1</b>	0.41708	0.30379	0.11037	0.02227	0.01808	0.01895	0.00055	0.00380	-0.00344		
<b>(173k-173k(xray))^2</b>	0.00000	0.00000	0.00000	0.00000	0.00000	0.00000	0.00000	0.00000	0.00000	0.00000	0.00000
<b>C2</b>	0.43626	0.22784	0.17979	0.02213	0.02214	0.01758	0.00162	0.00341	-0.00359		
<b>C2</b>	0.43629	0.22777	0.17972	0.02126	0.02140	0.01619	0.00181	0.00282	-0.00390		
<b>(173k-173k(xray))^2</b>	0.00000	0.00000	0.00000	0.00000	0.00000	0.00000	0.00000	0.00000	0.00000	0.00000	0.00000
<b>C3</b>	0.33949	0.18320	0.18963	0.02403	0.02430	0.01848	0.00298	0.00682	-0.00106		
<b>C3</b>	0.33943	0.18315	0.18959	0.02296	0.02385	0.01713	0.00325	0.00676	-0.00185		
<b>(173k-173k(xray))^2</b>	0.00000	0.00000	0.00000	0.00000	0.00000	0.00000	0.00000	0.00000	0.00000	0.00000	0.00000
<b>C4</b>	0.26032	0.23186	0.12662	0.02093	0.02505	0.02300	0.00444	0.00643	-0.00217		
<b>C4</b>	0.26035	0.23179	0.12671	0.02004	0.02376	0.02237	0.00470	0.00672	-0.00254		
<b>(173k-173k(xray))^2</b>	0.00000	0.00000	0.00000	0.00000	0.00000	0.00000	0.00000	0.00000	0.00000	0.00000	0.00000
<b>C5</b>	0.30843	0.30633	0.07767	0.02331	0.02027	0.02111	0.00406	0.00334	-0.00125		
<b>C5</b>	0.30844	0.30637	0.07771	0.02256	0.01917	0.02071	0.00449	0.00363	-0.00153		
<b>(173k-173k(xray))^2</b>	0.00000	0.00000	0.00000	0.00000	0.00000	0.00000	0.00000	0.00000	0.00000	0.00000	0.00000
<b>C6</b>	0.48960	0.32502	0.06193	0.02710	0.02107	0.02434	-0.00389	0.00744	-0.00401		
<b>C6</b>	0.48957	0.32506	0.06198	0.02600	0.01984	0.02335	-0.00364	0.00699	-0.00369		

(173k-173k(xray))^2	0.00000	0.00000	0.00000	0.00000	0.00000	0.00000	0.00000	0.00000	0.00000	0.00000	0.00000
C7	0.59246	0.28025	0.09609	0.02444	0.02846	0.03140	-0.00389	0.00935	-0.00701		
C7	0.59247	0.28009	0.09617	0.02282	0.02736	0.03044	-0.00433	0.00875	-0.00787		
(173k-173k(xray))^2	0.00000	0.00000	0.00000	0.00000	0.00000	0.00000	0.00000	0.00000	0.00000	0.00000	0.00001
H7	0.65599	0.29955	0.06490	0.03829	0.05817	0.05938	-0.00719	0.02386	-0.00282		
H7	0.65699	0.30518	0.06746	0.03169							
(173k-173k(xray))^2	0.00000	0.00003	0.00001	0.00004	0.00338	0.00353	0.00005	0.00057	0.00001		
C8	0.61131	0.20627	0.16421	0.02079	0.03007	0.02996	0.00107	0.00332	-0.00672		
C8	0.61135	0.20623	0.16419	0.01938	0.02908	0.02924	0.00075	0.00264	-0.00798		
(173k-173k(xray))^2	0.00000	0.00000	0.00000	0.00000	0.00000	0.00000	0.00000	0.00000	0.00000	0.00000	0.00001
H8	0.68898	0.16998	0.18385	0.02704	0.05833	0.05799	0.01029	0.00532	-0.00324		
H8	0.69037	0.17509	0.18790	0.03152							
(173k-173k(xray))^2	0.00000	0.00003	0.00002	0.00002	0.00340	0.00336	0.00011	0.00003	0.00001		
C9	0.52911	0.16920	0.20467	0.02183	0.02568	0.02077	0.00260	0.00034	-0.00440		
C9	0.52909	0.16925	0.20465	0.02184	0.02527	0.01852	0.00262	-0.00020	-0.00482		
(173k-173k(xray))^2	0.00000	0.00000	0.00000	0.00000	0.00000	0.00001	0.00000	0.00000	0.00000	0.00001	0.00001
C10	0.52207	0.06673	0.25301	0.02979	0.03003	0.02085	0.00577	-0.00149	0.00057		
C10	0.52188	0.06666	0.25303	0.02994	0.02962	0.01910	0.00674	-0.00126	-0.00012		
(173k-173k(xray))^2	0.00000	0.00000	0.00000	0.00000	0.00000	0.00000	0.00000	0.00000	0.00000	0.00000	0.00000
H10	0.59192	0.01709	0.27782	0.04350	0.04910	0.04751	0.01541	-0.00439	0.00726		
H10	0.59325	0.02247	0.28297	0.03260							
(173k-173k(xray))^2	0.00000	0.00003	0.00003	0.00012	0.00241	0.00226	0.00024	0.00002	0.00005		
C11	0.42692	0.02283	0.26241	0.03761	0.03028	0.01944	0.00421	0.00515	0.00491		
C11	0.42698	0.02290	0.26243	0.03662	0.02905	0.01825	0.00480	0.00492	0.00435		
(173k-173k(xray))^2	0.00000	0.00000	0.00000	0.00000	0.00000	0.00000	0.00000	0.00000	0.00000	0.00000	0.00000
H11	0.42554	-0.05876	0.29430	0.06348	0.04444	0.04401	0.00613	0.00822	0.01754		
H11	0.42585	-0.05498	0.29930	0.03372							
(173k-173k(xray))^2	0.00000	0.00001	0.00003	0.00089	0.00197	0.00194	0.00004	0.00007	0.00031		
C12	0.32956	0.07731	0.22480	0.03015	0.02846	0.02021	0.00190	0.01013	0.00137		
C12	0.32958	0.07724	0.22494	0.02970	0.02777	0.01894	0.00208	0.01029	0.00118		
(173k-173k(xray))^2	0.00000	0.00000	0.00000	0.00000	0.00000	0.00000	0.00000	0.00000	0.00000	0.00000	0.00000
C13	0.22607	0.02883	0.20399	0.03155	0.03498	0.03491	-0.00183	0.01794	0.00288		

<b>C13</b>	0.22606	0.02879	0.20405	0.03104	0.03327	0.03350	-0.00178	0.01788	0.00212		
<b>(173k-173k(xray))^2</b>	0.00000	0.00000	0.00000	0.00000	0.00000	0.00000	0.00000	0.00000	0.00000	0.00001	0.00001
<b>H13</b>	0.21052	-0.05206	0.23220	0.05772	0.04907	0.06782	-0.00713	0.02699	0.01639		
<b>H13</b>	0.20846	-0.04716	0.23760	0.03717							
<b>(173k-173k(xray))^2</b>	0.00000	0.00002	0.00003	0.00042	0.00241	0.00460	0.00005	0.00073	0.00027		
<b>C14</b>	0.14846	0.07670	0.14237	0.02362	0.03725	0.04370	-0.00135	0.01570	-0.00094		
<b>C14</b>	0.14861	0.07658	0.14239	0.02222	0.03672	0.04154	-0.00121	0.01543	-0.00101		
<b>(173k-173k(xray))^2</b>	0.00000	0.00000	0.00000	0.00000	0.00000	0.00000	0.00000	0.00000	0.00000	0.00001	0.00001
<b>H14</b>	0.07437	0.03199	0.12427	0.03347	0.06293	0.07799	-0.01159	0.01628	0.00175		
<b>H14</b>	0.07163	0.03710	0.12864	0.03865							
<b>(173k-173k(xray))^2</b>	0.00001	0.00003	0.00002	0.00003	0.00396	0.00608	0.00013	0.00027	0.00000		
<b>C15</b>	0.16697	0.17742	0.09565	0.01857	0.03205	0.03424	0.00387	0.00789	-0.00239		
<b>C15</b>	0.16700	0.17728	0.09581	0.01789	0.03143	0.03249	0.00421	0.00806	-0.00271		
<b>(173k-173k(xray))^2</b>	0.00000	0.00000	0.00000	0.00000	0.00000	0.00000	0.00000	0.00000	0.00000	0.00000	0.00000
<b>C16</b>	0.11410	0.21549	0.01329	0.01912	0.03991	0.03880	0.00638	0.00085	-0.00315		
<b>C16</b>	0.11415	0.21536	0.01328	0.01815	0.03837	0.03763	0.00641	0.00083	-0.00327		
<b>(173k-173k(xray))^2</b>	0.00000	0.00000	0.00000	0.00000	0.00000	0.00000	0.00000	0.00000	0.00000	0.00000	0.00000
<b>H16</b>	0.03813	0.18023	-0.01447	0.02761	0.07201	0.06687	-0.00469	-0.00306	-0.00190		
<b>H16</b>	0.03469	0.18648	-0.01173	0.03855							
<b>(173k-173k(xray))^2</b>	0.00001	0.00004	0.00001	0.00012	0.00519	0.00447	0.00002	0.00001	0.00000		
<b>C17</b>	0.16171	0.28782	-0.03508	0.02659	0.03497	0.03116	0.00921	-0.00279	0.00110		
<b>C17</b>	0.16171	0.28767	-0.03503	0.02536	0.03311	0.03071	0.00936	-0.00346	0.00033		
<b>(173k-173k(xray))^2</b>	0.00000	0.00000	0.00000	0.00000	0.00000	0.00000	0.00000	0.00000	0.00000	0.00001	0.00001
<b>H17</b>	0.12238	0.30558	-0.09966	0.04880	0.06561	0.04312	0.01001	-0.01208	0.00691		
<b>H17</b>	0.11873	0.31338	-0.09716	0.03733							
<b>(173k-173k(xray))^2</b>	0.00001	0.00006	0.00001	0.00013	0.00430	0.00186	0.00010	0.00015	0.00005		
<b>C18</b>	0.26629	0.32981	-0.00554	0.02929	0.02332	0.02458	0.00594	0.00170	0.00179		
<b>C18</b>	0.26633	0.32987	-0.00552	0.02795	0.02244	0.02341	0.00677	0.00074	0.00158		
<b>(173k-173k(xray))^2</b>	0.00000	0.00000	0.00000	0.00000	0.00000	0.00000	0.00000	0.00000	0.00000	0.00000	0.00001
<b>C19</b>	0.33982	0.37108	-0.05321	0.04099	0.02663	0.02353	0.00194	0.00447	0.00547		
<b>C19</b>	0.33994	0.37103	-0.05322	0.04076	0.02423	0.02290	0.00255	0.00438	0.00502		
<b>(173k-173k(xray))^2</b>	0.00000	0.00000	0.00000	0.00000	0.00001	0.00000	0.00000	0.00000	0.00000	0.00001	0.00001



H19	0.31193	0.39741	-0.11847	0.07036	0.05908	0.03277	0.00565	0.00486	0.01602		
H19	0.31094	0.40492	-0.11630	0.03557							
(173k-173k(xray))^2	0.00000	0.00006	0.00000	0.00121	0.00349	0.00107	0.00003	0.00002	0.00026		
C20	0.44640	0.36891	-0.02118	0.03841	0.02429	0.02648	-0.00400	0.01051	0.00177		
C20	0.44644	0.36871	-0.02114	0.03849	0.02234	0.02529	-0.00408	0.01033	0.00167		
(173k-173k(xray))^2	0.00000	0.00000	0.00000	0.00000	0.00000	0.00000	0.00000	0.00000	0.00000	0.00001	0.00001
H20	0.49810	0.39312	-0.06246	0.05953	0.05601	0.04539	-0.00855	0.02313	0.00863		
H20	0.49896	0.40065	-0.05964	0.03381							
(173k-173k(xray))^2	0.00000	0.00006	0.00001	0.00066	0.00314	0.00206	0.00007	0.00053	0.00007		
	X	Y	Z	U11	U22	U33	U12	U13	U23	0.00008	0.00009
<delta>	-0.00002	0.00005	-0.00003	0.00078	0.00113	0.00117	-0.00023	0.00022	0.00044	0.00103	
RMS:	0.00007	0.00010	0.00006	0.00093	0.00126	0.00128	0.00041	0.00042	0.00056	0.00117	0.00089
0.5 Angstroms	N - X										
CorH(B)											
ATOM	X	Y	Z	U11	U22	U33	U12	U13	U23	sum delUii	sum Uii+uij
C21	0.15533	0.69771	0.46696	0.02161	0.02335	0.02687	-0.00196	0.00847	-0.00252		
C21	0.15538	0.69758	0.46681	0.02014	0.02247	0.02640	-0.00283	0.00884	-0.00285		
(173k-173k(xray))^2	0.00000	0.00000	0.00000	0.00000	0.00000	0.00000	0.00000	0.00000	0.00000	0.00000	0.00000
C22	0.09997	0.69455	0.38236	0.01742	0.02334	0.02996	-0.00164	0.00512	-0.00197		
C22	0.10000	0.69465	0.38229	0.01583	0.02317	0.02883	-0.00208	0.00562	-0.00196		
(173k-173k(xray))^2	0.00000	0.00000	0.00000	0.00000	0.00000	0.00000	0.00000	0.00000	0.00000	0.00000	0.00000
C23	0.12434	0.59040	0.34638	0.01977	0.02434	0.02802	-0.00496	0.00687	-0.00458		
C23	0.12434	0.59028	0.34644	0.01787	0.02359	0.02713	-0.00527	0.00590	-0.00410		
(173k-173k(xray))^2	0.00000	0.00000	0.00000	0.00000	0.00000	0.00000	0.00000	0.00000	0.00000	0.00000	0.00001
C24	0.19520	0.52940	0.40861	0.02439	0.01889	0.02986	-0.00250	0.00946	-0.00051		
C24	0.19526	0.52953	0.40865	0.02331	0.01841	0.02922	-0.00338	0.00957	-0.00049		
(173k-173k(xray))^2	0.00000	0.00000	0.00000	0.00000	0.00000	0.00000	0.00000	0.00000	0.00000	0.00000	0.00000
C25	0.21496	0.59608	0.48276	0.02505	0.02334	0.02523	-0.00231	0.00886	0.00204		
C25	0.21499	0.59615	0.48276	0.02399	0.02202	0.02390	-0.00266	0.00854	0.00212		
(173k-173k(xray))^2	0.00000	0.00000	0.00000	0.00000	0.00000	0.00000	0.00000	0.00000	0.00000	0.00000	0.00000
C26	0.18275	0.79826	0.51024	0.02709	0.02650	0.03227	-0.00336	0.01030	-0.00755		

C26	0.18283	0.79827	0.51026	0.02597	0.02603	0.03152	-0.00355	0.01098	-0.00751		
(173k-173k(xray))^2	0.00000	0.00000	0.00000	0.00000	0.00000	0.00000	0.00000	0.00000	0.00000	0.00000	0.00000
C27	0.13577	0.89969	0.46731	0.03309	0.02348	0.05034	-0.00035	0.01208	-0.00846		
C27	0.13590	0.89959	0.46727	0.03113	0.02307	0.05023	-0.00028	0.01226	-0.00850		
(173k-173k(xray))^2	0.00000	0.00000	0.00000	0.00000	0.00000	0.00000	0.00000	0.00000	0.00000	0.00000	0.00000
H27	0.14864	0.98244	0.49844	0.07164	0.03172	0.07982	-0.00164	0.01636	-0.01936		
H27	0.14283	0.98083	0.50117	0.04112							
(173k-173k(xray))^2	0.00003	0.00000	0.00001	0.00093	0.00101	0.00637	0.00000	0.00027	0.00037		
C28	0.08230	0.89669	0.38420	0.02899	0.02445	0.05476	0.00468	0.00619	0.00090		
C28	0.08231	0.89675	0.38423	0.02790	0.02407	0.05391	0.00508	0.00646	0.00151		
(173k-173k(xray))^2	0.00000	0.00000	0.00000	0.00000	0.00000	0.00000	0.00000	0.00000	0.00000	0.00000	0.00000
H28	0.05554	0.97719	0.35324	0.06153	0.03597	0.08497	0.01555	0.00367	0.00979		
H28	0.04919	0.97601	0.35450	0.04274							
(173k-173k(xray))^2	0.00004	0.00000	0.00000	0.00035	0.00129	0.00722	0.00024	0.00001	0.00010		
C29	0.06909	0.79196	0.33591	0.01979	0.02864	0.03809	0.00186	0.00248	0.00260		
C29	0.06900	0.79187	0.33583	0.01807	0.02804	0.03807	0.00171	0.00219	0.00275		
(173k-173k(xray))^2	0.00000	0.00000	0.00000	0.00000	0.00000	0.00000	0.00000	0.00000	0.00000	0.00000	0.00000
C30	0.04807	0.77461	0.24587	0.02419	0.04448	0.03556	0.00130	-0.00247	0.00883		
C30	0.04803	0.77438	0.24583	0.02224	0.04339	0.03647	0.00042	-0.00303	0.00891		
(173k-173k(xray))^2	0.00000	0.00000	0.00000	0.00000	0.00000	0.00000	0.00000	0.00000	0.00000	0.00001	0.00001
H30	0.01807	0.84544	0.20416	0.05360	0.06557	0.05784	0.00917	-0.00486	0.02374		
H30	0.01197	0.84332	0.20447	0.04247							
(173k-173k(xray))^2	0.00004	0.00000	0.00000	0.00012	0.00430	0.00335	0.00008	0.00002	0.00056		
C31	0.07235	0.67236	0.21044	0.02410	0.05161	0.02764	-0.00511	-0.00197	-0.00023		
C31	0.07249	0.67243	0.21060	0.02259	0.05103	0.02676	-0.00548	-0.00188	-0.00011		
(173k-173k(xray))^2	0.00000	0.00000	0.00000	0.00000	0.00000	0.00000	0.00000	0.00000	0.00000	0.00000	0.00000
H31	0.06231	0.66729	0.14258	0.05284	0.09043	0.03264	-0.00491	0.00051	-0.00070		
H31	0.05584	0.66405	0.14231	0.04140							
(173k-173k(xray))^2	0.00004	0.00001	0.00000	0.00013	0.00818	0.00107	0.00002	0.00000	0.00000		
C32	0.11939	0.57700	0.26143	0.02168	0.03637	0.02822	-0.00774	0.00460	-0.00737		
C32	0.11939	0.57681	0.26153	0.02043	0.03554	0.02731	-0.00828	0.00371	-0.00788		
(173k-173k(xray))^2	0.00000	0.00000	0.00000	0.00000	0.00000	0.00000	0.00000	0.00000	0.00000	0.00000	0.00000

C33	0.17932	0.48145	0.24049	0.03264	0.03791	0.03597	-0.00961	0.01048	-0.01581		
C33	0.17935	0.48116	0.24057	0.03084	0.03761	0.03488	-0.01009	0.01073	-0.01645		
(173k-173k(xray))^2	0.00000	0.00000	0.00000	0.00000	0.00000	0.00000	0.00000	0.00000	0.00000	0.00000	0.00001
H33	0.17447	0.45890	0.17466	0.06015	0.07539	0.04501	-0.00743	0.01490	-0.02847		
H33	0.16943	0.45511	0.17497	0.04066							
(173k-173k(xray))^2	0.00003	0.00001	0.00000	0.00038	0.00568	0.00203	0.00006	0.00022	0.00081		
C34	0.24882	0.42169	0.30154	0.03559	0.02661	0.04637	-0.00432	0.01662	-0.01273		
C34	0.24902	0.42181	0.30163	0.03411	0.02531	0.04582	-0.00461	0.01667	-0.01306		
(173k-173k(xray))^2	0.00000	0.00000	0.00000	0.00000	0.00000	0.00000	0.00000	0.00000	0.00000	0.00000	0.00000
H34	0.29630	0.35505	0.28152	0.06398	0.04617	0.07240	0.00732	0.02776	-0.01868		
H34	0.29238	0.35032	0.28268	0.04064							
(173k-173k(xray))^2	0.00002	0.00002	0.00000	0.00054	0.00213	0.00524	0.00005	0.00077	0.00035		
C35	0.26592	0.45189	0.38966	0.03023	0.01869	0.04087	-0.00060	0.01310	-0.00095		
C35	0.26595	0.45179	0.38968	0.02895	0.01766	0.03905	-0.00106	0.01268	-0.00072		
(173k-173k(xray))^2	0.00000	0.00000	0.00000	0.00000	0.00000	0.00000	0.00000	0.00000	0.00000	0.00001	0.00001
C36	0.35492	0.43120	0.45672	0.03358	0.02299	0.04813	0.00562	0.01182	0.00954		
C36	0.35481	0.43123	0.45696	0.03311	0.02186	0.04636	0.00556	0.01233	0.00974		
(173k-173k(xray))^2	0.00000	0.00000	0.00000	0.00000	0.00000	0.00000	0.00000	0.00000	0.00000	0.00000	0.00000
H36	0.41192	0.36680	0.44866	0.05288	0.03927	0.07844	0.01795	0.01698	0.00904		
H36	0.40824	0.36186	0.45054	0.03983							
(173k-173k(xray))^2	0.00001	0.00002	0.00000	0.00017	0.00154	0.00615	0.00032	0.00029	0.00008		
C37	0.37428	0.49691	0.52942	0.03311	0.03258	0.03549	0.00429	0.00638	0.01444		
C37	0.37432	0.49692	0.52944	0.03193	0.03132	0.03494	0.00432	0.00591	0.01489		
(173k-173k(xray))^2	0.00000	0.00000	0.00000	0.00000	0.00000	0.00000	0.00000	0.00000	0.00000	0.00000	0.00000
H37	0.44633	0.48264	0.57545	0.05044	0.06375	0.05122	0.01161	-0.00165	0.01947		
H37	0.44264	0.47780	0.57846	0.03948							
(173k-173k(xray))^2	0.00001	0.00002	0.00001	0.00012	0.00406	0.00262	0.00013	0.00000	0.00038		
C38	0.30671	0.59003	0.54210	0.02993	0.03180	0.02459	-0.00061	0.00611	0.00733		
C38	0.30682	0.58999	0.54199	0.02906	0.03063	0.02312	-0.00121	0.00592	0.00740		
(173k-173k(xray))^2	0.00000	0.00000	0.00000	0.00000	0.00000	0.00000	0.00000	0.00000	0.00000	0.00000	0.00000
C39	0.32833	0.68868	0.59639	0.03568	0.04332	0.02190	-0.00518	0.00334	0.00029		
C39	0.32825	0.68883	0.59640	0.03410	0.04320	0.02096	-0.00570	0.00355	0.00077		

(173k-173k(xray))^2	0.00000	0.00000	0.00000	0.00000	0.00000	0.00000	0.00000	0.00000	0.00000	0.00000	0.00000
H39	0.39699	0.68854	0.64730	0.05532	0.07605	0.03831	-0.00375	-0.00838	-0.00033		
H39	0.39301	0.68543	0.65073	0.03970							
(173k-173k(xray))^2	0.00002	0.00001	0.00001	0.00024	0.00578	0.00147	0.00001	0.00007	0.00000		
C40	0.26890	0.78777	0.58165	0.03543	0.03865	0.02724	-0.00712	0.00813	-0.00959		
C40	0.26901	0.78763	0.58159	0.03465	0.03824	0.02653	-0.00828	0.00861	-0.00952		
(173k-173k(xray))^2	0.00000	0.00000	0.00000	0.00000	0.00000	0.00000	0.00000	0.00000	0.00000	0.00000	0.00000
H40	0.29318	0.86212	0.62143	0.06084	0.06005	0.05288	-0.01263	0.00751	-0.02728		
H40	0.28787	0.85955	0.62496	0.03939							
(173k-173k(xray))^2	0.00003	0.00001	0.00001	0.00046	0.00361	0.00280	0.00016	0.00006	0.00074		
	X	Y	Z	U11	U22	U33	U12	U13	U23	0.00007	0.00009
<delta>	-0.00004	0.00003	-0.00002	0.00136	0.00073	0.00080	0.00040	0.00002	-0.00006	0.00096	
RMS:	0.00009	0.00013	0.00009	0.00141	0.00083	0.00100	0.00054	0.00046	0.00032	0.00111	0.00085
0.6 Angstroms	N - X										
CorH(A)											
ATOM	X	Y	Z	U11	U22	U33	U12	U13	U23	sum delUii	sum Uii+uij
C1	0.41696	0.30379	0.11033	0.02205	0.01929	0.01920	0.00022	0.00406	-0.00294		
C1	0.41708	0.30379	0.11037	0.02227	0.01808	0.01895	0.00055	0.00380	-0.00344		
(173k-173k(xray))^2	0.00000	0.00000	0.00000	0.00000	0.00000	0.00000	0.00000	0.00000	0.00000	0.00000	0.00000
C2	0.43622	0.22786	0.17978	0.02160	0.02176	0.01686	0.00188	0.00327	-0.00361		
C2	0.43629	0.22777	0.17972	0.02126	0.02140	0.01619	0.00181	0.00282	-0.00390		
(173k-173k(xray))^2	0.00000	0.00000	0.00000	0.00000	0.00000	0.00000	0.00000	0.00000	0.00000	0.00000	0.00000
C3	0.33946	0.18320	0.18960	0.02356	0.02388	0.01807	0.00292	0.00702	-0.00106		
C3	0.33943	0.18315	0.18959	0.02296	0.02385	0.01713	0.00325	0.00676	-0.00185		
(173k-173k(xray))^2	0.00000	0.00000	0.00000	0.00000	0.00000	0.00000	0.00000	0.00000	0.00000	0.00000	0.00000
C4	0.26032	0.23188	0.12661	0.02033	0.02479	0.02264	0.00448	0.00639	-0.00194		
C4	0.26035	0.23179	0.12671	0.02004	0.02376	0.02237	0.00470	0.00672	-0.00254		
(173k-173k(xray))^2	0.00000	0.00000	0.00000	0.00000	0.00000	0.00000	0.00000	0.00000	0.00000	0.00000	0.00000
C5	0.30840	0.30635	0.07766	0.02266	0.01989	0.02056	0.00431	0.00315	-0.00104		
C5	0.30844	0.30637	0.07771	0.02256	0.01917	0.02071	0.00449	0.00363	-0.00153		
(173k-173k(xray))^2	0.00000	0.00000	0.00000	0.00000	0.00000	0.00000	0.00000	0.00000	0.00000	0.00000	0.00000

C6	0.48958	0.32503	0.06193	0.02658	0.02062	0.02382	-0.00387	0.00744	-0.00397		
C6	0.48957	0.32506	0.06198	0.02600	0.01984	0.02335	-0.00364	0.00699	-0.00369		
(173k-173k(xray))^2	0.00000	0.00000	0.00000	0.00000	0.00000	0.00000	0.00000	0.00000	0.00000	0.00000	0.00000
C7	0.59245	0.28034	0.09607	0.02416	0.02804	0.03091	-0.00395	0.00946	-0.00713		
C7	0.59247	0.28009	0.09617	0.02282	0.02736	0.03044	-0.00433	0.00875	-0.00787		
(173k-173k(xray))^2	0.00000	0.00000	0.00000	0.00000	0.00000	0.00000	0.00000	0.00000	0.00000	0.00000	0.00000
H7	0.65585	0.29955	0.06493	0.03807	0.05785	0.05925	-0.00739	0.02378	-0.00281		
H7	0.65699	0.30518	0.06746	0.03169							
(173k-173k(xray))^2	0.00000	0.00003	0.00001	0.00004	0.00335	0.00351	0.00005	0.00057	0.00001		
C8	0.61127	0.20629	0.16420	0.02023	0.02987	0.02960	0.00113	0.00289	-0.00715		
C8	0.61135	0.20623	0.16419	0.01938	0.02908	0.02924	0.00075	0.00264	-0.00798		
(173k-173k(xray))^2	0.00000	0.00000	0.00000	0.00000	0.00000	0.00000	0.00000	0.00000	0.00000	0.00000	0.00000
H8	0.68887	0.16997	0.18384	0.02688	0.05767	0.05798	0.01008	0.00553	-0.00358		
H8	0.69037	0.17509	0.18790	0.03152							
(173k-173k(xray))^2	0.00000	0.00003	0.00002	0.00002	0.00333	0.00336	0.00010	0.00003	0.00001		
C9	0.52907	0.16924	0.20466	0.02140	0.02512	0.02023	0.00261	0.00061	-0.00428		
C9	0.52909	0.16925	0.20465	0.02184	0.02527	0.01852	0.00262	-0.00020	-0.00482		
(173k-173k(xray))^2	0.00000	0.00000	0.00000	0.00000	0.00000	0.00000	0.00000	0.00000	0.00000	0.00000	0.00000
C10	0.52203	0.06672	0.25299	0.02942	0.02976	0.02019	0.00618	-0.00141	0.00068		
C10	0.52188	0.06666	0.25303	0.02994	0.02962	0.01910	0.00674	-0.00126	-0.00012		
(173k-173k(xray))^2	0.00000	0.00000	0.00000	0.00000	0.00000	0.00000	0.00000	0.00000	0.00000	0.00000	0.00000
H10	0.59178	0.01718	0.27773	0.04372	0.04847	0.04710	0.01559	-0.00436	0.00729		
H10	0.59325	0.02247	0.28297	0.03260							
(173k-173k(xray))^2	0.00000	0.00003	0.00003	0.00012	0.00235	0.00222	0.00024	0.00002	0.00005		
C11	0.42691	0.02287	0.26241	0.03732	0.03000	0.01875	0.00427	0.00520	0.00498		
C11	0.42698	0.02290	0.26243	0.03662	0.02905	0.01825	0.00480	0.00492	0.00435		
(173k-173k(xray))^2	0.00000	0.00000	0.00000	0.00000	0.00000	0.00000	0.00000	0.00000	0.00000	0.00000	0.00000
H11	0.42556	-0.05869	0.29422	0.06331	0.04405	0.04315	0.00616	0.00817	0.01799		
H11	0.42585	-0.05498	0.29930	0.03372							
(173k-173k(xray))^2	0.00000	0.00001	0.00003	0.00088	0.00194	0.00186	0.00004	0.00007	0.00032		
C12	0.32951	0.07734	0.22483	0.02984	0.02800	0.01988	0.00204	0.01025	0.00146		
C12	0.32958	0.07724	0.22494	0.02970	0.02777	0.01894	0.00208	0.01029	0.00118		

(173k-173k(xray))^2	0.00000	0.00000	0.00000	0.00000	0.00000	0.00000	0.00000	0.00000	0.00000	0.00000	0.00000
C13	0.22606	0.02884	0.20398	0.03111	0.03466	0.03446	-0.00179	0.01785	0.00321		
C13	0.22606	0.02879	0.20405	0.03104	0.03327	0.03350	-0.00178	0.01788	0.00212		
(173k-173k(xray))^2	0.00000	0.00000	0.00000	0.00000	0.00000	0.00000	0.00000	0.00000	0.00000	0.00000	0.00000
H13	0.21049	-0.05194	0.23215	0.05759	0.04825	0.06716	-0.00738	0.02693	0.01609		
H13	0.20846	-0.04716	0.23760	0.03717							
(173k-173k(xray))^2	0.00000	0.00002	0.00003	0.00042	0.00233	0.00451	0.00005	0.00073	0.00026		
C14	0.14841	0.07669	0.14233	0.02309	0.03720	0.04326	-0.00152	0.01559	-0.00117		
C14	0.14861	0.07658	0.14239	0.02222	0.03672	0.04154	-0.00121	0.01543	-0.00101		
(173k-173k(xray))^2	0.00000	0.00000	0.00000	0.00000	0.00000	0.00000	0.00000	0.00000	0.00000	0.00000	0.00000
H14	0.07440	0.03204	0.12432	0.03283	0.06261	0.07797	-0.01170	0.01688	0.00218		
H14	0.07163	0.03710	0.12864	0.03865							
(173k-173k(xray))^2	0.00001	0.00003	0.00002	0.00003	0.00392	0.00608	0.00014	0.00028	0.00000		
C15	0.16696	0.17738	0.09565	0.01796	0.03168	0.03433	0.00380	0.00804	-0.00196		
C15	0.16700	0.17728	0.09581	0.01789	0.03143	0.03249	0.00421	0.00806	-0.00271		
(173k-173k(xray))^2	0.00000	0.00000	0.00000	0.00000	0.00000	0.00000	0.00000	0.00000	0.00000	0.00000	0.00000
C16	0.11406	0.21543	0.01329	0.01849	0.03971	0.03838	0.00643	0.00079	-0.00343		
C16	0.11415	0.21536	0.01328	0.01815	0.03837	0.03763	0.00641	0.00083	-0.00327		
(173k-173k(xray))^2	0.00000	0.00000	0.00000	0.00000	0.00000	0.00000	0.00000	0.00000	0.00000	0.00000	0.00000
H16	0.03818	0.18021	-0.01440	0.02686	0.07191	0.06582	-0.00482	-0.00327	-0.00215		
H16	0.03469	0.18648	-0.01173	0.03855							
(173k-173k(xray))^2	0.00001	0.00004	0.00001	0.00014	0.00517	0.00433	0.00002	0.00001	0.00000		
C17	0.16169	0.28782	-0.03511	0.02601	0.03479	0.03071	0.00925	-0.00299	0.00104		
C17	0.16171	0.28767	-0.03503	0.02536	0.03311	0.03071	0.00936	-0.00346	0.00033		
(173k-173k(xray))^2	0.00000	0.00000	0.00000	0.00000	0.00000	0.00000	0.00000	0.00000	0.00000	0.00000	0.00000
H17	0.12238	0.30556	-0.09964	0.04826	0.06540	0.04213	0.00987	-0.01269	0.00718		
H17	0.11873	0.31338	-0.09716	0.03733							
(173k-173k(xray))^2	0.00001	0.00006	0.00001	0.00012	0.00428	0.00177	0.00010	0.00016	0.00005		
C18	0.26622	0.32981	-0.00557	0.02911	0.02302	0.02357	0.00620	0.00143	0.00186		
C18	0.26633	0.32987	-0.00552	0.02795	0.02244	0.02341	0.00677	0.00074	0.00158		
(173k-173k(xray))^2	0.00000	0.00000	0.00000	0.00000	0.00000	0.00000	0.00000	0.00000	0.00000	0.00000	0.00000
C19	0.33981	0.37107	-0.05324	0.04066	0.02613	0.02296	0.00156	0.00427	0.00535		

C19	0.33994	0.37103	-0.05322	0.04076	0.02423	0.02290	0.00255	0.00438	0.00502		
(173k-173k(xray))^2	0.00000	0.00000	0.00000	0.00000	0.00000	0.00000	0.00000	0.00000	0.00000	0.00000	0.00000
H19	0.31190	0.39729	-0.11844	0.07012	0.05824	0.03240	0.00545	0.00505	0.01616		
H19	0.31094	0.40492	-0.11630	0.03557							
(173k-173k(xray))^2	0.00000	0.00006	0.00000	0.00119	0.00339	0.00105	0.00003	0.00003	0.00026		
C20	0.44637	0.36894	-0.02119	0.03774	0.02390	0.02646	-0.00394	0.01051	0.00194		
C20	0.44644	0.36871	-0.02114	0.03849	0.02234	0.02529	-0.00408	0.01033	0.00167		
(173k-173k(xray))^2	0.00000	0.00000	0.00000	0.00000	0.00000	0.00000	0.00000	0.00000	0.00000	0.00000	0.00000
H20	0.49808	0.39312	-0.06238	0.05940	0.05528	0.04498	-0.00882	0.02276	0.00830		
H20	0.49896	0.40065	-0.05964	0.03381							
(173k-173k(xray))^2	0.00000	0.00006	0.00001	0.00065	0.00306	0.00202	0.00008	0.00052	0.00007		
	X	Y	Z	U11	U22	U33	U12	U13	U23	0.00004	0.00006
<delta>	-0.00005	0.00007	-0.00004	0.00030	0.00080	0.00071	-0.00019	0.00019	0.00047	0.00060	
RMS:	0.00009	0.00010	0.00007	0.00062	0.00098	0.00091	0.00038	0.00039	0.00059	0.00085	0.00068
0.6 Angstroms	N - X										
CorH(B)											
ATOM	X	Y	Z	U11	U22	U33	U12	U13	U23	sum delUii	sum Uii+uij
C21	0.15535	0.69770	0.46696	0.02115	0.02296	0.02651	-0.00210	0.00860	-0.00265		
C21	0.15538	0.69758	0.46681	0.02014	0.02247	0.02640	-0.00283	0.00884	-0.00285		
(173k-173k(xray))^2	0.00000	0.00000	0.00000	0.00000	0.00000	0.00000	0.00000	0.00000	0.00000	0.00000	0.00000
C22	0.09999	0.69455	0.38234	0.01682	0.02295	0.02953	-0.00164	0.00519	-0.00204		
C22	0.10000	0.69465	0.38229	0.01583	0.02317	0.02883	-0.00208	0.00562	-0.00196		
(173k-173k(xray))^2	0.00000	0.00000	0.00000	0.00000	0.00000	0.00000	0.00000	0.00000	0.00000	0.00000	0.00000
C23	0.12433	0.59040	0.34641	0.01942	0.02407	0.02734	-0.00499	0.00671	-0.00459		
C23	0.12434	0.59028	0.34644	0.01787	0.02359	0.02713	-0.00527	0.00590	-0.00410		
(173k-173k(xray))^2	0.00000	0.00000	0.00000	0.00000	0.00000	0.00000	0.00000	0.00000	0.00000	0.00000	0.00000
C24	0.19523	0.52941	0.40863	0.02413	0.01830	0.02955	-0.00283	0.00935	-0.00062		
C24	0.19526	0.52953	0.40865	0.02331	0.01841	0.02922	-0.00338	0.00957	-0.00049		
(173k-173k(xray))^2	0.00000	0.00000	0.00000	0.00000	0.00000	0.00000	0.00000	0.00000	0.00000	0.00000	0.00000
C25	0.21496	0.59609	0.48277	0.02470	0.02283	0.02511	-0.00225	0.00840	0.00209		
C25	0.21499	0.59615	0.48276	0.02399	0.02202	0.02390	-0.00266	0.00854	0.00212		

(173k-173k(xray))^2	0.00000	0.00000	0.00000	0.00000	0.00000	0.00000	0.00000	0.00000	0.00000	0.00000	0.00000
C26	0.18275	0.79825	0.51023	0.02655	0.02591	0.03205	-0.00358	0.01018	-0.00779		
C26	0.18283	0.79827	0.51026	0.02597	0.02603	0.03152	-0.00355	0.01098	-0.00751		
(173k-173k(xray))^2	0.00000	0.00000	0.00000	0.00000	0.00000	0.00000	0.00000	0.00000	0.00000	0.00000	0.00000
C27	0.13577	0.89965	0.46732	0.03238	0.02325	0.05012	-0.00048	0.01202	-0.00854		
C27	0.13590	0.89959	0.46727	0.03113	0.02307	0.05023	-0.00028	0.01226	-0.00850		
(173k-173k(xray))^2	0.00000	0.00000	0.00000	0.00000	0.00000	0.00000	0.00000	0.00000	0.00000	0.00000	0.00000
H27	0.14869	0.98235	0.49841	0.07116	0.03111	0.07967	-0.00200	0.01603	-0.01930		
H27	0.14283	0.98083	0.50117	0.04112							
(173k-173k(xray))^2	0.00003	0.00000	0.00001	0.00090	0.00097	0.00635	0.00000	0.00026	0.00037		
C28	0.08226	0.89669	0.38418	0.02871	0.02411	0.05446	0.00486	0.00639	0.00095		
C28	0.08231	0.89675	0.38423	0.02790	0.02407	0.05391	0.00508	0.00646	0.00151		
(173k-173k(xray))^2	0.00000	0.00000	0.00000	0.00000	0.00000	0.00000	0.00000	0.00000	0.00000	0.00000	0.00000
H28	0.05553	0.97714	0.35326	0.06075	0.03590	0.08443	0.01560	0.00403	0.00938		
H28	0.04919	0.97601	0.35450	0.04274							
(173k-173k(xray))^2	0.00004	0.00000	0.00000	0.00032	0.00129	0.00713	0.00024	0.00002	0.00009		
C29	0.06905	0.79195	0.33591	0.01949	0.02828	0.03741	0.00192	0.00234	0.00246		
C29	0.06900	0.79187	0.33583	0.01807	0.02804	0.03807	0.00171	0.00219	0.00275		
(173k-173k(xray))^2	0.00000	0.00000	0.00000	0.00000	0.00000	0.00000	0.00000	0.00000	0.00000	0.00000	0.00000
C30	0.04805	0.77461	0.24586	0.02368	0.04412	0.03526	0.00147	-0.00262	0.00891		
C30	0.04803	0.77438	0.24583	0.02224	0.04339	0.03647	0.00042	-0.00303	0.00891		
(173k-173k(xray))^2	0.00000	0.00000	0.00000	0.00000	0.00000	0.00000	0.00000	0.00000	0.00000	0.00000	0.00001
H30	0.01812	0.84539	0.20419	0.05348	0.06529	0.05698	0.00943	-0.00500	0.02401		
H30	0.01197	0.84332	0.20447	0.04247							
(173k-173k(xray))^2	0.00004	0.00000	0.00000	0.00012	0.00426	0.00325	0.00009	0.00003	0.00058		
C31	0.07232	0.67230	0.21044	0.02390	0.05125	0.02709	-0.00543	-0.00200	-0.00023		
C31	0.07249	0.67243	0.21060	0.02259	0.05103	0.02676	-0.00548	-0.00188	-0.00011		
(173k-173k(xray))^2	0.00000	0.00000	0.00000	0.00000	0.00000	0.00000	0.00000	0.00000	0.00000	0.00000	0.00000
H31	0.06223	0.66725	0.14263	0.05257	0.08968	0.03232	-0.00466	0.00086	-0.00045		
H31	0.05584	0.66405	0.14231	0.04140							
(173k-173k(xray))^2	0.00004	0.00001	0.00000	0.00012	0.00804	0.00104	0.00002	0.00000	0.00000		
C32	0.11938	0.57699	0.26143	0.02156	0.03573	0.02766	-0.00786	0.00444	-0.00745		



C32	0.11939	0.57681	0.26153	0.02043	0.03554	0.02731	-0.00828	0.00371	-0.00788		
(173k-173k(xray))^2	0.00000	0.00000	0.00000	0.00000	0.00000	0.00000	0.00000	0.00000	0.00000	0.00000	0.00000
C33	0.17932	0.48146	0.24049	0.03226	0.03750	0.03531	-0.00967	0.01064	-0.01594		
C33	0.17935	0.48116	0.24057	0.03084	0.03761	0.03488	-0.01009	0.01073	-0.01645		
(173k-173k(xray))^2	0.00000	0.00000	0.00000	0.00000	0.00000	0.00000	0.00000	0.00000	0.00000	0.00000	0.00000
H33	0.17449	0.45892	0.17477	0.06017	0.07478	0.04401	-0.00736	0.01492	-0.02864		
H33	0.16943	0.45511	0.17497	0.04066							
(173k-173k(xray))^2	0.00003	0.00001	0.00000	0.00038	0.00559	0.00194	0.00005	0.00022	0.00082		
C34	0.24886	0.42169	0.30158	0.03530	0.02636	0.04586	-0.00409	0.01657	-0.01297		
C34	0.24902	0.42181	0.30163	0.03411	0.02531	0.04582	-0.00461	0.01667	-0.01306		
(173k-173k(xray))^2	0.00000	0.00000	0.00000	0.00000	0.00000	0.00000	0.00000	0.00000	0.00000	0.00000	0.00000
H34	0.29617	0.35516	0.28152	0.06387	0.04600	0.07142	0.00685	0.02764	-0.01883		
H34	0.29238	0.35032	0.28268	0.04064							
(173k-173k(xray))^2	0.00001	0.00002	0.00000	0.00054	0.00212	0.00510	0.00005	0.00076	0.00035		
C35	0.26591	0.45191	0.38962	0.02974	0.01821	0.04015	-0.00073	0.01286	-0.00094		
C35	0.26595	0.45179	0.38968	0.02895	0.01766	0.03905	-0.00106	0.01268	-0.00072		
(173k-173k(xray))^2	0.00000	0.00000	0.00000	0.00000	0.00000	0.00000	0.00000	0.00000	0.00000	0.00000	0.00000
C36	0.35490	0.43118	0.45670	0.03341	0.02249	0.04809	0.00577	0.01207	0.00942		
C36	0.35481	0.43123	0.45696	0.03311	0.02186	0.04636	0.00556	0.01233	0.00974		
(173k-173k(xray))^2	0.00000	0.00000	0.00000	0.00000	0.00000	0.00000	0.00000	0.00000	0.00000	0.00000	0.00000
H36	0.41186	0.36687	0.44869	0.05244	0.03915	0.07795	0.01767	0.01670	0.00909		
H36	0.40824	0.36186	0.45054	0.03983							
(173k-173k(xray))^2	0.00001	0.00003	0.00000	0.00016	0.00153	0.00608	0.00031	0.00028	0.00008		
C37	0.37429	0.49687	0.52943	0.03268	0.03222	0.03532	0.00445	0.00611	0.01466		
C37	0.37432	0.49692	0.52944	0.03193	0.03132	0.03494	0.00432	0.00591	0.01489		
(173k-173k(xray))^2	0.00000	0.00000	0.00000	0.00000	0.00000	0.00000	0.00000	0.00000	0.00000	0.00000	0.00000
H37	0.44629	0.48261	0.57544	0.05051	0.06310	0.05069	0.01220	-0.00160	0.02019		
H37	0.44264	0.47780	0.57846	0.03948							
(173k-173k(xray))^2	0.00001	0.00002	0.00001	0.00012	0.00398	0.00257	0.00015	0.00000	0.00041		
C38	0.30677	0.59000	0.54210	0.02939	0.03151	0.02409	-0.00056	0.00591	0.00736		
C38	0.30682	0.58999	0.54199	0.02906	0.03063	0.02312	-0.00121	0.00592	0.00740		
(173k-173k(xray))^2	0.00000	0.00000	0.00000	0.00000	0.00000	0.00000	0.00000	0.00000	0.00000	0.00000	0.00000

C39	0.32837	0.68865	0.59637	0.03526	0.04296	0.02137	-0.00509	0.00309	0.00047		
C39	0.32825	0.68883	0.59640	0.03410	0.04320	0.02096	-0.00570	0.00355	0.00077		
(173k-173k(xray))^2	0.00000	0.00000	0.00000	0.00000	0.00000	0.00000	0.00000	0.00000	0.00000	0.00000	0.00000
H39	0.39693	0.68855	0.64729	0.05488	0.07468	0.03869	-0.00340	-0.00833	-0.00016		
H39	0.39301	0.68543	0.65073	0.03970							
(173k-173k(xray))^2	0.00002	0.00001	0.00001	0.00023	0.00558	0.00150	0.00001	0.00007	0.00000		
C40	0.26890	0.78777	0.58165	0.03529	0.03814	0.02695	-0.00723	0.00785	-0.00969		
C40	0.26901	0.78763	0.58159	0.03465	0.03824	0.02653	-0.00828	0.00861	-0.00952		
(173k-173k(xray))^2	0.00000	0.00000	0.00000	0.00000	0.00000	0.00000	0.00000	0.00000	0.00000	0.00000	0.00000
H40	0.29309	0.86200	0.62138	0.05996	0.05980	0.05260	-0.01234	0.00665	-0.02676		
H40	0.28787	0.85955	0.62496	0.03939							
(173k-173k(xray))^2	0.00003	0.00001	0.00001	0.00042	0.00358	0.00277	0.00015	0.00004	0.00072		
	X	Y	Z	U11	U22	U33	U12	U13	U23	0.00004	0.00005
<delta>	-0.00003	0.00002	-0.00002	0.00098	0.00032	0.00039	0.00038	-0.00007	-0.00010	0.00057	
RMS:	0.00008	0.00013	0.00009	0.00104	0.00052	0.00073	0.00051	0.00041	0.00028	0.00079	0.00063
0.7 Angstroms	N - X										
CorH(A)											
ATOM	X	Y	Z	U11	U22	U33	U12	U13	U23	sum delUii	sum Uii+uij
C1	0.41690	0.30378	0.11029	0.02244	0.01914	0.01917	0.00016	0.00417	-0.00273		
C1	0.41708	0.30379	0.11037	0.02227	0.01808	0.01895	0.00055	0.00380	-0.00344		
(173k-173k(xray))^2	0.00000	0.00000	0.00000	0.00000	0.00000	0.00000	0.00000	0.00000	0.00000	0.00000	0.00000
C2	0.43617	0.22785	0.17976	0.02119	0.02167	0.01756	0.00196	0.00321	-0.00371		
C2	0.43629	0.22777	0.17972	0.02126	0.02140	0.01619	0.00181	0.00282	-0.00390		
(173k-173k(xray))^2	0.00000	0.00000	0.00000	0.00000	0.00000	0.00000	0.00000	0.00000	0.00000	0.00000	0.00000
C3	0.33946	0.18316	0.18961	0.02366	0.02415	0.01805	0.00289	0.00733	-0.00105		
C3	0.33943	0.18315	0.18959	0.02296	0.02385	0.01713	0.00325	0.00676	-0.00185		
(173k-173k(xray))^2	0.00000	0.00000	0.00000	0.00000	0.00000	0.00000	0.00000	0.00000	0.00000	0.00000	0.00000
C4	0.26028	0.23181	0.12664	0.02088	0.02466	0.02240	0.00444	0.00645	-0.00219		
C4	0.26035	0.23179	0.12671	0.02004	0.02376	0.02237	0.00470	0.00672	-0.00254		
(173k-173k(xray))^2	0.00000	0.00000	0.00000	0.00000	0.00000	0.00000	0.00000	0.00000	0.00000	0.00000	0.00000
C5	0.30840	0.30633	0.07765	0.02295	0.01959	0.02106	0.00449	0.00366	-0.00100		

C5	0.30844	0.30637	0.07771	0.02256	0.01917	0.02071	0.00449	0.00363	-0.00153		
(173k-173k(xray))^2	0.00000	0.00000	0.00000	0.00000	0.00000	0.00000	0.00000	0.00000	0.00000	0.00000	0.00000
C6	0.48948	0.32510	0.06190	0.02653	0.02118	0.02350	-0.00383	0.00725	-0.00356		
C6	0.48957	0.32506	0.06198	0.02600	0.01984	0.02335	-0.00364	0.00699	-0.00369		
(173k-173k(xray))^2	0.00000	0.00000	0.00000	0.00000	0.00000	0.00000	0.00000	0.00000	0.00000	0.00000	0.00000
C7	0.59233	0.28040	0.09602	0.02422	0.02786	0.03105	-0.00374	0.00947	-0.00738		
C7	0.59247	0.28009	0.09617	0.02282	0.02736	0.03044	-0.00433	0.00875	-0.00787		
(173k-173k(xray))^2	0.00000	0.00000	0.00000	0.00000	0.00000	0.00000	0.00000	0.00000	0.00000	0.00000	0.00000
H7	0.65559	0.29944	0.06492	0.03865	0.05769	0.06074	-0.00771	0.02419	-0.00285		
H7	0.65699	0.30518	0.06746	0.03169							
(173k-173k(xray))^2	0.00000	0.00003	0.00001	0.00005	0.00333	0.00369	0.00006	0.00059	0.00001		
C8	0.61118	0.20623	0.16414	0.02027	0.02995	0.02958	0.00145	0.00273	-0.00728		
C8	0.61135	0.20623	0.16419	0.01938	0.02908	0.02924	0.00075	0.00264	-0.00798		
(173k-173k(xray))^2	0.00000	0.00000	0.00000	0.00000	0.00000	0.00000	0.00000	0.00000	0.00000	0.00000	0.00000
H8	0.68874	0.17005	0.18384	0.02677	0.05849	0.05833	0.01006	0.00514	-0.00376		
H8	0.69037	0.17509	0.18790	0.03152							
(173k-173k(xray))^2	0.00000	0.00003	0.00002	0.00002	0.00342	0.00340	0.00010	0.00003	0.00001		
C9	0.52908	0.16932	0.20473	0.02154	0.02513	0.02060	0.00257	0.00053	-0.00481		
C9	0.52909	0.16925	0.20465	0.02184	0.02527	0.01852	0.00262	-0.00020	-0.00482		
(173k-173k(xray))^2	0.00000	0.00000	0.00000	0.00000	0.00000	0.00000	0.00000	0.00000	0.00000	0.00000	0.00000
C10	0.52198	0.06676	0.25295	0.02929	0.03020	0.02038	0.00592	-0.00129	0.00056		
C10	0.52188	0.06666	0.25303	0.02994	0.02962	0.01910	0.00674	-0.00126	-0.00012		
(173k-173k(xray))^2	0.00000	0.00000	0.00000	0.00000	0.00000	0.00000	0.00000	0.00000	0.00000	0.00000	0.00000
H10	0.59178	0.01722	0.27769	0.04350	0.04875	0.04725	0.01506	-0.00343	0.00616		
H10	0.59325	0.02247	0.28297	0.03260							
(173k-173k(xray))^2	0.00000	0.00003	0.00003	0.00012	0.00238	0.00223	0.00023	0.00001	0.00004		
C11	0.42685	0.02284	0.26239	0.03738	0.03015	0.01940	0.00414	0.00525	0.00511		
C11	0.42698	0.02290	0.26243	0.03662	0.02905	0.01825	0.00480	0.00492	0.00435		
(173k-173k(xray))^2	0.00000	0.00000	0.00000	0.00000	0.00000	0.00000	0.00000	0.00000	0.00000	0.00000	0.00000
H11	0.42556	-0.05869	0.29429	0.06211	0.04511	0.04348	0.00655	0.00946	0.01824		
H11	0.42585	-0.05498	0.29930	0.03372							
(173k-173k(xray))^2	0.00000	0.00001	0.00003	0.00081	0.00203	0.00189	0.00004	0.00009	0.00033		

C12	0.32954	0.07738	0.22485	0.02972	0.02824	0.01973	0.00181	0.01013	0.00161		
C12	0.32958	0.07724	0.22494	0.02970	0.02777	0.01894	0.00208	0.01029	0.00118		
(173k-173k(xray))^2	0.00000	0.00000	0.00000	0.00000	0.00000	0.00000	0.00000	0.00000	0.00000	0.00000	0.00000
C13	0.22611	0.02878	0.20401	0.03144	0.03456	0.03441	-0.00180	0.01807	0.00321		
C13	0.22606	0.02879	0.20405	0.03104	0.03327	0.03350	-0.00178	0.01788	0.00212		
(173k-173k(xray))^2	0.00000	0.00000	0.00000	0.00000	0.00000	0.00000	0.00000	0.00000	0.00000	0.00000	0.00000
H13	0.21054	-0.05205	0.23212	0.05709	0.04795	0.06606	-0.00788	0.02665	0.01611		
H13	0.20846	-0.04716	0.23760	0.03717							
(173k-173k(xray))^2	0.00000	0.00002	0.00003	0.00040	0.00230	0.00436	0.00006	0.00071	0.00026		
C14	0.14846	0.07666	0.14230	0.02287	0.03736	0.04340	-0.00135	0.01555	-0.00160		
C14	0.14861	0.07658	0.14239	0.02222	0.03672	0.04154	-0.00121	0.01543	-0.00101		
(173k-173k(xray))^2	0.00000	0.00000	0.00000	0.00000	0.00000	0.00000	0.00000	0.00000	0.00000	0.00000	0.00000
H14	0.07454	0.03213	0.12457	0.03186	0.06273	0.07932	-0.01101	0.01724	0.00313		
H14	0.07163	0.03710	0.12864	0.03865							
(173k-173k(xray))^2	0.00001	0.00002	0.00002	0.00005	0.00394	0.00629	0.00012	0.00030	0.00001		
C15	0.16694	0.17734	0.09559	0.01797	0.03230	0.03367	0.00378	0.00801	-0.00263		
C15	0.16700	0.17728	0.09581	0.01789	0.03143	0.03249	0.00421	0.00806	-0.00271		
(173k-173k(xray))^2	0.00000	0.00000	0.00000	0.00000	0.00000	0.00000	0.00000	0.00000	0.00000	0.00000	0.00000
C16	0.11409	0.21535	0.01326	0.01912	0.03973	0.03855	0.00678	0.00123	-0.00306		
C16	0.11415	0.21536	0.01328	0.01815	0.03837	0.03763	0.00641	0.00083	-0.00327		
(173k-173k(xray))^2	0.00000	0.00000	0.00000	0.00000	0.00000	0.00000	0.00000	0.00000	0.00000	0.00000	0.00000
H16	0.03823	0.18024	-0.01448	0.02729	0.07184	0.06612	-0.00423	-0.00245	-0.00208		
H16	0.03469	0.18648	-0.01173	0.03855							
(173k-173k(xray))^2	0.00001	0.00004	0.00001	0.00013	0.00516	0.00437	0.00002	0.00001	0.00000		
C17	0.16158	0.28776	-0.03513	0.02550	0.03514	0.03078	0.00937	-0.00320	0.00100		
C17	0.16171	0.28767	-0.03503	0.02536	0.03311	0.03071	0.00936	-0.00346	0.00033		
(173k-173k(xray))^2	0.00000	0.00000	0.00000	0.00000	0.00000	0.00000	0.00000	0.00000	0.00000	0.00000	0.00000
H17	0.12242	0.30566	-0.09963	0.04846	0.06634	0.04191	0.01014	-0.01260	0.00731		
H17	0.11873	0.31338	-0.09716	0.03733							
(173k-173k(xray))^2	0.00001	0.00006	0.00001	0.00012	0.00440	0.00176	0.00010	0.00016	0.00005		
C18	0.26617	0.32974	-0.00557	0.02843	0.02327	0.02437	0.00647	0.00139	0.00192		
C18	0.26633	0.32987	-0.00552	0.02795	0.02244	0.02341	0.00677	0.00074	0.00158		

(173k-173k(xray))^2	0.00000	0.00000	0.00000	0.00000	0.00000	0.00000	0.00000	0.00000	0.00000	0.00000	0.00000
C19	0.33978	0.37099	-0.05321	0.04075	0.02646	0.02314	0.00175	0.00443	0.00542		
C19	0.33994	0.37103	-0.05322	0.04076	0.02423	0.02290	0.00255	0.00438	0.00502		
(173k-173k(xray))^2	0.00000	0.00000	0.00000	0.00000	0.00000	0.00000	0.00000	0.00000	0.00000	0.00001	0.00001
H19	0.31193	0.39720	-0.11836	0.07012	0.05804	0.03162	0.00536	0.00488	0.01640		
H19	0.31094	0.40492	-0.11630	0.03557							
(173k-173k(xray))^2	0.00000	0.00006	0.00000	0.00119	0.00337	0.00100	0.00003	0.00002	0.00027		
C20	0.44632	0.36889	-0.02120	0.03829	0.02396	0.02632	-0.00411	0.01064	0.00205		
C20	0.44644	0.36871	-0.02114	0.03849	0.02234	0.02529	-0.00408	0.01033	0.00167		
(173k-173k(xray))^2	0.00000	0.00000	0.00000	0.00000	0.00000	0.00000	0.00000	0.00000	0.00000	0.00000	0.00000
H20	0.49803	0.39304	-0.06226	0.06049	0.05570	0.04429	-0.00910	0.02354	0.00889		
H20	0.49896	0.40065	-0.05964	0.03381							
(173k-173k(xray))^2	0.00000	0.00006	0.00001	0.00071	0.00310	0.00196	0.00008	0.00055	0.00008		
	X	Y	Z	U11	U22	U33	U12	U13	U23	0.00005	0.00006
<delta>	-0.00008	0.00004	-0.00006	0.00036	0.00093	0.00082	-0.00015	0.00025	0.00042	0.00070	
RMS:	0.00011	0.00010	0.00009	0.00061	0.00109	0.00100	0.00042	0.00037	0.00055	0.00092	0.00073
0.7 Angstroms											
N - X											
CorH(B)											
ATOM	X	Y	Z	U11	U22	U33	U12	U13	U23	sum delUii	sum Uii+uij
C21	0.15536	0.69765	0.46694	0.02110	0.02311	0.02672	-0.00243	0.00866	-0.00265		
C21	0.15538	0.69758	0.46681	0.02014	0.02247	0.02640	-0.00283	0.00884	-0.00285		
(173k-173k(xray))^2	0.00000	0.00000	0.00000	0.00000	0.00000	0.00000	0.00000	0.00000	0.00000	0.00000	0.00000
C22	0.09997	0.69455	0.38233	0.01661	0.02341	0.02915	-0.00147	0.00531	-0.00202		
C22	0.10000	0.69465	0.38229	0.01583	0.02317	0.02883	-0.00208	0.00562	-0.00196		
(173k-173k(xray))^2	0.00000	0.00000	0.00000	0.00000	0.00000	0.00000	0.00000	0.00000	0.00000	0.00000	0.00000
C23	0.12431	0.59045	0.34633	0.01944	0.02464	0.02742	-0.00523	0.00675	-0.00449		
C23	0.12434	0.59028	0.34644	0.01787	0.02359	0.02713	-0.00527	0.00590	-0.00410		
(173k-173k(xray))^2	0.00000	0.00000	0.00000	0.00000	0.00000	0.00000	0.00000	0.00000	0.00000	0.00000	0.00000
C24	0.19521	0.52939	0.40858	0.02398	0.01869	0.02971	-0.00274	0.00935	-0.00043		
C24	0.19526	0.52953	0.40865	0.02331	0.01841	0.02922	-0.00338	0.00957	-0.00049		
(173k-173k(xray))^2	0.00000	0.00000	0.00000	0.00000	0.00000	0.00000	0.00000	0.00000	0.00000	0.00000	0.00000

C25	0.21499	0.59608	0.48278	0.02445	0.02304	0.02516	-0.00241	0.00848	0.00222		
C25	0.21499	0.59615	0.48276	0.02399	0.02202	0.02390	-0.00266	0.00854	0.00212		
(173k-173k(xray))^2	0.00000	0.00000	0.00000	0.00000	0.00000	0.00000	0.00000	0.00000	0.00000	0.00000	0.00000
C26	0.18276	0.79817	0.51022	0.02624	0.02643	0.03178	-0.00358	0.01021	-0.00783		
C26	0.18283	0.79827	0.51026	0.02597	0.02603	0.03152	-0.00355	0.01098	-0.00751		
(173k-173k(xray))^2	0.00000	0.00000	0.00000	0.00000	0.00000	0.00000	0.00000	0.00000	0.00000	0.00000	0.00000
C27	0.13584	0.89967	0.46735	0.03276	0.02349	0.04978	-0.00020	0.01201	-0.00842		
C27	0.13590	0.89959	0.46727	0.03113	0.02307	0.05023	-0.00028	0.01226	-0.00850		
(173k-173k(xray))^2	0.00000	0.00000	0.00000	0.00000	0.00000	0.00000	0.00000	0.00000	0.00000	0.00000	0.00000
H27	0.14868	0.98235	0.49850	0.06992	0.03192	0.07999	-0.00252	0.01640	-0.01961		
H27	0.14283	0.98083	0.50117	0.04112							
(173k-173k(xray))^2	0.00003	0.00000	0.00001	0.00083	0.00102	0.00640	0.00001	0.00027	0.00038		
C28	0.08230	0.89668	0.38420	0.02892	0.02396	0.05433	0.00509	0.00628	0.00098		
C28	0.08231	0.89675	0.38423	0.02790	0.02407	0.05391	0.00508	0.00646	0.00151		
(173k-173k(xray))^2	0.00000	0.00000	0.00000	0.00000	0.00000	0.00000	0.00000	0.00000	0.00000	0.00000	0.00000
H28	0.05567	0.97717	0.35332	0.06055	0.03558	0.08534	0.01587	0.00406	0.01056		
H28	0.04919	0.97601	0.35450	0.04274							
(173k-173k(xray))^2	0.00004	0.00000	0.00000	0.00032	0.00127	0.00728	0.00025	0.00002	0.00011		
C29	0.06906	0.79186	0.33592	0.01958	0.02822	0.03730	0.00166	0.00236	0.00241		
C29	0.06900	0.79187	0.33583	0.01807	0.02804	0.03807	0.00171	0.00219	0.00275		
(173k-173k(xray))^2	0.00000	0.00000	0.00000	0.00000	0.00000	0.00000	0.00000	0.00000	0.00000	0.00000	0.00000
C30	0.04804	0.77460	0.24592	0.02326	0.04426	0.03570	0.00123	-0.00284	0.00867		
C30	0.04803	0.77438	0.24583	0.02224	0.04339	0.03647	0.00042	-0.00303	0.00891		
(173k-173k(xray))^2	0.00000	0.00000	0.00000	0.00000	0.00000	0.00000	0.00000	0.00000	0.00000	0.00000	0.00000
H30	0.01803	0.84538	0.20422	0.05462	0.06577	0.05656	0.00951	-0.00491	0.02388		
H30	0.01197	0.84332	0.20447	0.04247							
(173k-173k(xray))^2	0.00004	0.00000	0.00000	0.00015	0.00433	0.00320	0.00009	0.00002	0.00057		
C31	0.07239	0.67228	0.21048	0.02383	0.05152	0.02737	-0.00516	-0.00200	-0.00022		
C31	0.07249	0.67243	0.21060	0.02259	0.05103	0.02676	-0.00548	-0.00188	-0.00011		
(173k-173k(xray))^2	0.00000	0.00000	0.00000	0.00000	0.00000	0.00000	0.00000	0.00000	0.00000	0.00000	0.00000
H31	0.06235	0.66738	0.14273	0.05257	0.08971	0.03370	-0.00389	0.00129	-0.00102		
H31	0.05584	0.66405	0.14231	0.04140							

(173k-173k(xray))^2	0.00004	0.00001	0.00000	0.00012	0.00805	0.00114	0.00002	0.00000	0.00000		
C32	0.11940	0.57702	0.26144	0.02175	0.03595	0.02736	-0.00776	0.00430	-0.00723		
C32	0.11939	0.57681	0.26153	0.02043	0.03554	0.02731	-0.00828	0.00371	-0.00788		
(173k-173k(xray))^2	0.00000	0.00000	0.00000	0.00000	0.00000	0.00000	0.00000	0.00000	0.00000	0.00000	0.00000
C33	0.17922	0.48149	0.24044	0.03180	0.03809	0.03573	-0.00980	0.01075	-0.01631		
C33	0.17935	0.48116	0.24057	0.03084	0.03761	0.03488	-0.01009	0.01073	-0.01645		
(173k-173k(xray))^2	0.00000	0.00000	0.00000	0.00000	0.00000	0.00000	0.00000	0.00000	0.00000	0.00000	0.00000
H33	0.17449	0.45875	0.17476	0.06032	0.07501	0.04492	-0.00693	0.01509	-0.02862		
H33	0.16943	0.45511	0.17497	0.04066							
(173k-173k(xray))^2	0.00003	0.00001	0.00000	0.00039	0.00563	0.00202	0.00005	0.00023	0.00082		
C34	0.24888	0.42177	0.30155	0.03519	0.02649	0.04621	-0.00436	0.01687	-0.01297		
C34	0.24902	0.42181	0.30163	0.03411	0.02531	0.04582	-0.00461	0.01667	-0.01306		
(173k-173k(xray))^2	0.00000	0.00000	0.00000	0.00000	0.00000	0.00000	0.00000	0.00000	0.00000	0.00000	0.00000
H34	0.29619	0.35544	0.28148	0.06390	0.04602	0.07071	0.00683	0.02713	-0.01869		
H34	0.29238	0.35032	0.28268	0.04064							
(173k-173k(xray))^2	0.00001	0.00003	0.00000	0.00054	0.00212	0.00500	0.00005	0.00074	0.00035		
C35	0.26588	0.45191	0.38959	0.02993	0.01832	0.03984	-0.00073	0.01297	-0.00102		
C35	0.26595	0.45179	0.38968	0.02895	0.01766	0.03905	-0.00106	0.01268	-0.00072		
(173k-173k(xray))^2	0.00000	0.00000	0.00000	0.00000	0.00000	0.00000	0.00000	0.00000	0.00000	0.00000	0.00000
C36	0.35486	0.43118	0.45669	0.03385	0.02244	0.04826	0.00612	0.01228	0.00996		
C36	0.35481	0.43123	0.45696	0.03311	0.02186	0.04636	0.00556	0.01233	0.00974		
(173k-173k(xray))^2	0.00000	0.00000	0.00000	0.00000	0.00000	0.00000	0.00000	0.00000	0.00000	0.00000	0.00000
H36	0.41184	0.36698	0.44866	0.05243	0.03946	0.07885	0.01815	0.01674	0.00893		
H36	0.40824	0.36186	0.45054	0.03983							
(173k-173k(xray))^2	0.00001	0.00003	0.00000	0.00016	0.00156	0.00622	0.00033	0.00028	0.00008		
C37	0.37431	0.49686	0.52941	0.03202	0.03248	0.03624	0.00472	0.00584	0.01469		
C37	0.37432	0.49692	0.52944	0.03193	0.03132	0.03494	0.00432	0.00591	0.01489		
(173k-173k(xray))^2	0.00000	0.00000	0.00000	0.00000	0.00000	0.00000	0.00000	0.00000	0.00000	0.00000	0.00000
H37	0.44633	0.48261	0.57536	0.04910	0.06285	0.05200	0.01192	-0.00225	0.02055		
H37	0.44264	0.47780	0.57846	0.03948							
(173k-173k(xray))^2	0.00001	0.00002	0.00001	0.00009	0.00395	0.00270	0.00014	0.00001	0.00042		
C38	0.30676	0.58999	0.54207	0.02924	0.03165	0.02395	-0.00036	0.00579	0.00751		

<b>C38</b>	0.30682	0.58999	0.54199	0.02906	0.03063	0.02312	-0.00121	0.00592	0.00740		
<b>(173k-173k(xray))^2</b>	0.00000	0.00000	0.00000	0.00000	0.00000	0.00000	0.00000	0.00000	0.00000	0.00000	0.00000
<b>C39</b>	0.32837	0.68866	0.59632	0.03501	0.04311	0.02164	-0.00550	0.00321	0.00021		
<b>C39</b>	0.32825	0.68883	0.59640	0.03410	0.04320	0.02096	-0.00570	0.00355	0.00077		
<b>(173k-173k(xray))^2</b>	0.00000	0.00000	0.00000	0.00000	0.00000	0.00000	0.00000	0.00000	0.00000	0.00000	0.00000
<b>H39</b>	0.39689	0.68861	0.64727	0.05499	0.07411	0.03822	-0.00333	-0.00851	-0.00086		
<b>H39</b>	0.39301	0.68543	0.65073	0.03970							
<b>(173k-173k(xray))^2</b>	0.00002	0.00001	0.00001	0.00023	0.00549	0.00146	0.00001	0.00007	0.00000		
<b>C40</b>	0.26887	0.78781	0.58157	0.03542	0.03882	0.02701	-0.00729	0.00815	-0.00949		
<b>C40</b>	0.26901	0.78763	0.58159	0.03465	0.03824	0.02653	-0.00828	0.00861	-0.00952		
<b>(173k-173k(xray))^2</b>	0.00000	0.00000	0.00000	0.00000	0.00000	0.00000	0.00000	0.00000	0.00000	0.00000	0.00000
<b>H40</b>	0.29308	0.86181	0.62145	0.06038	0.06035	0.05228	-0.01322	0.00706	-0.02607		
<b>H40</b>	0.28787	0.85955	0.62496	0.03939							
<b>(173k-173k(xray))^2</b>	0.00003	0.00001	0.00001	0.00044	0.00364	0.00273	0.00017	0.00005	0.00068		
	<b>X</b>	<b>Y</b>	<b>Z</b>	<b>U11</b>	<b>U22</b>	<b>U33</b>	<b>U12</b>	<b>U13</b>	<b>U23</b>	<b>0.00004</b>	<b>0.00005</b>
<b>&lt;delta&gt;</b>	<b>-0.00003</b>	<b>0.00002</b>	<b>-0.00003</b>	<b>0.00091</b>	<b>0.00057</b>	<b>0.00046</b>	<b>0.00037</b>	<b>-0.00004</b>	<b>-0.00007</b>	<b>0.00065</b>	
<b>RMS:</b>	<b>0.00007</b>	<b>0.00014</b>	<b>0.00010</b>	<b>0.00100</b>	<b>0.00068</b>	<b>0.00078</b>	<b>0.00048</b>	<b>0.00035</b>	<b>0.00029</b>	<b>0.00083</b>	<b>0.00065</b>



